Durham E-Theses

Synthesis and Characterisation of Complex Polymer Architectures based on Step-Growth Polymerisation

ANTONELLA PAGLIARULO

How to cite:

PAGLIARULO, ANTONELLA (2020) Synthesis and Characterisation of Complex Polymer Architectures based on Step-Growth Polymerisation. Doctoral thesis, Durham University.

Synthesis and Characterisation of Complex Polymer Architectures based on Step-Growth Polymerisation

Antonella Pagliarulo

Department of Chemistry

2020

Thesis submitted in fulfilment for the degree of Doctor of Philosophy

Antonella Pagliarulo

Synthesis and Characterisation of Complex Polymer Architectures based on Step-Growth Polymerisation

Abstract

Block copolymers have been proposed previously as compatibilizers in blends of incompatible polymers, being able to improve the blend morphology and mechanical properties by obtaining a finer dispersion of the minor component.
The main objective of this PhD project is the synthesis of complex polymer architectures, namely grafted block copolymers, in which the backbone is an aromatic polyester, with a view to being used as compatibilizers for blends of poly(ethylene terephthalate) (PET) and polystyrene (PS). Given the variety of possible applications of PET-PS blends, the design of a synthetic approach for PET-PS branched block copolymers is pursued, as a promising strategy towards blend compatibilization.

The proposed synthetic strategy comprises a first step in which macromonomers, functionalised at only one chain end with a bisphenol moiety, are obtained via living/controlled chain-growth mechanisms. For the synthesis of PS macromonomers, two different approaches using anionic polymerisation – the so-called initiating and the end-capping approach – have been compared by extensive characterisation, exploiting NMR, SEC, MALDI ToF and interaction chromatography. Moreover, the use of a bisphenol functionalised initiator for anionic polymerisation has been investigated. A second kind of macromonomer has been synthesised by the polymerisation of poly(poly(ethylene glycol) methyl ether methacrylate) (PolyPEGMEM), initially via anionic polymerisation, and subsequently developing an ATRP strategy, with the synthesis of a bisphenol functionalised ATRP initiator.

The second step of the synthetic approach of graft copolymers is the incorporation of macromonomers (PS and PolyPEGMEM) into step-growth polymerisation of polyesters, as a comonomer. The PET-PS graft copolymers have been investigated as compatibilizers for PET/PS blends, testing the effect of different PS graft lengths and different structures of copolymer, by measuring PS domain size by SEM. Even if no significant differences were detected among the blends with different copolymers, their effectiveness proved to be superior than existing commercial compatibilizers.

Finally, the versatility of the synthetic approach for graft copolymers with a step-growth polymer backbone was successfully demonstrated by the incorporation of macromonomers (both PS and PolyPEGMEM) into a polysulfone backbone. For PS macromonomers in particular, the effect of different amounts of PS macromonomer and different reaction solution viscosity was also investigated.

TABLE OF CONTENT

LIST OF FIGURES

LIST OF SCHEMES

LIST OF TABLES

LIST OF ABBREVIATIONS

%w.f.	Percentage Weight Fraction
AIBN	Azobisisobutyronitrile
ATRP	Atom Transfer Radical Polymerisation
BCPS	bis(4-chlorophenyl) sulfone
BHET	bis(2-hydroxyethyl) terephthalate
bipy	2,2'-bipyridyl
BOPET	Biaxially-Oriented poly(ethylene terephthalate)
BPA	Bisphenol A
BPF	Bisphenol F - 4,4' Dihydroxydiphenylmethane
BPFK	1,1-Bis(4-t-butyldimethylsiloxyphenyl)methylpotassium
BuLi	Butyllithium
CBDO	2,2,4,4-tetramethyl-1,3-cyclobutanediol
cc	Chain Coupling
Cp	Heat capacity at constant pressure
Đ	Dispersity
DCM	Dichloromethane
DMAc	Dimethylacetamide
DMF	Dimethyl formamide
dn/dc	Refractive index increment
DNA	Deoxyribonucleic Acid
DOSY	Diffusion Ordered Spectroscopy
DPE	1,1-diphenylethylene
DPE-OSi	1,1-bis(4-tert-butyldimethylsiloxyphenyl)ethylene
DPMK	Diphenylmethylpotassium
DSC	Differential Scanning Calorimetry
EG	Ethylene glycol
EPDM	Ethylene/propylene/diene terpolymer
EPR	Ethylene/propylene copolymer
ESI-LC	Electrospray-Liquid Chromatography
FA	Formic Acid

GMA	Styrene-glycidyl methacrylate copolymers
GPC	Gel Permeation Chromatography
HPLC	High Pressure Liquid Chromatography
HRMS	High Resolution Mass Spectrometry
HT	High-temperature
IC	Interaction Chromatography
IPCl	Isophthaloyl chloride
IUPAC	International Union of Pure and Applied Chemistry
LAP	Living Anionic Polymerisation
LRMS	Low Resolution Mass Spectrometry
MALDI	Matrix Assisted Laser Desorption Ionisation
MMA	Methyl methacrylate
M_n	Number-average molar mass
M_w	Weight-average molar mass
MW	Molecular Weight
NMP	Nitroxide Mediated Polymerisation
NMP	1-Methyl-2-pyrrolidinone
NMR	Nuclear Magnetic Resonance
NP-IIC	Normal Phase Isothermal Interaction Chromatography
PCL	Poly(ε-caprolactone)
PE	Polyethylene
PEG	Polyethylene glycol
PEGMEM	Poly(ethylene glycol) methyl ether methacrylate
PEI	Poly(ethylene isophthalate)
PEO	Poly(ethylene oxide)
PET	Poly(ethylene therephthalate)
PMDETA	N,N,N',N'',N''-pentamethyldiethylenetriamine
PMPI	Poly[methylene(phenylene isocyanate)]
PO	Propylene oxide
PP	Polypropylene
PS	Polystyrene
PSf	Polysulfone

Py	Pyridine
r.u.	Repeat Unit
RAFT	Reversible Addition Fragmentation chain Transfer
RALS	Right Angle Light Scattering
RDRP	Reversible Deactivation Radical Polymerisation
RI	Refractive Index
RNA	Ribonucleic Acid
ROMP	Ring Opening Metathesis Polymerisation
RP-IC	Reverse Phase Interaction Chromatography
rpm	Revolutions Per Minute
SEBS	Styrene-ethylene/butylene-styrene
SEC	Size Exclusion Chromatography
SEM	Scanning Electron Microscopy
Sf	Sulfone repeat unit
SMA	Polystyrene-co-maleic anhydride copolymer
sp	Solution Polycondensation
St	Styrene
TBAF	Tetrabutylammonium fluoride
TBDMS	ter-buthyldimethylsilyl
TEMPO	2,2,6,6-tetramethyl-1-piperidynyl-N-oxy
T_g	Glass transition Temperature
THF	Tetrahydrofuran
TMEDA	N,N,N',N'-tetramethylethylendiamine
ToF	Time of Flight
wt.%	Weight percent
σ	Standard deviations

STATEMENT OF COPYRIGHT

CHAPTER 1

1.1 POLYMERS – DEFINITIONS AND MOLECULAR WEIGHT DISTRIBUTION

The term 'polymer' derives from the Ancient Greek word πολύς (*polús*, 'many') and μέρος (*méros*, 'part'),[1] and refers to a molecule of high relative molecular mass, whose structure is composed of multiple repeating units, monomers, from which originates attendant properties.[2]

The chain length and thus the molecular weight of polymers are, among others, important parameters that can determine the main properties of the material. Some biopolymers, such as polypeptides, DNA or RNA, can have a single molecular weight, given by a well-defined monomer sequence. Synthetic polymers, on the other hand, without exception, present a distribution of molecular weights, because of the intrinsic imperfections of any polymerisation mechanism. For this reason, a statistical treatment is necessary when dealing with the molecular weight of synthetic polymers.

The number of monomer repeat units in a polymer chain can be calculated by simply dividing the polymer molar mass by the molar mass of the monomer. This quantity defines the degree of polymerisation (X), however, as stated earlier, the molar mass of any given polymer sample is not a single value, but an average, extrapolated from a distribution of values, and it is, therefore, more correct to talk about an average degree of polymerisation ($\overline{X}$).

Considering a polymer sample comprising of chains with a distribution of molar masses, where M_i is the molar mass of a given chain, N_i is the total number of

chains with molar mass M_i and w_i is the weight fraction of chains with molar mass M_i, the molar mass of the entire sample can be expressed statistically as either:

1. Number-average molar mass $\qquad M_n = \dfrac{\sum_i N_i M_i}{\sum_i N_i} = \dfrac{1}{\sum (w_i/M_i)}$

or

2. Weight-average molar mass $\qquad M_w = \dfrac{\sum_i N_i M_i^2}{\sum_i N_i M_i} = \sum_i w_i M_i$

The ratio of the two averages is a measurement of how broad the molecular weight distribution is, and defines the dispersity, Đ, as:

$$Đ = \frac{M_w}{M_n}$$

Since $M_w > M_n$, Đ is always greater than 1. The closer to 1.0 the dispersity, the more similar the polymer is to a so-called monodisperse polymer, where all chains are identical, which is usually the case for monodisperse biopolymers, such as peptides, DNA and RNA. Synthetic polymers are, instead, polydisperse, with a dispersity that can be more or less broad, usually according to the polymerisation mechanism used.[3]

The synthetic mechanisms used for polymerisation can be classified into two main categories: chain-growth and step-growth. The former comprises all the mechanisms in which the chain only grows upon reaction between the chain-end and a monomer, while the latter comprises polymerisations through stepwise reactions of polyfunctional monomers. Both kinds of mechanism allow the synthesis of linear polymers or more complex architectures, such as branched polymers or polymer networks, when multifunctional monomers are used.

1.2 CHAIN-GROWTH POLYMERISATION

When polymerisation occurs by chain-growth mechanisms, the monomer is consumed one unit at a time, by addition to an active centre, always located at the chain-end of the growing polymer. The reactions can, in theory, continue until the complete consumption of monomer or deactivation of the active centre, via

various possible termination reactions. The active centre can be, for example, a radical or an ion, giving Free Radical Polymerisation in the former case, and Anionic or Cationic Polymerisations in the latter. The great academic and commercial interest around this kind of polymerisation lead to the development of many more mechanisms, including Ziegler-Natta polymerisation, metallocene catalysed polymerisation, controlled radical polymerisation, and ring opening metathesis polymerisation.

1.2.1 FREE RADICAL POLYMERISATION

Free radical polymerisation was first reported by Flory in 1937,[4] who described the mechanism of vinyl polymerisation as a chain reaction involving free radicals and being terminated by bimolecular combination or disproportionation reactions between two active growing chains.

Nowadays, it remains the most important industrial technology for the production of low-density polyethylene, polystyrene, polyacrylates, and polymethacrylates, due to its versatility and synthetic ease. The compatibility with a wide variety of functional groups (e.g. -OH, $-NR_2$, -COOH), coupled with its tolerance to water and protic media, makes possible the development of emulsion and suspension techniques which greatly simplify the experimental setup. The only requirement for its effectiveness is the absence of oxygen. Despite these advantages, free radical procedures do have a few drawbacks, since the materials obtained are often polydisperse with very limited control over architecture. Indeed, block copolymers and well-defined branched polymer architectures – e.g. star-branched polymers, cannot be obtained by conventional free radical mechanisms.[5]

Despite good reproducibility over the average molecular weight achieved, usually polymers obtained by free radical polymerisation are heterogeneous in terms of molar mass, and it is very difficult to control architecture and composition in case of copolymerisation. The general lack of control (on a molecular level) arises because the active centre, a free radical, is able to propagate and/or terminate at a very high rate, that is only limited by the diffusion of the radicals. It is this high

rate of termination and propagation, compared to the relative slow rate of initiation, that makes the control, in terms of molar mass distribution and copolymer composition, very complicated.

As is common with all chain-growth mechanisms, free radical polymerisation consists of three steps: initiation, comprising the formation of the first radical and the subsequent reaction with the first monomer; propagation, when the radical active centre reacts sequentially with monomers, giving chain growth; termination, that causes the end of the chain growth, by the destruction of the active centres.

There are different kinds of species that can easily generate radicals upon homolytic rupture of a covalent bond – radical initiators. The most commonly used initiators include peroxides, in which the (R-O-O-R) bond undergoes homolytic scission, usually by thermolysis, to form two (R-O$^{\bullet}$) radical species, or azo compounds (-N=N-), which can be used to generate initiating radicals by the action of both temperature or light (photolysis). Scheme 1.1 shows of the structure of benzoyl peroxide and azobisisobutyronitrile (AIBN), which are common examples of each of the aforementioned classes of radical initiators, respectively.[6]
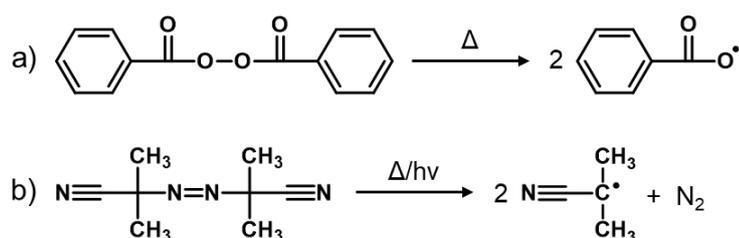
Scheme 1.1 Thermo or photolytic formation of radical initiators from a) benzoyl peroxide and b) azobisisobutyronitrile (AIBN).
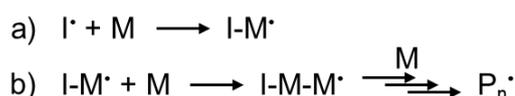
Scheme 1.2 a) Radical initiator, I$^{\bullet}$, attack to the first monomer, M, and b) subsequent propagation step.

Once formed, the radical is usually unstable and thus very reactive towards monomers (Scheme 1.2a), forming a new propagating radical species and

starting the next step of the process, propagation, in which n-1 monomers are added to form the still active radical chain $P_n{}^{\bullet}$, with degree of polymerisation n (Scheme 1.2b).

The radical addition happens on the π bond of unsaturated monomers, typically on the less substituted carbon (Scheme 1.3). In this way, the more substituted (stable) radical is formed, resulting in a head-to-tail polymerisation.[6]
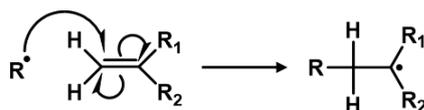
Scheme 1.3 Regioselectivity of the radical attack on the double bond of an unsaturated monomer.

Theoretically, the chain can propagate until all the monomers in the system are consumed, but the high reactivity of free radicals results in a series of termination reactions, yielding inactive covalent bonds and thus ending the growth of the polymer chains. These termination reactions are frequent, especially when high degrees of polymerisation are reached. There are two common termination mechanisms, illustrated in Scheme 1.4.
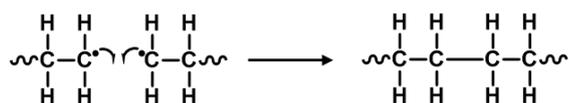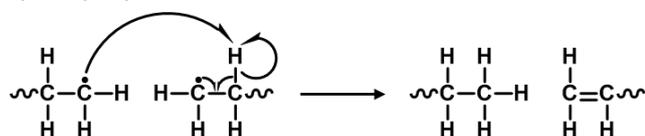
Scheme 1.4 Termination mechanisms in free radical polymerisation: a) recombination and b) disproportionation.

Recombination is caused by two radical chains coupling together through the formation of a covalent bond (Scheme 1.4a). Disproportionation occurs when a proton is abstracted from the chain-end of another species, resulting in two deactivated chains (Scheme 1.4b).

A further kind of reaction, which can also occur during a radical polymerisation, is the chain transfer reaction, in which the propagating active centre is transferred to another molecule. The activation energy for these reactions is higher than propagation, therefore they become more significant at higher temperatures.[7] Typical chain transfer reactions can occur between the active site on a chain and a monomer, another or the same chain (backbiting reaction), and sometimes the solvent. Since the propagating site is deactivated and another active radical is formed to potentially continue the polymerisation, with the exception of chain transfer to polymer, chain transfer has the effect of reducing the number average molecular weight achievable. However, the transfer of the active site to another polymer chain (intermolecular), or to a difference position on the same chain (intramolecular) instead, causes the formation of branched structures and the number average molar mass is not affected. Some species, such as halogen compounds (chloroform and carbon tetrachloride), certain aromatic hydrocarbons and thiols (mercaptans), can be deliberately added to the polymerisation reaction, with the specific purpose to control and lower the final molecular weight via chain transfer.[8]

The occurrence of barely controllable termination and chain transfer reactions usually yields product with a broad molecular weight distribution, and makes this mechanism very unsuitable for the creation of well-defined polymers. For this reason, there have been many efforts to develop 'controlled radical polymerisation' strategies, with aim of retaining the versatility of a radical mechanism, with a better control over the molecular parameters of the final product.

1.2.2   REVERSIBLE DEACTIVATION RADICAL POLYMERISATION - RDRP

The way to make a radical polymerisation more controllable is to try to suppress the contribution of termination reactions. This can be achieved by lowering the concentration of the growing radical species via fast equilibria with a dormant species, thus promoting the reversible deactivation of the majority of the propagating species. Therefore, IUPAC has defined the controlled radical

polymerisation mechanisms as Reversible Deactivation Radical Polymerisation (RDRP).[9] The low concentration of active species also slows down the rate of propagation, but to a different extent compared to the rate of termination. Termination, whether via recombination or disproportionation (Scheme 1.4), is a bimolecular mechanism, thus its rate is much more affected by the low concentration of active species than the rate of propagation.

Radicals may either be reversibly trapped in a deactivation/activation process (Scheme 1.5a), or they can be involved in a reversible exchange equilibrium (Scheme 1.5b).[7]
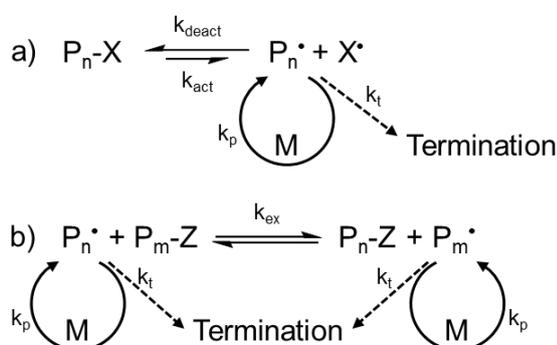
Scheme 1.5 General mechanisms in a RDRP reaction, involving a) a deactivation/activation process or b) a reversible exchange equilibrium.[7]

In the former case, the propagating radicals $P_n^\bullet$ are rapidly deactivated, with a rate constant k_{deact}, to give a dormant species, which can, in turn, be activated (k_{act}) either spontaneously/thermally, through light, or with an appropriate catalyst to reform the active centres. Once formed, radicals can react with monomers (M) and propagate (k_p), but of course this is also the stage at which termination (k_t) can happen. Since $k_{deact} \gg k_{act}$, the instantaneous concentration of active radicals that can undergo termination is kept extremely low, thus significantly reducing the probability that bimolecular termination could happen. Moreover, $X^\bullet$ (Scheme 1.5a) is typically incapable of reacting with itself or monomer, but only (reversibly) with the active growing chain. Therefore, in the case of unavoidable irreversible bimolecular radical-radical termination, the concentration of $X^\bullet$ progressively and irreversibly increases, causing an even higher probability that the growing radicals react with $X^\bullet$ rather than with themselves to give termination.

The most common mechanisms working with this kind of equilibria are nitroxide mediated polymerisation (NMP) and atom transfer radical polymerisation (ATRP).

1.2.2.1   Reversible Addition Fragmentation chain Transfer - RAFT

A different approach, among the RDRP mechanisms, consists of reversible exchange equilibria with a transfer agent (Scheme 1.5b). The most common example, due to its applicability to a wide range of monomers, is Reversible Addition Fragmentation chain Transfer polymerisation (RAFT), developed by Rizzardo in 1998.[10] The transfer agents are typically dithio or trithio compounds (Figure 1.1).

$$Z = \text{-Ph}, \quad \text{—N}\bigcirc, \quad \text{—N}\bigcirc^N, \quad \text{-OR'}$$

$$R = \text{-C(CH}_3)_2\text{CN}, \ \text{-C(CH}_3)_2\text{Ph}, \ \text{-CH}_2\text{Ph}, \ \text{-C(CH}_3)_2\text{COOH}$$
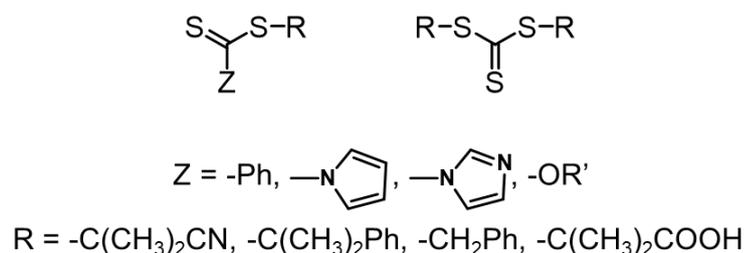
Figure 1.1 Examples of dithio and trithio compounds commonly used as RAFT agents.

A general RAFT mechanism is shown in Scheme 1.6.
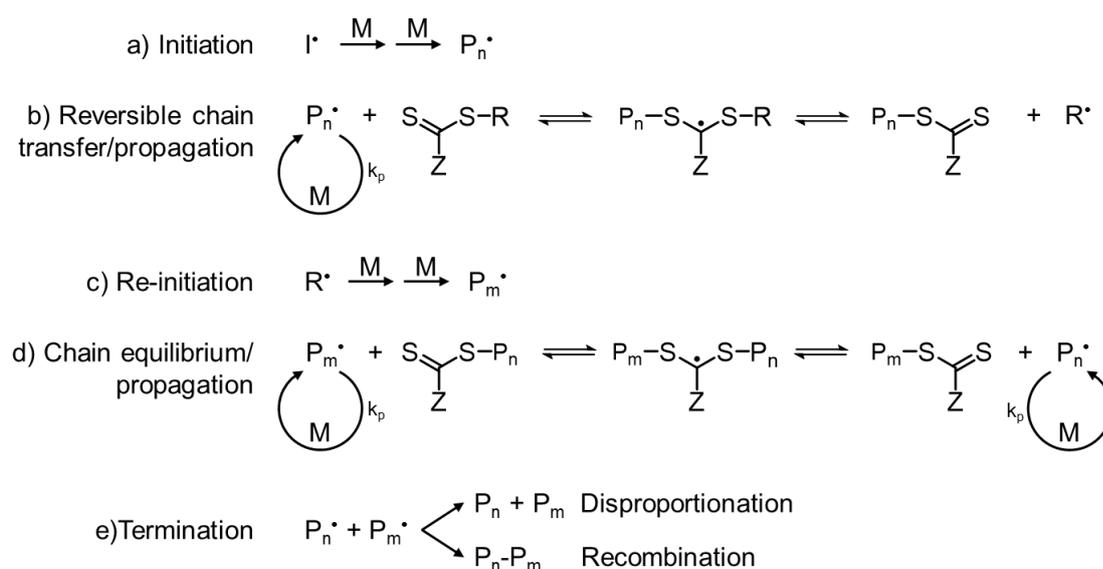
Scheme 1.6 General mechanism of RAFT polymerisation.

The initiation step (a) is the same as free radical polymerisation, with the formation of the initiator radical, I•, for example from AIBN or benzoyl peroxide, and the reaction with monomers, M, to give a growing radical chain P_n•. At this point the active species reacts with the RAFT agent (b), producing an intermediate – dormant - radical and, from the equilibrium, a new radical R• is released, which can initiate the growth of a different chain, P_m•, in the re-initiation step (c). The following equilibrium (d) is, now, between two active chains and the dormant polymeric RAFT agent. At this stage, propagation also occurs, when either P_n• or P_m• are released from the dormant species. The chains have equal probability to grow, thus allowing the production of narrow distribution polymers. Termination is suppressed, as is the case for all RDRP mechanisms, but is not eliminated and occurs as in conventional radical polymerisation (e). When the polymerisation is complete (or stopped), the chains that have not undergone termination will retain the thiocarbonylthio end group.[11]

The choice of the RAFT agent is a key factor for the success of the polymerisation, and one of the drawbacks of this mechanism is the lack of a generic RAFT agent suitable for every class of monomers, and the consequent need to design and synthesise a specific one each time. This also makes it difficult to find a RAFT agent suitable for different monomers, in case a copolymer, block or statistical, is to be synthesised. Moreover, these species are often brightly coloured, and the final polymer might require an additional step to remove the RAFT agent residue from the chain end. All these limitations, combined with high cost of the reagents, have slowed down the industrial application of RAFT.[12]

1.2.2.2   Nitroxide Mediated Polymerisation - NMP

Among the controlled radical mechanisms involving a dormant/active species equilibrium, in NMP the dormant species is an alkoxyamine, obtained via the (reversible) covalent addition of the stable free radical 2,2,6,6-tetramethyl-1-piperidynyl-N-oxy (TEMPO) to the propagating chain-end (Scheme 1.7).[7] TEMPO-based systems have been proven to be successful for the controlled radical polymerisation of styrene and its derivatives,[13] but they are

not very effective with acrylates, because the covalent bond created in the dormant species is too strong.
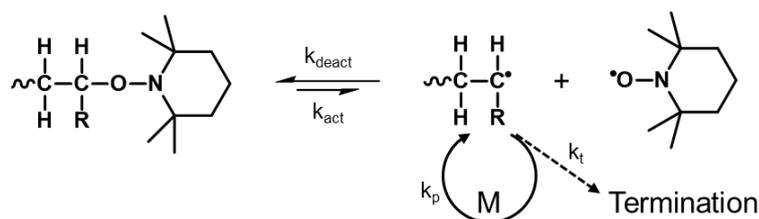
Scheme 1.7 Active/dormant species equilibrium in an NMP mechanism.

Different structures of alkoxyamines, such as phosphonate[14] and arene nitroxide[15] (Figure 1.2), have been proposed to improve the efficiency of NMP with a wider range of monomers.
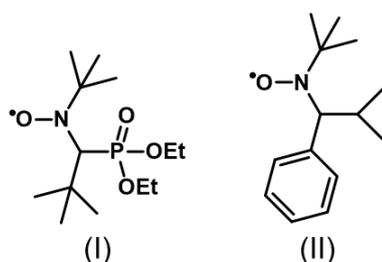
Figure 1.2 Structures of two nitroxides used in NMP: phosphonate (I) and arene nitroxide (II).

1.2.2.3   Atom Transfer Radical Polymerisation - ATRP

ATRP is another mechanism based on the active/dormant species equilibrium[16-17] and was first reported independently and almost simultaneously by both Sawamoto[18] and Matyjaszewski[19] in 1995. A halogen atom (X) is transferred from an alkyl halide to a metal catalyst (M), usually coordinated to a nitrogen-based ligand (L), oxidising the metal centre and producing the active organic radical (Scheme 1.8).

The active radical concentration is kept very low because in the equilibrium the deactivation is kinetically favoured ($k_{deact} \gg k_{act}$), thus suppressing the termination reactions. Termination is not completely eliminated, especially when attempting to make high molecular weight polymers or to drive reactions to high

conversions. In these conditions the control of the molecular weight and the dispersity of the polymers is very poor.

$$P_m\text{-}X + M^n/L \underset{k_{act}}{\overset{k_{deact}}{\rightleftharpoons}} P_m{}^\bullet + X\text{-}M^{n+1}/L$$

$$k_p \quad M \quad k_t \quad \text{Termination}$$
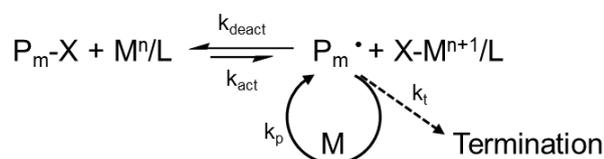
Scheme 1.8 Active/dormant species equilibrium in an ATRP mechanism.

ATRP is effective for a variety of monomers, including styrene, acrylates, methacrylates, acrylonitriles and acrylamides, however some monomers containing functional groups with acidic protons, such as (meth)acrylic acid, cannot be used because of incompatibility with the reaction conditions. The application of ATRP on industrial scale is strongly limited by: (i) the need to remove all oxygen and oxidants, to prevent the reduction of ATRP catalysts; (ii) the presence of transition metal catalysts (copper, the most popular), which are often considered to be mildly toxic, in concentrations that can approach 0.1 M in bulk monomer, meaning that expensive post-polymerisation purification of the product is often necessary, together with the removal/disposal of large quantities of catalysts.[7]

1.2.3 LIVING IONIC POLYMERISATION

A polymerisation mechanism can be defined as living if chain transfer and termination are absent.[20] The rate of initiation is comparable or faster than the rate of chain propagation, resulting in the growth of all the polymer chains essentially at a similar rate during polymerisation. These characteristics lead to a very low dispersity and a good control of compositional and structural parameters. Therefore, living polymerisation is one of the most effective for the synthesis of polymers with well-defined structures and functionalisation.

For any polymerisation mechanism, to be defined as living, there are a number of criteria that need to be met:[20]

i. Polymerisation proceeds until all monomer is consumed and if more monomer is added, the polymerisation continues.

ii. The number average molecular weight (M_n) is a linear function of conversion. M_n is related to the mass of monomer by the following equation:

$$M_n = \frac{\text{Mass of monomer [g]}}{\text{Moles of initiator}} \qquad (1.1)$$

At any intermediate degree of conversion, this equation becomes:

$$M_n = \frac{\text{Mass of monomer consumed [g]}}{\text{Moles of initiator}} \qquad (1.2)$$

In the absence of chain transfer reactions, M_n vs conversion is linear, however this is true also in presence of termination reactions. Thus, this criterion alone is not rigorous enough to define alone a living polymerisation.

iii. The number of polymer molecules - and active centres - is constant, independent of conversion.

This criterion excludes the possibility of chain transfer reactions, that increase the number of polymer molecules, and chain terminations, which also reduce the number of active centres.

iv. The molecular weight can be controlled by the stoichiometry of the reaction.

It has been shown in criterion *ii* that theoretical M_n can be calculated by Equation 1.1. Deviations of the experimentally obtained molecular weight from this calculated value can indicate whether the system is stoichiometrically controlled.

v. Narrow molecular weight distribution polymers are produced.

Low Đ values are possible when the rate of initiation is competitive with the rate of propagation, and every chain is allowed to grow for the same period of time. Moreover, no chain transfer or termination reactions should occur, all active centres are readily available to react with monomers and propagation reactions must be irreversible. However, low Đ polymers have been obtained by non-living

mechanisms. As a consequence, a narrow molecular weight distribution cannot alone be used as a criterion to identify living polymerisation.

vi. Block copolymers can be prepared by sequential monomer addition.

Following criterion *i*, this criterion states that polymerisation continues upon further addition of monomer, yielding block copolymers, if the added monomer is different from the first polymerised block. If termination reactions occur, the addition of a new monomer to the reaction can result in the presence of two different distributions of polymers, detectable in an SEC chromatogram as separate peaks.

vii. Chain-end functionalised polymers can be prepared in quantitative yield.

This is possible because the active centres in a living polymerisation should be available for end-capping reactions with various terminating or functionalising agents.

In conclusion, it is clear that no single criterion can be used alone to determine whether or not a system is a living polymerisation, but all the criteria have to be used together.

The first time a living polymerisation was reported was in 1956, when Michael Szwarc[21] published his work about the anionic polymerisation of styrene initiated by an alkali metal and naphthalene in THF. Subsequently, other types of living polymerisation have been developed; such as living cationic polymerisation[22] and ring opening metathesis polymerisation.[23]

1.2.3.1   Cationic polymerisation

When, in a chain-growth polymerisation, the reactive propagating species carries an ionic charge, it is called ionic polymerisation. In cationic polymerisation in particular, the active chain end is a positively charged species. As with other chain-growth mechanisms, cationic polymerisations consist of initiation, propagation and termination reactions, but it can be classified as living polymerisation, when the latter is excluded. Initiators in these reactions are

electrophilic species, such as protic acid (HCl, H$_2$SO$_4$, HClO$_4$), or Lewis acids (BF$_3$, AlCl$_3$, SnCl$_4$) in equilibrium with a co-catalyst, to give the electrophilic initiator:

$$BF_3 + H_2O \rightleftharpoons H^+(BF_3OH)^-$$

$$AlCl_3 + RCl \rightleftharpoons R^+(AlCl_4)^-$$
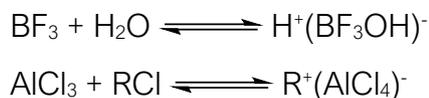
Because of the very high reactivity of the propagating species, cationic polymerisation is usually carried out at low temperatures, in order to inhibit side reactions such as chain transfer. Great care must also be taken to eliminate impurities that may cause termination.[22]

1.2.3.2   Anionic polymerisation

When the active species is negatively charged, the polymerisation is called anionic. In many cases, it meets each of the living polymerisation criteria listed above and can therefore be considered living. As with cationic polymerisation, it comprises the steps of initiation, propagation and termination, even if actually there is no inherent termination step. Compared to other chain growth methods, anionic polymerisation is the best way to control both molecular weight and dispersity and it is the optimal way for the synthesis of copolymers and well-designed complex architectures.

The first living anionic polymerisation of styrene was performed and studied by Szwarc and co-workers in 1956.[21] The suggested mechanism is shown in Scheme 1.9. Upon electron transfer from sodium metal to naphthalene in THF, a dark green solution of sodium naphthalenide radical anion is formed. This species can in turn transfer an electron to styrene, forming a styrene radical anion, which will rapidly dimerise to form a typically deep red solution of styrene dianion. The latter is the actual initiator of the polymerisation, being able to propagate polystyrene chains from both ends. Szwarc and co-workers noted that the solution remained red even after complete monomer consumption and, upon further addition of monomer, polymerisation continued. They concluded that termination did not occur, and this is always true in anionic polymerisation,

provided that no acidic protons or any other environmental impurities, such as moisture, oxygen or CO_2 are present.
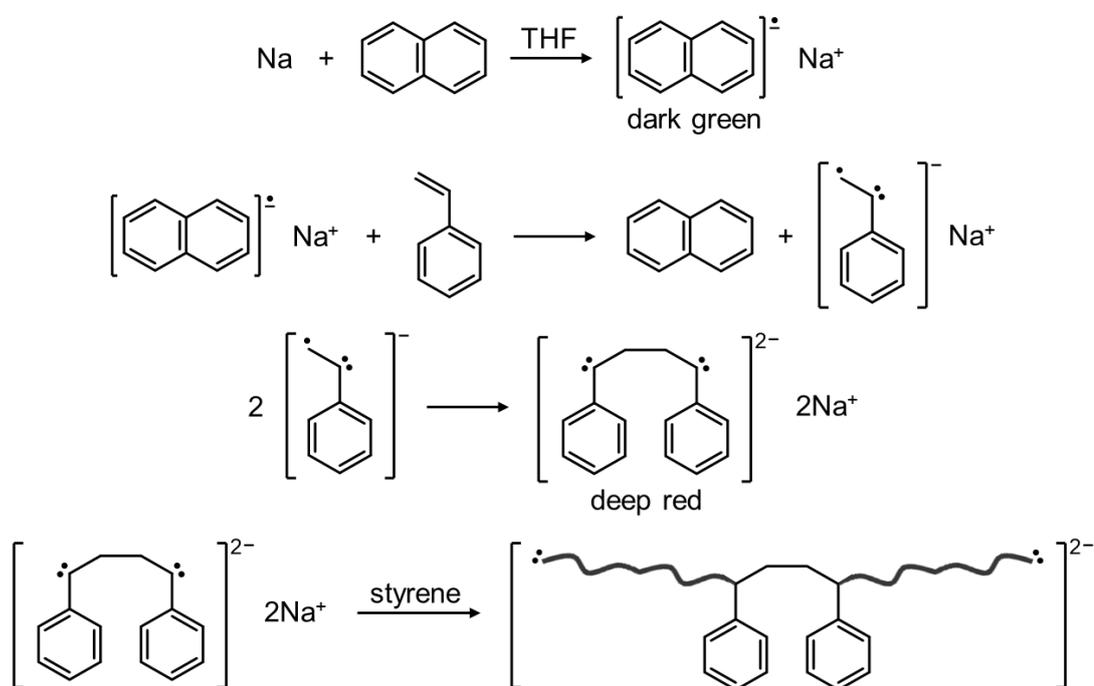
Scheme 1.9 Anionic polymerisation of styrene initiated by sodium naphthalide.[21]

The reaction is indeed very sensitive to tiny quantities of these compounds, that can deactivate the carbanion. Therefore, the system must be free of any acidic protons, the solvent must be aprotic and the reagents must undergo rigorous purification. An inert atmosphere is required, with no air, CO_2 or oxygen, even better if under high vacuum conditions.

Despite all these procedural challenges, anionic polymerisation, along with free radical polymerisation, is one of the most widely used techniques in industry for polymer synthesis, especially in the rubber industry, for the synthesis of elastomers, thermoplastic elastomers, thermoplastic resins, and other specialty polymers.[20,24]

1.2.3.2.1 Monomers

Because of the high reactivity of carbanions there are relatively few monomers which are compatible with anionic polymerisation in comparison to other mechanisms, such as radical polymerisations. Thus, monomers which have

acidic, proton donating groups (e.g. amino, hydroxyl, carboxyl, alkyne functional groups), or strongly electrophilic functional groups or bases that react with nucleophiles are unsuitable. Those monomers which are suitable for anionic polymerisation are divided into vinyl monomers, such as styrene, diene and carbonyl-type, and cyclic monomers, in which the ring can be opened by a nucleophile and result in propagation. Some monomers commonly used in anionic polymerisation are listed in Figure 1.3.
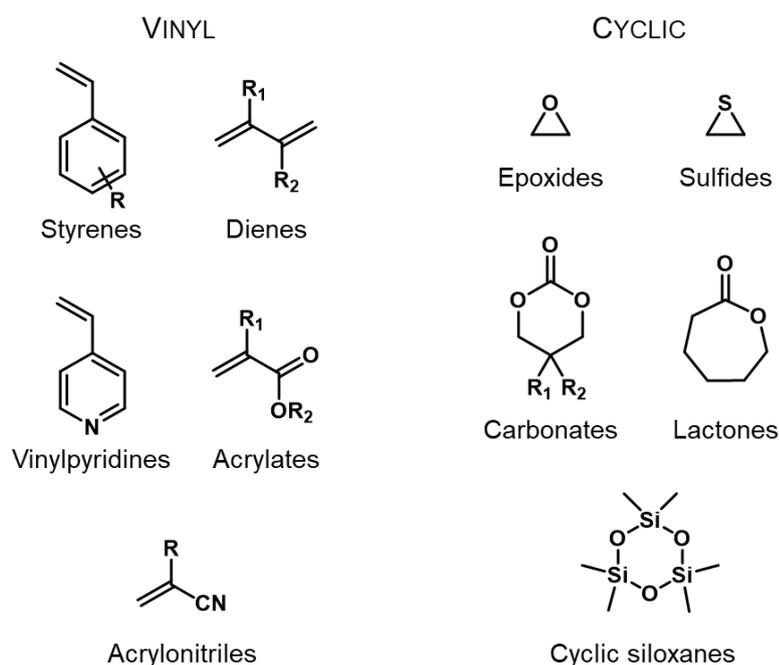
Figure 1.3 Monomers suitable for anionic polymerisation.

Moreover, the monomer must be able to stabilise the negative charge of the resulting propagating carbanionic species. This happens usually by delocalisation, as shown in Figure 1.4.[20]
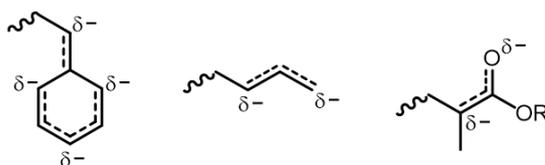
Figure 1.4 Delocalisation of negative charge on vinyl, diene and carbonyl-type monomers.

The presence of electrophilic substituents, such as carbonyl, cyano and nitro groups, though, make anionic polymerisation complicated, because of the presence of a second site for nucleophilic attack by the carbanion, that leads to side reactions.

As an example, the side reactions occurring during the anionic polymerisation of methyl methacrylate are shown in Scheme 1.10.[25]

Initiator destruction

Nucleophilic attack on carbonyl of monomer
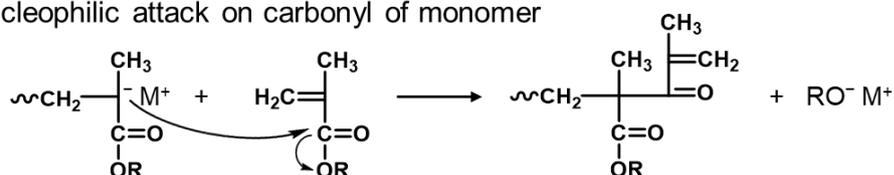
Inter-molecular polymer termination
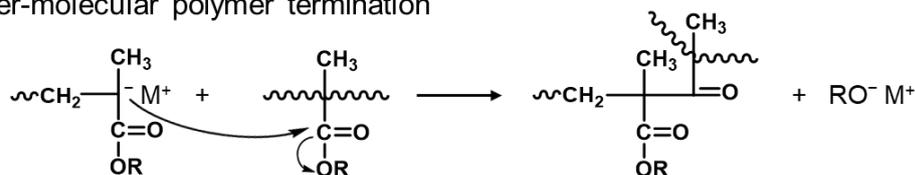
Intra-molecular back-biting termination
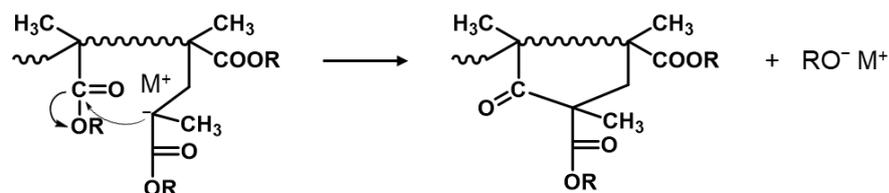
Scheme 1.10 Side reactions in the anionic polymerisation of methacrylates. R=CH$_3$, CH$_2$CH$_3$, C(CH$_3$)$_3$, (CH$_2$)$_3$CH$_3$, (CH$_2$CH$_2$O)$_n$CH$_3$.[25]

It is possible to add monomers with functional groups which are not stable to the anionic charges, provided that the group is protected with a protective group which remains stable during polymerisation and is easily removed afterwards. Silyl ether derivatives, for example, are commonly used with hydroxyl functionalities, and can be removed via mild acid deprotection, after the polymerisation.[20]

1.2.3.2.2   Initiators

As first reported by Szwarc and co-workers,[21] anionic polymerisation can be initiated with radical anions and alkali metals, but nowadays organometallic compounds based on lithium, sodium and potassium, are more commonly used. Alkyllithium compounds are the most widespread because of their fast initiation rates, hydrocarbon solubility, commercial availability and for their ability to form diene polymers with predominantly 1,4-microstructures.

Apart from monomer and solvent choice, and of course the reaction temperature, the rate of initiation by alkyllithium species is related to their degree of aggregation, which in turn is mainly dependent on steric factors, and solvent polarity. In non-polar solvents the initiation step can be seen as comprising of two stages (Scheme 1.11): a) the dissociation equilibrium of the aggregated alkyllithium species and b) the actual initiation, which occurs only when a unaggregated free RLi attacks a monomer molecule M.[20]

$$\text{a)} \quad 1/x \; (RLi)_x \; \underset{}{\overset{K_d}{\rightleftharpoons}} \; RLi$$

$$\text{b)} \quad RLi + M \; \xrightarrow{k_i} \; R\text{-}MLi$$
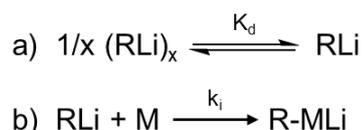
Scheme 1.11 Mechanism of alkyllithium-initiated polymerisation of monomer M.

The kinetics of the initiation process described in Scheme 1.11 exhibit a first-order dependence on monomer concentration and a 1/x order dependence on initiator concentration, as shown in the following equation:

$$R_i = k_i K_d [RLi]^{1/x} [M] \qquad\qquad (1.3)$$

Where x is the degree of aggregation. Therefore, the lower the degree of aggregation x, the higher the rate of initiation R_i, for a given monomer M and in a specific solvent. For instance, for the polymerisation of styrene in non-polar aromatic solvents, menthyllithium, which has a degree of aggregation of 2, is the most reactive, followed by *sec*-butyllithium, with a degree of aggregation of 4, and the less reactive, *n*-butyllithium, which is characterised by a degree of aggregation of 6.[20,26] The solvent also affects significantly the rate of initiation by

enhancing, or not, the dissociation of alkyllithiums. Aromatic solvents tend to partially dissociate the aggregates, leading to higher reactivity than in aliphatic solvents; completely unaggregated initiators can be observed in polar solvents, such as THF, however, care needs to be exercised with the use of ethers since they can react with both the organometallic initiators and the growing polymer chains, leading to chain termination reactions.[20]

The fastest initiation possible is preferable in most cases, in order to make sure it is faster than propagation, thus obtaining narrow distribution polymers; as such, for styrene and diene polymerisations, *sec*-BuLi is preferred over *n*-BuLi.

1.3   STEP-GROWTH POLYMERISATION

In contrast to chain-growth polymerisation, in step-growth mechanisms, the polymer chains grow stepwise, as a result of reactions between two mutually reactive functional groups. That means that the reaction can occur between the functional groups of any two molecular species (monomers, dimers, …, x-mers) present, as schematically shown in Figure 1.5. An initiator is not needed, but often a catalyst is required.
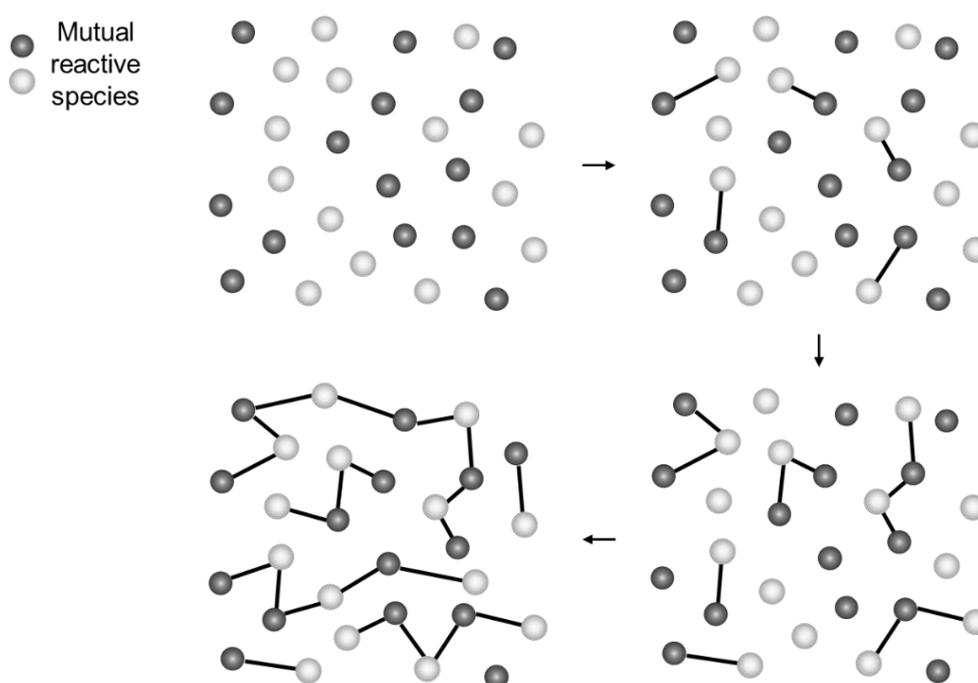
Figure 1.5 Schematic illustration of a step-growth polymerisation.

The mutually reactive functional groups can be either on the same monomer (Scheme 1.12b) or the reaction can happen between two comonomers, each one carrying a pair of one of the functional groups required to react (Scheme 1.12a).

a) x-Ⓐ-x + y-Ⓑ-y ⟶ x-Ⓐ-Ⓑ-y ⟶ {Ⓐ-Ⓑ}$_n$
b) n x-Ⓒ-y ⟶ x-Ⓒ-Ⓒ-y ⟶ {Ⓒ}$_n$
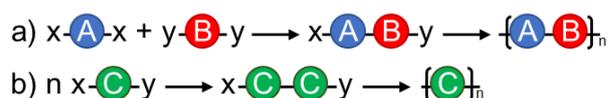
Scheme 1.12 Possible reaction between two mutual reactive functional groups (x and y), either on a) two different comonomers, A and B, or b) the same monomer, C.

Among step-growth mechanisms, a further distinction can be made between step-growth polycondensation, in which a small molecule is eliminated as by-product, and step-growth polyaddition, when no by-product is produced. Table 1.1 summarises some of the most common step-growth polymers, named according to the linking group in their chain backbone.[3]

Table 1.1 Common classes of step-growth polymers, named according to the linking group in the chain backbone.[3]

	Class of Polymer	Structure of linking group
Polycondensation	Polyether	⟿—O—⟿
	Polyester	⟿—C(=O)—O—⟿
	Polycarbonate	⟿—O—C(=O)—O—⟿
	Polysulfone	⟿—S(=O)(=O)—⟿
	Polyamide	⟿—C(=O)—N(H)—⟿
Polyaddition	Polyurethane	⟿—O—C(=O)—N(H)—⟿
	Polyurea	⟿—N(H)—C(=O)—N(H)—⟿

1.3.1 MOLECULAR WEIGHT IN STEP-GROWTH POLYMERISATION

The molecular weight is an important parameter for a polymer, because it can affect significantly the final properties of the material. In step-growth polymerisation the control over this parameter is intrinsically complicated, but a theoretical treatment was developed by Carothers, to analyse and predict the resulting molar mass in a step-growth mechanism.

Before that, Flory demonstrated that the reaction kinetics in step-growth polymerisation are only determined by the mutually reactive functional groups involved, regardless of the size of the species to which they are attached and the potential increase in viscosity, as the polymerisation proceeds.[3,27] Despite the fact that the increasing molecular weight of polymer chains might reduce the ease with which reactive ends come together, the large molecules, acting as a 'cage', also reduce the possibility that reactive ends diffuse away from each other. These two effects essentially neutralise each other, so that the rate of reaction during the polymerisation process depends only on the concentration of reactive groups.[28]

The principle of equal reactivity of functional groups is an assumption that must be kept in mind in the following theoretical treatment, to analyse and predict the molecular weight in step-growth polymerisation.

The number-average degree of polymerisation - the average number of structural units per polymer chain - is given by the equation:

$$\overline{X}_n = \frac{N_0}{N} \tag{1.4}$$

where N_0 is the initial number of molecules and N is the remaining number of unreacted molecules, at time *t*. This parameter can be related to the extent of reaction, p, assuming that there is an equimolar quantity of mutually reactive functional groups:

$$p = \frac{\text{Number of reacted functinal groups}}{\text{Number of initial functional groups}} = \frac{N_0 - N}{N_0} \tag{1.5}$$

which can be rearranged to:

$$\frac{N_0}{N} = \frac{1}{1-p} \tag{1.6}$$

giving the *Carothers equation*:

$$\overline{X_n} = \frac{1}{1-p}$$

(1.7)

This equation proves numerically that a high extent of reaction ($p \rightarrow 1$), is required to achieve a high degree of polymerisation ($\overline{X_n} \rightarrow +\infty$), and therefore polymers with useful physical properties. A high value of p means high monomer conversion (>99%), and to achieve a high conversion, besides the stoichiometric equivalence of mutually reactive functional groups, there is a requirement for high monomer purity, an absence of side reactions (e.g. cyclisation), highly efficient chemical reactions, or reactions which can be easily forced to completion.[3]

The weight average degree of polymerisation is given by:

$$\overline{X_w} = \frac{1+p}{1-p}$$

(1.8)

Therefore the ratio between $\overline{X_w}$ and $\overline{X_n}$ gives a measure of the dispersity of the polymer, Đ, which for a linear polycondensation reaction at completion ($p=1$) is expected to be 2.[28]

In the case of a stoichiometric imbalance, the *general Carothers equation* is needed:

$$\overline{X_n} = \frac{1+r}{1+r-2rp}$$

(1.9)

where r – the reactant ratio - is the ratio between N_A (number of functional groups A) and N_B (number of functional groups B), initially present in the reaction. Conventionally, the excess reactant is the denominator, so that $r < 1$. When $r = 1$, this equation reduces to the equimolar case (Equation 1.7)

The general Carothers equation is a tool to use the stoichiometric imbalance as a strategy to control the degree of polymerisation and, in the end, the molecular weight. For example, for $p \rightarrow 1$ (full conversion of the limiting reagent monomer):

$$\overline{X_n} \rightarrow \frac{1+r}{1-r}$$

(1.10)

considering $r = 0.99$ (1% excess), $\overline{X_n} = 199$, instead of $+\infty$ for the equimolar case.

An alternative approach to tune the degree of polymerisation, and hence the molecular weight, involves the introduction of a mono-functional monomer, carrying either a single A or B functional group. In this case, the reactant ratio, r, is defined as:

$$r = \frac{N_{AA}}{N_{BB} + 2N_B} \qquad (1.11)$$

where N_{AA} and N_{BB} are the number of monomers with two functional groups each, and N_B is the number of species with a single B group. This strategy also results in the end-capping of polymers with the mono B functionalised monomer, in the case that the total number of moles of B functional groups is equal to the number of moles of A functional groups:[3]

$$N_{AA} = N_{BB} + N_B \qquad (1.12)$$

1.3.2   COPOLYMERISATION IN STEP-GROWTH POLYMERISATION

It is possible to form copolymers by step-growth polymerisation, if comonomers with the same reactive groups but different chemical structures are used. We cited before the principle of equal reactivity of functional groups demonstrated by Flory.[27] Indeed, the sequence distribution in a step-growth polymer is mainly related to the relative reactivity of the functional group of each monomer, consequently these polymerisations offer limited options for controlling primary monomer sequences.

For example, if the polymerisation proceeds via the mechanism in Scheme 1.12b, i.e. the mutually reactive functional groups are both on the same monomer, the addition of a comonomer with both the same mutually reactive moieties will yield a statistical copolymer (Scheme 1.13a).[29] When the copolymerisation is based on two comonomers xx and yy functionalised (Scheme 1.12a), a third copolymer, carrying either xx or yy functionality, can be incorporated into the AB alternating sequence (Scheme 1.13b), leading to statistical sequences as well. A few attempts to create an ABC ordered sequence in a step-growth polymerisation, have been reported, using sequential approaches or monomers with selected reactivities (Scheme 1.13c).[30]
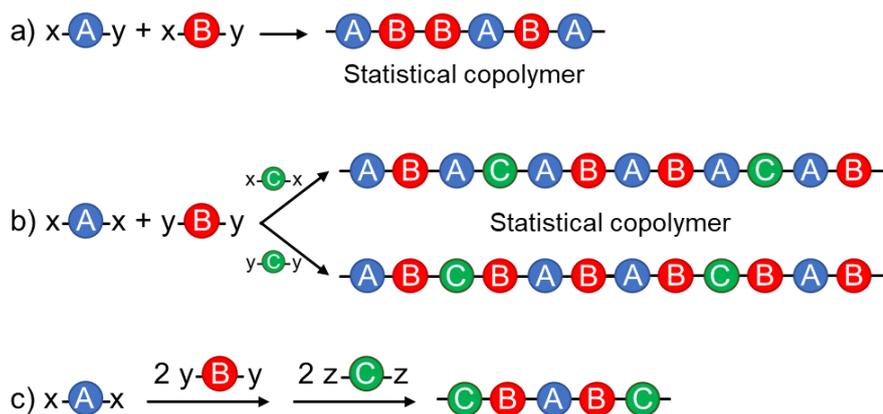
Scheme 1.13 Sequence distribution for copolymers following step-growth polymerisation. The capital letters A, B, C represent different monomer units. The letters x, y, and z represent different types of reactive functions (x reacts with y; y reacts with z).[29]

Linear block copolymers comprising repeated long sequences of A followed by long sequences of B, are rarely observed in step-growth polymers. Some examples of block copolymers have been synthesised by Zhang *et al.*,[31] via a one-pot melt transesterification approach, to synthesize segmented multiblock copolyesters from high-T_g polyester precursors containing the rigid cyclic monomer 2,2,4,4-tetramethyl-1,3-cyclobutanediol (CBDO) (Scheme 1.14).
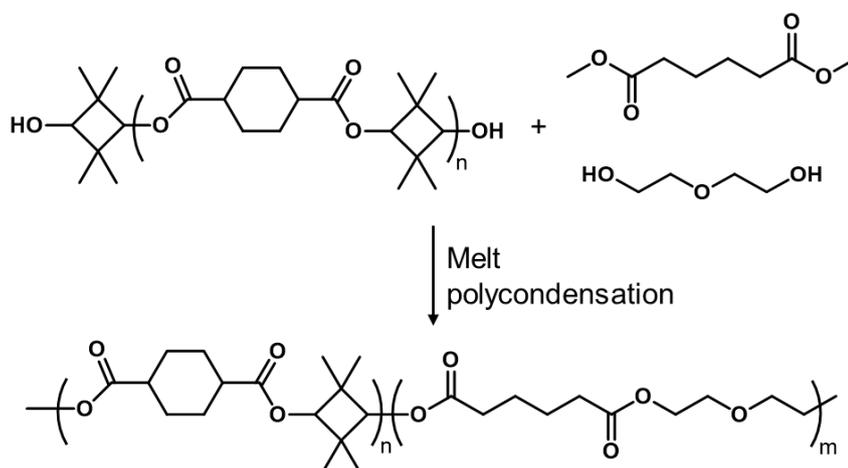
Scheme 1.14 Example of synthesis of a linear block copolymer by step-growth polymerisation.[31]

They demonstrated that the different alcohol steric hindrance and the reaction temperature (180°C) can affect the degree of transesterification and prevent the segment sequence scrambling.

Finally, in a step-growth mechanism it is possible to add multifunctional monomers, in order to obtain branched or crosslinked polymers. If not controlled, polycondensation reactions with multifunctional comonomers may form a polymer network, or gel. The onset of gelation, however, occurs at a critical point of conversion and depends on the concentration of the multifunctional comonomer, thus giving a certain degree of control.[32]

1.4 COMPLEX POLYMER ARCHITECTURES

Chain architecture is a very important feature for polymers, since it can strongly affect a variety of properties, such as rheology, phase separation, crystallinity and other mechanical properties. There are three main classes of polymer architectures, linear, branched and crosslinked (network). For the aim of this project, branched polymers, in which the main chains are connected to each other through branch points, are of particular interest. Many different structures can be classified as branched and some of them are schematically represented in Figure 1.6.
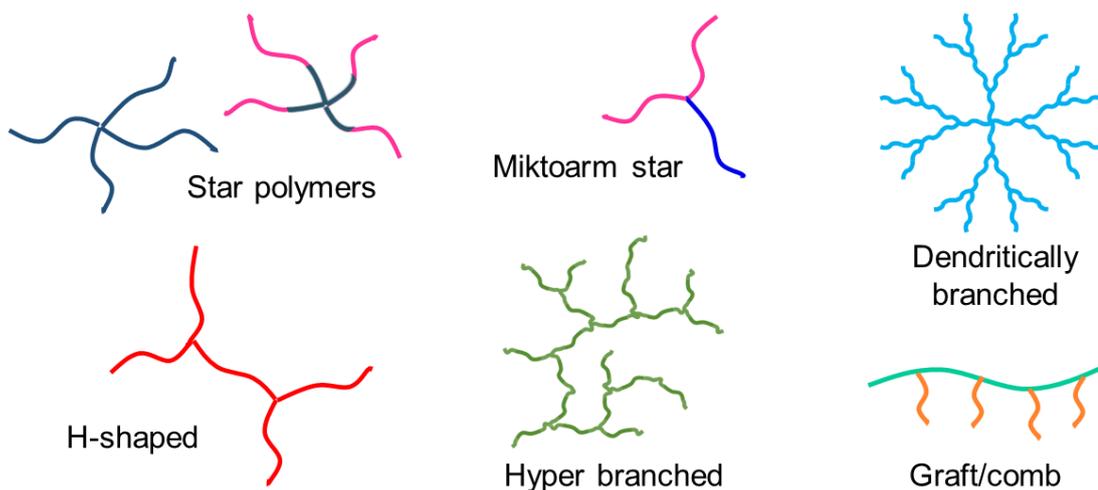
Figure 1.6 Examples of branched polymer architectures.

The possibilities are unlimited, especially if considering that every arm can have the same monomer composition, or the structure can comprise arms of different polymers, as in the case of miktoarm stars (Figure 1.6). Moreover, the monomer composition of each arm can include one type of monomer (homopolymer) or

different kind of monomers (copolymers). According to the sequential arrangement of the monomer units, copolymers can be classified as alternating, random or statistical, gradient or block copolymers (Figure 1.7).
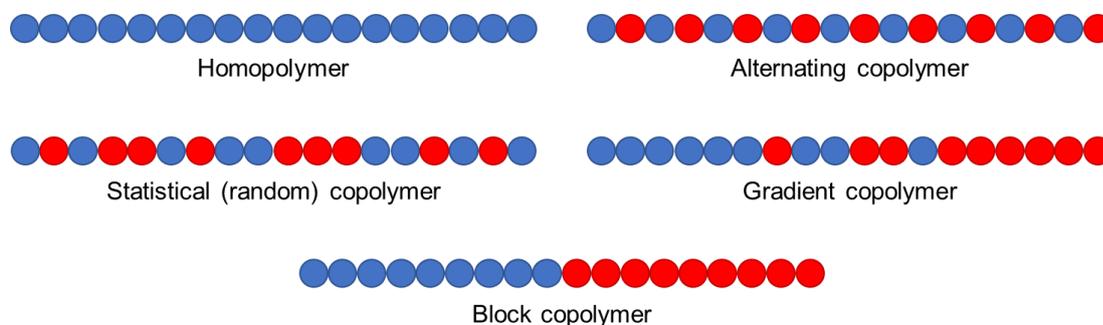
Figure 1.7 Classification of polymers by monomer sequence.

This classification, however, is not exhaustive, because of the almost infinite combinations of different monomers in different number of sequences. It is possible, for example, to have terpolymers, which contain three different monomer types, or copolymers in which monomer sequence distribution is not regular, but follows the same arrangement in all chains, currently known as 'aperiodic copolymers', but whose name is still under discussion.[33]

Over the years, many approaches have been developed for the synthesis of complex polymer architectures, and these approaches employ different mechanisms, from controlled/living chain growth polymerisation, to step-growth polycondensation and 'click chemistry' reactions. A deeper overview of the topic can be gained by reference to recent and exaustive reviews.[34-36] Since the aim of this work is the synthesis of graft copolymer structures the approaches developed for this kind of architecture will be briefly reported in the following paragraph.

1.4.1 GRAFT/COMB ARCHITECTURES

The structure of graft or comb polymers, the target architecture of this project, comprises a main linear backbone and multiple side chains, grafted to the backbone. In comparison with the corresponding linear counterparts, in general

graft architectures show more compact molecular dimensions and significant chain-end effects, resulting from their confined and compact structures. This aspect clearly increases with graft density. The three general strategies to prepare these architectures, 'grafting from', 'grafting onto' and 'grafting through' are illustrated schematically in Figure 1.8.
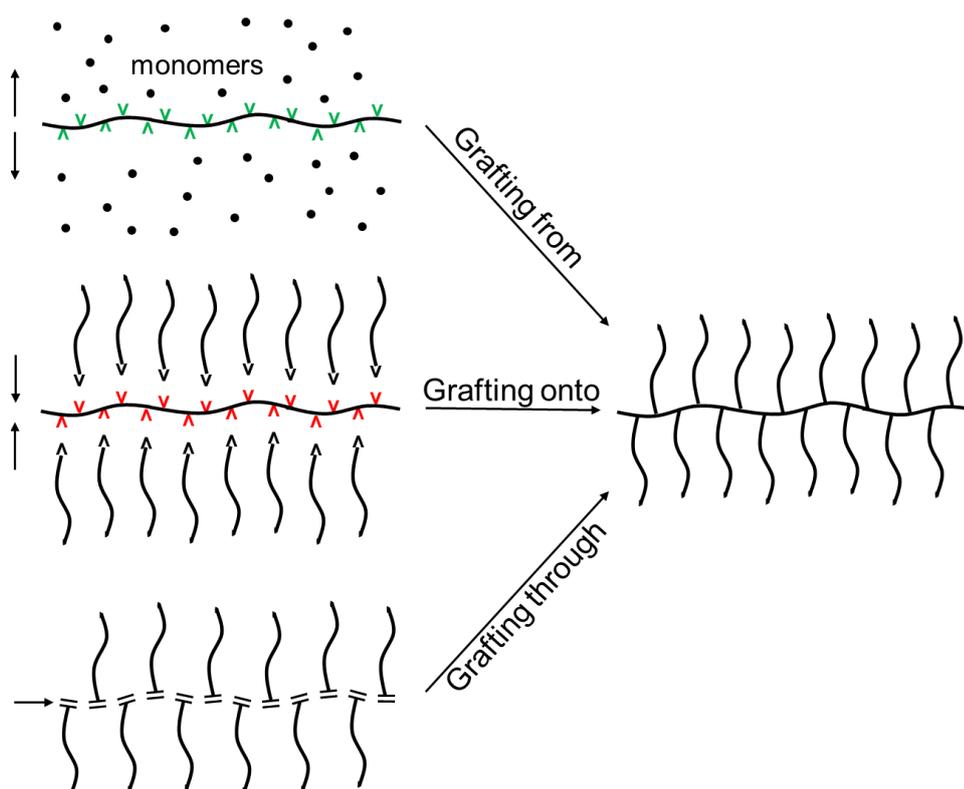
Figure 1.8 Three main strategies for the synthesis of graft polymer architectures.[37]

In the 'grafting from' strategy, the linear backbone is effectively a macroinitiator, with multiple initiating groups along the chain, from which another monomer can be polymerised to form the side chains. The macroinitiator can be synthesised by incorporating monomers carrying functional groups suitable for the initiation of the grafts, or alternatively, the backbone can be functionalised via post-polymerisation reactions.

Typical initiating sites on the backbone are chloromethyl[38] and α-bromoisobutyrate[39-41] groups, to initiate ATRP , and hydroxy groups, as initiators for ring opening polymerisation.[42] The gradual growth of side chains effectively decreases the steric effect that can limit the homogeneous growth of

the side chains, and the absence of unreacted macroinitiator makes the purification of the final product easier. On the other hand, to avoid cross-linking reactions between the multifunctional macroinitiators, the polymerisation of side chains is normally carried out in a highly dilute system, with relatively low monomer conversions. This means that long reaction times and a significant waste of monomers and solvent are inevitable.[37]

The 'grafting onto' strategy is based on the attachment of side chains onto a linear backbone by a coupling reaction. An advantage of this approach is that, since the linear backbone and side chains are prepared independently, their synthesis can be carefully controlled, and their properties fully characterised before coupling. However, a highly efficient coupling reaction and the removal of unreacted side chains are required.[37] Grafts synthesised by living anionic polymerisation and, therefore, carrying a reactive carbanion chain end have been used to attack backbone functional groups such as ester, benzylic halide, nitrile, chlorosilane, anhydride and epoxide, via the corresponding nucleophilic reactions.[43] Other examples of robust coupling reactions employed in a 'grafting onto' approach include azide/alkyne cycloaddition,[44-45] atom transfer nitroxide radical coupling reaction,[46] thiol-ene reaction,[47] and photo-induced coupling reactions.[48]
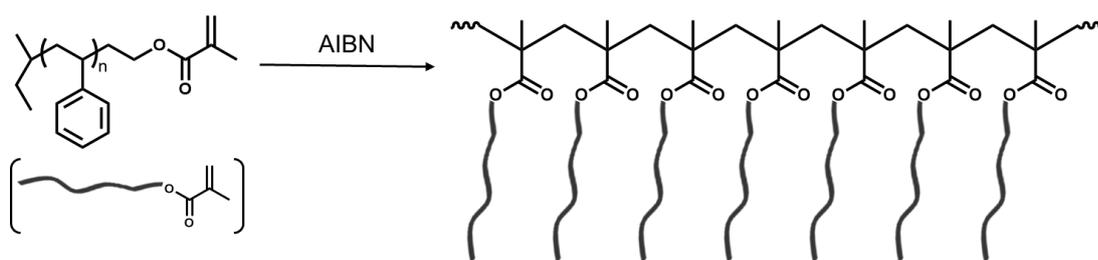
Scheme 1.15 Polymerisation of methacrylate-terminated polystyrene macromonomers to obtain grafted copolymers.[49]

The third approach, the 'grafting through', is based on the use of macromonomers, usually linear polymers synthesised by a living/controlled polymerisation mechanism, with functional groups at one chain end which can undergo polymerisation. The term 'macromonomer' was first used by

Milkovich *et al.*[49-50], who polymerised methacrylate-terminated polystyrene macromonomers by free radical polymerisation, to obtain graft copolymers (Scheme 1.15).

This approach enables control over the degree of polymerisation of both side chains and backbone, thus adjusting also the length of side chains and the grafting density. There are many examples of macromonomers polymerised by different chain-growth mechanisms, such as free radical,[49] ROMP,[51-52] controlled radical polymerisation,[53-54] and living anionic polymerisation.[55] Theoretically, graft copolymers with 100% grafting density (every repeating unit containing one side chain) can be prepared. However, especially with radical polymerisations, avoiding side reactions is difficult and high conversion cannot be reached. Even for more effective mechanisms, the complete conversion of macromonomer is not easy. Therefore, frequently residual unreacted macromonomers need to be removed.[37]

1.4.2 MACROMONOMER APPROACH FOR COMPLEX ARCHITECTURES

Besides being used in the 'grafting through' approach, as seen before, macromonomers with functional groups at one or both chain ends have been also used for the construction of complex architectures – not only graft polymers – with a high compositional and molecular homogeneity,[24,56] by coupling and condensation reactions. The first example was reported by Hedrick *et al.*, who synthesised long-chain hyperbranched poly(ε-caprolactone) (PCL) from an AB$_2$ poly(ε-caprolactone) macromonomer.[57-58]

Jikei at al. have successfully synthesised hyperbranched polylactides[59-60] and branched poly(ether sulfone)s[61] by the self-polycondensation of AB$_2$-type macromonomers. Kong *et al.* have reported the synthesis of polystyrene hyperbranched architectures by an alkyne-azide click reaction between AB$_2$ macromonomers obtained by ATRP, with a bis-functionalised initiator.[62] The same click reaction was used by Wu *et al.* to synthesise 'Defect-Free' hyperbranched polystyrene, but with a different kind of AB$_2$ macromonomer, the

so-called seesaw-type, in which there is one reactive B group at each chain end and A group is in the middle (Figure 1.9).[63-64]
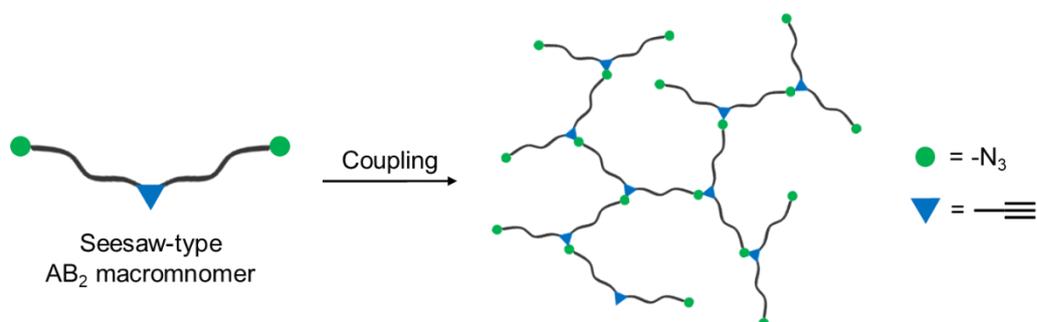
Figure 1.9 Coupling reaction of seesaw-type AB_2 macromonomers to obtain hyperbranched architectures.[63]

Frey *et al.* synthesised AB_n polybutadiene macromonomers by anionic polymerisation, in which the A group was added at the chain end by end-capping reaction with chlorodimethylsilane, and the *n* B groups are pendant vinyl groups, distributed randomly along the backbone, arising from the 1,2 addition during the anionic polymerisation of butadiene. A hydrosilylation polyaddition reaction leads to the formation of the branched structures.[65-66]

In recent years, cyclodextrins have been investigated as polymer functional group for macromonomers, as they form supramolecular inclusion complexes with hydrophobic guest molecules in aqueous solution, giving the possibility to combine a large variety of building blocks to form novel macromolecular architectures.[67]

Hutchings *et al.* have exploited and developed the macromonomer concept for the synthesis of a variety of complex branched polymers, including miktoarm stars,[68] DendriMacs,[69-70] HyperMacs[71-75] and more recently HyperBlocks.[76-77] For instance, AB_2 polystyrene macromonomers were synthesised by anionic polymerisation, using a mono-functionalised initiator and a bi-functional end-capping agent based on diphenylethylene (DPE) (Scheme 1.16).
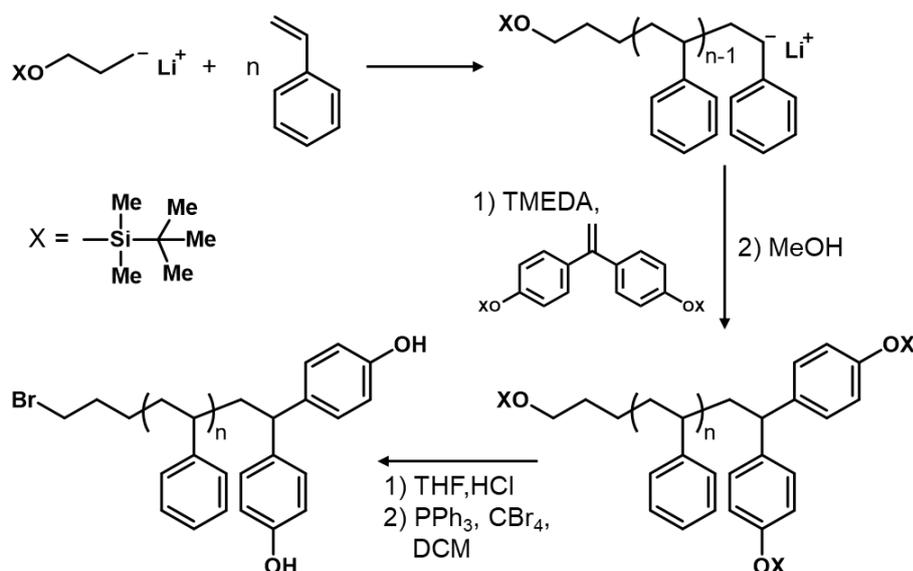
Scheme 1.16 Synthesis of AB$_2$ polystyrene macromonomers.[69]

The macromonomers can be then coupled through polycondensation mechanisms, such as Williamson reaction between an alkyl halide group and the phenol groups of the macromonomers, giving different architectures. Polystyrene HyperMacs has been obtained this way, as shown in Scheme 1.17.
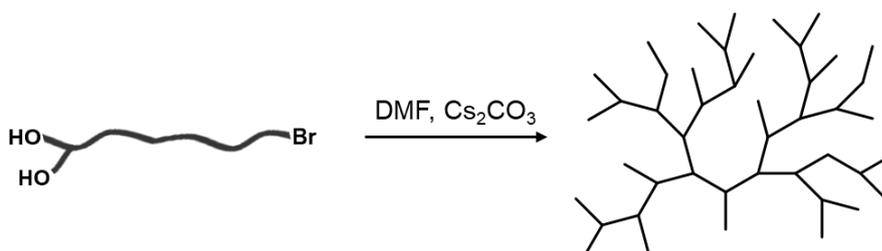
Scheme 1.17 Schematic reactions for the synthesis of polystyrene HyperMacs by macromonomer approach.[73]

The technique is very versatile and also polybutadiene and poly(methyl methacrylate) HyperMacs have been reported.[76] Moreover, block AB$_2$ macromonomers can be synthesised, to be coupled to produce the so called 'Hyperblocks', long chain hyperbranched block copolymers.[76-77] Asymmetric structures can be obtained by reacting macromonomers of different nature, so long as the end-group functionalities are compatible. For example, polystyrene miktostar were synthesised by coupling of two 'long' arms with 'short' AB$_2$ arms of different molecular weights (Scheme 1.18).[68]
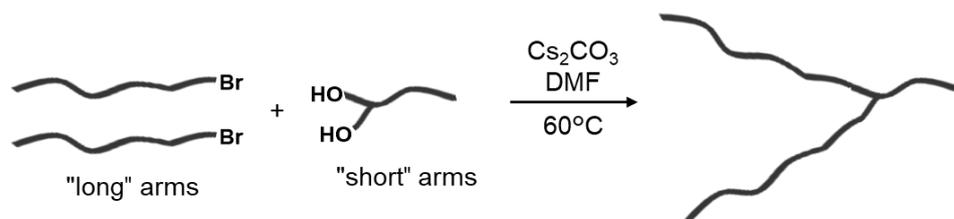
Scheme 1.18 Schematic reactions for the synthesis of polystyrene miktostar by macromonomer approach.[68]

The drawback of the coupling reactions between macromonomers is that they are often incomplete, therefore, the use of excess starting materials is required. This in turn may lead to the need for time-consuming fractionation and purification of the final products, not only from the unreacted macromonomer, but also from partially reacted structure with lower degree of branching than expected.

Macromonomers of different natures have been polymerised by many chain-growth mechanisms, for the synthesis of graft/comb architectures, as mentioned above in Section 1.4.1. There are in the literature, however, fewer cases of the synthesis and use of macromonomers in a 'grafting through' approach, with macromonomers bonded by a step-growth polymerisation.
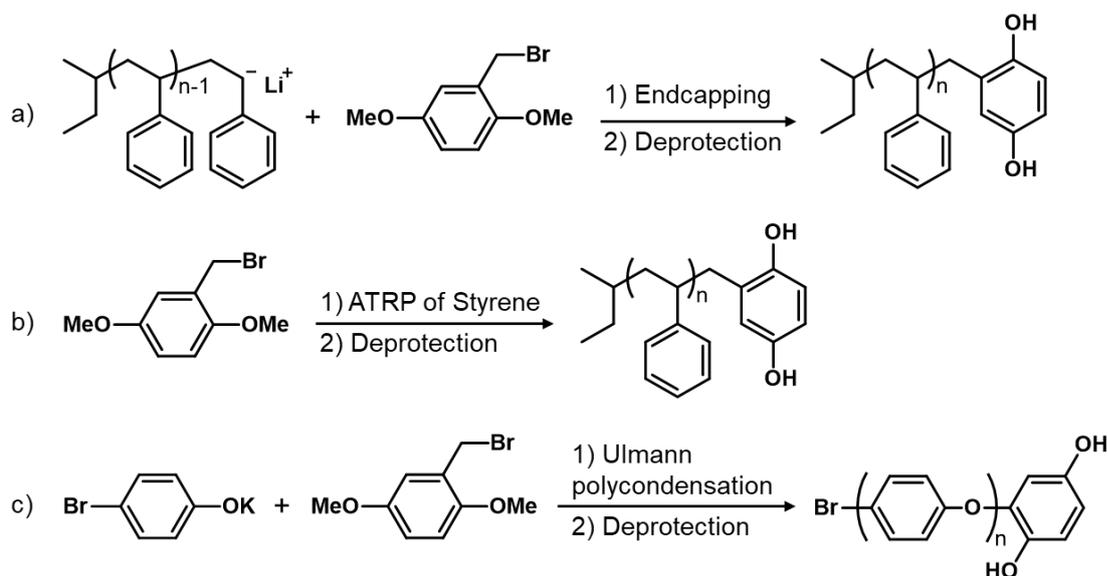
Scheme 1.19 Use of 2,5-dimethoxybenzyl bromide for the synthesis of bis-hydroxy functionalised macromonomers by a) anionic polymerisation,[78] b) ATRP[79] and c) Ulmann polycondensation.[80]

For example, 2,5-dimethoxybenzyl bromide has been used as an end-capping agent in anionic polymerisation (Scheme 1.19a), or as an initiator for ATRP synthesis of polystyrene macromonomers (Scheme 1.19b) with bis-hydroxy functionality, which can be incorporated into a polycarbonate backbone via a polycondensation reaction.[78-79] The same 2,5-dimethoxybenzyl bromide has been used in a Ullmann reaction with potassium 4-bromophenolate to obtain poly(oxy-1,4-phenylene) macromonomers (Scheme 1.19c) that were then added into a polycondensation reaction to get a polyester backbone.[80]

Heitz[78] and Quirk[81] separately suggested the use of a protected 1,1-bis(4-hydroxyphenyl)ethylene as end-capping agent for polystyryllithium (Scheme 1.20) to obtain a macromonomer with a bisphenol functionality that can be polymerised in the polycondensation reaction of polycarbonate.
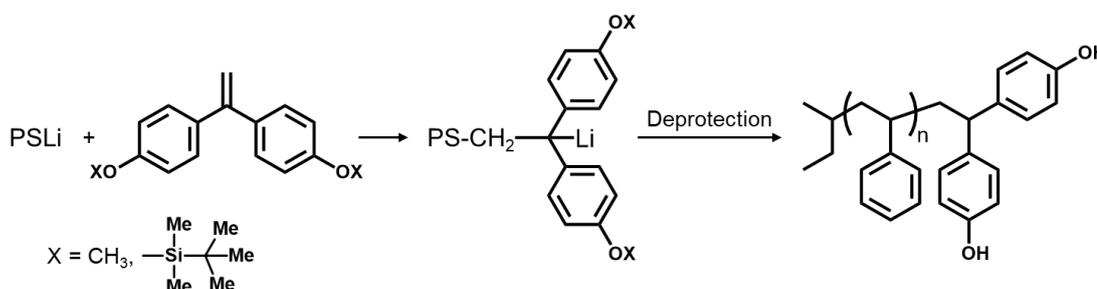
Scheme 1.20 Synthesis of polystyrene macromonomers via end-capping with a protected 1,1-bis(4-hydroxyphenyl)ethylene.[78,81]

A PMMA macromonomer with a bis-carboxylic acid moiety at one chain end (Scheme 1.21) has been used for the synthesis of grafted polycarbonate and polyamide.[82-83]
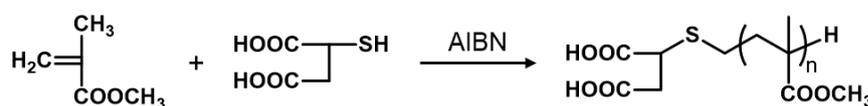
Scheme 1.21 Synthesis of bis-carboxylic acid functionalised PMMA macromonomer with thiomalic acid.[82]

Finally, 4-aminobenzoic acid ester macromonomers[84] and aromatic diamine macromonomers[85] have been incorporated into a polyamide synthesis, to obtain grafted copolymers with a step-growth polymer backbone.

In order to obtain the desired architecture by any of the macromonomer approaches listed before, a strict control over the functionalisation of the chains is needed in respect of the number of functional moieties per chain and for the position of the functionality within the chain. For this reason, living/controlled polymerisation mechanisms are usually exploited for this purpose.

1.4.2.1   Macromonomer synthesis: end-functionalisation of polymers by anionic polymerisation

Living anionic polymerisation is particularly useful for the purpose of synthesising macromonomers, because this mechanism offers a strict control over the functionalisation of polymers, whether it be chain-end or in-chain.

The absence of termination reactions is useful for the synthesis of block copolymers or homopolymers with functionalised end groups. As mentioned in Section 1.2.3, two of the criteria to define living polymerisation are (*criterion vi*) the possibility to add, once all the first monomer is consumed, a second monomer to obtain a block copolymer, and (*criterion vii*) to add another compound, that is itself incorporated to give a useful end group.

a) $P\text{-Li}$ $\xrightarrow{CO_2,\ H^+}$ $P\text{-COOH} + P_2CO + P_3COH$

b) $P\text{-Li} + $ [epoxide] $\longrightarrow \xrightarrow{H^+}$ $P\text{-CH}_2CH_2OH$

c) $P\text{-Li} + \text{Cl-(CH}_2)_3\text{-NR}_2 \longrightarrow P\text{-(CH}_2)_3\text{-NR}_2$

d) $P\text{-Li} + $ [sultone SO_2] $\longrightarrow P\text{-(CH}_2)_3\text{-SO}_3^-\text{Li}^+$

     $\searrow PH + $ [sultone anion SO_2, $^-\text{Li}^+$]
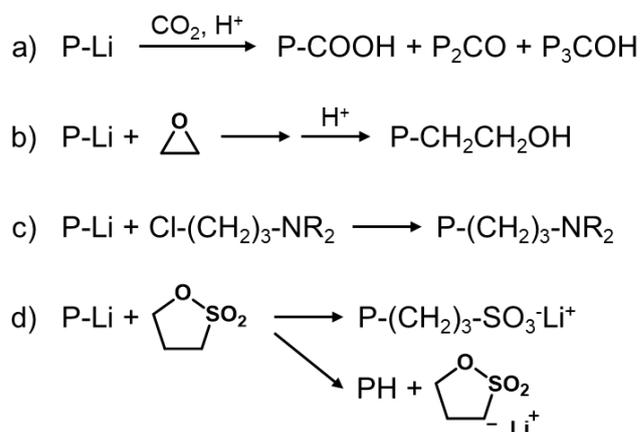
Scheme 1.22 End-functionalisation reactions – and some possible side reactions – of living polyorganolithium anion with electrophilic species.[20]

There are two main ways to introduce desired functionalities at one end of a polymer chain. Traditionally, chain-end functionalisation was achieved through a post-polymerisation reaction of the living anionic polymer with an electrophilic species carrying the desired functional group (Scheme 1.22).

Numerous functionalities may be introduced by the controlled termination of alkyllithium-initiated living polymers with special reagents. For example, a carboxylic acid group can be introduced by the reaction with gaseous carbon dioxide with a solution of the living polymeric organolithium compound (Scheme 1.22a).[86-87] It has been shown that the addition of large amount of a Lewis base, such as THF (25 vol.%) or N,N,N',N'-tetramethylethylendiamine (TMEDA) ([TMEDA]/[PLi]=146), can promote the disaggregation of polymeric organolithium chain ends, thus giving >99% carboxylated polymer (P-COOH in Scheme 1.22a).[20] Hydroxyl terminated polymers can be obtained by reaction with ethylene oxide (Scheme 1.22b),[88-89] and amino groups can be added through the addition of protected α-halo-ω-aminoalkanes (Scheme 1.22c).[90-92]

Sulfonate end-capped polymers has been synthesised through the reaction of polymeric organolithium compounds directly with cyclic sultones (Scheme 1.22d).[93] There is, however, the competitive reaction of polymeric organolithium with the acidic α-hydrogen of the sultone, yielding unfunctionalised chains. The use of THF at low temperature (-78°C) and/or the presence of a hindered chain-end structure (poly(α-methyl-styryl)lithium) proved successful in increasing the percentage of sulfonated chains to higher than 90%.[20]

Alternatively, a (protected) functionalised initiator can be used for anionic polymerisation of, for example styrene or dienes.
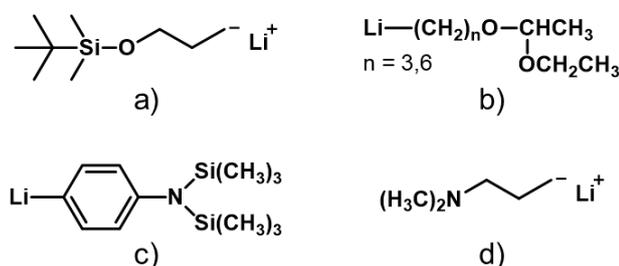
Figure 1.10 Examples of functionalised alkyllithium initiators for anionic polymerisation.

Organolithium initiators with a silyl-protected hydroxy functionality, such as 3-(t-butyldimethylsilyloxy)-1-propyllithium (Figure 1.10a),[68,70-71,94-95] or with acetal-

protected hydroxy functionalities, such as (6-lithiohexyl)acetaldehyde acetal,[96] and (3-lithiopropyl)acetaldehyde acetal (Figure 1.10b),[96-97] have been used to obtain (essentially) quantitative hydroxy end-functionalised polymers. Some examples of amino functionalisation can also be found, in which the initiator is p-lithio-N,N-bis(trimethylsilyl)aniline[98] or 3-(N,N-dimethylamino)propyl-lithium (Figure 1.10c and d, respectively).[99]

Even though quantitative functionalisation is assured with a (protected) functionalised initiator, limited availability and often limited solubility of the initiators strongly impact on the practical application of this strategy.[20,88] In each case, the protection of reactive functional groups is needed, because of the high reactivity of the organolithium reagents.[20]

Of particular interest for the introduction of functionalisation in living anionic polymerisation is the family of monomers based on 1,1-diphenylethylene (DPE). Many reports can be found in the literature which describe the use of functionalised derivatives of DPE, mainly via one of two functionalisation strategies (Scheme 1.23):[100]
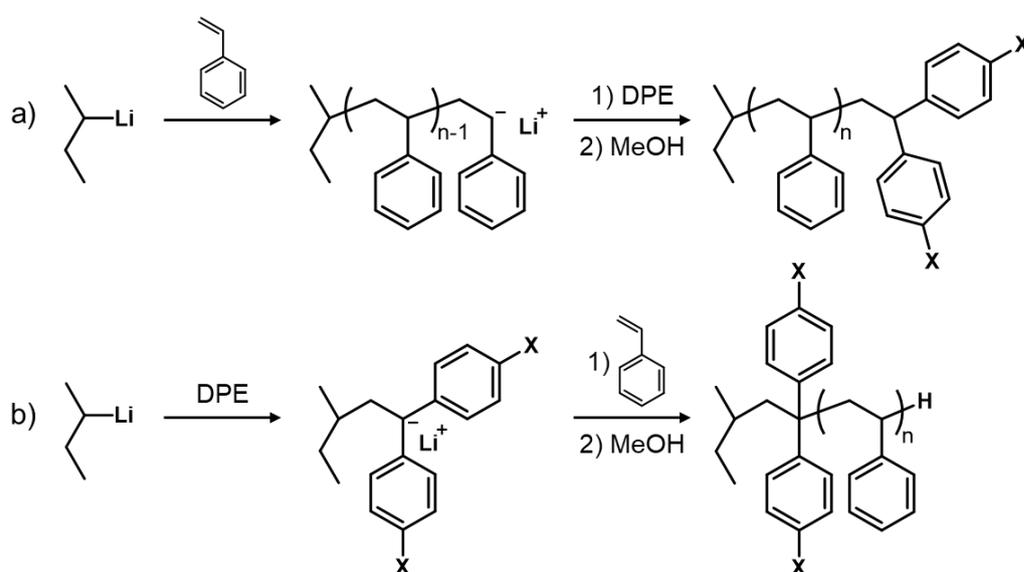
Scheme 1.23 Example of a) end-capping and b) initiating procedure using a generic X-functionalised DPE in the anionic polymerisation of styrene.

The functionalised DPE can be added either post-polymerisation, as an end-capping agent, before the termination of the polymer,[69,71,76] or it can be

activated by the alkyl lithium initiator, and the adduct used to initiate the polymerisation.

The end-capping strategy (Scheme 1.23a) involves the simple addition of DPE to the living polymeric organolithium species, usually in the presence of a Lewis base such as TMEDA to reduce the aggregation of polymer anionic chain ends and thus speed up the end-capping. The addition of DPE to poly(styryl)lithium or poly(dienyl)lithium is a very favourable reaction since the corresponding 1,1-diphenylalkyllithium is approximately 64.5 kJ·mol^{-1} more stable than the organolithium species it reacts with.[100] The functionalisation is, thus, practically quantitative.[101-102] The steric bulk of the two phenyl rings bonded directly to the propagating carbanion, however, prevents DPE from self-propagating. The DPE monomer is unable to homopolymerize, and therefore only mono-addition happens, even with an excess of DPE.[68,100,103] Finally, after the addition of DPE, the product is still a living chain and the obtained polymeric 1,1-diphenylalkyllithium can be used as a macro-initiator to synthesise (block)copolymers, by the sequential addition of monomers.

As an alternative to the end-capping procedure, the reaction of DPE (and derivatives) with a simple alkyllithium compound (e.g. butyllithium) to form the corresponding 1,1-diphenylalkyllithium gives an effective initiator in anionic polymerisation (Scheme 1.23b). As previously noted, the diphenylmethyl carbanion is more stable than the carbanions resulting from the subsequent addition of monomers (usually benzyl and allyl carbanion). Thus, it would be expected that this initiation reaction would be energetically unfavourable. However, the energy released by the conversion of a π-bond in the monomer to a more stable σ-bond in the adduct is enough to start the polymerisation.[100] Moreover, it is well known that a lower degree of association in alkyllithium species results in increased reactivity. 1,1-diphenylalkyllithium is associated into dimers in hydrocarbon solutions, while other organolithium species often have a higher degree of association.[20,100] This contributes to making DPE an effective species to initiate anionic polymerisation. Homopolymerisation resulting in the dimerisation of DPE has been reported when using a large excess of DPE (10-fold

excess),[104] however, under normal circumstances the 1,1-diphenylalkyllithium initiator would not be expected to attack another DPE molecule, and homopolymerisation of DPE is avoided. The use of 1,1-diphenylalkyllithium (and its derivatives) as an initiator for anionic polymerisation is particularly advantageous for some specific purposes. For example, in the polymerisation of methyl methacrylate (MMA), the use of DPE is essential. The steric hindrance caused by the two bulky phenyl groups adjacent to the carbanion, prevents attack by the initiator on the carbonyl group of MMA – which would otherwise occur if butyllithium were used.[76,100] Other authors have also exploited functionalised DPE for living anionic surface initiated polymerisation, to produce surface grafted polymer. Fan *et al.*[105] produced montmorillonite clay nanoparticles, intercalated with a quaternised-amine modified DPE derivative which was immobilised on the clay surface by electrostatic attraction. After being dispersed in benzene, the initiator-clay complex was activated by n-BuLi to initiate polymerisation. Quirk *et al.*[106] used a surface bound 1,1-diphenylethylene monolayer to prepare diblock copolymer brushes on oxide surfaces by anionic polymerisation.
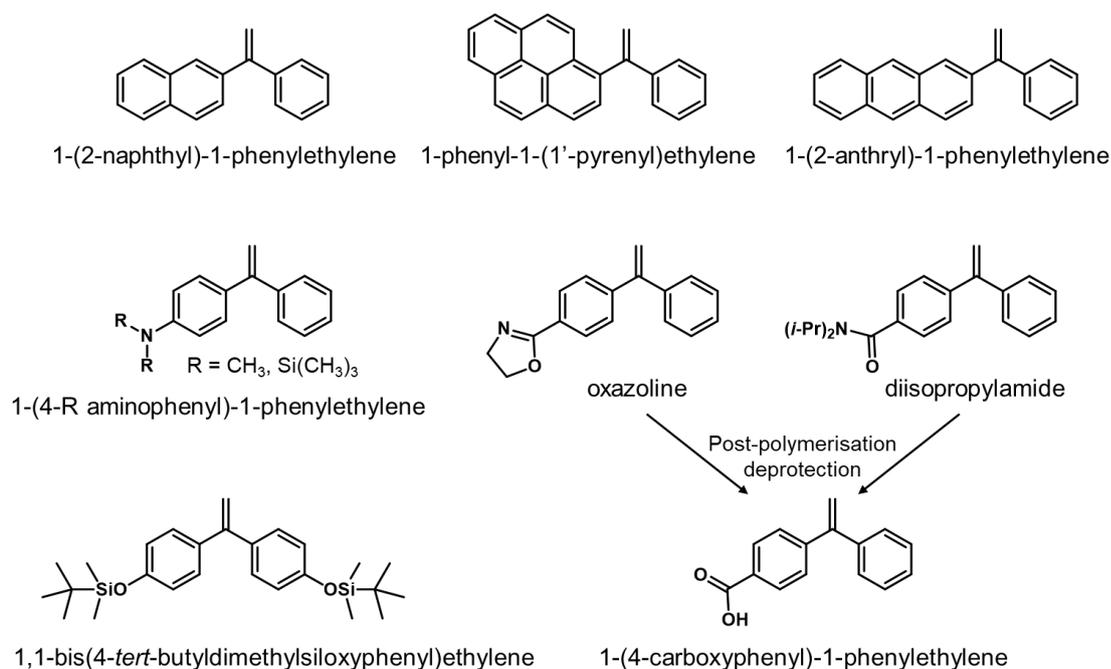
Figure 1.11 Examples of functionalised DPE, used in anionic polymerisation to functionalise polymers.

Whether functionalisation with DPE (derivative) is performed at the chain-end, via the initiating step or in-chain, this particular species is very versatile and allows the introduction of many different functional groups (Figure 1.11) onto the polymer chain. DPE carrying fluorescent moieties, such as naphthyl and pyrenyl groups, have been used to label polymer chains, via the reaction with 1-(2-naphthyl)-1-phenylethylene or 1-phenyl-1-(1'-pyrenyl)ethylene.[103,107-112] More recently, 1-(2-anthryl)-1-phenylethylene has been used to monitor polymer-polymer coupling by size exclusion chromatography coupled with fluorescence detection.[101-102] DPE derivatives with amino groups on the aromatic rings, e.g. 1-(4-dimethylaminophenyl)-1-phenylethylene and 1-(4-(N,N-bis(trimethylsilyl)-amino)phenyl)-1-phenylethylene, have been widely used to obtain amino-functionalised chains of styrene and dienes. The presence even of a small number of these polar groups can dramatically change the solution and aggregation behaviour of non-polar macromolecules. There are examples of such kind of functionalisation at the beginning of the chain,[105] the terminus of the chain,[113-115] in-chain,[116-117] or to prepare telechelic copolymers.[113,118] The carboxyl functionality can also be added to a polymer chain through a DPE carboxyl derivative, after protection with an oxazoline group or a diisopropylamide. A post-polymerisation deprotection reaction gives the desired carboxy functionalised product.[20,119] Similarly, DPE derivatives have been used to introduce a phenol group at the chain terminus.[120] In order to prepare macromonomers with two phenol polymerisable groups at one chain end, 1,1-bis(4-tert-butyldimethylsiloxyphenyl)ethylene (DPE-OSi) has been used as both initiator or end-capping agent in living anionic polymerisation.[68,73,81,100] The use of functionalised DPE as monomer has also been exploited in studies of monomer sequence control in anionic polymerisation.[103,107-112]

1.4.2.2 Macromonomer synthesis: end-functionalisation of polymers by ATRP

The introduction of a functional moiety selectively at one polymer chain end can be achieved by ATRP essentially in two ways: use of functionalised ATRP initiators and chemical transformations of end-groups.[121]

A functional initiator yields direct α-functionalisation of the polymer, without any post-polymerisation reaction. A wide variety of functionalised ATRP initiators have been reported and recently reviewed by Matyjaszewski and co-workers.[122-123] Some examples are presented in Figure 1.12. Difunctional initiators can also be employed to introduce functionality into the midpoint of a chain. For instance, the use of an initiator with an internal disulfide bond (bottom right species in Figure 1.12) has been studied, with the aim of synthesising degradable polymers. The disulfide bond can degrade under a reducing environment to yield oligopolymeric fragments.[124-125]
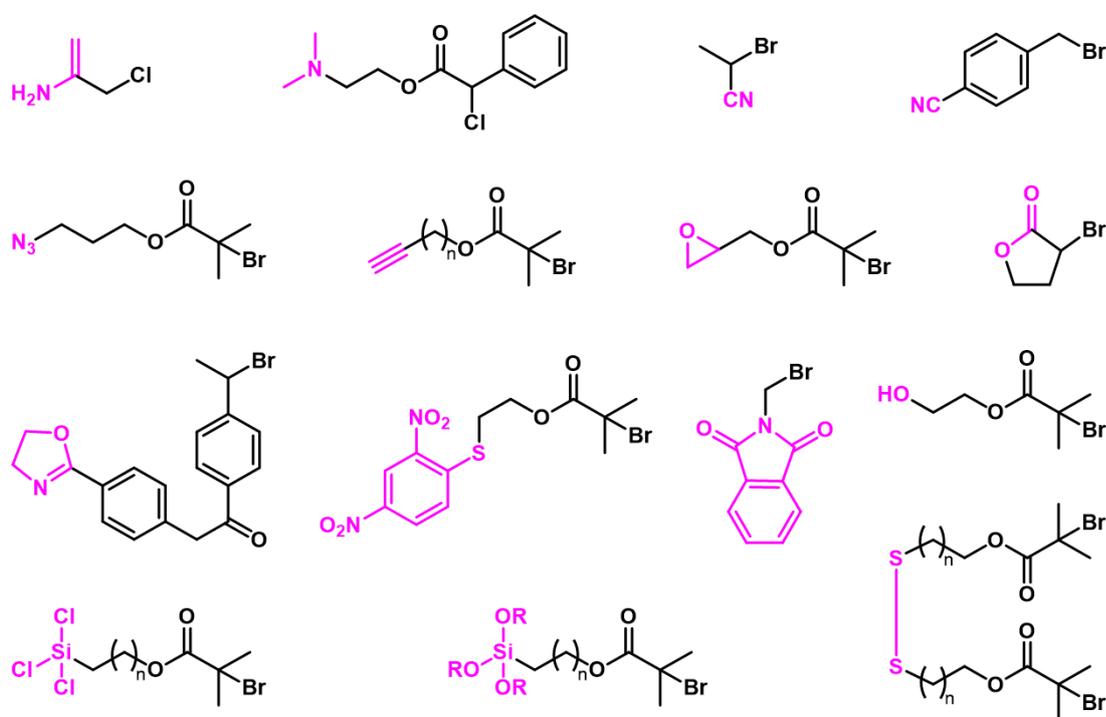
Figure 1.12 Functional alkyl halide ATRP initiators with the functional moiety highlighted in purple.[122]

Theoretically, in an ATRP reaction, provided termination and other side reactions are avoided, the resulting polymer chains are halogen-terminated and can be further used as macroinitiators to propagate a different monomer in the formation of block copolymers. Alternatively, via an end group transformation, α,ω-end-functionalised polymers can be synthesised.

Regardless of the presence or not of a functional group in the α chain position, chemical transformation of the halide end group is the second way to obtain end-functionalised polymers by ATRP. This end-functionality can participate in nucleophilic substitution reactions, to give a plethora of end-functionalised, well-defined polymeric materials, including functionalities which are incompatible with the polymerisation process.[122-123,126] Some examples are reported in Figure 1.13.
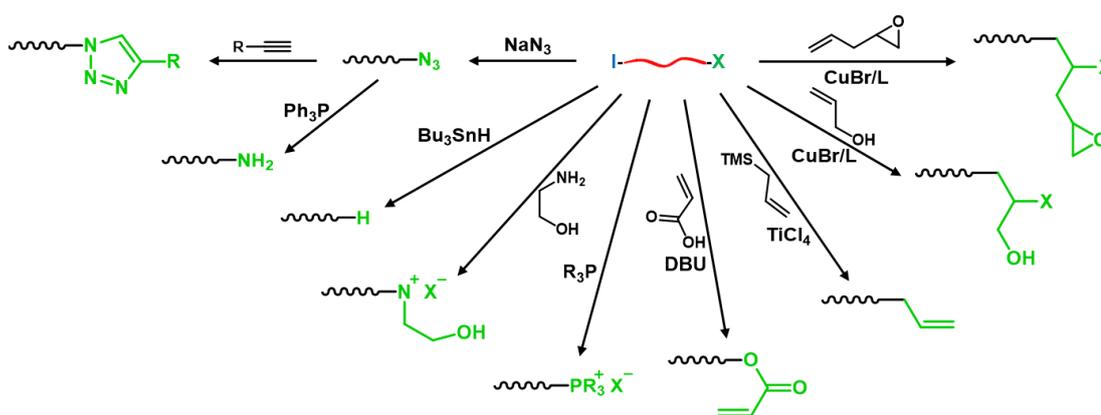
Figure 1.13 Examples of transformations of the halide end group (X) of polymer chains synthesised by ATRP.[122]

Of particular interest is the reaction of halogen-capped polymers with sodium azide to obtain azido-terminated polymers that can be used in click chemistry reactions with acetylene derivatives, to incorporate further functional groups.[122]

1.5   COMPATIBILIZATION OF BLENDS

Among many different potential applications, block copolymers have been tested as compatibilizers for polymer blends. Whilst a blend of two different polymers is highly desirable, because of the great potential to join in one material the properties of each component, usually the blend components are immiscible and interfacial adhesion between the polymer phases is poor, leading to mechanically unstable materials, poor processability, low impact strength and mechanical properties. In an ideal blend, satisfactory properties will critically depend on strong interfacial adhesion and low interfacial tension, to generate small domain sizes and a good dispersion of the two components.

One strategy to achieve this is to use as a compatibilizer linear or graft block copolymers, in which each individual segment is miscible or compatible with each of the blend components. The chosen copolymer will tend to concentrate at the interface (Figure 1.14), often resulting in stabilised morphology with a finer dispersion of the minor phase.
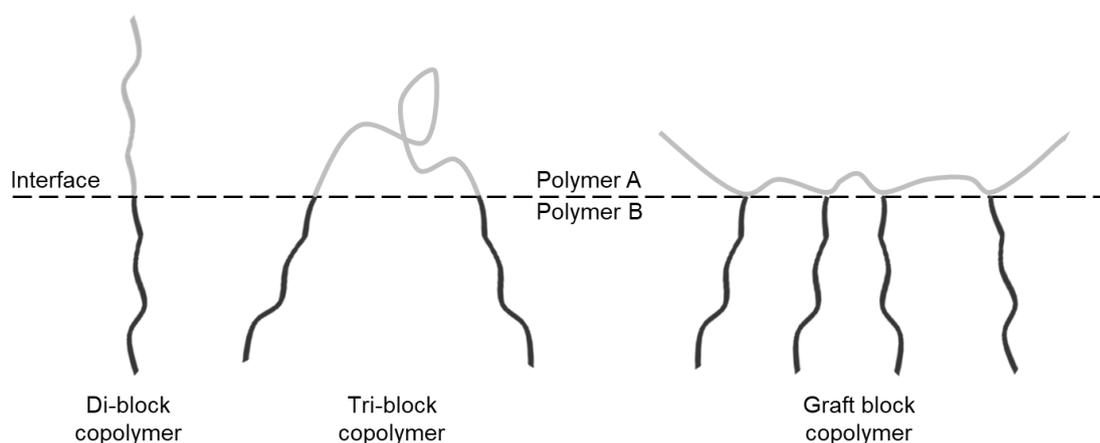
Figure 1.14 Interface behaviour of linear and graft block copolymers, used as compatibilizer in a blend of immiscible polymers.

It has been shown that, segment molecular weights and concentration of the block copolymer added in the blend are essential parameters to have interface segregation and compatibilization. The segments of the block copolymer need to have a minimum molecular weight, otherwise the blocks would not be able to entangle far enough into the respective polymer phase. Moreover, only the amount necessary to form a thin film around the dispersed particles should be added (typical block copolymer concentrations in the blend from 0.5 to 5% are used). Otherwise, the block copolymers tends to form micelles as a further separate phase, enhancing the overall heterogeneity of the blend.[127-128]

The effect of copolymer structure (linear di- or multi-block, graft copolymers) can also impact the effectiveness of the compatibilization and many comparisons have been performed in different blends conditions. The results of the various studies are not always consistent, but in general it has been seen that conformational restraints of the copolymer structure are important to ensure the proper distribution of the different blocks between the two polymers at the interface. On this basis, a linear block copolymer is expected to be superior to a

graft, because its segments would be less restrained. In the case of graft copolymers, multiple branches can restrict the opportunities of the backbone to penetrate its homopolymer phase, even if this, of course, would not preclude adhesion of the backbone to this phase. For the same reasons, di-block copolymers are more effective than tri- and multi-blocks.[128]

1.5.1 COMPATIBILIZED POLYMER BLENDS AS A PROMISING MATERIAL TO OBTAIN POROUS MEMBRANES

The biaxial stretching of thin films comprised of homopolymers or blends of incompatible polymers has been reported for the production of porous membranes.[129-131]

Usually, they are based on semi-crystalline polyolefin materials, including polyethylene (PE),[132] polypropylene (PP)[133] and their blends such as PE–PP[134] and high density polyethylene–ultrahigh molecular weight polyethylene.[135] The method for manufacturing the microporous membranes basically includes an extrusion step to make thin films, and then one or more orientation steps, to impart porosity and increase the tensile strength by stretching.[136]

It has been suggested that the introduction of a compatibilizing copolymer into the blend would improve the blend morphology and the dispersion of the minor component into the major component, thus achieving uniformly distributed micro-craks of relatively uniform dimensions, upon the stretching phase.[137]

1.6 AIMS AND OBJECTIVES

The main objective of this PhD project is the synthesis of complex polymer architectures, namely grafted block copolymers, in which the graft backbone is an aromatic polyester. The long-term potential application is as an additive in the production of porous polyester (especially PET) membranes or films, with improved transport and/or barrier properties.

As explained above, one of the proposed techniques for the production of porous films involves the biaxial stretching of thin films comprised of blends of PET and another incompatible polymer, such as polystyrene, polypropylene or

polyethylene. In order to improve the blend morphology, with a better/controlled dispersion of the minor component, and to achieve a better control on the porosity, many different block copolymers have been proposed as compatibilizer between the incompatible components of blends. In this perspective, given the variety of possible applications of PET-PS blends, the synthesis of PET-PS branched block copolymers is pursued, as a promising strategy towards blend compatibilization.

The specific aims and objectives are;

1.   The synthesis of well-defined polystyrene macromonomers by anionic polymerisation, strictly functionalised at one chain end with a bisphenol moiety. Two different approaches – the initiating and the end-capping approach – will be compared using extensive characterisation, including NMR, size exclusion chromatography, interaction chromatography and MALDI ToF MS, in order to identify chains with different degree of functionalisation (mono-, di- and unfunctionalised).

2.   The synthesis and use of a bisphenol functionalised initiator for anionic polymerisation of PS macromonomers.

3.   The synthesis of well-defined poly(poly(ethylene glycol) methyl ether methacrylate) (PolyPEGMEM) macromonomers by living/controlled polymerisation, strictly functionalised at one end with a bisphenol moiety.

4.   The incorporation of macromonomers (PS and PolyPEGMEM) into a polyester polymer backbone by step-growth polymerisation to yield graft block copolymers. In particular, the synthesis of PEI-*g*-PS copolymers prepared by two different procedures – solution polycondensation and chain coupling – will be investigated.

5.   The preparation and characterisation of PET-PS blends using PEI-*g*-PS copolymers as a blend compatibilizer. The effect of different weight percent of compatibilizer on the PS domain size will be investigated by SEM.

6.   The incorporation of macromonomers - both PS and PolyPEGMEM - into a polysulfone backbone, to prove the versatility of the macromonomer approach to synthesise graft copolymers with a step-growth polymer backbone.

REFERENCES

1. https://en.wiktionary.org/wiki/polymer.
2. McNaught, A.D.; Wilkinson, A., *IUPAC. Compendium of Chemical Terminology, 2nd ed. (the "Gold Book")*. Online version (2019); Blackwell Scientific Publications, Oxford, **1997**.
3. Young, R.J.; Lovell, P.A., *Introduction to Polymers*. 3rd Edition; Taylor and Francis, Boca Raton, **2011**.
4. Flory, P.J., *Journal of the American Chemical Society*, **1937,** *59* (2), 241-253.
5. Hawker, C.J.; Piotti, M.E.*, et al.*, *Nitroxide-Mediated Free Radical Polymerization*, in *Reference Module in Materials Science and Materials Engineering*, Elsevier, **2016**.
6. Braun, D., *International Journal of Polymer Science*, **2009,** *2009*, 893234.
7. Braunecker, W.A.; Matyjaszewski, K., *Progress in Polymer Science*, **2007,** *32* (1), 93-146.
8. https://polymerdatabase.com/polymer%20chemistry/Chain%20Transfer.html.
9. Jenkins Aubrey, D.; Jones Richard, G.*, et al.*, *Pure and Applied Chemistry*, **2009,** *82* (2), 483.
10. Chiefari, J.; Chong, Y.K.*, et al.*, *Macromolecules*, **1998,** *31* (16), 5559-5562.
11. Moad, G.; Rizzardo, E.*, et al.*, *Accounts of Chemical Research*, **2008,** *41* (9), 1133-1142.
12. Nesvadba, P., *Radical Polymerization in Industry*, in *Encyclopedia of Radicals in Chemistry, Biology and Materials*, John Wiley & Sons, Ltd., **2012**.
13. Georges, M.K.; Veregin, R.P.N.*, et al.*, *Macromolecules*, **1993,** *26* (11), 2987-2988.
14. Benoit, D.; Grimaldi, S.*, et al.*, *Journal of the American Chemical Society*, **2000,** *122* (25), 5929-5939.
15. Benoit, D.; Chaplinski, V.*, et al.*, *Journal of the American Chemical Society*, **1999,** *121* (16), 3904-3920.
16. Matyjaszewski, K., *Macromolecules*, **2012,** *45* (10), 4015-4039.
17. Matyjaszewski, K.; Xia, J., *Chemical Reviews*, **2001,** *101* (9), 2921-2990.
18. Kato, M.; Kamigaito, M.*, et al.*, *Macromolecules*, **1995,** *28* (5), 1721-1723.
19. Wang, J.-S.; Matyjaszewski, K., *Journal of the American Chemical Society*, **1995,** *117* (20), 5614-5615.
20. Hsieh, H., Quirk, R. P., *Anionic Polymerization: Principles and Practical Applications*. Marcel Dekker, Inc., **1996**.
21. Szwarc, M.; Levy, M.*, et al.*, *Journal of the American Chemical Society*, **1956,** *78* (11), 2656-2657.
22. Aoshima, S.; Kanaoka, S., *Chemical Reviews*, **2009,** *109* (11), 5245-5287.
23. Bielawski, C.W.; Grubbs, R.H., *Progress in Polymer Science*, **2007,** *32* (1), 1-29.
24. Hirao, A.; Goseki, R.*, et al.*, *Macromolecules*, **2014,** *47* (6), 1883-1905.
25. Baskaran, D., *Progress in Polymer Science*, **2003,** *28* (4), 521-581.
26. Reich, H.J., *Chemical Reviews*, **2013,** *113* (9), 7130-7178.
27. Flory, P.J., *Journal of the American Chemical Society*, **1939,** *61* (12), 3334-3340.
28. Saunders, J.H.; Dobinson, F., *Chapter 7 The Kinetics of Polycondensation Reactions*, in *Comprehensive Chemical Kinetics*, Elsevier, **1976**; Vol. 15, pp 473-581.
29. Lutz, J.-F., *Polymer Chemistry*, **2010,** *1* (1), 55-62.
30. Ueda, M., *Progress in Polymer Science*, **1999,** *24* (5), 699-730.
31. Zhang, M.; Moore, R.B.*, et al.*, *Journal of Polymer Science Part A: Polymer Chemistry*, **2012,** *50* (18), 3710-3718.

32.   McKee, M.G.; Unal, S.*, et al.*, *Progress in Polymer Science*, **2005,** *30* (5), 507-539.
33.   Rowan, S.J.; Barner-Kowollik, C.*, et al.*, *ACS Macro Letters*, **2016,** *5* (1), 1-3.
34.   Polymeropoulos, G.; Zapsas, G.*, et al.*, *Macromolecules*, **2017,** *50* (4), 1253-1290.
35.   Ren, J.M.; McKenzie, T.G.*, et al.*, *Chemical Reviews*, **2016,** *116* (12), 6743-6836.
36.   Zheng, Y.; Li, S.*, et al.*, *Chemical Society Reviews*, **2015,** *44* (12), 4091-4130.
37.   Feng, C.; Li, Y.*, et al.*, *Chemical Society Reviews*, **2011,** *40* (3), 1282-1295.
38.   Grubbs, R.B.; Hawker, C.J.*, et al.*, *Angewandte Chemie International Edition in English*, **1997,** *36* (3), 270-272.
39.   Beers, K.L.; Gaynor, S.G.*, et al.*, *Macromolecules*, **1998,** *31* (26), 9413-9415.
40.   Börner, H.G.; Beers, K.*, et al.*, *Macromolecules*, **2001,** *34* (13), 4375-4383.
41.   Zhang, Y.; Shen, Z.*, et al.*, *Macromolecules*, **2010,** *43* (1), 117-125.
42.   Lee, H.-i.; Matyjaszewski, K.*, et al.*, *Macromolecules*, **2008,** *41* (16), 6073-6080.
43.   Hadjichristidis, N.; Pitsikalis, M.*, et al.*, *Chemical Reviews*, **2001,** *101* (12), 3747-3792.
44.   Gao, H.; Matyjaszewski, K., *Journal of the American Chemical Society*, **2007,** *129* (20), 6633-6639.
45.   Engler, A.C.; Lee, H.-i.*, et al.*, *Angewandte Chemie International Edition*, **2009,** *48* (49), 9334-9338.
46.   Fu, Q.; Lin, W.*, et al.*, *Macromolecules*, **2008,** *41* (7), 2381-2387.
47.   Lowe, A.B., *Polymer Chemistry*, **2010,** *1* (1), 17-36.
48.   Durmaz, Y.Y.; Kumbaraci, V.*, et al.*, *Macromolecules*, **2009,** *42* (11), 3743-3749.
49.   Schulz, G.O.; Milkovich, R., *Journal of Applied Polymer Science*, **1982,** *27* (12), 4773-4786.
50.   Milkovich, R.; Chiang, M., US3786116A, **1972.**
51.   Xia, Y.; Kornfield, J.A.*, et al.*, *Macromolecules*, **2009,** *42* (11), 3761-3766.
52.   Li, Z.; Zhang, K.*, et al.*, *Journal of Polymer Science Part A: Polymer Chemistry*, **2009,** *47* (20), 5557-5563.
53.   Weber, C.; Becer, C.R.*, et al.*, *Macromolecules*, **2009,** *42* (8), 2965-2971.
54.   Gu, L.; Shen, Z.*, et al.*, *Macromolecules*, **2007,** *40* (13), 4486-4493.
55.   Christodoulou, S.; Iatrou, H.*, et al.*, *Journal of Polymer Science Part A: Polymer Chemistry*, **2005,** *43* (18), 4030-4039.
56.   Konkolewicz, D.; Monteiro, M.J.*, et al.*, *Macromolecules*, **2011,** *44* (18), 7067-7087.
57.   Trollsås, M.; Atthoff, B.*, et al.*, *Macromolecules*, **1998,** *31* (11), 3439-3445.
58.   Trollsås, M.; Hedrick, J.L., *Macromolecules*, **1998,** *31* (13), 4390-4395.
59.   Jikei, M.; Terata, C.*, et al.*, *Materials Today Communications*, **2019,** *20*, 100528.
60.   Jikei, M.; Suzuki, M.*, et al.*, *Macromolecules*, **2012,** *45* (20), 8237-8244.
61.   Jikei, M.; Uchida, D.*, et al.*, *Journal of Polymer Science Part A: Polymer Chemistry*, **2014,** *52* (13), 1825-1831.
62.   Kong, L.-Z.; Sun, M.*, et al.*, *Journal of Polymer Science Part A: Polymer Chemistry*, **2010,** *48* (2), 454-462.
63.   He, C.; Li, L.-W.*, et al.*, *Macromolecules*, **2011,** *44* (16), 6233-6236.
64.   Li, L.; He, C.*, et al.*, *Macromolecules*, **2011,** *44* (20), 8195-8206.
65.   Hilf, S.; Wurm, F.*, et al.*, *Journal of Polymer Science Part A: Polymer Chemistry*, **2009,** *47* (24), 6932-6940.
66.   Wurm, F.; López-Villanueva, F.-J.*, et al.*, *Macromolecular Chemistry and Physics*, **2008,** *209* (7), 675-684.
67.   Schmidt, B.V.K.J.; Hetzer, M.*, et al.*, *Progress in Polymer Science*, **2014,** *39* (1), 235-249.
68.   Agostini, S.; Hutchings, L.R., *European Polymer Journal*, **2013,** *49* (9), 2769-2784.

69. Hutchings, L.R.; Roberts-Bleming, S.J., *Macromolecules*, **2006,** *39* (6), 2144-2152.

70. Kimani, S.M.; Hutchings, L.R., *Macromolecular Rapid Communications*, **2008,** *29* (8), 633-637.

71. Hutchings, L.R.; Dodds, J.M.*, et al.*, *Macromolecules*, **2005,** *38* (14), 5970-5980.

72. Dodds, J.M.; De Luca, E.*, et al.*, *Journal of Polymer Science Part B: Polymer Physics*, **2007,** *45* (19), 2762-2769.

73. Clarke, N.; Luca, E.D.*, et al.*, *European Polymer Journal*, **2008,** *44* (3), 665-676.

74. Dodds, J.M.; Hutchings, L.R., *Macromolecular Symposia*, **2010,** *291-292* (1), 26-35.

75. Hutchings, L.R.; Dodds, J.M.*, et al.*, *Macromolecular Symposia*, **2006,** *240* (1), 56-67.

76. Hutchings, L.R.; Dodds, J.M.*, et al.*, *Macromolecules*, **2009,** *42* (22), 8675-8687.

77. Hutchings, L.R.; Agostini, S.*, et al.*, *Macromolecules*, **2015,** *48* (24), 8806-8822.

78. Heitz, T.; Höcker, H., *Die Makromolekulare Chemie*, **1988,** *189* (4), 777-789.

79. Yamamoto, M.; Uchimura, N.*, et al.*, *Designed Monomers & Polymers*, **2010,** *13* (5), 445-458.

80. Nießner, N.; Heitz, W., *Die Makromolekulare Chemie*, **1990,** *191* (6), 1463-1475.

81. Quirk, R.P.; Wang, Y., *Polymer International*, **1993,** *31* (1), 51-59.

82. Okamoto, M., *Journal of Applied Polymer Science*, **2001,** *80* (14), 2670-2675.

83. Yamashita, Y.; Chujo, Y.*, et al.*, *Polymer Bulletin*, **1981,** *5* (7), 361-366.

84. Sugi, R.; Tate, D.*, et al.*, *Journal of Polymer Science Part A: Polymer Chemistry*, **2013,** *51* (12), 2725-2729.

85. Nagase, Y.; Mori, S.*, et al.*, *Die Makromolekulare Chemie*, **1990,** *191* (10), 2413-2421.

86. Quirk, R.P.; Yin, J., *Journal of Polymer Science Part A: Polymer Chemistry*, **1992,** *30* (11), 2349-2355.

87. Quirk, R.P.; Yin, J.*, et al.*, *Macromolecules*, **1989,** *22* (1), 85-90.

88. Tonhauser, C.; Frey, H., *Macromolecular Rapid Communications*, **2010,** *31* (22), 1938-1947.

89. Quirk, R.P.; Ma, J.-J., *Journal of Polymer Science Part A: Polymer Chemistry*, **1988,** *26* (8), 2031-2037.

90. Ueda, K.; Hirao, A.*, et al.*, *Macromolecules*, **1990,** *23* (4), 939-945.

91. Quirk, R.P.; Lee, Y., *Journal of Polymer Science Part A: Polymer Chemistry*, **2000,** *38* (1), 145-151.

92. Ganß, M.; Satapathy, B.K.*, et al.*, *European Polymer Journal*, **2009,** *45* (9), 2549-2563.

93. Quirk, R.P.; Kim, J., *Macromolecules*, **1991,** *24* (16), 4515-4522.

94. Elkins, C.L.; Viswanathan, K.*, et al.*, *Macromolecules*, **2006,** *39* (9), 3132-3139.

95. Hwang, J.; Foster, M.D.*, et al.*, *Polymer*, **2004,** *45* (3), 873-880.

96. Gauthier, M.; Tichagwa, L.*, et al.*, *Macromolecules*, **1996,** *29* (2), 519-527.

97. Búcsi, A.; Forcada, J.*, et al.*, *Macromolecules*, **1998,** *31* (7), 2087-2097.

98. Schulz, D.N.; Halasa, A.F., *Journal of Polymer Science: Polymer Chemistry Edition*, **1977,** *15* (10), 2401-2410.

99. Pispas, S.; Hadjichristidis, N., *Macromolecules*, **1994,** *27* (7), 1891-1896.

100. Quirk, R.P.; Yoo, T.*, et al.*, *Applications of 1,1-Diphenylethylene Chemistry in Anionic Synthesis of Polymers with Controlled Structures*, in *Biopolymers · PVA Hydrogels, Anionic Polymerisation Nanocomposites*, Springer, Berlin, **2000.**pp 67-162.

101. Moon, B.; Hoye, T.R.*, et al.*, *Journal of Polymer Science Part A: Polymer Chemistry*, **2000,** *38* (12), 2177-2185.

102. Jeon, H.K.; Macosko, C.W.*, et al.*, *Macromolecules*, **2004,** *37* (7), 2563-2571.

103. Hutchings, L.R.; Brooks, P.P.*, et al.*, *Macromolecules*, **2015,** *48* (3), 610-628.
104. Quirk, R.P.; Garcés, C.*, et al.*, *Polymer*, **2012,** *53* (11), 2162-2167.
105. Fan, X.; Zhou, Q.*, et al.*, *Langmuir*, **2002,** *18* (11), 4511-4518.
106. Quirk, R.P.; Mathers, R.T.*, et al.*, *Macromolecules*, **2002,** *35* (27), 9964-9974.
107. Brooks, P.P.; Natalello, A.*, et al.*, *Macromolecular Symposia*, **2013,** *323* (1), 42-50.
108. Natalello, A.; Hall, J.N.*, et al.*, *Macromolecular Rapid Communications*, **2011,** *32* (2), 233-237.
109. Liu, P.; Ma, H.*, et al.*, *Polymer*, **2016,** *97*, 167-173.
110. Liu, P.; Ma, H.*, et al.*, *Polymer Chemistry*, **2017,** *8* (11), 1778-1789.
111. Natalello, A.; Werre, M.*, et al.*, *Macromolecules*, **2013,** *46* (21), 8467-8471.
112. Ma, H.; Han, L.*, et al.*, *Macromolecular Chemistry and Physics*, **2017,** *218* (12).
113. Quirk, R.P.; Zhu, L.-F., *British Polymer Journal*, **1990,** *23* (1-2), 47-54.
114. Quirk, R.P.; Lynch, T., *Macromolecules*, **1993,** *26* (6), 1206-1212.
115. Pispas, S.; Hadjichristidis, N., *Journal of Polymer Science Part A: Polymer Chemistry*, **2000,** *38* (20), 3791-3801.
116. Wu, L.; Wang, Y.*, et al.*, *Polymer*, **2013,** *54* (12), 2958-2965.
117. Hirao, A.; Karasawa, Y.*, et al.*, *Designed Monomers and Polymers*, **2004,** *7* (6), 647-660.
118. Hayashi, M., *Macromolecular Symposia*, **2004,** *215* (1), 29-40.
119. Summers, G.J.; Quirk, R.P., *Journal of Polymer Science Part A: Polymer Chemistry*, **1998,** *36* (8), 1233-1241.
120. Quirk, R.P.; Zhu, L.-f., *Die Makromolekulare Chemie*, **1989,** *190* (3), 487-493.
121. https://www.cmu.edu/maty/index.html.
122. Matyjaszewski, K.; Tsarevsky, N.V., *Nature Chemistry*, **2009,** *1* (4), 276-288.
123. Coessens, V.; Pintauer, T.*, et al.*, *Progress in Polymer Science*, **2001,** *26* (3), 337-377.
124. Tsarevsky, N.V.; Matyjaszewski, K., *Macromolecules*, **2002,** *35* (24), 9009-9014.
125. Tsarevsky, N.V.; Matyjaszewski, K., *Macromolecules*, **2005,** *38* (8), 3087-3092.
126. Anastasaki, A.; Willenbacher, J.*, et al.*, *Polymer Chemistry*, **2017,** *8* (4), 689-697.
127. Pospiech, D., *Influencing the Interface in Polymer Blends by Compatibilization with Block Copolymers*, in *Polymer Surfaces and Interfaces: Characterization, Modification and Applications*, Springer, Berlin, **2008**.pp 275-298.
128. Anastasiadis, S.H., *Interfacial Tension in Binary Polymer Blends and the Effects of Copolymers as Emulsifying Agents*, in *Polymer Thermodynamics: Liquid Polymer-Containing Mixtures*, Springer, Berlin, **2011**.pp 179-269.
129. Druin, M.; Loft, J.*, et al.*, US3801404, **1972**.
130. Bierenbaum, H.S.; Daley, L.R.*, et al.*, US3843761, **1974**.
131. Brazinsky, I.; Cooper, W.M.*, et al.*, US4138459, **1975**.
132. Kaimai, N.; Takita, K.*, et al.*, US6153133, **1998**.
133. Lee, S.Y.; Ahn, B.I.*, et al.*, US6830849, **2001**.
134. Sogo, H., US5641565, **1994**.
135. Ihm, D.; Noh, J.*, et al.*, *Journal of Power Sources*, **2002,** *109* (2), 388-393.
136. Zhang, S.S., *Journal of Power Sources*, **2007,** *164* (1), 351-364.
137. Chandavasu, C.; Xanthos, M.*, et al.*, US6824680, **2001**.

CHAPTER 2

SYNTHESIS OF BISPHENOL FUNCTIONALISED POLYSTYRENE MACROMONOMERS BY ANIONIC POLYMERISATION

2.1 INTRODUCTION

The 'macromonomer' approach has become widely adopted as a route to make a variety of complex branched polymers with high compositional and molecular homogeneity. In this project, linear macromonomers were synthesised by living/controlled polymerisation mechanisms, with a bisphenol functional group at one chain end, to allow reaction of the macromonomer in a subsequent step-growth polycondensation, leading to the construction of graft block copolymers.
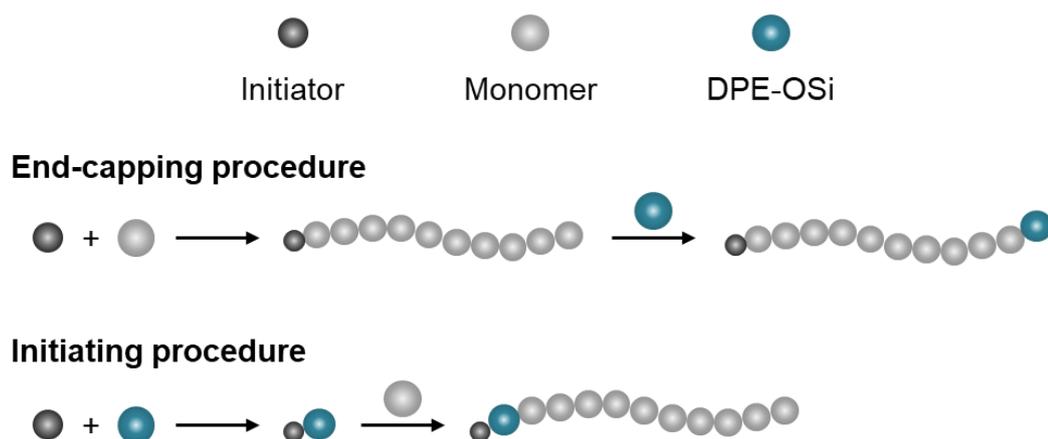
Figure 2.1 General mechanism for end-capping and initiating procedures to functionalise polymers by anionic polymerisation.

In this Chapter, polystyrene macromonomers were synthesised by living anionic polymerisation (LAP). As discussed in Chapter 1, various protected

functionalised DPE species have been used to produce end-functionalised macromonomers using LAP and the DPE can be added either as an end-capping agent, before the termination of the polymer,[1-3] or, following reaction of the DPE with butyllithium, the adduct can be used to initiate the polymerisation (see Figure 2.1).

Previous studies have reported that the end-capping strategy is practically quantitative,[1-5] and that the steric bulk of DPE prevents it from self-propagation.[4,6-7] Moreover, the reaction of DPE (and derivatives) with butyllithium has proved to provide an effective initiator for LAP.[6,8] However, there are potential problems associated with each approach, especially if the objective is to produce chains with 100% end-functionalisation and with accurate control over the number of functional DPE moieties per chain.

In this Chapter, the results of a systematic comparison of the relative effectiveness of the two approaches, with the aim to evaluate which approach is best able to produce mono-end-functionalised polymer chains using functionalised DPE derivatives, is reported.[9] For this purpose, polystyrene was synthesised *via* LAP and functionalised with 1,1-bis(4-*tert*-butyl dimethylsiloxyphenyl)ethylene (DPE-OSi) via both the initiating and the end-capping procedures. A combination of NMR, SEC, MALDI ToF mass spectrometry and Normal-Phase Isothermal Interaction Chromatography (NP-IIC) analysis was used to characterise the resulting polymers with a view to calculating the average degree of functionalisation and to go further and identify the presence of chains with different numbers of DPE units.

Temperature Gradient (TGIC) or Isothermal Interaction Chromatography is a valuable, but rarely used, characterisation technique for polymers. In particular, normal phase (NP) IC allows the resolution of polymers in terms of functionality and molecular weight. NP-IIC was therefore chosen to complete the characterisation of the macromonomers described in this Chapter, and to fulfil the comparison between the two functionalisation procedures.

Although the functionalised DPE-OSi 'monomer' is incapable of self-propagation, it is able to copolymerise with styrene[7,10] and this can result in the introduction of more than one DPE-OSi unit per chain – especially when using the initiating

procedure (Figure 2.1). The use of a functionalised initiator as an alternative approach to synthesise well-defined end-functionalised macromonomers (see Section 1.4.1.1) was also investigated. Such a functionalised species should be capable of initiation, but unable to participate in propagation, i.e. it cannot behave as a monomer, as DPE does, thus preventing any possibility of having more than one functional moiety into the chain. To this end, a bisphenol-derivative of diphenylmethylpotassium (DPMK) – a well-known initiator most frequently used for the polymerisation of ethylene oxide - was synthesised from bisphenol F (BPF) and investigated as a functionalised initiator for polystyrene (PS) macromonomers.

2.2 EXPERIMENTAL

2.2.1 MATERIALS

Benzene (Aldrich, HPLC grade, ≥99%), cyclohexane (Sigma-Aldrich, ≥99%) and styrene (Sigma-Aldrich, ≥99%) were dried and degassed over calcium hydride (CaH_2) (Acros Organics, 93%) and stored under high vacuum. Tetrahydrofuran (THF) (in-house solvent purification) was dried over sodium wire (Aldrich, 99.9%) and benzophenone (Aldrich, 99%), and degassed using freeze-thaw techniques. *sec*-Butyllithium (*sec*-BuLi, 1.4 M solution in cyclohexane), *N,N,N',N'*-tetramethylethylenediamine (TMEDA), cesium carbonate (all Sigma-Aldrich), were used as received. Methanol (AR grade) and hydrochloric acid (37 wt.%), (both Fischer Scientific) were used as received. *N,N*-dimethylacetamide (DMAc, 99.5%, Extra Dry, AcroSeal™, ACROS Organics) was used as received. Naphthalene and potassium chunks (both Sigma-Aldrich) were used as received. 4,4'-Dihydroxydiphenylmethane (bisphenol F, (BPF)) (Tokyo Chemical Industry) was used as received. Dimethyl formamide (DMF) (Sigma-Aldrich, 99.8%) was stored over molecular sieves (Sigma-Aldrich) under an inert atmosphere. Dimethylacetamide, (DMAc, Acros Organics, 99.5%, Extra Dry) was used as received.

1,1-Bis(4-*tert*-butyldimethyl siloxyphenyl)ethylene (DPE-OSi) was synthesised in two steps from dihydroxybenzophenone (Sigma-Aldrich, 99%) according to the procedure of Quirk and Wang.[11] Yield 65%

^{1}H NMR (400 MHz, CDCl$_3$, δ): 7.23 (4H, d, *J*=2.2 Hz, Ar H), 7.81 (4H, d, *J*=2.2 Hz, Ar H), 5.31 (2H, s, =CH$_2$), 1.02 (18H, s, (CH$_3$)$_3$C-Si), 0.24 (12H, s, (CH$_3$)$_2$Si).

1,1-Bis(4-t-butyldimethylsiloxyphenyl)methane was synthesised by protection of BPF hydroxyl groups with *t*-butyldimethylsilyl chloride (Sigma-Aldrich, 97%) according to the procedure of Quirk and Wang.[11] Yield 87%

^{1}H NMR (400 MHz, CDCl$_3$, δ): 7.09 (4H, d, *J*=2.1 Hz, Ar H), 6.83 (4H, d, *J*=2.1 Hz, Ar H), 3.91 (2H, s, -CH$_2$-), 1.06 (18H, s, (CH$_3$)$_3$C-Si), 0.26 (12H, s, (CH$_3$)$_2$Si).

2.2.2 CHARACTERISATION

^{1}H NMR spectra were measured on a Bruker DRX-400 MHz spectrometer and on a Varian VNMRS-700 spectrometer, using CDCl$_3$ as solvent.

Triple detection size exclusion chromatography (SEC) with refractive index (RI), viscosity, and right angle light scattering (RALS) detectors was used for the analysis of molar mass and molar mass distribution of the macromonomers, using a Viscotek TDA 302. THF was used as the eluent, at a flow rate of 1.0 ml·min^{-1} and at a temperature of 35°C. Separation was achieved using 2×300 mm PLgel 5 µm mixed C-columns. A value of 0.185 ml·g^{-1} was used as the dn/dc of polystyrene, while a value of 0.124 ml·g^{-1} (measured in house) was used as the dn/dc of polybutadiene for the analysis of prepared mikto-star polymers.

MALDI ToF MS analysis was carried out on an Autoflex II TOF/TOF mass spectrometer (Bruker Daltonik GmBH) equipped with a 337 nm nitrogen laser. A linear mode of analysis was used typically above *m/z* 5,000. Samples were dissolved in THF or chloroform (~1 mg·ml^{-1}) and mixed with a matrix solution (dithranol or trans-2-[3-(4-*tert*-butylphenyl)-2-methyl-2-propenylidene]

malononitrile, ~20 mg·ml^{-1}). 1 μl of this mixture was spotted on to a metal target and placed into the MALDI ion source. Ag$^+$ was used as dopant.

Isothermal interaction chromatography analysis was performed under normal phase conditions using a diol modified silica column (Nucleosil 100 Å pore, 250×4.6 mm I.D., 5 μm). A mixture of THF/isooctane (Fisher, GPC and HPLC grade respectively) was used in a ratio 45/55 (v/v) with a flow rate of 0.5 ml·min^{-1}. The temperature was maintained at 15°C using a ThermoScientific circulating bath and thermostat. Samples were prepared with a concentration of 2.5 mg·ml^{-1} in the eluent mixture and the injection volume was 100 μl. The analysis was performed using a modified Viscotek TDA 301, mainly using the RALS detector and a Viscotek UV2600 detector, set to a wavelength of 260 nm. For the calculation of the molecular weight by NP-IIC, the dn/dc utilised was 0.1 ml·g^{-1}, previously determined in house. The calibration was achieved using a narrow dispersity PS standard (66 kg·mol^{-1}).

2.2.3 SYNTHESIS OF 1,1-BIS(4-*t*-BUTYLDIMETHYLSILOXYPHENYL) METHYL POTASSIUM - BPFK

The synthesis of 1,1-bis(4-*t*-butyldimethylsiloxyphenyl) methyl potassium (BPFK) was adapted from the procedure already described in literature for diphenyl methane (DPMK).[12]

A 50 ml reaction flask was initially put under vacuum to remove air and backfilled with dry nitrogen. Naphthalene (0.41 g, 3.2 mmol) was added to the reaction flask against a continuous flow of nitrogen. After sealing the flask, 9 ml of dry THF was injected via a rubber septum and stirred until complete dissolution of naphthalene. Potassium chunks (0.32 g, 8.1 mmol) were added against a continuous flow of N$_2$, before the flask was sealed and stirred for 20 hours at room temperature. 1,1-Bis(4-t-butyldimethylsiloxyphenyl)methane (3.04 g, 7.1 mmol) was dissolved in 9 ml of dry cyclohexane and the solution injected into the reaction flask and vigorously stirred for 5 days at room temperature (after the first day the solution turned from a dark green colour to a deep red). Finally, the solution was stored in the fridge under an inert atmosphere of N$_2$.

2.2.3.1   Calculation of BPFK concentration by synthesis of BPFK initiated PS

In order to determine the concentration of BPFK initiator solution, benzene (~50 ml) and styrene (2.22 g, 21 mmol) were distilled under vacuum into the reaction flask, then a known volume of the synthesised BPFK initiator solution (5000 µl) was injected through a septum. The reaction was stirred at room temperature for 3 hours, then terminated with nitrogen-sparged methanol. The polymer was precipitated into methanol, re-dissolved in THF, precipitated again into methanol, recovered by filtration and then dried under vacuum. Yield 97%

M_n 32,800 g·mol^{-1}, M_w 36,600 g·mol^{-1}, Đ 1.12.

^{1}H NMR (400 MHz, CDCl$_3$, δ): 7.4 – 6.2 (Ar $\underline{H}$), 2.4 – 1.2 (aliphatic $\underline{H}$), 1.1 – 0.9 (18H, (C$\underline{H_3}$)$_3$C-Si), 0.3 – 0.1 (12H, (C$\underline{H_3}$)$_2$Si).

BPFK calculated concentration 0.14M.

2.2.4   SYNTHESIS OF POLYSTYRENE MACROMONOMERS BY LAP

The synthesis of polystyrene macromonomers by LAP was performed using standard high vacuum techniques.

2.2.4.1   Synthesis of polystyrene macromonomer via 'initiating procedure'
          (iPS-OSi)

In a typical reaction and for a target molar mass of 10,000 g·mol^{-1}, DPE-OSi (0.26 g, 0.6 mmol) was added to the reaction vessel, sealed and evacuated overnight, then azeotropically dried through the addition by distillation and subsequent removal by distillation of ~20 ml of dry benzene (3 times). Finally, ~50 ml of fresh benzene was distilled into the reactor to dissolve the DPE-OSi. *sec*-BuLi was added drop wise to the DPE-OSi solution, to titrate out any residual impurities, until the red colour of living DPE-OSi persisted. The required amount of *sec*-BuLi (430 µl, 0.6 mmol) to initiate the polymerisation was then injected, allowed to react for 4 hours, followed by the addition of styrene (5.74 g, 55.1 mmol). The propagation was allowed to proceed for 4 hours at room

temperature, before the reaction was terminated with nitrogen-sparged methanol. The polymer was recovered by precipitation into excess methanol, re-dissolved in THF, precipitated again into methanol, collected by filtration and dried to constant mass under vacuum. Yield 92%

M_n 12,000 g·mol^{-1}, M_w 12,500 g·mol^{-1}, Đ 1.04.

^{1}H NMR (400 MHz, CDCl$_3$, δ): 7.4 – 6.3 (Ar $\underline{H}$), 2.3 – 1.2 (aliphatic $\underline{H}$), 1.1 - 0.9 (18H, (C$\underline{H}_3$)$_3$C-Si), 0.8 – 0.4 (3H, C$\underline{H}_3$CH$_2$), 0.8 – 0.4 (3H, CHC$\underline{H}_3$), 0.3 – 0.1 (12H, (C$\underline{H}_3$)$_2$Si).

A second polymerisation reaction was carried out to establish the reproducibility of the procedure, with the amount of reagents, the yield, the molar mass and the molar mass distribution data reported in Table 2.2 and 2.3.

2.2.4.2   Synthesis of polystyrene macromonomer via 'end-capping procedure' (ePS-OSi)

In a typical reaction and for a target molar mass of 10,000 g·mol^{-1}, benzene (~50 ml) and styrene (6.44 g, 62 mmol) were distilled under vacuum into the reaction flask, then *sec*-BuLi (460 μl, 0.6 mmol) was injected through a septum. The reaction was stirred at room temperature for 3 hours before the addition of a purified solution of DPE-OSi (0.44 g, 1.0 mmol) in benzene. The purified solution of DPE-OSi was prepared by azeotropically drying the desired amount of DPE-OSi 3 times with dry benzene and then dissolving the DPE-OSi into ~5 ml of freshly distilled benzene. To this solution, TMEDA was added in a molar ratio of 1: 1 with respect to the initiator. *sec*-BuLi was added drop wise to titrate out any residual impurities until the red colour of living DPE-OSi persisted. The end-capping reaction between the living polymer chain and DPE-OSi was stirred at room temperature for 5 days and then terminated with nitrogen-sparged methanol. The polymer was precipitated into methanol, redissolved in THF, precipitated again into methanol, recovered by filtration and then dried under vacuum. Yield 91%

M_n 11,300 g·mol^{-1}, M_w 11,900 g·mol^{-1}, Đ 1.05.

^{1}H NMR (400 MHz, CDCl$_3$, δ): 7.4 – 6.3 (Ar $\underline{H}$), 3.5 – 3.4 (1H, $\underline{H}$C(Ph)$_2$), 2.3 - 1.2 (aliphatic $\underline{H}$), 1.1 – 0.9 (18H, (C$\underline{H}_3$)$_3$C-Si), 0.8–0.4 (3H, C$\underline{H}_3$CH$_2$), 0.8 - 0.4 (3H, CHC$\underline{H}_3$), 0.3–0.1 (12H, (C$\underline{H}_3$)$_2$Si).

One more replicated polymerisation was carried out for reproducibility of the procedure, with the amount of reagents, the yield, the molar mass and the molar mass distribution data are summarised in Table 2.2 and 2.3.

The same procedure, namely the end-capping procedure, was followed to synthesise all of the PS macromonomers (ePS2.9k, ePS6.4k, ePS9.1k, ePS6.2k in Section 2.3.2) used in this study. Their use in various polycondensation reactions will be discussed in the following Chapters. The amount of reagents for ePS2.9k, ePS6.4k, ePS9.1k, ePS6.2k are summarised in Table 2.1, while the yields and SEC data are reported in Table 2.5.

Table 2.1 Quantity of reagents in mmol used in the scale-up synthesis of end-capped polystyrene macromonomers.

	DPE-OSi	Sty	*sec*-BuLi	TMEDA
ePS2.9k	20	192	10	10
ePS6.4k	20	473	9.8	10
ePS9.1k	0.4	24	0.2	0.2
ePS6.2k	40	960	20	20

2.2.4.3   Deprotection of iPS-OSi to yield iPS-OH

The protected iPS-OSi1 (4.14 g, 0.52 mmol) was dissolved in THF (10% w/v solution) and HCl$_{aq}$ (1.1 ml, 11 mmol) was added dropwise. The solution was stirred at reflux overnight. Finally, the solution was cooled and the polymer recovered by precipitation into methanol, re-dissolved in THF, precipitated again into methanol, recovered by filtration and then dried under vacuum. Yield 97%

^{1}H NMR (400 MHz, CDCl$_3$, δ): 7.4 – 6.3 (Ar $\underline{H}$), 4.7 – 4.4 (2H, $\underline{H}$OPh), 2.3 - 1.2 (aliphatic $\underline{H}$), 0.8–0.4 (3H, C$\underline{H}_3$CH$_2$), 0.8 – 0.4 (3H, CHC$\underline{H}_3$).

2.2.4.4 Deprotection of ePS-OSi to yield ePS-OH

ePS-OSi2 (6.30 g, 0.56 mmol) was deprotected using HCl_{aq} (1.1 ml, 11 mmol) according to the procedure described above for iPS-OSi. Yield 97%

^{1}H NMR (400 MHz, $CDCl_3$, δ): 7.4 – 6.3 (Ar $\underline{H}$), 4.6 – 4.4 (2H, $\underline{H}$OPh), 3.5 - 3.4 (1H, $\underline{H}$C(Ph)$_2$), 2.3 – 1.2 (aliphatic $\underline{H}$), 0.8–0.4 (3H, C$\underline{H}_3$CH$_2$), 0.8 – 0.4 (3H, CHC$\underline{H}_3$).

2.2.4.5 Synthesis of bisphenol F end-functionalised polystyrene (BPF-PS-OSi) initiated by BPFK

In a typical reaction and for a target molar mass of 10,000 g·mol^{-1}, benzene (~20 ml) and styrene (1.54 g, 14.8 mmol) were distilled under vacuum into the reaction flask. BPFK initiator solution in cyclohexane (1.1 ml, 0.15 mmol) was then injected through a rubber septum. The reaction was stirred at room temperature for 3 hours, then terminated with nitrogen-sparged methanol. The polymer was precipitated into methanol, redissolved in THF, precipitated again into methanol, recovered by filtration and then dried under vacuum. Yield 77%.

M_n 15,800 g·mol^{-1}, M_w 17,700 g·mol^{-1}, Đ 1.12.

^{1}H NMR (400 MHz, $CDCl_3$, δ): 7.4 – 6.2 (Ar $\underline{H}$), 2.4 – 1.2 (aliphatic $\underline{H}$), 1.1 - 0.9 (18H, (C$\underline{H}_3$)$_3$C-Si), 0.3 – 0.1 (12H, (C$\underline{H}_3$)$_2$Si).

2.2.4.6 Deprotection of BPF-PS-OSi to yield BPF-PS-OH

BPF-PS-OSi (1.01 g, 0.06 mmol) was deprotected using HCl_{aq} (130 µl, 1.3 mmol) according to the procedure described above for iPS-OSi. Yield 62%

^{1}H NMR (400 MHz, $CDCl_3$, δ): 7.4 – 6.3 (Ar $\underline{H}$), 4.6 – 4.4 (2H, $\underline{H}$OPh), 2.4 - 1.2 (aliphatic $\underline{H}$).

2.2.5 SYNTHESIS OF MIKTO-ARM STARS VIA WILLIAMSON COUPLING REACTION

Linear polybutadiene brominated arms, with a molecular weight of about 40,000 g·mol^{-1} (PB40-Br), used for the coupling reaction, were previously synthesised in our group by Matthew Oti, according to a previously reported procedure.[13] Yield 96%.

M_n 40,300 g·mol^{-1}, M_w 41,600 g·mol^{-1}, Đ 1.03

^{1}H NMR (400 MHz, CDCl$_3$, δ): 5.64 – 5.49 (-C$\underline{H}$=CH$_2$), 5.49 – 5.27 (-C$\underline{H}$=C$\underline{H}$-), 5.02 -4.88 (-CH=C$\underline{H_2}$), 3.40 (-C$\underline{H_2}$-Br), 2.24 – 1.85 (backbone aliphatic $\underline{H}$), 1.34 – 1.20 (backbone aliphatic $\underline{H}$), 0.92 – 0.79 (*sec*-BuLi C$\underline{H_3}$).

In a typical reaction, PB40-Br (1.78 g, 0.044 mmol), deprotected end-capped polystyrene ePS-OH1 (0.20 g, 0.017 mmol) and cesium carbonate (Cs$_2$CO$_3$) (0.11 g, 0.35 mmol) were dissolved in 10 ml of dry THF under an inert atmosphere of nitrogen. Dry DMAc (10 ml) was then added to this solution, the reaction was heated with an oil bath at 60°C and stirred with a mechanical stirrer. The reaction was followed by SEC analysis and when the peak corresponding to PB40-Br no longer decreased, the reaction was stopped. The polymer was precipitated into methanol, re-dissolved in THF, precipitated again into methanol, collected by filtration and dried under vacuum. Yield 67%.

M_n 42,100 g·mol^{-1}, M_w 44,400 g·mol^{-1}, Đ 1.05
M_n 97,900 g·mol^{-1}, M_w 104,700 g·mol^{-1}, Đ 1.07.

2.3 RESULTS AND DISCUSSION

The aim of this PhD project is the design and synthesis of graft block copolymer architectures, by a combination of chain growth and step growth polymerisation. The first step in this process involves the synthesis of macromonomers with particular chain-end functionalisation, in this case a single bisphenol functionality. LAP represents probably the best way to do so, especially with styrenic and diene monomers, and this mechanism was therefore employed for PS macromonomer

synthesis. An ATRP strategy has been developed for the synthesis of macromonomers derived from PEGMEM (discussed in Chapter 3) since LAP is more challenging and complex with methacrylate monomers. Moreover, the presence of a PEO side chain in PEGMEM makes this monomer highly hygroscopic, with a high boiling point, making it difficult to distil and purify for use in LAP.

2.3.1   SYNTHESIS OF END-FUNCTIONALISED POLYSTYRENE BY LAP A COMPARISON OF DIFFERENT APPROACHES

LAP was chosen for the synthesis of functionalised polystyrene macromonomers, using a bisphenol functionalised DPE derivative to introduce the desired functional moiety strictly at one chain end of the final product. The functionalisation of polymers prepared by LAP with DPE derivatives, especially using styrenic and diene monomers, has been widely studied before. However, a comprehensive characterisation of the end-functionalised product has not previously been reported, especially as regards the actual number of functional DPE moieties introduced into the chain. For this reason, a comparison of two different strategies for end-functionalisation was performed, with a view to choosing the best way to synthesise the desired macromonomers to be used into the following polycondensation reactions. The first strategy uses a functionalised monomer, DPE-OSi and the second, a functionalised initiator (BPFK).

2.3.1.1   Synthesis of end-functionalised polystyrene using a functionalised monomer, DPE-OSi

The first strategy, i.e. exploiting the use of DPE-OSi for the synthesis of mono end-functionalised polystyrene, can itself be achieved by two approaches, namely using either an end-capping or an initiation procedure (Scheme 2.1). These two approaches have been compared to establish which provides the optimal approach for introducing a single (and no more than one) DPE-OSi end group per chain. Although both approaches have been widely used, by the Hutchings group and others,[1-6] with apparent success, it is clear that both have potential advantages and disadvantages. For a comprehensive comparison of

the two approaches, and in an attempt to highlight the potential disadvantages/limitations of each approach, a combination of NMR, SEC, MALDI ToF mass spectrometry and NP-IIC characterisation is required, in order to determine precisely the average degree of functionalisation and to identify the presence of chains with different numbers of DPE-OSi units.
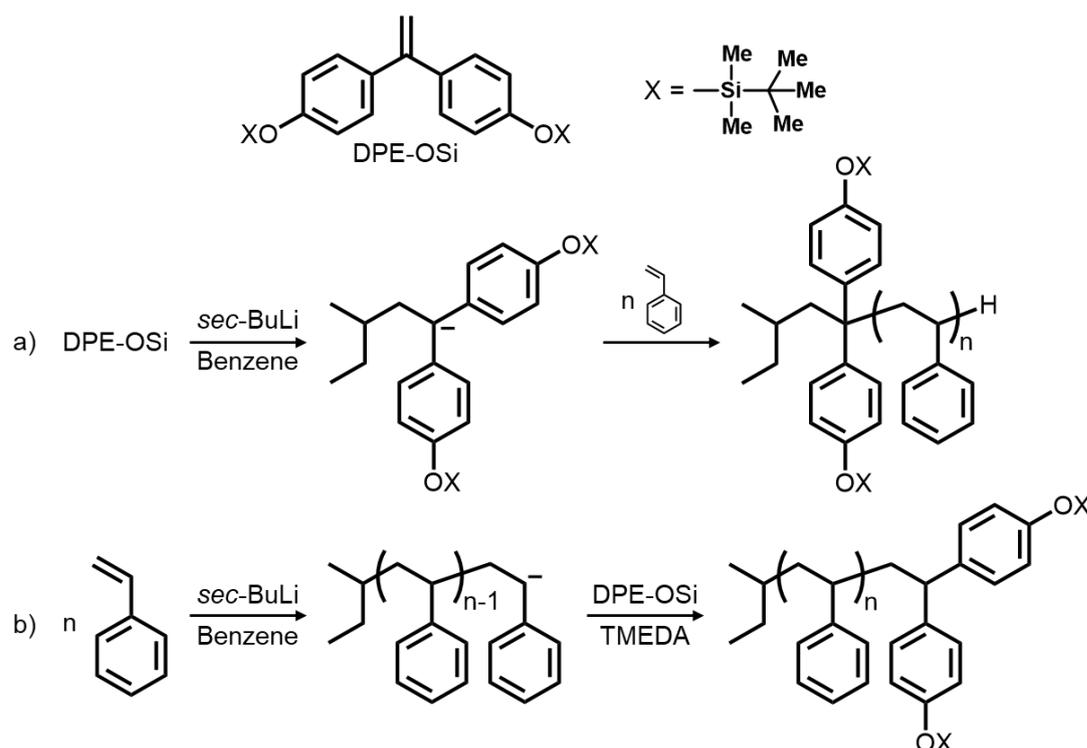
Scheme 2.1 Synthesis of functionalised polystyrene by LAP using a functionalised monomer, DPE-OSi, via: a) initiating procedure and b) end-capping procedure.

Both procedures require high vacuum techniques, and each has its pros and cons. The initiation approach (Scheme 2.1a), i.e. initiating polymerisation with the adduct of butyllithium and DPE-OSi, relies on very careful control of the stoichiometry of the reaction between BuLi and DPE-OSi, which in turn also requires careful management of impurities. Should there be an excess of BuLi with respect to DPE-OSi, then some chains will be initiated by BuLi and remain un-functionalised. However, if there is an excess of DPE-OSi with respect to BuLi, then some propagating chains may react with the excess DPE-OSi and end up with more than one DPE-OSi per chain. Achieving perfect stoichiometry between BuLi and DPE-OSi is practically impossible, although, in an attempt to minimise

any imbalance, butyllithium was added dropwise to the DPE-OSi in the reaction vessel, prior to the addition of styrene, to 'titrate' out any residual impurities. The presence of the characteristic deep red colour of diphenylhexyllithium, indicates the end-point of the titration. Even so, any slight variation in the concentration of active BuLi in the stock initiator solution may still result in a stoichiometric imbalance. However, the significant advantages of this approach are i) that at the end of the reaction the propagating chain-end is still available for further functionalisation and ii) that the reaction is complete in less than one day.

In contrast, the end-capping approach (Scheme 2.1b) does not rely on careful control of stoichiometry and an excess of DPE-OSi can be added to end-functionalise the chains, following complete consumption of styrene, since the DPE moiety is incapable of homopolymerisation. Of course, one still must ensure that the DPE-OSi solution – in which TMEDA is added as Lewis base, in order to decrease the degree of association of the polystyryllithium aggregates and speed up the reaction with the end-capping agent - is scrupulously free of impurities to ensure a clean end-capping reaction, and since the end-capping reaction itself requires up to 5 days to reach completion, the reaction mixture must be kept free of impurities for the duration of the end-capping reaction. Should any impurities be introduced with the DPE-OSi, some chain termination may occur and less than quantitative end-capping will result. A series of initial experiments were carried out in which two reactions were performed using each approach. The quantities of reagents are reported in Table 2.2.

Table 2.2 Quantity of reagents in mmol of the initiated and end-capped polystyrene samples. Two replicated polymerisations were performed for each procedure.

	DPE-OSi	Sty	*sec*-BuLi	TMEDA
iPS-OSi1	0.55	47.4	0.56	\
iPS-OSi2	0.60	55.1	0.60	\
ePS-OSi1	1.1	47.5	0.50	0.60
ePS-OSi2	1.0	61.8	0.64	0.60

SEC analysis of the polymers made by each approach reveals that, in each case, good control over the molecular weight and the dispersity of the products was achieved (Table 2.3) although SEC alone can tell us nothing about the extent of end-capping.

Table 2.3 Yield, molar mass data and degree of functionalisation of the initiated and end-capped polystyrene samples. Two replicated polymerisations were performed for each procedure.

	Yield[a]	M_n[b]	M_w[b]	Đ[b]	n[c]	%F[d]
iPS-OSi1	81%	8,000	8,300	1.05	0.68	44%
iPS-OSi2	92%	12,000	12,500	1.04	1.00	49%
ePS-OSi1	91%	12,500	13,000	1.04	1.00	93%
ePS-OSi2	91%	11,300	11,900	1.05	0.91	81%

a) After the deprotection reaction.
b) Calculated by SEC, in g·mol^{-1}.
c) Average number of DPE-OSi per chain, calculated by ^{1}H NMR.
d) Percentage of mono end-functionalised chains calculated by NP-IIC.

^{1}H NMR spectroscopy of the resulting polymers enables a calculation of the average number of DPE-OSi units per chain. By way of an example, the ^{1}H NMR spectrum of iPS-OSi1 is shown in Figure 2.2.
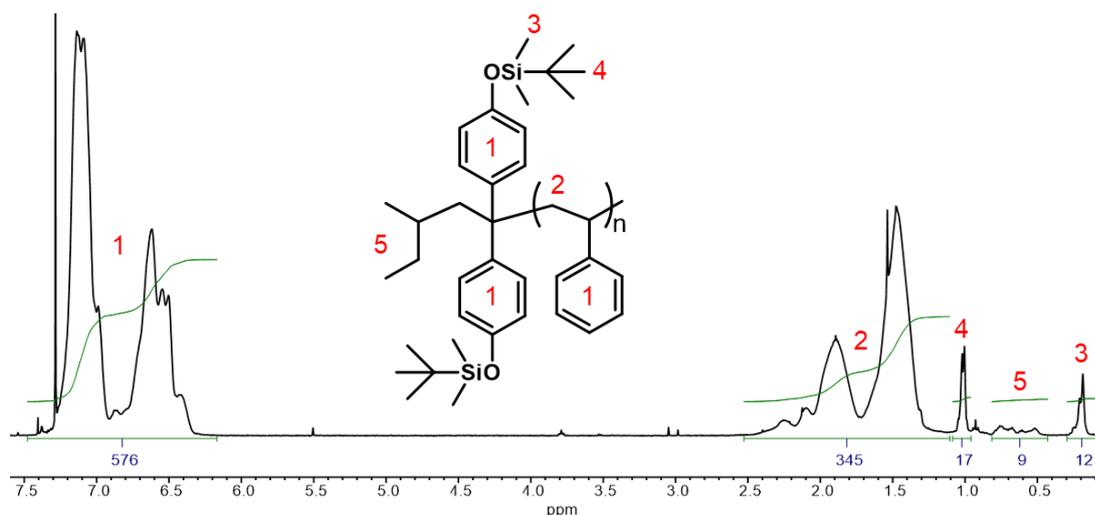
Figure 2.2 ^{1}H NMR spectra (CDCl$_3$, 400 MHz) of iPS-OSi1 synthesised by the initiating approach.

The average number of DPE-OSi units was determined by comparing the integrals of the aromatic protons (styrene repeat unit and DPE-OSi) to the methyl protons of the silyl groups. The broad signals between 6.2 and 7.4 ppm represents 8 aromatic protons per DPE-OSi unit and $n \times 5$ aromatic protons of the n styrene units per chain (where n is the degree of polymerisation), while the signal between 0.1 and 0.3 ppm can be ascribed to 12 equivalent $Si-(C\underline{H}_3)_2$ protons per DPE-OSi unit – indicated as proton '3' in Figure 2.2.

Setting a value of 12 for the integral of the silyl group protons, the following equation can be solved to give the chain composition:

$$8 + 5n = 576$$

The above equation gives as a result a DPE-OSi:styrene ratio of 114:1. According to the M_n value calculated by SEC analysis (8,000 g·mol^{-1}), there are an average of 77 styrene monomers in each chain (M_n/styrene molecular weight, 104.15 g·mol^{-1}) which implies an average of 0.68 DPE-OSi monomers per chain (number of styrene repeat units in each chain / number of styrene units per DPE-OSi units). We acknowledge that in this way we are ignoring the contribution of end-groups and DPE-OSi units to M_n, and that this will introduce an error into the calculation of average degree of polymerisation of styrene, however we expect the error to be small. The data for all the macromonomers are summarised in Table 2.3. If one ONLY considered the NMR data, one might simply conclude that the obvious/only difference between the two functionalisation approaches, in terms of average number of DPE-OSi units per chain, is that the initiating approach resulted in worse reproducibility in so much that iPS-OSi1, had a low degree of functionalisation and iPS-OSi2 a high degree of functionalisation with only 0.7 and 1.0 DPE-OSi units per chain respectively. This poor reproducibility is consistent with the challenge of maintaining good control over the reaction stoichiometry by the initiating procedure, and would appear to suggest that in the case of iPS-OSi1 an excess of BuLi was present. In contrast, the NMR data would suggest that the end-capping approach delivers a consistently higher degree of end-capping.

However, NMR can tell us the average number of DPE-OSi units per chain, but it cannot give any information about the distribution of DPE-OSi units per chain. In order to identify the (potential) presence of chains with different numbers of DPE-OSi units (0, 1, 2, etc.), a combination of NMR and SEC with MALDI ToF mass spectrometry and NP-IIC analysis is essential.

2.3.1.1.1 MALDI ToF characterisation

MALDI ToF MS analysis was performed on the 4 samples of functionalised polystyrene obtained via the two procedures. Using this technique, the molar mass corresponding to each individual polymer chain could be found, and it was possible to identify different series of peaks ascribable to different degrees of DPE-OSi incorporation. The MALDI ToF spectra (Figure 2.3 and 2.4) provide an excellent indication of the samples' composition and suggest that the effectiveness, in terms of introducing a single DPE-OSi moiety per chain, is not the same for each approach.

The MALDI spectra for the macromonomers produced via the initiating procedure clearly show three series of peaks (see Figure 2.3), which correspond to mono-, di- and un-functionalised chains. For example (see the insert in Figure 2.3a), the peak of mono-functionalised chains in iPS-OSi1, with an *m/z* of 9,147 u corresponds to 82 units of styrene (82×104.15 u) + 1 units of DPE-OSi (440.77 u) + 1 counterion, Ag (107.87 u) + 1 *sec*-butyl end-group (57.12 u) + 1 hydrogen end-group (1.01 u). The peak of un-functionalised chains in the same sample, with an *m/z* of 9,123 u corresponds to 86 units of styrene (86×104.15 u) + 1 counterion, Ag (107.87 u) + 1 *sec*-Butyl end-group (57.12 u) + 1 hydrogen end-group (1.01 u). Finally, the peak of di-functionalised chains, with an *m/z* of 9,171 u corresponds to 78 units of styrene (78×104.15 u) + 2 units of DPE-OSi (2 × 440.77 u) + 1 counterion, Ag (107.87 u) + 1 *sec*-Butyl end-group (57.12 u) + 1 hydrogen end-group (1.01 u).
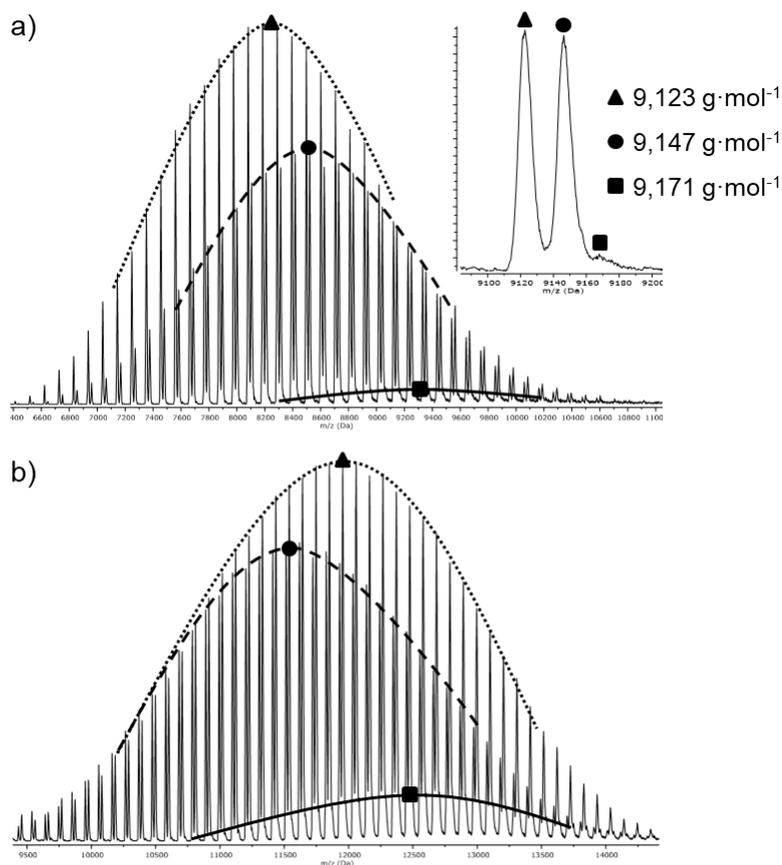
Figure 2.3 MALDI ToF spectra for a) iPS-OSi1; b) iPS-OSi2. The different series of peaks are highlighted respectively with a triangle for un-functionalised chains, a circle for the mono-functionalised chains, and with a square for the di-functionalised chains.

On the other hand, the MALDI spectra for the macromonomers produced via the 'end-capping procedure' reveal one dominant series of peaks (Figure 2.4) corresponding to mono-functionalised polymer chains. For example, the most intense peak of mono-functionalised chains in the ePS-OSi2 sample, with an *m/z* of 10,603 u corresponds to 96 units of styrene (96×104.15 u) + 1 unit of DPE-OSi (440.77 u) + 1 counterion, Ag (107.87 u) + 1 *sec*-Butyl end-group (57.12 u) + 1 hydrogen end-group (1.01 u). However, close inspection does indicate a trace amount of un-functionalised chains (see the insert in Figure 2.4b).

It should be noted that the relative intensity of individual peaks in MALDI analysis is not a reliable quantitative measure of abundance, since some chains may be more or less prone to ionisation than others.[14] Nevertheless, the MALDI analysis clearly and unambiguously indicates that the initiating procedure is less effective

than the end-capping one, for control over the degree of functionalisation of polystyrene with DPE-OSi.
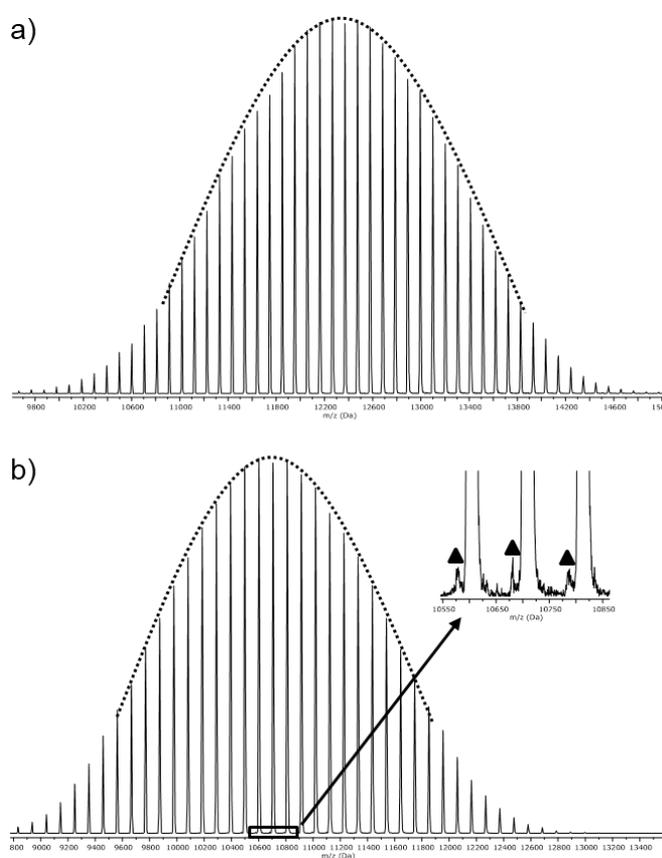
Figure 2.4 MALDI ToF spectra for a) ePS-OSi1; b) ePS-OSi2. The main visible series of peaks is ascribable to mono-functionalised chains, while the triangles indicate un-functionalised chains.

2.3.1.1.2 NP-IIC characterisation

The MALDI analysis described above gives initial proof that the samples obtained through the two procedures are different in terms of the degree of functionalisation, even if MALDI data does not allow us to quantify, neither relatively nor absolutely, the abundance of chains with different degrees of functionalisation in each sample. Interaction chromatography (IC), on the other hand, allows a relative quantification of the separated species, by measuring the area under the different peaks of the chromatogram, when UV or refractive index (RI) detector (both proportional to concentration) are used.

Temperature gradient (TGIC) or isothermal (IIC) interaction chromatography has recently emerged as a valuable characterisation technique for polymers, to

complement SEC. The latter is intrinsically incapable of separating polymers with identical or nearly identical hydrodynamic volumes, which may differ in other molecular parameters such as molecular weight, chain architecture or chain functionality. In IC, on the other hand, separation is driven by enthalpic interactions between the solute molecules and the stationary phase. Reversed phase (RP) IC resolves polymer samples based on molecular weight, not hydrodynamic volume, and thus it is a powerful tool for studying the structural heterogeneity of branched polymers.[15] Normal phase (NP) IC allows the resolution of polymers in terms of functionality and molecular weight, with polymer separation achieved by partition between a polar stationary phase (bare silica or diol bonded silica) and a less polar mobile phase.[13,16] Most recently,[13,15] it has been shown that end-functionalised polymers can be resolved from un-functionalised polymers of identical molar mass, for polymers with molecular weights up to 200,000 g·mol^{-1}. At such molecular weights any attempt to analyse the extent of end-functionalisation by NMR or MALDI-ToF MS would be an exercise in futility.

For the purposes of this section, the work by Hutchings *et al.*[13] is of particular interest, because of the application of NP-IIC to a series of linear PS samples of identical molar mass which differ only in the nature of the chain-end functionality. Thus, a *t*-BuMe$_2$Si-protected mono-hydroxy functionalised linear PS, was compared to the same polymer with the (deprotected) hydroxyl group and a third sample, following the transformation of the OH group to bromide. A schematic representation of the chemical modification of the functionalised polymer performed in aforementioned work is shown in Scheme 2.2.

Scheme 2.2 Schematic representation of chemical modification of functionalised PS.[13]

The NP-IIC analysis of these samples shows a significant change of retention volume upon deprotection of the hydroxyl group: the higher polarity of OH cause a significant delay in the elution of the functionalised chains, because of a stronger interaction with the polar stationary phase.

In light of these previously reported results, it was decided to carry out IC analysis after the deprotection of samples (labelled iPS-OH and ePS-OH, 1 and 2). In this way any functionalised polymer would be more clearly resolved from the possible un-functionalised polymer peak.

The deprotection was achieved by acid hydrolysis and was followed by ^{1}H NMR, until the complete disappearance of the signals corresponding to the *t*-BuMe$_2$Si-protective groups at δ 0.3–0.1 ppm ((C$\underline{H}_3$)$_2$Si) and δ 1.1 - 0.9 ppm ((C$\underline{H}_3$)$_3$C-Si). The appearance of a new peak at δ 4.6 – 4.4 ppm, corresponding to the phenol groups ($\underline{H}$OPh), was also detected. By way of example, the sections of NMR spectra before and after deprotection of ePS-OH1 are shown in Figure 2.5.
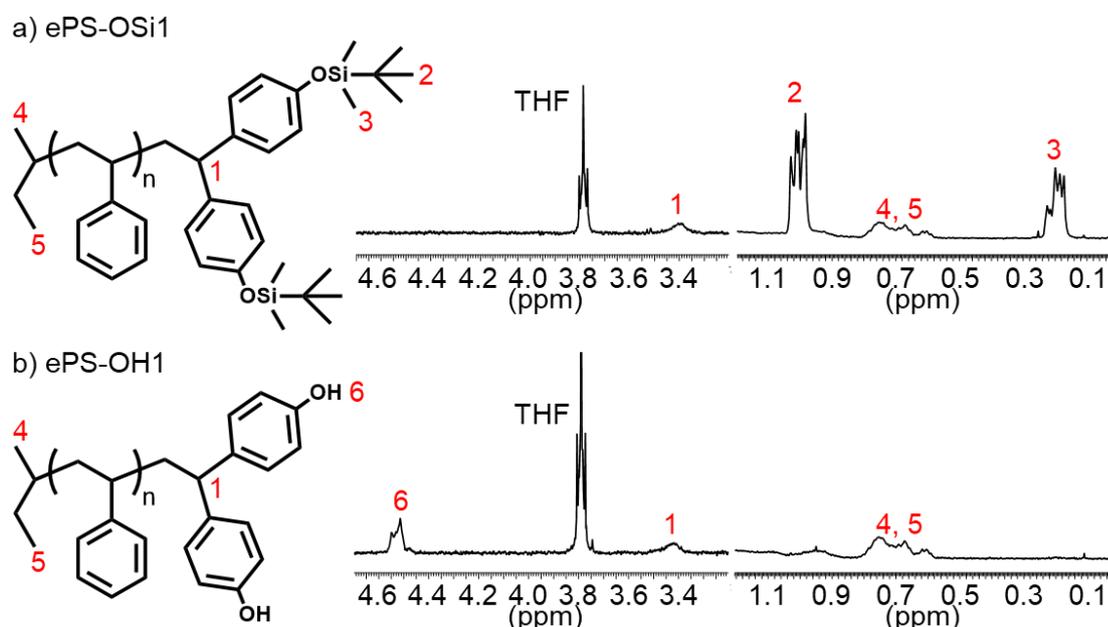
Figure 2.5 ^{1}H NMR (CDCl$_3$, 400 MHz) spectra fragments of a) protected and b) deprotected end-capped polystyrene.

The NP-IIC chromatograms of the deprotected samples recorded by UV detector are shown in Figure 2.6.

It should be remembered that it is a normal phase chromatography, with a polar column, thus the most polar species, the functionalised polystyrene in this case, elutes at longer retention times than un-functionalised polystyrene. Moreover, where polymers have the same polarity (functionalised or un-functionalised), lower molecular weight polymers elute at shorter times. It is clear from the

multimodal distributions in Figure 2.6a and b that each sample contains more than one species.
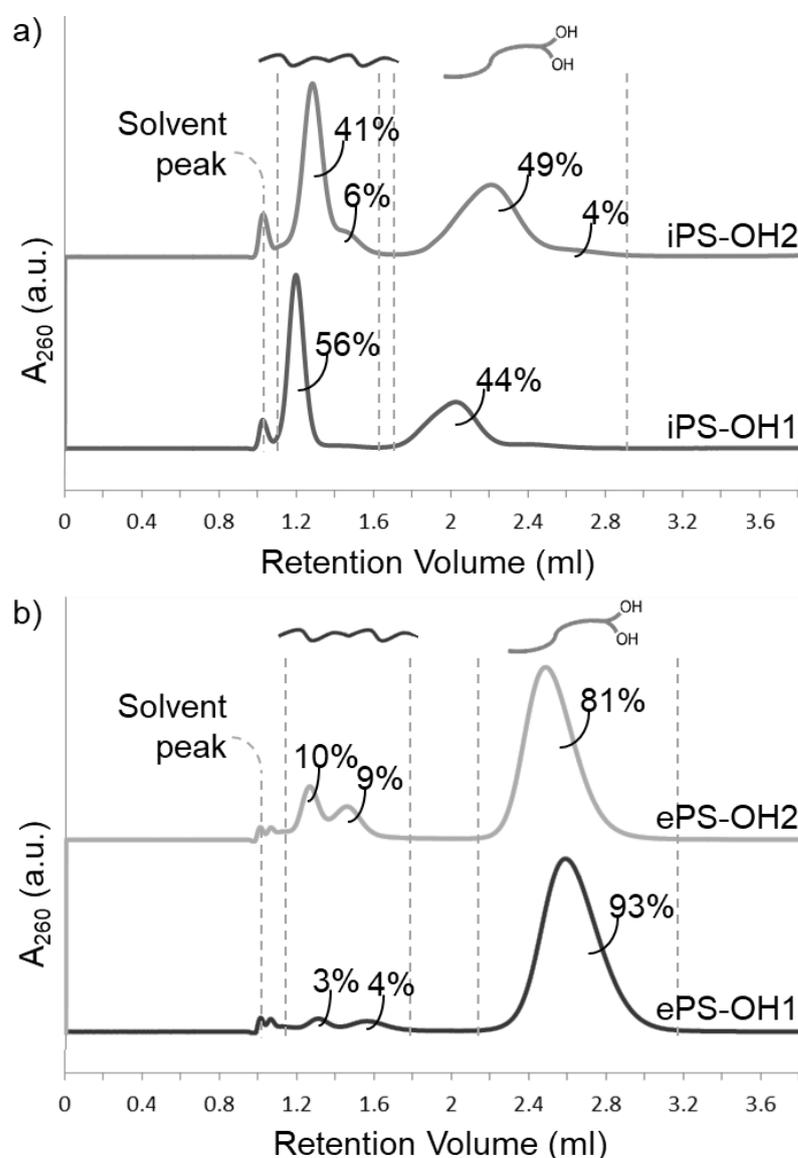
Figure 2.6 NP-IIC chromatograms of a) iPS-OH1 and iPS-OH2; b) ePS-OH1 and ePS-OH2, all recorded by UV detector. The relative amount (weight fraction %) of each species was estimated by deconvolution of the chromatograms using a Gaussian distribution and measuring the area under the curve.

These data are in good agreement with the MALDI spectra. Indeed, it is possible to identify two main groups of peaks in each sample. Considering firstly the samples prepared by the initiating approach (iPS-OH1 and iPS-OH2 in Figure 2.6a), it can be seen that there is a broad peak between 1.8 - 2.2 ml (for iPS-OH1) and 1.8 - 3.0 ml (for iPS-OH2) which in each case can be ascribed to

bisphenol functionalised polystyrene – the presence of the polar functional groups resulting in stronger retention by the column – and peaks eluting at low retention volumes (ca. 1.0 – 1.6 ml) which can be ascribed to un-functionalised polystyrene. In the case of iPS-OH2 there are two low retention volume peaks, a major peak at 1.3 ml and a shoulder at ca 1.5 ml. It is believed that these both arise due to un-functionalised polymer, but of different molar masses. Specifically, the later eluting peak of this pair corresponds to chains with approximately double the molecular weight of the earlier eluting peak. This higher molar mass peak arises due to post-polymerisation chain-coupling, which can be caused by the reaction with environmental impurities, such as oxygen or carbon dioxide, introduced during the termination reaction. The MALDI data in Figure 2.3a indicated that a small fraction of polymer chains produced via the 'initiation procedure' were di-functionalised, i.e. possessed two DPE-OSi groups per chain, however, the presence of such species could not be confirmed by NP-IIC. It would be expected that due to the presence of 4 phenolic –OH groups such chains would elute at greater retention volumes, however, even with the application of a temperature gradient with a maximum of 40°C, nor with a more polar solvent (Isooctane:THF 50:50), could further peaks be detected.

NP-IIC also allows the abundance of un-functionalised and mono-functionalised chains in each sample to be quantified. The relative amount of each species revealed in the NP-IIC chromatogram was estimated by deconvolution of the peaks from the UV or Refractive Index (RI) detector (both proportional to concentration), using a standard Gaussian distribution, and calculating the area under each curve. In the case of polymers produced using the initiating procedure, this process indicates that almost equal amounts of mono- and un-functionalised chains are produced (44 and 49% of functionalisation for iPS-OH1 and 2, respectively), which also suggests that there must be a significant quantity of undetected di-functionalised chains, since NMR analysis indicated an average number of DPE-OSi units per chain of 0.68 and 1.0 for iPS-OH1 and iPS-OH2 respectively.

Similarly for the samples obtained by end-capping (Figure 2.6b), peaks eluting in two main retention volume regions can be identified: peaks at 2.2 - 3.2 ml for both

samples can be ascribed to bisphenol functionalised polystyrene, the most polar species, while at lower retention volumes (ca. 1.2 – 1.8 ml) the un-functionalised polystyrene peaks are eluted. The presence of two peaks at low retention volume for both of the end-capped samples, as seen before with initiated polymers, is due to un-functionalised polymer, but of different molar masses, with the later eluting peak (species with higher MW) arising due to post-polymerisation chain-coupling. Analysing the area under the different peaks quantifies the amount of each species and in this case indicates that much higher percentage of the desired mono-functionalised chains are produced (93 and 81% for ePS-OH1 and 2, respectively), also in accordance with NMR analysis (1.0 and 0.9 average number of DPE-OH units per chain) and MALDI spectra (Figure 2.4), confirming that the end-capping procedure is far more effective than the initiating procedure.

When considering all the analytical data combined, a reasonably clear picture emerges about the relative effectiveness of the two different functionalisation approaches. The NMR analysis only gives information about the average number of DPE-OSi units per chain and did not show any significant differences between the two approaches. On the other hand, MALDI demonstrated the existence of different species of functionalised polystyrene in the samples, i.e. polystyrene chains with different numbers of DPE-OSi units. For polymer chains produced via the initiating procedure, MALDI revealed the desired mono-functionalised polymer, together with an (apparently) large fraction of un-functionalised chains, and small peaks corresponding to di-functionalised chains. However, for chains produced via the end-capping procedure, MALDI indicated predominantly peaks corresponding to the desired mono-functionalised chains with very small peaks corresponding to un-functionalised chains. The relative abundance of each species, however, cannot be accurately quantified by MALDI. Finally, the IC analysis was qualitatively in agreement with the MALDI data but also allowed us to quantify the relative abundance of each species identified, indicating that initiating procedure resulted in almost equal quantities of mono- and

un-functionalised chains whereas the end-capping approach yielded 80-90% of the desired mono functionalised chains.

There are, however, some discrepancies in the data, which are most evident for the samples produced via the initiating procedure. For example, the NMR analysis of iPS-OSi1 indicates that the resulting chains possess an average of 0.68 DPE-OSi units whereas the IC analysis of the same polymer suggests that less than 50% of the chains are functionalised. Moreover, MALDI clearly indicates the presence of a third distribution of chains with two DPE-OSi units. The abundance of these di-functionalised chains cannot be quantified by MALDI, although their prevalence looks to be low compared to the other species. Their presence was not detected at all by NP-IIC, probably due to a much stronger interaction with the stationary phase, which resulted in much longer retention times and possibly very shallow/broad (undetectable) peaks. If one was to assume as little as 5% of chains were difunctionalised, then the discrepancies between NMR and NP-IIC are significantly diminished. For example, for iPS-OH1, the presence of a peak for di-functionalised PS, accounting for 5% of the total peak area, would have caused the area under the peak for mono-functionalised chain to account for 42% of the total instead of 44%. Calculating the average number of DPE-OH units in a sample comprising 42% of chains with 1 DPE-OH unit, 53% with 0 DPE-OH unit and 5% with 2 DPE-OH unit gives an average of 0.52 DPE-OH units per chain. Although this value is closer to that indicated by NMR (0.68) there is still a significant difference. For iPS-OH2, if we rely on MALDI spectrum, the di-functionalised species seem to be in higher amount. If we assume that, in this case, 10% of chains are di-functionalised, then according to the previous calculation, a value of 0.64, instead of 0.49 DPE-OH units per chain is obtained. This value is still far from the one obtained by NMR (1.00), but it comes from assumptions that are affected by significant errors. It is evident that MALDI significantly underestimates the amount of di-functionalised chains and NP-IC (in these conditions) does not detect the di-functional species at all.

Despite some discrepancies, however, the overall picture is clear. The effectiveness of the initiating procedure is compromised by the reliance upon controlling the stoichiometry of the reaction between BuLi and DPE-OSi, and the

fate of the DPE-OSi, that can act as a comonomer. An imperfect molar ratio will result in either a slight excess of BuLi, which can initiate un-functionalised chains upon addition of styrene, or DPE-OSi, which, as a monomer, can be incorporated into a PS chain which may be carrying already another bisphenol moiety at the initial end. This hypothesis however does not fully explain the presence of both chains with no DPE-OSi and 2 DPE-OSi moieties. Indeed, the hypothesis above would suggest either chains with no DPE-OSi or with 2 DPE-OSi, but not both outcomes. One possible explanation for the presence of both, is a slow rate of the reaction between BuLi and DPE-OSi. If, at the time of styrene addition, this reaction is not complete, there will be the adduct formed by reaction between the two along with both unreacted BuLi and unreacted DPE-OSi, thus yielding both un-functionalised PS and di-functionalised PS. The result is a varying extent of functionalisation and a degree of functionalisation which varies from chain to chain.

On the other hand, the end-capping procedure is far more effective, in so much that an excess of DPE-OSi can be used to end-cap, since propagation with DPE-OSi is not possible, and therefore no di-functionalisation can occur. However, careful control of impurities is required to ensure a high degree of end-capping (up to 93% end-capping was achieved in this work). In conclusion, it is clear that the end-capping procedure can be used effectively to obtain almost quantitative mono-functionalisation of polymer, although the end-capping reaction is very slow. As an alternative, it was considered that the use of a functionalised initiator could simplify the process, eliminating the possibility of un-functionalised chains, which are still present after the end-capping reaction.

2.3.1.1.3   *Mikto-arm stars synthesis*

Since, the polymers prepared by the end-capping approach showed the highest level of end-functionalisation with no evidence of chains containing more than a single DPE-OH, ePS-OH1, with 93% end-functionalisation, was used as a macromonomer for the synthesis of asymmetric three-arm mikto stars, in which

the 'short' arm was DPE-OH mono-functionalised polystyrene, while the 'long' arms were brominated polybutadiene of 40,000 g·mol^{-1} (PB40-Br) (Scheme 2.3).
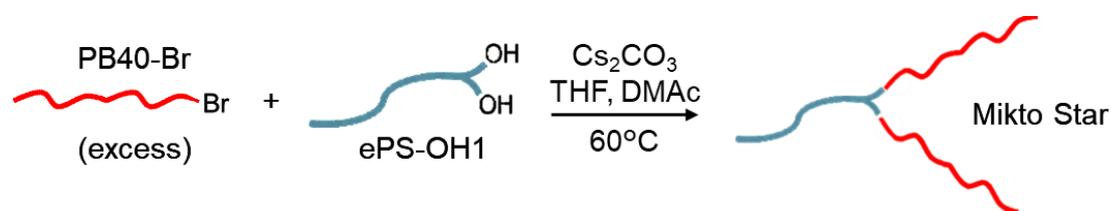
Scheme 2.3 Synthesis of mikto star copolymers from Williamson coupling between brominated polybutadiene (PB40-Br) and bisphenol functionalised polystyrene (ePS-OH1).

This experiment was carried out for two reasons, firstly to demonstrate one of the potential applications of well-defined end-functionalised polymers, namely macromonomers, but also to supplement the characterisation data above. Assuming that the NP-IIC data is correct, we would expect to see all of the ePS-OH react and this should be evident by SEC analysis. The arms were coupled together by a Williamson coupling reaction - a nucleophilic substitution of halides with a deprotonated alcohol (alkoxide) forming an ether – after the deprotection of the OH groups of the polystyrene macromonomer by acid hydrolysis. The Williamson coupling with the 'long' arms (PB40-Br) was carried out in the presence of Cs$_2$CO$_3$, whose role is to deprotonate the phenol groups of ePS-OH. A slight excess (mole ratio long arm:short arm of 2.5:1) of the long arm was used in an attempt to drive the reaction to high degrees of coupling, as previously demonstrated.[2,4,17]

Figure 2.7 compares the SEC chromatograms of the polymer mixture at the beginning of the reaction (grey trace) and at the end after 27 hours (black trace). It is clear from the SEC chromatograms in Figure 2.7 and molar mass data presented in Table 2.4 that this demonstration coupling reaction was a success. The reaction mixture at the start of the reaction (grey trace) had peaks at 13.7 ml and 15.5 ml, for the PB40-Br and ePS-OH, respectively. The final product (black trace) had a bimodal distribution comprising a new peak at c. 12.8 ml (M$_n$ 97,900 g·mol^{-1}), which can be attributed to the desired mikto-arm star, and a second peak at 13.5 ml (M$_n$ 42,100 g·mol^{-1}). This second peak is shifted to slightly

lower retention volume and has a slightly higher molecular weight than PB40-Br, suggesting that it represents predominantly unreacted PB40-Br and a small quantity of partial coupled product – i.e. a single chain of PB40-Br coupled to ePS-OH.
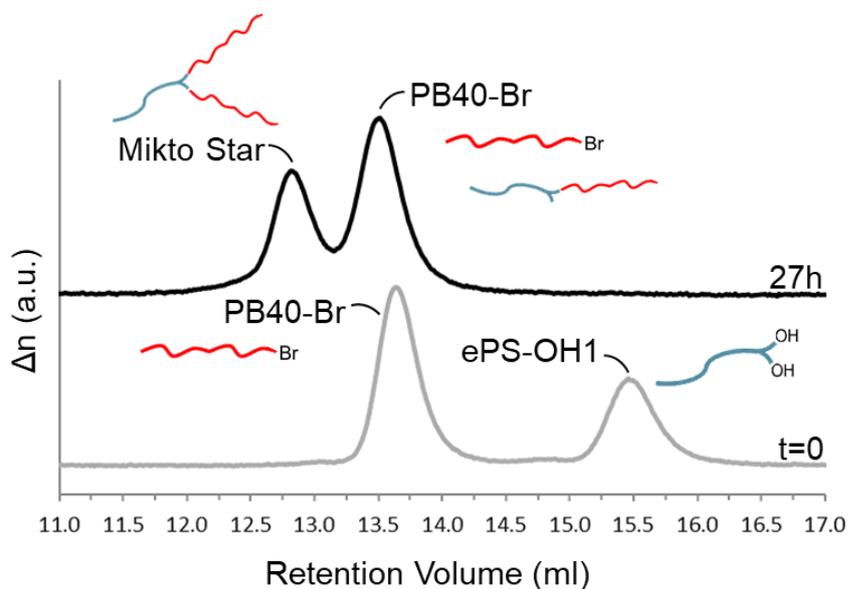
Figure 2.7 SEC (RI detector) chromatograms of mikto-arm stars polymer synthesised by Williamson coupling reaction between 'short' arm ePS-OH1 and 'long' arm PB40-Br. Reaction at time 0 (grey trace) and after 27 hours (black trace).

Table 2.4 Molar mass and dispersity data for starting materials and mikto-arm star produced via Williamson coupling of PB40-Br and ePS-OHa.

	ePS-OH1	PB40-Br	Target	Mikto Star	Residual PB40-Br
M_n (g·mol^{-1})	12,500	40,300	93,100	97,900	42,100
M_w (g·mol^{-1})	13,000	41,600	\	104,700	44,400
Đ	1.04	1.03	\	1.07	1.05

However, of prime significance to the current study is the complete absence of any unreacted 'short' arm (ePS-OH) at 15.5 ml, evidence that the polystyrene macromonomers were almost quantitatively end-capped with DPE-OSi.

2.3.1.2   Synthesis of end-functionalised polystyrene using a functionalised
         initiator - BPFK

Although the end-capping approach for the end-functionalisation of polystyrene
with DPE-OSi proved to be the better of the two options, it is not perfect. Even if
levels of end-capping can exceed 90%, 100% functionalisation is practically
impossible due to the inevitable introduction of traces of impurities accompanying
the addition of the DPE-OSi. Moreover, the end-capping reaction takes up to five
days to complete. With this in mind, a novel approach to introduce the same
bisphenol functionality to the chain end of polymers produced by LAP was
conceived and is reported here. This new approach uses a functionalised initiator
which overcomes the limitations of using the adduct of BuLi and DPE as an
initiator - namely the need to use an exact stoichiometric equivalence of BuLi and
DPE. As reported above, an excess of BuLi results in the production of
un-functionalised chains and an excess of DPE results in chains with more than
one functional DPE moiety per chain, since DPE can copolymerise. The proposed
solution is to use a functional initiator based on bisphenol F (BPF) (Scheme 2.4),
a functional derivative of diphenylmethyl potassium, which has been widely used
for the anionic ring opening polymerisation of ethylene oxide.[8,18]
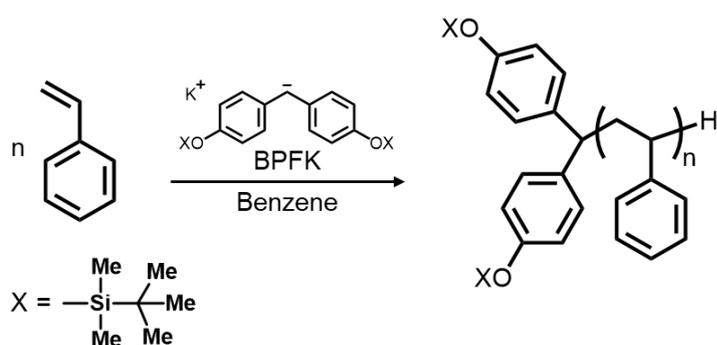
Scheme 2.4 Synthesis of functionalised polystyrene by LAP using a functionalised
initiator, BPFK.

The advantage of this approach is that the BPF is cheap and readily available;
the resulting initiator carries the two required protected phenol groups but is an
initiator in its own right, so does not need to be produced in-situ, avoiding the
issues of stoichiometry described above. Moreover, whilst DPE-OSi is also a
monomer, the protected BPFK is not a monomer and can only take part in

initiation reactions. It should therefore be impossible to produce polymer chains with more than one functionalised bisphenyl moiety. This approach should allow the production of polymers in which each and every chain has one and only one bisphenol functionality.

This novel initiator was prepared according to Scheme 2.5, set out below.
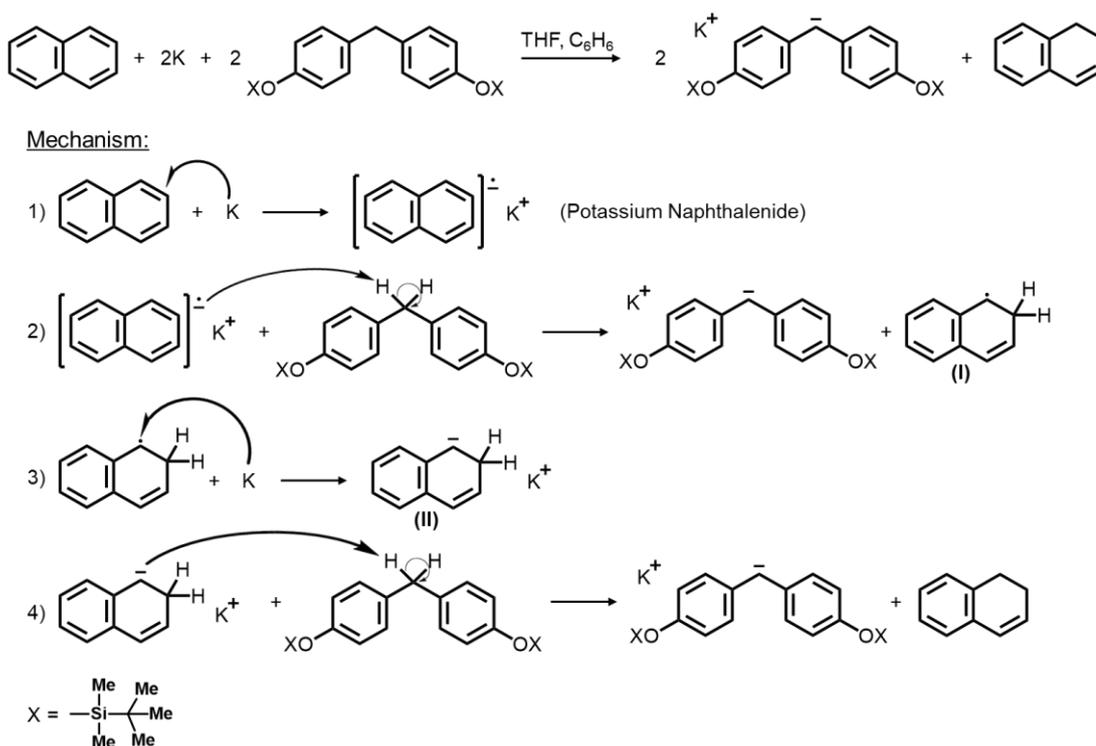
Scheme 2.5 Synthesis of BPFK and mechanism in 4 steps.

Firstly, the two phenol groups of bisphenol F (BPF) were protected in the same manner as DPE-OSi. The protected BPF-OSi was converted to its potassium salt, according to a previously reported procedure for the synthesis of the potassium salt of diphenylmethane.[12] Thus, potassium naphthalenide (a green solution in THF) was formed by the reaction of naphthalene with excess potassium metal in dry THF under an inert atmosphere (Scheme 2.5 step 1). At this point (step 2) BPF was added and the strongly basic naphthalenide removes one methylene proton from BPF, giving one equivalent of BPFK and a radical species (I). The latter forms another anionic species (II) upon electron transfer from residual potassium metal (step 3), which forms a second equivalent of BPFK plus

dihydronaphthalene (step 4). During the formation of the BPF anion, the colour of the solution gradually shifted from dark green to deep red.

The polymerisation of styrene with 1,1-bis(4-*t*-butyldimethylsiloxy phenyl)methyl potassium (BPFK) as initiator, was performed in benzene under high vacuum conditions, according to the standard procedure for LAP. Initially, a polymerisation was carried out in order to determine the concentration of the initiator. To styrene (2.22 g, 21 mmol) in benzene, 500 μl of BPFK solution were added, yielding a polymer of M_n 32,800 g·mol⁻¹ and Đ 1.12. Knowing the volume of initiator solution injected, it was possible to calculate the concentration of the initiator by the following equation:

$$M_n = \frac{M_m}{I}$$

where M_n is the number average molecular weight of PS, M_m is the mass of monomer in grams used and I is the number of moles of initiator. These data gave a value of 0.14 M. Using this concentration, the synthesis of polystyrene with a target molar mass of 10,000 g·mol⁻¹ was carried out, followed by characterisation of the resulting polymer. SEC analysis gave M_n 15,800 g·mol⁻¹ and Đ 1.12. Despite a reasonable control over the molecular weight, the dispersity was a little broader than analogous polymers prepared using alkyllithium initiators (usually Đ<1.1), in line with what has been previously reported in literature as regards the DPMK initiator.[18] However, the dispersity value obtained for the polymerisation of styrene with BPFK (Đ=1.12) is much better than the values obtained when using (un-functionalised) DPMK initiator for the polymerisation of styrene in benzene (in-house attempt gave a Đ>1.3). The lower dispersity of polystyrene initiated with BPFK in benzene compared to initiation with DPMK arises for two reasons. Firstly, DPMK is insoluble in benzene and precipitates upon addition, meaning that initiation is a heterogeneous process, although the reaction mixture becomes homogeneous as propagation proceeds. On the other hand, no precipitation of initiator was seen when BPFK was used, ensuring homogeneous initiation. Secondly, the electron-donating effect of the (protected) OH groups makes the

BPF anion more nucleophilic, thus making the initiation step faster in relation to propagation.

In the ^{1}H NMR spectrum (Figure 2.8 a and b), the peaks of the TBDMS protecting groups at δ 0.3-0.1 ppm ((C$\underline{H}_3$)$_2$Si) and δ 1.1-0.9 ppm ((C$\underline{H}_3$)$_3$C-Si) are clearly visible, proving the successful functionalisation of the chains.
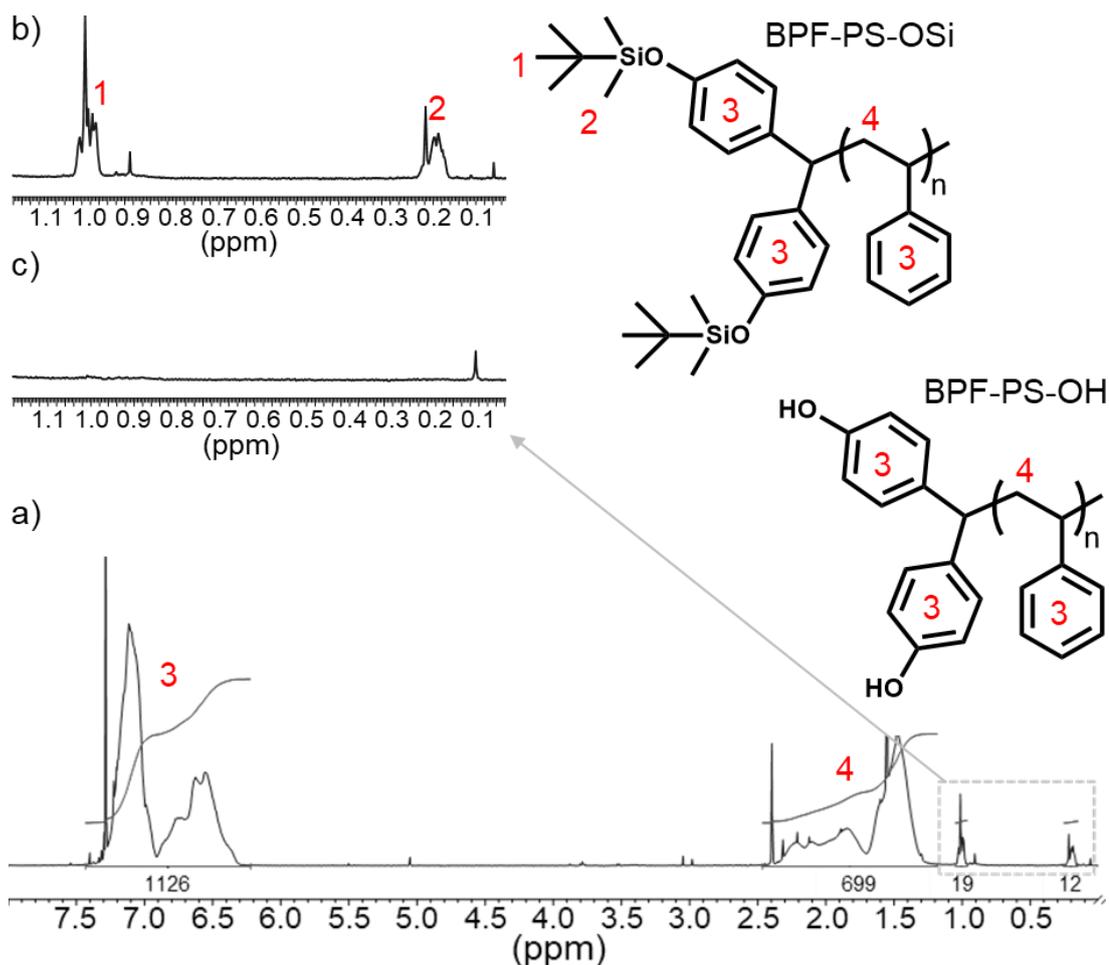
Figure 2.8 a) ^{1}H NMR spectra (CDCl$_3$, 400 MHz) of BPF-PS-OSi before the deprotection. b) TBDMS peaks area in the spectra of BPFK initiated polystyrene before the deprotection (BPF-PS-OSi); c) TBDMS peaks area in the spectra of BPFK initiated polystyrene after the deprotection (BPF-PS-OH).

After deprotection, the same signals completely disappear (Figure 2.8c). The calculation by NMR of the average number of bisphenol units per chain gave a value of 0.68, which might suggest the presence of un-functionalised chains,

even if the use of a functionalised initiator should exclude the presence of un-functionalised chains.

NP-IIC analysis of the BPFK initiated polystyrene, before and after the deprotection, was carried out using a RALS detector. The use of RALS coupled with a refractive index detector enables the calculation of both molar mass and abundance of each species and the results are shown in Figure 2.9.
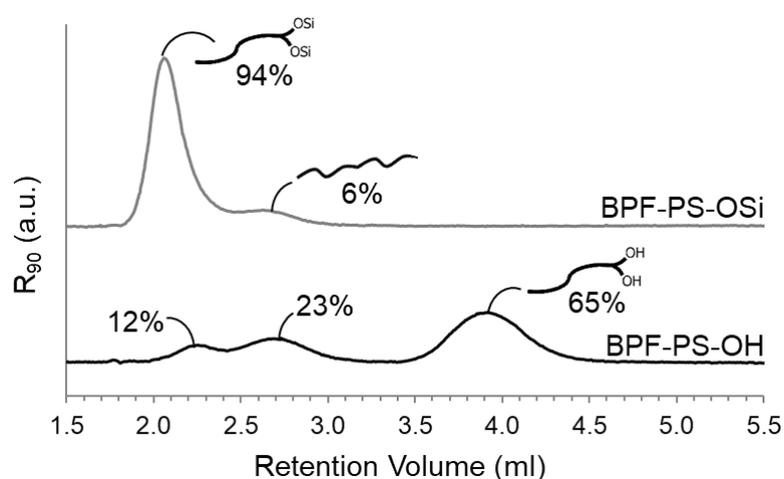
Figure 2.9 NP-IIC chromatograms of BPFK initiated polystyrene, recorded by RALS detector. The upper curve is related to the sample before the deprotection of the phenol groups (BPF-PS-OSi), while the lower curve to the sample after the deprotection of the phenol groups (BPF-PS-OH).

In the chromatogram of the sample before the deprotection (upper curve), two peaks are clearly visible. The first, eluting at ~2.2 ml, with a molar mass of 16,900 g·mol^{-1} and comprising the majority of the total peak area (94%), can be ascribed to the desired BPF-initiated polystyrene, while the second, at ~2.6 ml, with a molar mass of 28,600 g·mol^{-1} comprises of only 6% of the total polymer. Although we cannot be certain, it is proposed that the higher molar mass and later retention volume of the smaller peak, indicates un-functionalised chains that may have been initiated by residual potassium naphthalenide radical anion, which may still be present in the initiator solution. The higher molecular weight is in accordance with initiation by the naphthalenide radical anion, which reacts with monomers such as styrene by reversible electron transfer, followed by radical

coupling, leading to a di-anionic initiator that grows in two directions, giving longer chains.[8]

Following deprotection (Figure 2.9, lower trace), a significant decrease in the intensity of the peak at ~2.2 ml can be seen, accompanied by a new peak at 3.9 ml (16,600 g·mol^{-1}), which can be ascribed to the deprotected functionalised polymer. This is consistent with the stronger interaction between the OH groups and the polar column, compared to the interaction between the protected OH groups and the same polar column, and in agreement with expectations based on a previous report.[13] Moreover, the calculated M_n for this peak (16,600 g·mol^{-1}) is in accordance with the one obtained for the peak of protected chains at 2.2 ml, before the deprotection. Analysis of the area under the peaks indicates that the functionalised, deprotected polymer represents about 65% of the total mass of sample. This value is in good agreement with NMR analysis of the protected sample which indicated 68% of chains were end-functionalised.

Beside the main peak at higher retention volume, the chromatogram after the deprotection shows two more residual peaks, in the area between 2.0 and 3.2 ml. One hypothesis could be that the second peak, at ~2.7 ml, is due to the presence of un-functionalised chains, since it seems to be the same peak – same retention volume - identified in the trace before the deprotection. Moreover, it is expected that the retention onto the stationary phase would not change before and after the deprotection, because the reaction does not affect an un-functionalised chain. The calculated M_n (18,900 g·mol^{-1}), however, is again higher, but not double the one of the desired product, as seen in the chromatogram before the deprotection reaction. A possible explanation that was considered for the appearance of these peaks at low retention volume and with similar molar mass to the desired end-functionalised polymer is that the deprotection reaction was incomplete or only partially complete. However, NMR analysis (Figure 2.8) indicates the complete disappearance of peaks associated with the protecting groups, suggesting that deprotection was quantitative. Thus, we do not believe that these low retention volume peaks in the NP-IIC data represent end-functionalised chains which are still protected.

Once the possibility of incomplete deprotection is excluded, the only possible explanation for those peaks is the presence of chains with the same molecular weight of the desired product, but with a different kind of functionalisation. These species are eluted at retention volumes similar to the protected chains, meaning similar polarity of the functional group, but they are not, or only slightly, affected by the deprotection reaction. The second peak at 2.7 ml with a higher molecular weight of 18,900 g·mol^{-1}, could be actually due to an overlapping of the un-functionalised chains of circa double the molecular weight, also seen in the trace before the deprotection, and an unidentified species which has been affected by the deprotection, causing a shift to higher retention volumes. It is difficult to explain what could have caused the presence of this unknown functionalisation, also because the NMR spectra does not show any characteristic signals that could help in the identification. The relative signals can easily be covered by the broad peaks of polystyrene, or be too weak to be actually seen.

It is clear that the polymer sample - nominally - initiated with BPFK, is not fully functionalised as intended, as the NP-IIC chromatogram of the polymer post deprotection contains unresolved peaks between 2 and 3 ml, which are probably due to a different – unknown - kind of functionalisation. At the present time we don't have an entirely satisfactory explanation for the origin of these peaks or for the cause of the less than quantitative end-capping when using BPFK, except for the possibility to have un-functionalised chains initiated by potassium naphthalenide with double the molecular weight.

Accepting that this new strategy is not yet perfect, the characterisation data of the polystyrene initiated with BPFK demonstrates that this strategy presents a viable potential approach to achieve selective mono-functionalisation of polymers, albeit further optimisation is needed to overcome some issues encountered during the synthesis of the initiator and during the polymerisation step. It is a promising procedure, though, because BPFK acts exclusively as an initiator and cannot behave like a monomer, as DPE and its derivatives do. Thus, each chain initiated by BPFK carries the functional groups of the functionalised

diphenylmethane moiety, thereby removing the issue of incomplete activation of DPE by *sec*-BuLi or incomplete end-capping, which leads to un-functionalised chains. Moreover, the possibility that a second DPE monomer could be included into the chain during the propagating phase, resulting in a di-functionalisation, is avoided. Finally, it is a straightforward polymerisation procedure that does not require long reaction times to reach completion, as in the case of the end-capping procedure with DPE-OSi. We believe with further studies this new initiator could allow the synthesis of mono-functionalised macromonomers, with a bisphenol functionality exclusively at one end, whilst allowing further functionalisation to be carried out at the still-living chain end, on completion of propagation.

2.3.2 SYNTHESIS OF END-FUNCTIONALISED POLYSTYRENE MACROMONOMERS VIA END-CAPPING PROCEDURE WITH DPE-OSi AND SCALE-UP

Although the use of a functional initiator such as BPFK is desirable for various resaons, given the issues discussed above, the use of a functional monomer such as DPE-OSi and the end-capping procedure was considered the most effective approach to make well-defined mono-end-functionalised polystyrene macromonomers. Above all, this approach gives certainty in avoiding the presence of more than one functional monomer per chain. Thus, the synthesis was scaled-up and the resulting macromonomers were used in polycondensation reactions for the synthesis of grafted copolymers, as extensively described in the following chapters.

As discussed above, a combination of NMR, SEC and NP-IIC analysis to characterise the resulting macromonomers is essential to quantitatively determine the extent of functionalisation achieved.

A series polystyrene macromonomers have been prepared of varying molar mass and on a scale of up to 150 g. Molar mass (SEC) and degree of functionalisation (NMR) data is included in Table 2.5. From now on, the macromonomers will be labelled as ePSX.Xk where *e* indicates end-capping procedure and X.Xk indicates number average molar mass in kg·mol^{-1}. Thus ePS9.1k is a polystyrene

macromonomer with M_n equal to 9.1 kg·mol⁻¹ produced using the end-capping approach.

Table 2.5 Yield, SEC data and degree of functionalisation parameters of PS macromonomers.

	Yield[a]	MW[b]	M_n[c]	Đ	n[d]	%F[e]
ePS2.9k	33%	2,000	2,900	1.03	1.1	99%
ePS6.4k	97%	5,000	6,400	1.05	0.8	97%
ePS9.1k	94%	7,100	9,100	1.07	1.0	92%
ePS6.2k	91%	5,000	6,200	1.08	0.91	98%

a) After the deprotection reaction.
b) Target molecular weight, in g·mol⁻¹.
c) Calculated by SEC, in g·mol⁻¹.
d) Average number of DPE-OSi per chain, calculated by ¹H NMR.
e) Percentage of mono end-functionalised chains calculated by NP-IIC.

¹H NMR spectra (example in Figure 2.10 for ePS9.1k), combined with the SEC data (Table 2.5), enable a calculation of the average number of DPE-OSi per chain.
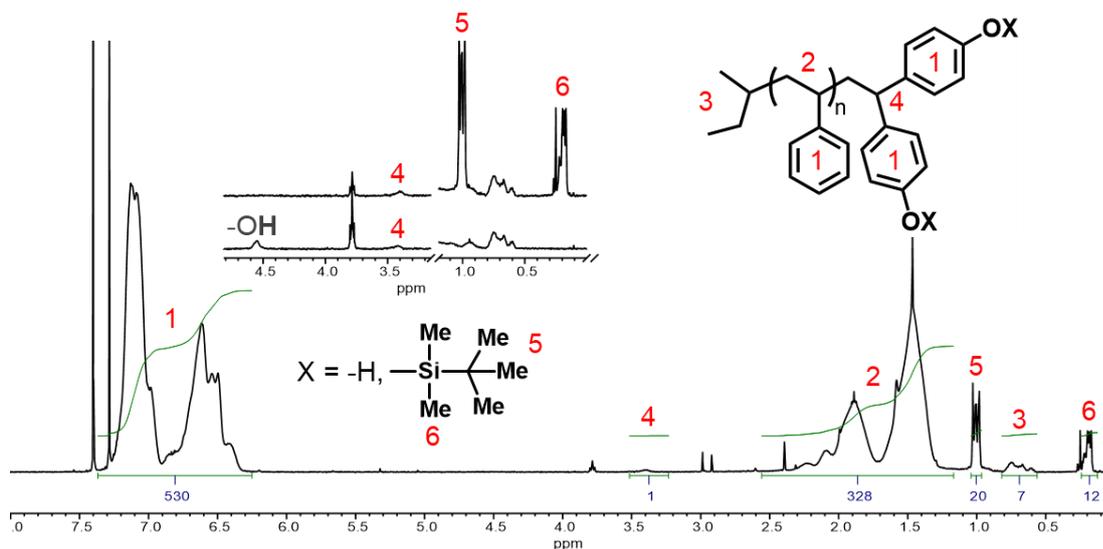
Figure 2.10 ¹H NMR spectra (CDCl₃, 400 MHz) of ePS9.1k macromonomer synthesised by the end-capping procedure with DPE-OSi. Insert: comparison of sections of the spectra before (top trace) and after (bottom trace) the deprotection of the phenol groups.

As seen in Section 2.3.1, the average number was determined by comparing the integrals of the aromatic protons to the methyl protons of the Si groups. The results for all the macromonomers synthesised are summarised in Table 2.5.

The NP-IIC analysis (example for ePS6.4k in Figure 2.11) indicates that the extent of functionalisation is greater than 92% for all the macromonomers, proving once again that the end-capping procedure is a very effective approach to obtain the desired functionalisation, even when the synthesis is scaled up, as in the case of ePS9.1k and ePS6.2k, to 100 g and 150 g.
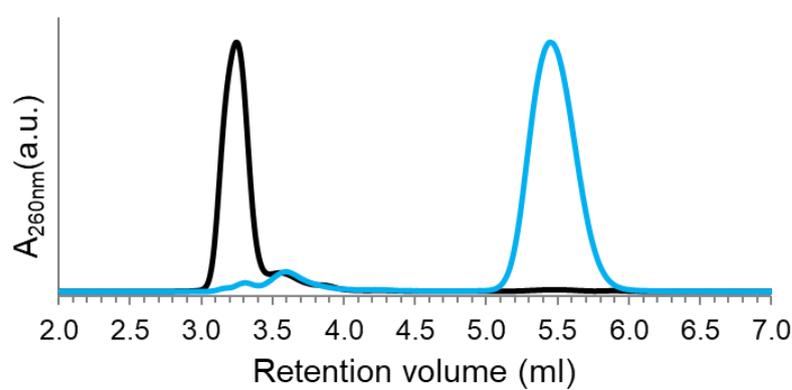
Figure 2.11 NP-IIC chromatogram of ePS6.4k before (black trace) and after (blue trace) deprotection.

2.4 CONCLUSIONS

The first step of this PhD project is the synthesis and characterisation of macromonomers with absolute control of the degree of functionalisation, such that a single functional group - a bisphenol functionality - could be introduced, selectively at one end of the chain.

To this end we investigated the effectiveness of the use of the monomer DPE-OSi in LAP to functionalise polystyrene via two approaches: the end-capping and the initiating procedures. The combined characterisation using NMR, SEC, MALDI ToF and NP-IIC allowed us to compare the two procedures and to better understand the outcome in terms of number of functional DPE-OSi units per chain. MALDI and NP-IIC data proved particularly useful in showing that the initiating procedure gave only ~50% of a mono-functionalised product, along with both un-functionalised and di-functionalised polymer. Even if the end-capping

procedure proved to give much better results, both procedures showed intrinsic limitations: 100% functionalisation is practically impossible, due to the inevitable introduction of traces of impurities and, in the case of the initiating procedure, the need to precisely control the stoichiometry of *sec*-BuLi and DPE-OSi, which together with the slow rate of reaction between the two, resulted in a mixture of products. As a final consideration, the end-capping reaction takes up to five days to complete.

With this in mind, we developed a new approach to introduce the same bisphenol functionality to the chain end of polymers obtained by LAP. By using a functional initiator based on bisphenol F (BPF), the initiation process is simplified, avoiding the issues of stoichiometry and, in contrast to DPE-OSi, the protected BPF is not a monomer and cannot copolymerise, thus avoiding also the possibility to add more than one functionalised bisphenyl moiety. However, despite the encouraging early results and potential for the use of the BPF initiator, this approach still needs further optimisation, to overcome some issues encountered during the synthesis of the initiator and the polymerisation step.

In conclusion, the end-capping approach using DPE-OSi was chosen for the scaled-up synthesis of PS macromonomers, as the most effective and reliable method to obtain the desired control over the functionalisation of the chains, despite the long reaction time. These macromonomers were subsequently used in step-growth polycondensation reaction, as described in the following Chapters.

REFERENCES

1. Hutchings, L.R.; Dodds, J.M.*, et al.*, *Macromolecules*, **2005,** *38* (14), 5970-5980.
2. Hutchings, L.R.; Roberts-Bleming, S.J., *Macromolecules*, **2006,** *39* (6), 2144-2152.
3. Hutchings, L.R.; Dodds, J.M.*, et al.*, *Macromolecules*, **2009,** *42* (22), 8675-8687.
4. Agostini, S.; Hutchings, L.R., *European Polymer Journal*, **2013,** *49* (9), 2769-2784.
5. Zhang, H.; He, J.*, et al.*, *Macromolecules*, **2012,** *45* (2), 828-841.
6. Quirk, R.P.; Yoo, T.*, et al.*, *Applications of 1,1-Diphenylethylene Chemistry in Anionic Synthesis of Polymers with Controlled Structures*, in *Biopolymers · PVA Hydrogels, Anionic Polymerisation Nanocomposites*, Springer, Berlin, **2000**.pp 67-162.
7. Hutchings, L.R.; Brooks, P.P.*, et al.*, *Macromolecules*, **2015,** *48* (3), 610-628.
8. Hsieh, H., Quirk, R. P., *Anionic Polymerization: Principles and Practical Applications*. Marcel Dekker, Inc., **1996**.
9. Pagliarulo, A.; Hutchings, L.R., *Macromolecular Chemistry and Physics*, **2018,** *219* (1), 1700386.
10. Brooks, P.P.; Natalello, A.*, et al.*, *Macromolecular Symposia*, **2013,** *323* (1), 42-50.
11. Quirk, R.P.; Wang, Y., *Polymer International*, **1993,** *31* (1), 51-59.
12. Candau, F.; Afchar-Taromi, F.*, et al.*, *Polymer*, **1977,** *18* (12), 1253-1257.
13. Hutchings, L.R.; Agostini, S.*, et al.*, *European Polymer Journal*, **2015,** *73*, 105-115.
14. Li, L., *MALDI Mass Spectrometry for Synthetic Polymer Analysis*. John Wiley & Sons, New York, **2009**.
15. Hutchings, L.R., *Macromolecules*, **2012,** *45* (14), 5621-5639.
16. Lee, W.; Cho, D.*, et al.*, *Journal of Chromatography A*, **2001,** *910* (1), 51-60.
17. Kimani, S.M.; Hutchings, L.R., *Macromolecular Rapid Communications*, **2008,** *29* (8), 633-637.
18. Ekizoglou, N.; Hadjichristidis, N., *Journal of Polymer Science Part A: Polymer Chemistry*, **2001,** *39* (8), 1198-1202.

CHAPTER 3

SYNTHESIS OF BISPHENOL FUNCTIONALISED POLYPEGMEM MACROMONOMERS BY ATRP

3.1 INTRODUCTION

The aim of this project is to synthesise graft block copolymers by incorporating suitable macromonomers in a step-growth polycondensation reaction. Therefore, a bisphenol functional group has been introduced at one chain end, to obtain linear macromonomers by living/controlled polymerisation mechanisms. A bisphenol derivative based on 1,1-diphenylethylene (DPE-OSi), was chosen to introduce the desired functionality to the macromonomers, via both anionic polymerisation and ATRP.
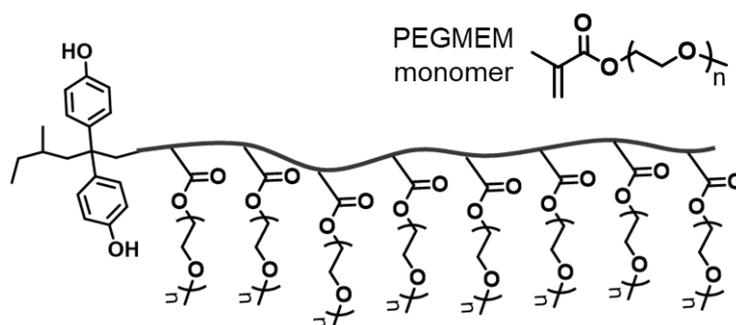
Figure 3.1 PolyPEGMEM macromonomer.

In addition to PS macromonomers, whose synthesis has been described in Chapter 2, the versatility of the macromonomer approach is demonstrated by the synthesis of a hydrophilic macromonomer using poly(ethylene glycol) methyl ether methacrylate (PEGMEM) (Figure 3.1).

The polymerisation of methacrylates such as PEGMEM by anionic polymerisation is feasible but challenging, due to potential side reactions between the carbanions of both the initiator and propagating chain end and the carbonyl group of either a free monomer or within the chain. These side reactions result in termination reactions.[1] For this reason, atom transfer radical polymerisation (ATRP), a (controlled) reversible deactivation radical polymerisation was also investigated as a route to obtain the desired bisphenol functionalised PolyPEGMEM macromonomer. DPE-OSi was picked again to introduce the desired bisphenol functionality, at first as a monomer and then to synthesise a novel functionalised initiator for ATRP.

3.2 EXPERIMENTAL

3.2.1 MATERIALS

Benzene (Aldrich, HPLC grade, ≥99%), was dried and degassed over calcium hydride (CaH_2) (Acros Organics, 93%) and stored under high vacuum. Tetrahydrofuran (THF) (in-house solvent purification) was dried over sodium wire (Aldrich, 99.9%) and benzophenone (Aldrich, 99%), and degassed using freeze-thaw techniques. *sec*-Butyllithium (*sec*-BuLi, Sigma-Aldrich, 1.4 M solution in cyclohexane) was used as received. Methanol (AR grade) and hydrochloric acid (37 wt.%), (both Fischer Scientific) were used as received. 1,1-Bis(4-*tert*-butyl dimethylsiloxyphenyl)ethylene (DPE-OSi) was synthesised in two steps from dihydroxybenzophenone (Sigma-Aldrich, 99%) according to the procedure of Quirk and Wang.[2]

Lithium chloride (⩾99.98% trace metals basis, Aldrich) and triethylaluminium (25 wt.% in toluene, Aldrich) were used as received. Toluene (CHROMASOLV™, for HPLC, 99.9%, Fischer Scientific), poly(ethylene glycol) methyl ether methacrylate (PEGMEM, average M_n 300, Sigma-Aldrich), copper(I) bromide (98%, ACROS Organics), 2,2'-bipyridyl (bipy, Sigma-Aldrich), anisole (99%, ACROS Organics), ethyl 2-bromoisobutyrate (Tokyo Chemical Industry), N,N,N',N'',N'' pentamethyldiethylenetriamine (PMDETA, Tokyo Chemical Industry), hexane (SLR, Fisher Chemical), aluminium oxide (neutral,

Brockmann I, for chromatography, 50-200μm, 60A, ACROS Organics) were all used as received.

(±)-Propylene oxide (PO) (99%), α-bromoisobutyryl bromide (98%), triethylamine (≥99%), tetrabutylammonium fluoride (TBAF) (solution 1.0 M in THF), ammonium chloride (ACS grade), all Sigma-Aldrich, were used as received.

3.2.2 CHARACTERISATION

^{1}H NMR spectra were measured on a Bruker DRX-400 MHz spectrometer and on a Varian VNMRS-700 spectrometer, using $CDCl_3$ as solvent.

Triple detection size exclusion chromatography (SEC) with refractive index (RI), viscosity, and right angle light scattering (RALS) detectors was used for the analysis of molar mass and molar mass distribution of the macromonomers, using a Viscotek TDA 302. THF was used as the eluent, at a flow rate of 1.0 ml·min^{-1} and at a temperature of 35°C. Separation was achieved using 2×300 mm PLgel 5 μm mixed C-columns. A dn/dc value of 0.069 ml·g^{-1} (measured in house) was used for PolyPEGMEM.

Isothermal interaction chromatography analysis was performed under normal phase conditions using a diol modified silica column (Nucleosil 100 Å pore, 250×4.6 mm I.D., 5 μm). A mixture of THF/isooctane (Fisher, GPC and HPLC grade respectively) was used in a ratio 45/55 (v/v) with a flow rate of 0.5 ml·min^{-1}. The temperature was maintained at 15°C using a ThermoScientific circulating bath and thermostat. Samples were prepared with a concentration of 2.5 mg·ml^{-1} in the eluent mixture and the injection volume was 100 μl. The analysis was performed using a modified Viscotek TDA 301, mainly using the RALS detector and a Viscotek UV2600 detector, set to a wavelength of 260 nm. For the calculation of the molecular weight by NP-IIC, the dn/dc utilised was 0.1 ml·g^{-1}, previously determined in house. The calibration was achieved using a narrow dispersity PS standard (66 kg·mol^{-1}).

Electrospray-Liquid chromatography (ESI-LC) low resolution (LR) and high resolution (HR) mass spectra were recorded using a *LCT Premier XE* mass spectrometer and an *Acquity UPLC* (Waters Ltd, UK).

3.2.3 SYNTHESIS OF POLYPEGMEM MACROMONOMERS BY ANIONIC POLYMERISATION (POLYPEGMEM-OSI)

The synthesis of PolyPEGMEM macromonomers by anionic polymerisation was performed using standard high vacuum techniques.

Before the reaction, LiCl (42mg, 1mmol) was added to the reaction flask, which was kept open up to the high-vacuum pump overnight, while heating it up at 120°C. In a separate flask, DPE-OSi (133 mg, 0.3 mmol) was azeotropically dried 3 times with benzene (~10 ml), solubilised in dry THF (~5 ml), and then injected by syringe into the flask with LiCl. The solution was stirred until complete dissolution of LiCl and then *sec*-BuLi was added drop wise until an orange/red colour of DPE-OSi anion persisted. The required amount of *sec*-BuLi (150µl, 0.2 mmol) for a target molar mass of 10,000 g·mol^{-1} was injected to activate DPE-OSi (deep red colour) and form the initiator for this polymerisation. After waiting 2 hours, to ensure the complete activation of DPE-OSi, the initiator mixture was cooled to -78°C, before the addition of the monomer.

PEGMEM (2.0 g, 6.7 mmol) was dried and degassed over CaH$_2$ under high vacuum, before being distilled into another flask, where Et$_3$Al was injected dropwise until a pale yellow colour appeared. The purified monomer was then distilled into reaction flask containing the initiator solution at −78°C. After 3 hours the polymerisation was terminated with nitrogen-sparged methanol. The polymer was precipitated in hexane as a viscous liquid, allowed to settle to the bottom of the beaker, and the supernatant liquor was decanted away. The polymer was, finally, dried under vacuum. Yield 86%.

M$_n$ 17,700 g·mol^{-1}, M$_w$ 19,600 g·mol^{-1}, Đ 1.11.

^{1}H NMR (400 MHz, CDCl$_3$, δ): 7.1 – 6.9 (4H, DPE-OSi aromatics), 6.8 – 6.6 (4H, DPE-OSi aromatics), 4.2 – 4.0 (2H, COOC$\underline{H}_2$CH$_2$O), 3.8 – 3.5 (18H, COOCH$_2$C$\underline{H}_2$O(C$\underline{H}_2$C$\underline{H}_2$O)$_4$CH$_3$), 3.4 – 3.3 (3H, (CH$_2$CH$_2$O)$_4$C$\underline{H}_3$), 2.2 – 1.7 (2H, backbone C$\underline{H}_2$CCH$_3$), 1.0 – 0.7 (3H, backbone CH$_2$CC$\underline{H}_3$), 0.9 (18H, (C$\underline{H}_3$)$_3$C-Si), 0.1 (12H, (C$\underline{H}_3$)$_2$Si).

3.2.3.1 Deprotection of PolyPEGMEM-OSi to yield PolyPEGMEM-OH

The protected PolyPEGMEM-OSi was deprotected by treating the polymer (1.45 g, 0.08 mmol) with TBAF (160 μl of a solution 1M in THF, 0.16 mmol) in 15 ml of THF at 0°C for 15 minutes. The reaction was quenched with an aqueous solution of NH_4Cl, then the polymer was collected by precipitation in hexane. Yield 98%.

M_n 18,000 g·mol^{-1}, M_w 19,600 g·mol^{-1}, Đ 1.09.

^{1}H NMR (400 MHz, CDCl$_3$, δ): 7.1 – 6.9 (4H, DPE aromatics), 6.8 – 6.6 (4H, DPE-OH aromatics), 4.2 – 4.0 (2H, COOC$\underline{H_2}$CH$_2$O), 3.8 – 3.5 (18H, COOCH$_2$C$\underline{H_2}$O(C$\underline{H_2}$C$\underline{H_2}$O)$_4$CH$_3$), 3.4 – 3.3 (3H, COOCH$_2$CH$_2$O(CH$_2$CH$_2$O)$_4$ C$\underline{H_3}$), 2.2 – 1.7 (2H, backbone C$\underline{H_2}$CCH$_3$), 1.0 – 0.7 (3H, backbone CH$_2$CC$\underline{H_3}$).

3.2.4 SYNTHESIS OF DPE-OSi DERIVED ATRP INITIATOR (BP-Br)

DPE-OSi (4.99 g, 11.3 mmol) was azeotropically dried 3 times through the vacuum distillation into and out of ~5 ml of dry benzene. Finally, ~20 ml of fresh dry benzene was distilled to dissolve the DPE-OSi and the solution was titrated with *sec*-BuLi, until the typical red colour of diphenylhexyl anion persisted. Afterwards, the required amount of *sec*-BuLi (9.7 ml, 13.6 mmol) was injected. After 1 hour, propylene oxide (1.6 ml, 22.7 mmol) was injected, causing the colour of the reaction to change to orange. The reaction was stirred overnight at room temperature, then quenched with acidic (HCl) methanol. Upon complete removal of benzene by distillation, the crude product was dissolved in DCM, washed with distilled water and dried with MgSO$_4$. Upon evaporation of solvent, a sample was collected for NMR analysis.
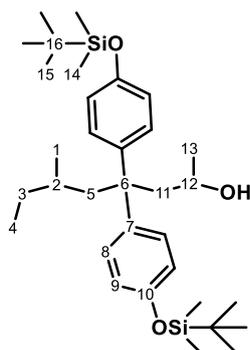
^{1}H NMR (700 MHz, CDCl$_3$, δ)*: 7.15 - 7.00 (8H, m, H8), 6.81 - 6.69 (8H, m, H9), 3.84 - 3.75 (2H, m, H12), 2.31 (2H, dd, *J*=14.3, 1.9 Hz, H11$_1$), 2.15 - 2.08 (2H, overlapping, H11$_2$), 2.15 - 2.12 (1H, overlapping, H5$_1$), 2.05 (1H, dd, *J*=13.8, 3.8 Hz, H5$_1$'), 1.97 (1H, dd, *J*=13.7, 5.6 Hz, H5$_2$'), 1.89 (1H, dd, *J*=13.8, 5.8 Hz, H5$_2$),1.22 – 1.12 (2H, m, H2), 1.07 (6H, t, *J*=6.4 Hz, H13), 1.04 – 0.96 (2H, overlapping, H3$_1$), 0.96 (36H, s, H15), 0.95 – 0.88 (2H, m, H3$_2$), 0.72 – 0.67 (3H, m, H4), 0.64 - 0.60 (3H, overlapping, H4'), 0.61 - 0.57 (3H, overlapping, H1), 0.47 (3H, d, *J*=6.7 Hz, H1'), 0.16 (24H, s, H14z).

^{13}C NMR (176 MHz, CDCl$_3$, δ)*: 153.8 (C10), 153.6 (C10), 141.5 (C7), 140.9 (C7'), 129.2 (C8), 128.9 (C8'), 119.7 (C9), 119.4 (C9'), 65.0 (C12), 47.9 (C6), 47.8 (C11), 46.0 (C5'), 45.9 (C5), 31.7 (C3), 31.4 (C3'), 30.3 (C2), 30.1 (C2'), 25.7 (C15), 24.5 (C13), 24.4 (C13'), 21.3 (C1), 21.1 (C1'), 18.2 (C16), 11.4 (C4), 11.2 (C4'), -4.5 (C14).

The product was azeotropically dried 3 times with benzene and dissolved in dry DCM with Et$_3$N (3.2 ml, 22.7 mmol). The solution was cooled at 0°C before the addition of α-bromoisobutyryl bromide (4.2 ml, 33.9 mmol), then kept at that temperature for 3 hours and finally allowed to warm to room temperature and stirred overnight. After that time, the reaction was washed with saturated NaHCO$_3$ in a separating funnel, the organic phase collected, dried over MgSO$_4$ and, after removal of the MgSO$_4$ by filtration, the solvent was evaporated by rotavap. The residue was dissolved in THF (~10 ml), to perform the deprotection of the phenyl groups. For this purpose, TBAF (23 ml, 22.7 mmol) was added at 0°C and after 15 minutes the reaction was quenched with NH$_4$Cl. Upon evaporation of THF, the crude mixture was solubilised in DCM, transferred in a separating funnel, washed with distilled water, and the organic phase dried with MgSO$_4$. The crude product, obtained upon filtering MgSO$_4$ and evaporating the

---

* The molecule is synthesised as two couples of enantiomers. For some of them, the same proton or carbon can have different δ, if belonging to one of the other couple of enantiomers. In that case the different signals are labelled as X and X'. There are also 3 diasterotopic protons (3, 5, 11), whose different signals are labelled as X$_1$ and X$_2$.

solvent, was then purified by silica column chromatography using hexane/ethyl acetate (30:70 respectively) as eluent. Yield 42%.

R_f = 0.49, 0.37 (2 spots for each pair of enantiomers).
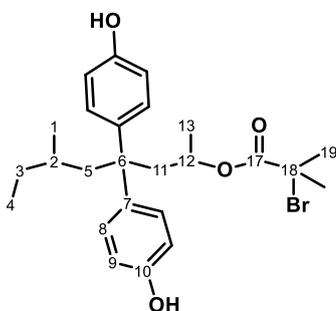
^{1}H NMR (700 MHz, CDCl$_3$, δ)*: 7.03 - 6.95 (8H, m, H8), 6.72 - 6.65 (8H, m, H9), 4.84 (2H, m, H12), 2.55 (2H, m, H11$_1$), 2.24 (2H, m, H11$_2$), 2.13 – 2.09 (1H, m, H5$_1$), 2.07 – 2.03 (1H, m, H5$_1$'), 1.96 – 1.90 (1H, m, H5$_2$'), 1.90 – 1.86 (1H, m, H5$_2$), 1.77 (6H, d, *J*=2.5 Hz, H19$_1$), 1.67 (6H, d, *J*=2.5 Hz, H19$_2$), 1.18 (2H, m, H2), 1.06 (2H, m, H3$_1$), 1.02 - 0.93 (6H, m, H13), 0.90 (2H, m, H3$_2$), 0.69 (3H, dd, *J*=7.4 Hz, H4), 0.66 (3H, dd, *J*=7.4 Hz, H4'), 0.55 (3H, d, *J*=6.7 Hz, H1), 0.50 (3H, d, *J*=6.7 Hz, H1').

^{13}C NMR (176 MHz, CDCl$_3$, δ)*: 170.6 (C17'), 153.4 (C10), 140.6 (C7), 140.3 (C7'), 129.4 (C8), 114.7 (C9), 114.5 (C9'), 70.6 (C12), 70.5 (C12'), 56.5 (C18), 47.8 (C6), 46.0 (C5'), 45.9 (C5), 44.9 (C11), 31.5 (C3), 31.3 (C3'), 30.5 (C19), 30.4 (C19'), 30.3 (C2), 21.3 (C13), 21.2 (C13'), 21.0 (C1), 20.9 (C1'), 11.3 (C4).

LRMS (ESI-TOF) m/z: 475.1 (9.7%), 477.2 (6.6%) [M-H]$^-$; 521.2 (35.0%), 523.2 (38.3%) [M+FA-H]$^-$; 951.2 (47.3%), 953.2 (100.0%), 955.2 (39.7%) [2M-H]$^-$. HRMS (ESI-TOF) m/z: calculated for C25H32O4Br: 475.1484 [M-H]$^-$, found: 475.1497.

3.2.5   SYNTHESIS OF POLYPEGMEM MACROMONOMERS BY ATRP

3.2.5.1   Synthesis of iPolyPEGMEM-OSi via 'initiating procedure'

DPE-OSi (439 mg, 1 mmol), CuBr (145 mg, 1 mmol), bipy (473 mg, 3 mmol) and anisole (~15 ml) were added into a Schlenck flask. In order to follow the reaction over time by NMR, DMF (1.316 ml, 17 mmol) was added as an internal standard.

---

* The molecule is synthesised as two couples of enantiomers. For some of them, the same proton or carbon can have different δ, if belonging to one of the other couple of enantiomers. In that case the different signals are labelled as X and X'. There are also 3 diasterotopic protons (3, 5, 11), whose different signals are labelled as X$_1$ and X$_2$.

The mixture was degassed by 3 freeze-pump-thaw cycles and then backfilled with nitrogen. The reaction solution temperature was raised to 110°C in an oil bath. Ethyl 2-bromoisobutyrate (150 µl, 1 mmol) was then injected and immediately a sample was collected (time t=0). More samples were collected periodically and analysed by NMR. When NMR analysis indicated that the vinyl proton signal of DPE-OSi had almost disappeared, a solution of the PEGMEM monomer (5 g, 17 mmol) in ~5 ml of anisole, which had previously been subjected to a freeze-pump-thaw cycle, was injected and the temperature lowered to 90°C. The reaction was quenched after 48 hours by exposing it to air, diluted with THF, and filtered through activated neutral alumina to remove copper salts. The polymer was precipitated in hexane as a viscous liquid, allowed to settle to the bottom of the beaker, and the supernatant liquor was decanted away. The polymer was, finally, dried under vacuum. Yield 6%.

M_n 10,200 g·mol^{-1}, M_w 14,100 g·mol^{-1}, Đ 1.38.

^{1}H NMR (400 MHz, CDCl$_3$, δ): 4.2 – 4.0 (2H, COOC<u>H$_2$</u>CH$_2$O), 4.0 – 3.4 (18H, COOCH$_2$C<u>H$_2$</u>O(C<u>H$_2$</u>C<u>H$_2$</u>O)$_4$CH$_3$), 3.4 – 3.2 (3H, COOCH$_2$CH$_2$O(CH$_2$CH$_2$O)$_4$ C<u>H$_3$</u>), 2.2 – 0.6 (5H, backbone C<u>H$_2$</u>C(CO)C<u>H$_3$</u>).

3.2.5.2   Synthesis of ePolyPEGMEM-OSi via 'Direct end-capping procedure'

For ePolyPEGMEM1, PEGMEM (5 g, 17 mmol), CuBr (158 mg, 1 mmol), bipy (466 mg, 3 mmol) and anisole (15 ml) were added into a flask. In order to follow the conversion over time by NMR, DMF (1.316 ml, 17 mmol) was added as an internal standard. The mixture was degassed by 3 freeze-pump-thaw cycles and then backfilled with nitrogen.

After raising the reaction temperature to 90°C using an oil bath, the polymerisation was initiated by injecting ethyl 2-bromoisobutyrate (150 µl, 1 mmol) for a theoretical M_n of 5,000 g·mol^{-1}. A sample was immediately collected for analysis (time t=0) and further samples were collected periodically and analysed by NMR, in order to calculate the conversion. When the reaction was at completion (conversion >90%), a solution of DPE-OSi (881 mg, 2 mmol) in

anisole (5 ml), which had previously been degassed by 3 freeze-pump-thaw cycles and back-filled with nitrogen, was injected and a sample immediately collected for NMR analysis, followed by further samples collected periodically. When no more changes in the DPE-OSi vinyl protons NMR signals were detected, the reaction was cooled and quenched by exposing it to air, diluted with THF, and filtered through activated neutral alumina to remove the copper salts. The polymer was precipitated in hexane as a viscous liquid, allowed to settle to the bottom of the beaker, and the supernatant liquor was decanted away. The polymer was, finally, dried under vacuum. Yield 52%.

M_n 8,100 g·mol^{-1}, M_w 9,900 g·mol^{-1}, Đ 1.22.

^{1}H NMR (400 MHz, CDCl$_3$, δ): 4.2 – 4.0 (2H, COOC$\underline{H}_2$CH$_2$O), 3.8 – 3.5 (18H, COOCH$_2$C$\underline{H}_2$O(C$\underline{H}_2$C$\underline{H}_2$O)$_4$CH$_3$), 3.4 (3H, COOCH$_2$CH$_2$O(CH$_2$CH$_2$O)$_8$C$\underline{H}_3$), 2.0 - 0.8 (5H, backbone C$\underline{H}_2$C(CO)C$\underline{H}_3$).

A second reaction was performed, ePolyPEGMEM2, keeping the same conditions - PEGMEM (5 g, 17 mmol), CuBr (150 mg, 1 mmol), bipy (474 mg, 3 mmol), anisole (15 ml), DMF (1.316 ml, 17 mmol), oil bath at 90°C, ethyl 2-bromoisobutyrate (150 μl, 1 mmol), DPE-OSi (884 mg, 2 mmol) in anisole (5 ml) - but in this case the temperature was raised to 110ºC after the addition of DPE-OSi. Yield 56%.

M_n 7,400 g·mol^{-1}, M_w 9,100 g·mol^{-1}, Đ 1.23.

^{1}H NMR (400 MHz, CDCl$_3$, δ): 4.2 – 4.0 (2H, COOC$\underline{H}_2$CH$_2$O), 3.7 – 3.5 (18H, COOCH$_2$C$\underline{H}_2$O(C$\underline{H}_2$C$\underline{H}_2$O)$_4$CH$_3$), 3.4 (3H, COOCH$_2$CH$_2$O(CH$_2$CH$_2$O)$_8$C$\underline{H}_3$), 2.0 - 0.7 (5H, backbone C$\underline{H}_2$C(CO)C$\underline{H}_3$).

3.2.5.3 <u>Synthesis of ePolyPEGMEM-OSi via 'Post polymerisation end-capping procedure'</u>

For the synthesis of ePolyPEGMEM3, PEGMEM (5 g, 17 mmol), CuBr (152 mg, 1 mmol), bipy (324 mg, 2 mmol) and toluene (15 ml) were added into a flask. In order to follow the conversion over time by NMR, DMF (1.316 ml, 17 mmol) was

added as internal standard. The mixture was degassed by 3 freeze-pump-thaw cycles and then backfilled with nitrogen.

After raising the reaction temperature in an oil bath to 80ºC, the polymerisation was initiated by injecting ethyl 2-bromoisobutyrate (147 μl, 1 mmol) for a theoretical M_n of 5,000 g·mol^{-1}. A sample was immediately collected for analysis (time t=0) and then more samples were collected periodically and analysed by NMR, in order to calculate the conversion. When the reaction was at completion (conversion >90%), it was quenched by exposure to air, diluted with THF, and filtered through activated neutral alumina to remove copper salts. The polymer was precipitated in hexane as a viscous liquid, allowed to settle to the bottom of the beaker, and the supernatant liquor was decanted away. The polymer was, finally, dried under vacuum. Yield 64%.

M_n 8,300 g·mol^{-1}, M_w 10,700 g·mol^{-1}, Đ 1.29.

^{1}H NMR (400 MHz, CDCl$_3$, δ): 4.2 – 4.0 (2H, COOC$\underline{H_2}$CH$_2$O), 3.8 – 3.5 (18H, COOCH$_2$C$\underline{H_2}$O(C$\underline{H_2}$C$\underline{H_2}$O)$_4$CH$_3$), 3.4 (3H, COOCH$_2$CH$_2$O(CH$_2$CH$_2$O)$_4$C$\underline{H_3}$), 2.0 - 0.8 (5H, backbone C$\underline{H_2}$C(CO)C$\underline{H_3}$).

To perform the end-capping reaction to produce ePolyPEGMEM3A, PolyPEGMEM3, (0.999g, 0.1 mmol), DPE-OSi (0.264 mg, 0.6 mmol), PMDETA (42 μl, 0.2 mmol) and toluene (~5 ml) were added into one flasks of a 2-flask reactor, together with DMF (93 μl, 1.2 mmol) as an internal standard for NMR. The mixture (solution 1) was degassed by 3 freeze-pump-thaw cycles and then backfilled with nitrogen. In the second flask of the reactor, CuBr (20 mg, 0.1 mmol) was degassed and backfilled with nitrogen. The end-capping reaction was started by pouring solution 1 into the flask with CuBr and heating it in an oil bath at 80°C. A sample was immediately collected for analysis (time t=0). After 4 days the reaction was cooled and quenched by exposing it to air, diluted with THF, and filtered through activated neutral alumina to remove copper salts. The polymer was precipitated in hexane as a viscous liquid, allowed to settle to the bottom of the beaker, and the supernatant liquor was decanted away. The polymer was, finally, dried under vacuum. Yield 44%.

^{1}H NMR (400 MHz, CDCl$_3$, δ): 4.2 – 4.0 (2H, COOC**H$_2$**CH$_2$O), 3.8 – 3.5 (18H, COOCH$_2$C**H$_2$**O(C**H$_2$**C**H$_2$**O)$_4$CH$_3$), 3.4 (3H, COOCH$_2$CH$_2$O(CH$_2$CH$_2$O)$_4$C**H$_3$**), 2.0 - 0.8 (5H, backbone C**H$_2$**C(CO)C**H$_3$**).

A second attempt was made, ePolyPEGMEM3B, using PolyPEGMEM3 (0.998 g 0.1 mmol), CuBr (21 mg, 0.1 mmol), DPE-OSi (266 mg, 0.6 mmol) and DMF (93 µl, 1.2 mmol), but with bipy as the ligand (37 mg, 0.2 mmol) and anisole as the solvent at 90°C. Yield 15%.

^{1}H NMR (400 MHz, CDCl$_3$, δ): 4.2 – 4.0 (2H, COOC**H$_2$**CH$_2$O), 3.7 – 3.5 (18H, COOCH$_2$C**H$_2$**O(C**H$_2$**C**H$_2$**O)$_4$CH$_3$), 3.4 (3H, COOCH$_2$CH$_2$O(CH$_2$CH$_2$O)$_4$C**H$_3$**), 2.0 - 0.8 (5H, backbone C**H$_2$**C(CO)C**H$_3$**).

3.2.5.4   Synthesis of bisphenol end-functionalised PolyPEGMEM-OH macromonomers using a functionalised ATRP initiator (BP-Br)

PEGMEM (3.25 g, 11 mmol), CuBr (102 mg, 0.71 mmol), PMDETA (407 µg, 1.95 mmol) and toluene (20 ml) were added into a flask, together with DMF (851 µl, 11 mmol) as internal standard for NMR analysis. The mixture was degassed by 3 freeze-pump-thaw cycles and then backfilled with nitrogen. After raising the reaction temperature in an oil bath to 60°C, the polymerisation was initiated by injecting a solution of BP-Br (312 mg, 0.65 mmol) in toluene (5 ml) previously degassed by a 3-freeze-pump-thaw cycles, for a theoretical M_n of 5,000 g·mol^{-1}. A sample was immediately collected for analysis (time t=0). By NMR analysis of subsequent samples it was possible to follow the conversion, and when it was at ~70%, it was quenched by cooling with liquid nitrogen and exposing it to air, the solution diluted with THF, and filtered through activated neutral alumina to remove the copper salts. The polymer was precipitated in hexane as a viscous liquid, allowed to settle to the bottom of the beaker, and the supernatant liquor was decanted away. The recovered polymer was dried under vacuum. Yield 82%.

M_n 12,700 g·mol^{-1}, M_w 17,200 g·mol^{-1}, Đ 1.35.

A second attempt was performed, PolyPEGMEM-OH2, with the same conditions, using PEGMEM (5 g, 16.7 mmol), CuBr (165 mg, 1.2 mmol), PMDETA (420 µg, 2.0 mmol), anisole (20 ml), DMF (1.3 ml, 16.7 mmol), oil bath at 90°C, BP-Br (481 mg, 1.0 mmol) in anisole (5 ml). Yield 53%.

M_n 21,200 g·mol^{-1}, M_w 23,700 g·mol^{-1}, Đ 1.12.

^{1}H NMR (400 MHz, CDCl$_3$, δ): 7.2 – 6.9 (8H, DPE aromatics), 6.8 – 6.6 (8H, DPE aromatics), 4.8 – 4.6 (2H, BP-Br H12), 4.2 – 4.0 (2n·H, COOC$\underline{H_2}$CH$_2$O), 3.8 - 3.5 (18n·H, COOCH$_2$C$\underline{H_2}$O(C$\underline{H_2}$C$\underline{H_2}$O)$_4$CH$_3$), 3.4 (3n·H, COOCH$_2$CH$_2$O(CH$_2$CH$_2$O)$_4$C$\underline{H_3}$), 2.0 – 0.8 (5n·H, backbone C$\underline{H_2}$C(CO)C$\underline{H_3}$).

3.2.5.5 Synthesis of bisphenol end-functionalised Poly(PEGMEM-*co*-MMA)-OH macromonomers using a functionalised ATRP initiator (BP-Br)

PEGMEM (990 mg, 3.3 mmol), MMA (330 mg, 3.3 mmol), CuBr (87 mg, 0.6 mmol), bipy (159 mg, 1.0 mmol), DMF (255 µl, 3.3 mmol) as internal standard for NMR analysis and anisole (10 ml) were added into a flask. The mixture was degassed by 3 freeze-pump-thaw cycles and then backfilled with nitrogen. After raising the reaction temperature in an oil bath to 90°C, the polymerisation was initiated by injecting a solution of BP-Br (242 mg, 0.5 mmol) in anisole (2 ml) previously degassed by a 3-freeze-pump-thaw cycles, for a theoretical M_n of 2,600 g·mol^{-1}. A sample was immediately collected for analysis (time t=0). After 2 hours and 30 minutes, the reaction was quenched by cooling and exposing it to air, the solution was diluted with THF (~20 ml) and filtered through activated neutral alumina to remove the copper salts. The polymer was precipitated in hexane as a viscous liquid, allowed to settle to the bottom of the beaker, and the supernatant liquor was decanted away. The polymer was, finally, dried under vacuum. Yield 86%.

M_n 15,300 g·mol^{-1}, M_w 18,700 g·mol^{-1}, Đ 1.22.

^{1}H NMR (400 MHz, CDCl$_3$, δ): 7.2 – 6.9 (8H, DPE aromatics), 6.8 – 6.6 (8H, DPE aromatics), 4.8 – 4.6 (2H, HO-DPE-Br H12), 4.2 – 4.0 (2n·H, COOC$\underline{H_2}$CH$_2$O),

3.8 - 3.5 (18n·H, COOCH$_2$C$\underline{H_2}$O(C$\underline{H_2}$C$\underline{H_2}$O)$_4$CH$_3$), 3.4 (3n·H, COOCH$_2$CH$_2$O (CH$_2$CH$_2$O)$_4$C$\underline{H_3}$), 2.0 – 0.8 (5n·H, backbone C$\underline{H_2}$C(CO)C$\underline{H_3}$).

3.2.5.6 Synthesis of bisphenol end-functionalised PS-OH macromonomers using a functionalised ATRP initiator (BP-Br)

Styrene (1.1 g, 10.5 mmol), CuBr (91 mg, 0.6 mmol), PMDETA (208 µl, 1.0 mmol) and anisole (516 µl, 4.7 mmol) as internal standard for NMR were added into a flask. The solution was degassed by 3 freeze-pump-thaw cycles and then backfilled with nitrogen. After raising the reaction temperature in an oil bath to 130°C, the polymerisation was initiated by injecting a solution of BP-Br (255 mg, 0.5 mmol) in styrene (0.9 g, 8.6 mmol) previously degassed by a 3-freeze-pump-thaw cycles. A sample was immediately collected for analysis (time t=0). After 2 hours and 20 minutes the reaction was quenched by cooling and exposing it to air, the solution was diluted with THF (~20 ml) and filtered through activated neutral alumina to remove the copper salts. The polymer was precipitated into excess methanol, re-dissolved in THF, precipitated again into methanol, collected by filtration and dried to constant mass under vacuum. Yield 52%.

M_n 29,700 g·mol^{-1}, M_w 55,200 g·mol^{-1}, Đ 1.86.

^{1}H NMR (400 MHz, CDCl$_3$, δ): 7.3 – 6.2 (Ar $\underline{H}$), 2.5 – 1.1 (aliphatic $\underline{H}$), 0.8 - 0.4 (BP-Br H1 H1' and H4 H4').

3.3 RESULTS AND DISCUSSION

The 'macromonomer' approach for the synthesis of complex branched architectures has been shown to be very versatile. To demonstrate the versatility of this approach in the context of this project, and to allow the synthesis of graft block copolymers with varying properties, different macromonomers have been synthesised. In the previous Chapter the synthesis of hydrophobic, non-polar polystyrene macromonomers was described, and now the synthesis of

hydrophilic poly(ethylene glycol) methyl ether methacrylate (PEGMEM) macromonomers will be described.

Initial attempts to synthesise PEGMEM macromonomers using anionic polymerisation were successful, but not without significant practical challenges. For this reason, synthetic approaches to prepare PEGMEM macromonomers using atom transfer radical polymerisation will also be described.

3.3.1   SYNTHESIS OF POLYPEGMEM MACROMONOMERS BY AP

The polymerisation of methacrylate monomers by anionic polymerisation is complicated by the presence of the carbonyl group as a site for side reactions by nucleophilic attack by the carbanion of both the initiator and the propagating chain. In the initiating step, these side reactions are usually kept under control using a bulky and less nucleophilic initiator. A common strategy is the use of DPE carbanion, obtained upon alkyllithium attack.[1,3]

The kinetics of the propagation step of methacrylate monomers is also complicated by the presence of multiple equilibria between species with different degrees of charge separation (Scheme 3.1), each one having its own propagation rate constant, k_p^x, and resulting usually in a broad dispersity of the final polymer.
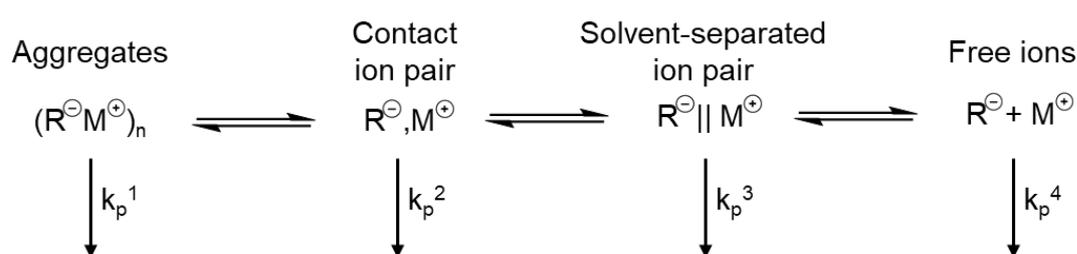
Scheme 3.1 Equilibria among different degree of charge separation of ion species during the propagation step in anionic polymerisation of methacrylate monomers.[3]

In general, polar solvents tend to shift the equilibria in Scheme 3.1 to the right, thus giving lower degree of aggregation and, therefore, a more homogeneous distribution. However, it is only with the addition of lithium chloride or alkoxides, that it is possible to effectively control the anionic polymerisation of methacrylate

monomers, obtaining dispersity below 1.1 and high conversion. It has been proved that lithium chloride effectively promotes the dissociation of aggregated propagating anions, while alkali metal alkoxides also contribute to reduce the rate of termination caused by intramolecular backbiting reaction.[3] The latter is a common side reaction during the propagation step, caused by the attack of the lithium ester enolate onto one of the carbonyl group on the same chain. These reactions are usually promoted when intramolecularly solvated species (A in Scheme 3.2) are formed. The presence of polar solvent, such as THF, and alkali metal alkoxides has been found to prevent backbiting by the formation of solvated contact ion pairs (B in Scheme 3.2).[1] Moreover, the rate of this unimolecular termination reaction at low temperatures ($<$-75 $^{\circ}$C) has been found to be lower than the rate of propagation by a factor of approximately 10^4.[3]
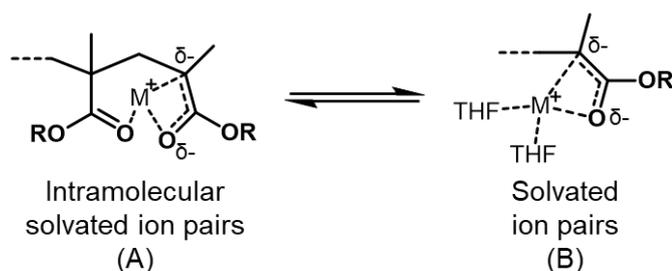
Scheme 3.2 Propagation via contact ion pairs in PMMA.[1]

Among methacrylate monomers, the anionic polymerisation of PEGMEM is further complicated by the presence of the PEO side chains, making the monomer highly hygroscopic, and by the high boiling point of PEGMEM (141°C), which make its distillation difficult even under high-vacuum conditions. The common methods of monomer purification require drying over CaH_2 and degassing under high vacuum, and then, following distillation in a separate flask, the dropwise addition of Et_3Al, which reacts with traces of moisture, alcohol and other protic impurities. Complete removal of protic impurities is indicated by a pale yellow colour arising from the formation of a complex between free Et_3Al and the carbonyl group of PEGMEM monomers. [1] Usually, the trialkyl aluminium is chosen with a higher boiling point than that of the monomer to avoid co-distillation, which will contaminate the pure monomer. In this case, this was

basically impossible, because of the high boiling point of PEGMEM, therefore the possible presence of free Et$_3$Al was accepted, whilst being careful in the addition of the purifying agent, so that the minimum amount of free Et$_3$Al was present in the monomer.

The reaction conditions chosen for the LAP synthesis of PolyPEGMEM macromonomers are summarised in Scheme 3.3.
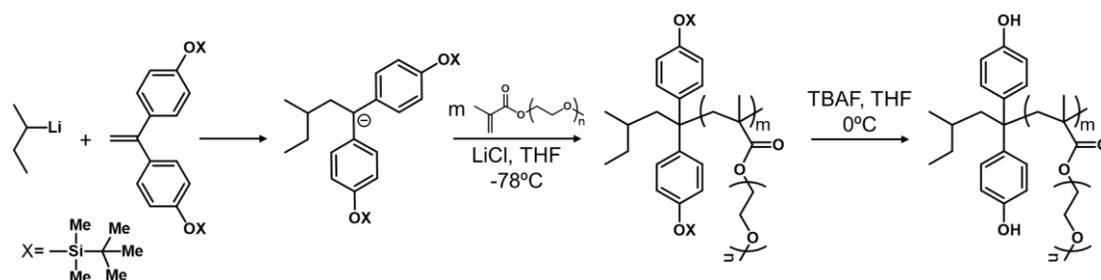
Scheme 3.3 Synthesis of PolyPEGMEM macromonomer by anionic polymerisation, via initiating approach with DPE-OSi.

The approach is the same as the initiating procedure used for the synthesis of PS macromonomers in Chapter 2. Even though it was shown that the end-capping approach is much better for the aim of obtaining strict control over the functionalisation of macromonomers, in this case, with a methacrylate derivative monomer, there is no alternative. Bulky DPE initiators are commonly used for the initiation of methacrylate monomers in anionic polymerisation, and the presence of the silyl ether in para positions contributes to make the species even less nucleophilic. In this way the attack on the carbonyl carbon by the initiator is prevented. Moreover, the end-capping reaction with DPE-OSi is not possible, because the delocalisation of the negative charge on the electrophilic oxygen atom makes the carbanion on a methacrylic unit less nucleophilic and, therefore, not reactive enough to attack DPE. The use of a polar solvent at low temperatures reduce the side reactions (termination) during the propagation step, and the presence of lithium chloride also enhances the dissociation of the anionic propagating species. All these chosen conditions contribute to improve the final conversion and the dispersity.

An initial attempt to prepare PolyPEGMEM with a target molar mass of 10 kg·mol^{-1} resulted in a polymer with a SEC-determined M$_n$ of 17.7 kg·mol^{-1}, almost double

the target. This was most likely due to incomplete purification of the hygroscopic monomer: residual impurities introduced with the monomer can deactivate part of the initiator, giving higher MW. The dispersity (1.11), on the other hand, is a little high for an anionic polymerisation, but still acceptable, and the yield (89%) is acceptable , suggesting that the reaction conditions chosen were effective to improve charge separation and prevent intramolecular reactions that cause termination, as discussed above.
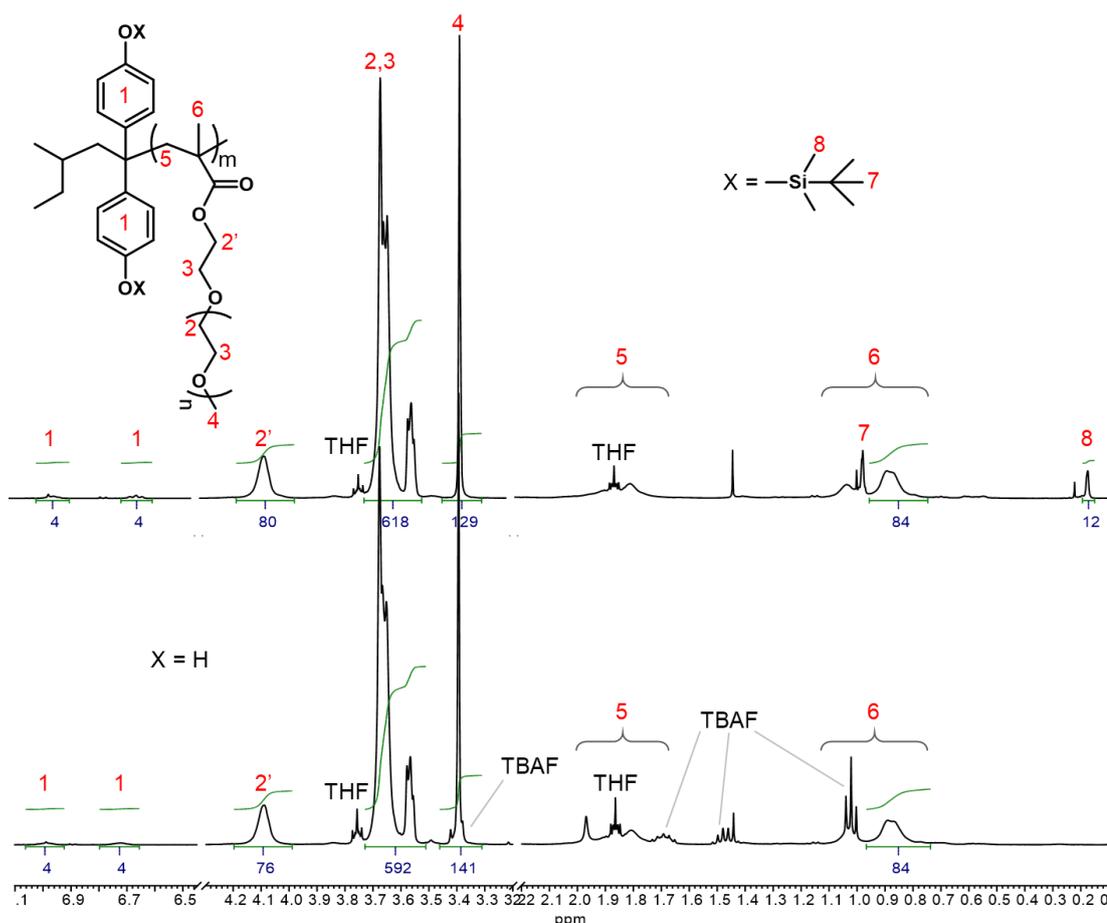
Figure 3.2 ^{1}H NMR (CDCl$_3$, 400 MHz) spectra of PolyPEGMEM macromonomer synthesised by anionic polymerisation, before (upper trace) and after (lower trace) the deprotection reaction with TBAF.

^{1}H NMR analysis of the resulting polymer (see Figure 3.2) confirms the presence of the bisphenol functionality with peaks due the aromatic protons of DPE-OSi at 7.0 and 6.7 ppm and peaks at 0.15 and 0.95 ppm due to the TBDMS protecting group. The average number of DPE-OSi units per chain was determined by comparing the integral of the peak at 3.4 ppm (129, due to 3 equivalent protons

numbered 4 in Figure 3.2 (upper trace) of the PEGMEM repeat unit) to the integral of the methyl protons (peak 8) of TBDMS protecting group: there are 129/3 = 43 PEGMEM repeat units per DPE-OSi units. Moreover, dividing the SEC-calculated (by triple detection, with the relative dn/dc measured in house) M_n of 17,700 g·mol^{-1} by PEGMEM molar mass (300 g·mol^{-1}), gives us a number average degree of polymerisation of 59. Finally, the number average degree of polymerisation (59) divided by the number of PEGMEM monomers per each DPE-OSi unit gives an average value of 1.4 DPE-OSi units per PolyPEGMEM macromonomer chain. We know, from the discussion in Chapter 2 for the synthesis of PS macromonomers, that the initiating procedure gives species with different degrees of functionalisation, because of the difficulty to control the stoichiometry in the initiating step, in which an excess of BuLi would give un-functionalised chains, whereas an excess of DPE-OSi would cause more than one functionalised monomer to be incorporated into the chain. Moreover, the slow reaction between the two can cause the presence of both free BuLi and DPE-OSi at the time of monomer addition, thus explaining the presence of un- and di-functionalised chains simultaneously. The situation is different with methacrylates monomers. It is well known that the reactivity of a propagating methacrylate chain-end is insufficient to allow reaction with styrene monomer – it is not possible to make a PMMA-PS block copolymer by sequential addition of MMA and then styrene.[4] Therefore DPE-OSi, which is even less reactive than styrene as a monomer, because of the electron-donating effect of the silyl-ether groups in para position, could not react as a comonomer in this reaction. Hence, we believe that a value of 1.4 DPE-OSi units per chains, instead of indicating the unlikely presence of chains with more than 1 DPE-OSi unit, must can be due to an error in the analytical techniques. The NMR calculation relies on the relatively small signal of the functional group (CH_3 of the TBDMS protecting group at 0.2 ppm), which may thus cause a certain error. The signal to noise ratio, nevertheless, is good (the signal is sharp and well defined, over the baseline), making us believe that the NMR calculation is reasonably accurate. As for SEC analysis, there can be an error in the determination of dn/dc, which relies on the preparation of a solution of known concentration, to be analysed by SEC.

PEGMEM is difficult to dry properly and therefore the actual concentration of the sample could be lower than expected, because part of the weighed mass could actually be water. Moreover, the dn/dc ($0.069 \, ml \cdot g^{-1}$) value found for PolyPEGMEM is very low, which results in a weak response in the RALS detector, especially for lower MW chains (RALS detector response is proportional to molar mass). This can cause an overestimation of M_n by SEC and may contribute to the high value of DPE-OSi units per chain calculated. In light of all these considerations, it is possible that the M_n calculated by NMR is closer to the real one and that, considering the possible overestimation of M_n by SEC, the discrepancy between the two values might be lower, thus giving a value of DPE-OSi units per chain closer to the unity, instead 1.4 calculated.

The typical deprotection procedure described before for polystyrene macromonomers, using HCl, was deemed unsuitable because of possible hydrolysis of the ester group of PEGMEM. Tetrabutylammonium fluoride (TBAF), which selectively attacks the Si-O bond,[5] was chosen instead. The effective deprotection of the phenol groups is confirmed by NMR (Figure 3.2, lower trace) with the complete disappearance of the TBDMS peaks. Moreover, the integral values of the main peaks in the spectra show only slight changes before and after the deprotection. In particular the ratio between peak 2, 3, 4 (ascribable to PEG side chains[6-7]) and 6 (methyl group in the backbone[6-7]) remains the same (2:15:3:2 respectively), proving that the deprotection was effectively selective for the Si-O ether and did not affect the ester and ether bonds of the PEG side chain. To be thorough, there are small inaccuracies in the integral values considered in the latter discussion, namely: i) peak 4, after deprotection (lower trace), overlaps with a peak arising from residual TBAF used for deprotection of TBDMS group, and shows an integral value which is slightly higher than expected; ii) peak 6, which can be ascribed to the methyl group on the PEGMEM backbone, actually comprises two broad peaks between 1.1 and 0.7 ppm, but only one of it was integrated, because of the overlap with other signals (*t*-Bu of TBDMS protecting group and TBAF) in both spectra. For this reason, the respective value in the ratio is lower than expected (2 instead of 3).

Although reasonably successful, it was concluded that, due to the practical challenges associated with the anionic polymerisation of PEGMEM, and also after the previously discussed issues associated with the initiating approach encountered in the synthesis of PS macromonomers in Chapter 2, this was not a viable way to obtain PolyPEGMEM macromonomers on a reasonable scale. For this reason, efforts were redirected towards the development of an alternative approach based on ATRP.

3.3.2   SYNTHESIS OF POLYPEGMEM-OH MACROMONOMERS BY ATRP

For the reasons discussed above an ATRP-based strategy was developed to synthesise the desired bisphenol functionalised PolyPEGMEM macromonomer. As a first step a series of ATRP reactions were carried out with the aim of optimising the reactions general conditions for the ATRP of PEGMEM. Although there are many examples of the ATRP of PEGMEM reported in the literature, the polymerisation is usually performed in water.[8-11] However, it was considered best to avoid water to limit the need to dry the macromonomer for the subsequent polycondensation reactions. CuBr and ethyl 2-bromoisobutyrate were chosen as catalyst and initiator, respectively, as examples of those commonly used also for the polymerisation of PEGMEM with different side chain lengths. These were used with different combinations of solvent, ligand and reaction temperature. Anisole and toluene were chosen as solvents, having been used as solvent in a limited number of cases for the ATRP of PEGMEM monomers with different side chain lengths[12-14]; 2,2'-bipyridyl (bipy) and pentamethyldiethylenetriamine (PMDETA) were investigated as suitable ligands, and temperatures ranging from 40 to 110°C were used. No particular trend in effectiveness was identified during this preliminary study, and all reactions gave the desired polymer in good yield. None of the reagents seemed to offer any particular advantage, either in terms of control over the molar mass or Đ. Only an increase of temperature, as expected, affected the rate of propagation, making it faster, but usually resulting in a higher dispersity. In light of these results both solvents and both ligands were considered

viable choices for subsequent attempts to prepare bisphenol end-functionalised polyPEGMEM macromonomers.

When using the ATRP mechanism, as with anionic polymerisation, the functional moiety can potentially be introduced as a functionalised monomer - to initiate the polymerisation or to end-cap the chains - or by using a functionalised initiator. In the next sections the results of both approaches will be discussed, whereby DPE-OSi was first used as a monomer via the initiating and end-capping approach, and then used to synthesise a novel functionalised initiator for ATRP.

3.3.2.1   Use of DPE-OSi as functionalised monomer

As seen with anionic polymerisation, the synthesis of a chain-end functionalised macromonomer via ATRP can (theoretically) be achieved by using a functionalised monomer, either as an end-capping agent or at the initiation stage, prior to adding monomer. For the potential use of DPE-OSi, the two approaches are shown in Scheme 3.4.
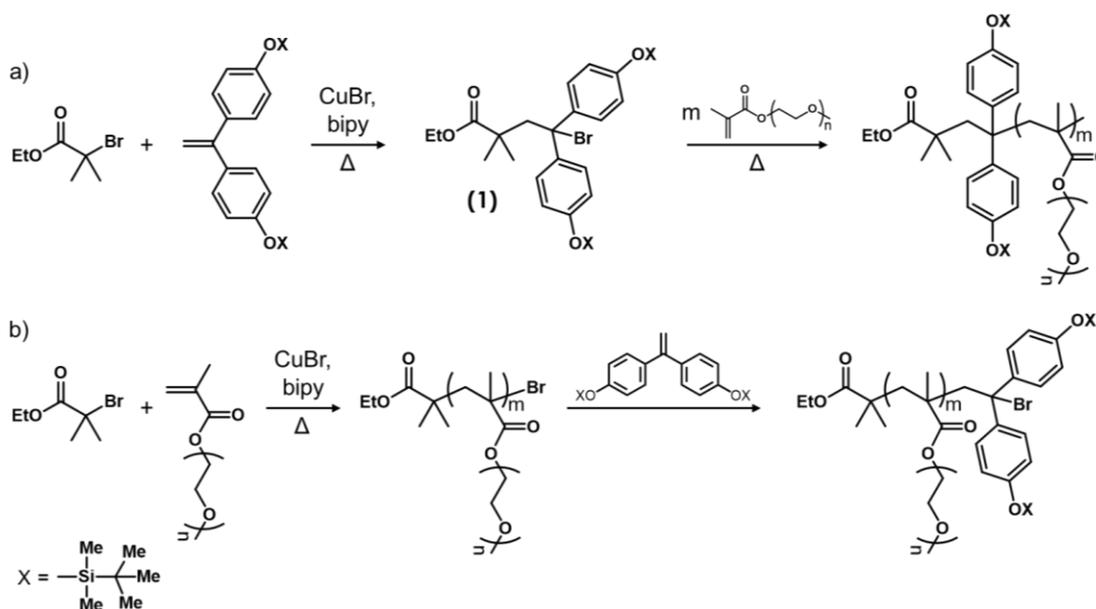
Scheme 3.4 Approaches to end-functionalise PolyPEGMEM via ATRP, using DPE-OSi as monomer: a) by initiation and b) by end-capping procedures.

3.3.2.1.1   The Initiating Approach – iPolyPEGMEM-OSi

A single attempt was carried out to produce a PolyPEGMEM macromonomer via the initiating approach, namely iPolyPEGMEM-OSi. A ratio of 1:1:3:1:17 of initiator, catalyst, ligand, DPE-OSi and monomer, respectively, was used, for a target M_n of 5,000 g·mol^{-1}.

The reaction proceeds in two steps (Scheme 3.4a). Step 1 involves the reaction between the ATRP initiator and DPE-OSi. This was followed by ^{1}H NMR (Figure 3.3), by comparing the intensity of peak due to the vinyl protons of DPE-OSi (peak 1 at 5.3 ppm) with the DMF (internal standard) aldehyde proton peak at 8.1 ppm.
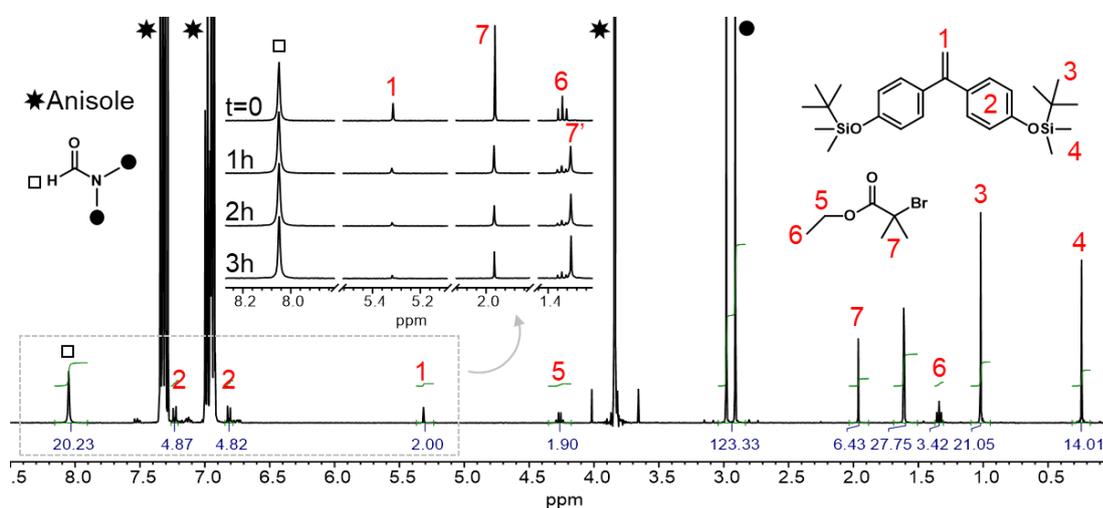
Figure 3.3 ^{1}H NMR (CDCl$_3$, 400 MHz) spectrum of the reaction solution at time 0 for the attempted synthesis by initiating approach of iPolyPEGMEM-OSi. In the insert, the evolution over time of the DPE-OSi vinyl peak (1) and CH$_3$ peak (7) of the initiator, shifting to peak 7' in the adduct initiator-DPE-OSi, during step 1.

The insert in Figure 3.3 shows the rapid disappearance of the vinyl protons peak of DPE-OSi and the shift of peak 7 (CH$_3$ of the ATRP initiator) from 1.9 to 1.3 ppm (peak 7'), suggesting that the DPE-OSi had reacted with the ATRP initiator, giving the ethyl isobutyrate-DPE-OSi bromide adduct (species 1 in Scheme 3.4a).

Step 2 involves the addition of PEGMEM monomer to the product of step 1, with the aim that adduct should initiate the polymerisation, resulting in the functionalised PolyPEGMEM macromonomer. The polymerisation conditions chosen (CuBr as catalyst, bipy as ligand, anisole as solvent, at 90°C) had proved

to be effective in the ATRP of PolyPEGMEM in previous attempts. Progress of step 2 was also analysed by NMR (Figure 3.4), in which the intensity of the vinyl protons peaks (5) of the monomer was monitored.
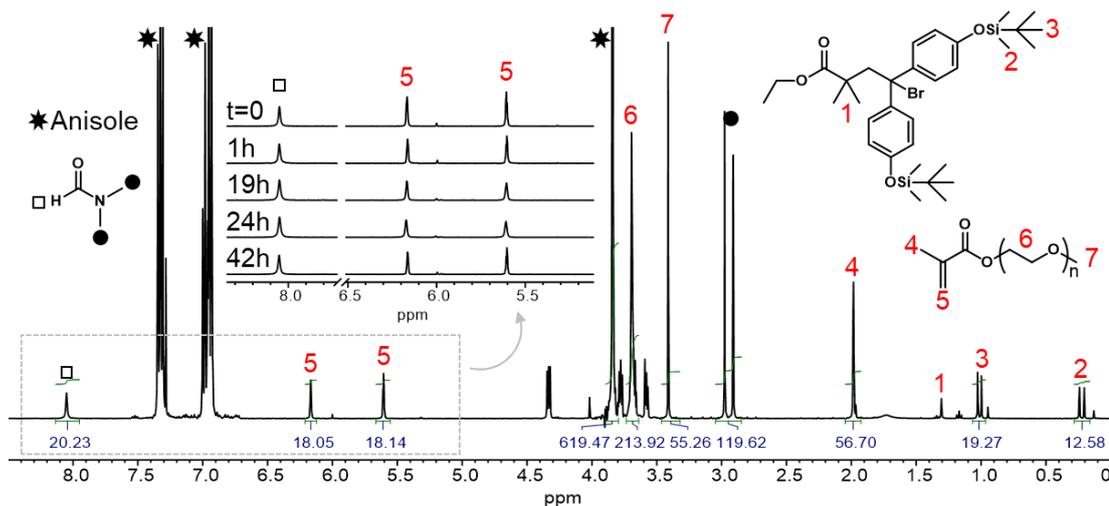
Figure 3.4 ^{1}H NMR (CDCl$_3$, 400 MHz) spectra of the reaction solution at time 0 of step 2 for the attempted synthesis by initiating approach of iPolyPEGMEM-OSi, when the monomer, PEGMEM, is added. In the insert, the evolution over time of the vinyl peaks (5) of PEGMEM.

After 1 hour, the reduction in the integral values of peaks 5 indicated a conversion of about 20%, but only rose to around 30% and remained at this level until the reaction was quenched after 42 hours, as better shown in Figure 3.5.
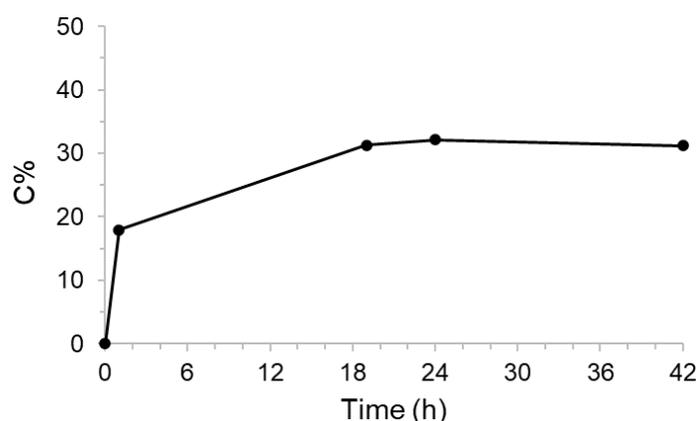
Figure 3.5 Conversion percentage (C%) over time, calculated during step 2 of the attempted synthesis of iPolyPEGMEM-OSi by initiating approach.

This evidence suggests that DPE-OSi adduct is not effective at all as initiator, and the little polymerisation observed (6% yield) is due to traces of residual ethyl 2-bromoisobutyrate. SEC analysis gave a M_n of 10,200 g·mol^{-1}, with Đ 1.38.

The reason why the polymerisation of the monomer was so ineffective can be explained by the role of 1,1-diphenylethene (DPE) in free radical polymerisation: in 2001 Nuyken and coworkers[15] developed a new alternative for controlled radical polymerisation (CRP) by using DPE. The general strategy to make radical polymerisation more or less controllable is to establish an equilibrium between the active radical and a dormant species, so that the instantaneous concentration of active species is kept extremely low. In the so-called DPE method (Scheme 3.5), Nuyken and coworkers found out that such an equilibrium exists between an active propagating chain ($P_1^•$) and the radical formed upon addition of DPE ($P_2^•$).
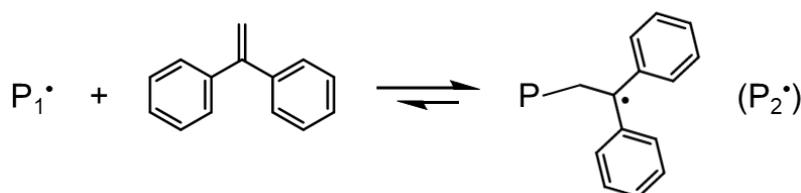
Scheme 3.5 Equilibrium between active and dormant species in the DPE method for CRP.[15]

In this case, therefore, the dormant species is $P_2^•$, as the addition of a monomer to it is very slow due to the stability of the radical, on the benzyl position between two aromatic rings. The reversibility of the reaction in Scheme 3.5, however, would allow the presence of a certain amount of $P_1^•$, which could undergo propagation and continue to grow.

Considering now the use of functionalised DPE-OSi for the initiation of ATRP, what we hoped may occur is summarised in Scheme 3.6. According to the NMR data presented in Figure 3.3 and 3.4, it would appear that step 1 and 2 of Scheme 3.6 were successful. Moreover, the NMR data may suggest that some propagation of PEGMEM occurred after the formation of I-DPE-OSi$^•$ radical species in step 2. However, according to Nuyken[15] step 2 is actually an

equilibrium between two dormant species (the bromide and the bis-benzyl radical), therefore no further propagation can take place after that point and step 3 does not proceed.
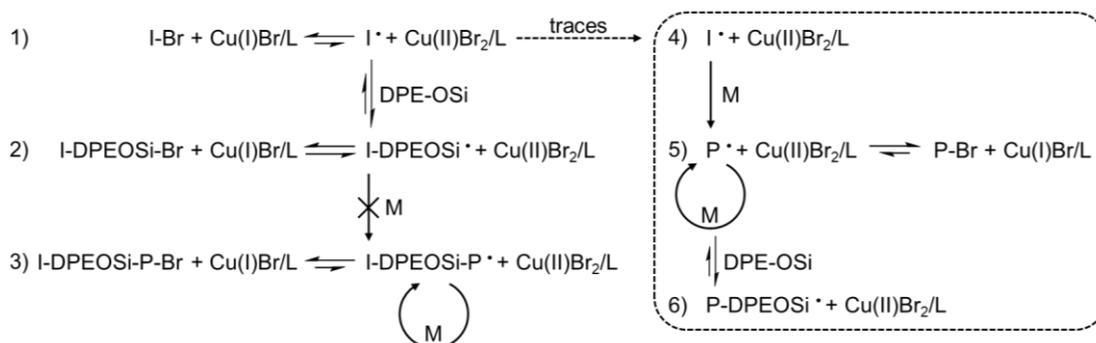
Scheme 3.6 Mechanism of the (ineffective) use of functionalised DPE in an initiating approach by ATRP. L = ligand.

On the other hand, Nuyken also reports that the reaction between ethyl 2-bromoisobutyrate and DPE should also be reversible (Scheme 3.5) and therefore there will be a very low concentration of I$^\bullet$ (derived from ethyl 2-bromoisobutyrate) which can initiate propagation of monomer (step 4 in Scheme 3.6). However, propagation will be really slow because the active species, P$^\bullet$, can either be deactivated by Br (step 5) or DPE-OSi (step 6), to become dormant species.

3.3.2.1.2 End-capping approach – ePolyPEGMEM-OSi

Although it has been shown that the initiating approach was unsuccessful, the role of DPE in radical polymerisation theorised by Nuyken and co-workers does not rule out the possibility of the addition of DPE-OSi as an end-capping agent in an ATRP reaction (Scheme 3.7). In fact, the end-capping of a chain with DPE-OSi should actually be favoured, given the stability of the resulting radical (P-DPEOSi$^\bullet$).

1)   I-Br + Cu(I)Br/L $\rightleftharpoons$ I $^{\bullet}$ + Cu(II)Br$_2$/L

$\downarrow$ M

2)   P-Br + Cu(I)Br/L $\rightleftharpoons$ P $^{\bullet}$ + Cu(II)Br$_2$/L

M

DPE-OSi

3)   P-DPEOSi-Br + Cu(I)Br/L $\rightleftharpoons$ P-DPEOSi $^{\bullet}$ + Cu(II)Br$_2$/L
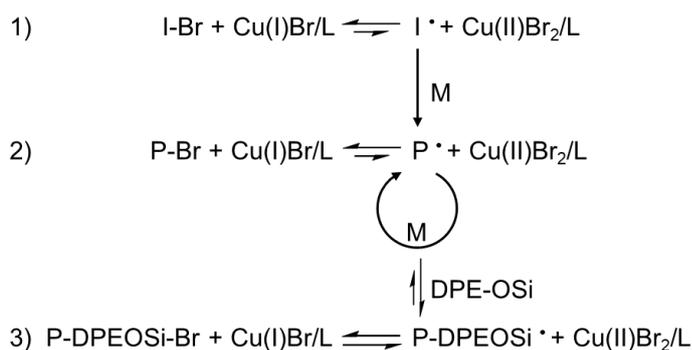
Scheme 3.7 Mechanism of the use of functionalised DPE in an end-capping approach by ATRP. L = ligand.

Thus, a series of ATRP reactions were carried out using DPE-OSi as a monomer, via the end-capping approach. The end-capping approach can itself be performed in two different ways; i) in a so-called direct approach, whereby DPE-OSi is added directly into the reaction mixture after the polymerisation of PEGMEM, without any work-up or; ii) in a post-polymerisation approach, whereby the polymer is first isolated and purified by filtration over alumina, to remove the copper, and recovered by precipitation. The resulting polymer can then be used as a macroinitiator to be end-capped with a DPE-OSi in a brand new ATRP reaction. Each of these procedures were carried out using CuBr as catalyst, ethyl 2-bromoisobutyrate as initiator, and different ligands, solvents and temperatures.

3.3.2.1.2.1 Direct End-Capping Approach

Two reactions (ePolyPEGMEM1 and ePolyPEGMEM2) were performed in which the end-capping was carried out directly after the propagation step. The reaction conditions, together with results for each polymerisation for the macromonomers prepared by direct end-capping approach are summarised in Table 3.1.

The process (Scheme 3.7) consists of 2 steps and the progress of each one was followed by ^{1}H NMR.

Table 3.1 Reagents and polymerisation conditions, yield, molar mass and dispersity values of the ePolyPEGMEM-OSi samples obtained by direct end-capping approach.

	L[a]	S[b]	T(ºC)	r[c]	Conv.	Yield[d]	M_n[e]	Đ
ePolyPEGMEM1	bipy	A	90	1:1:3:2:17	95%	52%	8,100	1.22
ePolyPEGMEM2	bipy	A	90 110	1:1:3:2:17	92%	56%	7,400	1.23

a) Ligand. bipy = 2,2' bipyridyl.
b) Solvent: A = anisole.
c) Ratio among initiator, catalyst, ligand, DPE-OSi and monomer, respectively.
d) Calculated as ratio between the mass of the final product and the percentage of initial mass of monomer given by conversion.
e) Number average molecular weight measured by SEC, in g·mol⁻¹.

For both the attempts made, step 1 consists of the ATRP of PEGMEM, and a successful polymerisation was confirmed by the rapid disappearance of the monomer vinyl peaks (2 in Figure 3.6) at 6.2 and 5.6 ppm.
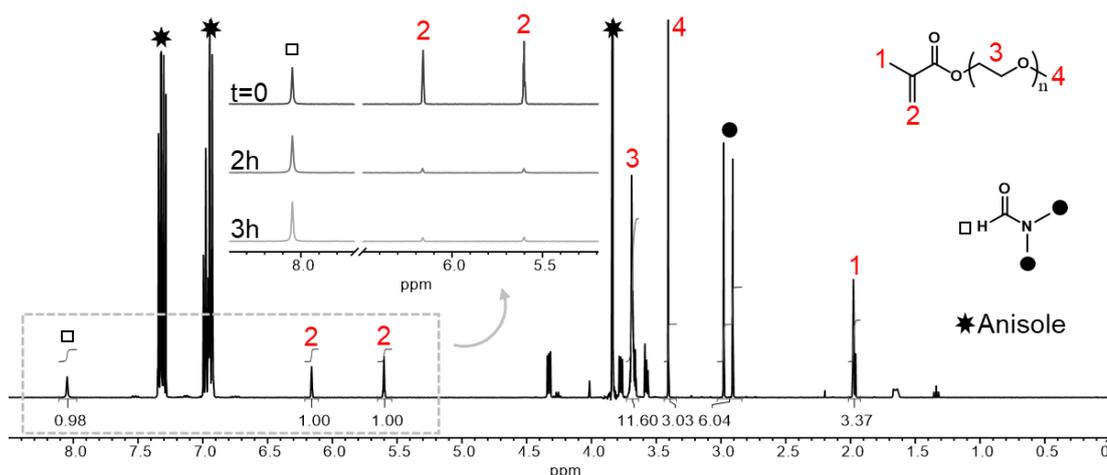
Figure 3.6 ¹H NMR spectra (CDCl₃, 400 MHz) of the reaction solution at time 0 for the synthesis of ePolyPEGMEM1 and, in the insert, the evolution of the vinyl peaks of the monomer (2) over time.

In the case of ePolyPEGMEM1, step 2 - the direct addition of DPE-OSi as end-capping agent - was carried out at 90°C, while for ePolyPEGMEM2 at 110°C. The extent of end-capping with time was followed by NMR (Figure 3.7). In both cases, the signal of DPE-OSi (triangle) shows some fluctuations over time, with respect to the integral value of the reference DMF (circle).

For ePolyPEGMEM1 (Figure 3.7a) there is a small decrease in peak intensity after 21 hours, but then the value remains more or less the same.
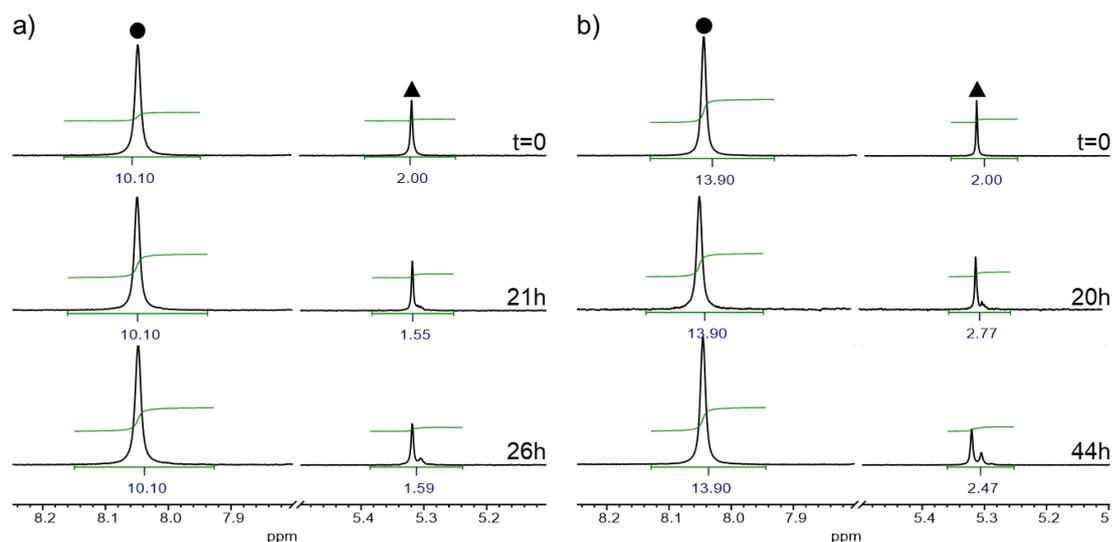
Figure 3.7 Sections of ^{1}H NMR spectra (CDCl$_3$, 400 MHz) of the reaction solution for the synthesis of a) ePolyPEGMEM1 and b) ePolyPEGMEM2 over time, after the addition of DPE-OSi as end-capping agent. (●) DMF aldehyde proton signal; (▲) DPE-OSi vinyl protons signal.

For ePolyPEGMEM2 (Figure 3.7b), the values are even higher than the one at the start of the reaction. As discussed before, it is very unlikely that DPE-OSi is released again, once the active propagating chain attacks it, because of the high stability of the so-formed radical (Scheme 3.5). At the same time, it is not possible to have an increase of DEP-OSi in the reaction solution, as the measurements over time for ePolyPEGMEM2 seem to suggest. Therefore, the fluctuations are probably within the error of the NMR instrument, meaning that no DPE-OSi, or a very little quantity of it, end-capped the PolyPEGMEM chains.

3.3.2.1.2.2 Post Polymerisation End-capping Approach

In a variation to the direct end-capping approach described above, a post-polymerisation approach was also investigated, i.e. the end-capping step was performed after the work-up of the polymer, which was then used as macroinitiator in a new ATRP reaction. Again, this is a two-step process, as shown in Scheme 3.7. In step 1 the polymerisation of PEGMEM worked well, giving a polymer in good yield and dispersity (PolyPEGMEM3 M$_n$ 8,300 g·mol^{-1}, Đ 1.29). In step 2, the end-capping step, the PolyPEGMEM3 was added into one flask of a two-flask reactor acting as a macroinitiator, together with solvent, ligand

and DPE-OSi. After 3 cycles of freeze-pump-thaw, the degassed solution was transferred into the second side flask containing degassed CuBr, with the aim to start the reaction. Two different attempts (ePolyPEGMEM3A and B) were performed, with different reagents and conditions (Table 3.2).

Table 3.2 Reagents and polymerisation conditions, yield, molar mass and dispersity values of the ePolyPEGMEM-OSi samples obtained by post polymerisation end-capping approach.

	L[a]	S[b]	T(°C)	r[c]	Conv.	Yield[d]	M_n[e]	Đ
ePolyPEGMEM3A	PMDETA	T	80	1:1:2:6	\	28%	\	\
ePolyPEGMEM3B	bipy	A	90	1:1:2:6	\	10%	\	\

a) Ligand. bipy = 2,2' bipyridyl
b) Solvent: A = anisole, T = toluene.
c) Ratio among ePolyPEGMEM3, catalyst, ligand and DPE-OSi, respectively.
d) Total yield after step 1 and 2.
e) Number average molecular weight measured by SEC, in g·mol^{-1}.
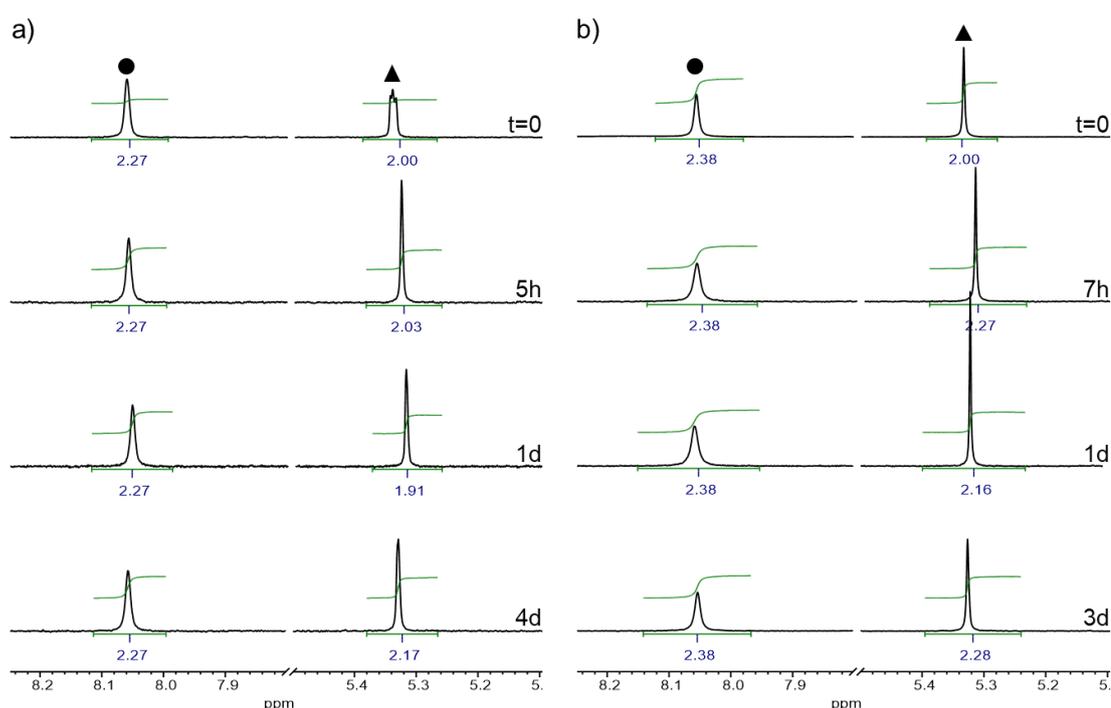
Figure 3.8 Sections of ^{1}H NMR spectra (CDCl$_3$, 400 MHz) of the reaction solution for the synthesis of a) ePolyPEGMEM3A and b) ePolyPEGMEM3B over time, after the addition of DPE-OSi as end-capping agent. (●) DMF aldehyde proton signal; (▲) DPE-OSi vinyl protons signal.

Figure 3.8 shows the signals of the vinyl protons of DPE-OSi (triangles) compared to the reference DMF (circle) over time, for both the attempts of post polymerisation end-capping. As seen previously for the direct approach, the integral values fluctuate around the initial value, suggesting that probably the end-capping was unsuccessful.

To finally verify the potential presence, or not, of the functionalised moiety of DPE-OSi in the PolyPEGMEM synthesised so far by ATRP, via both initiating and end-capping approaches, the NMR spectra are reported in Figure 3.9.
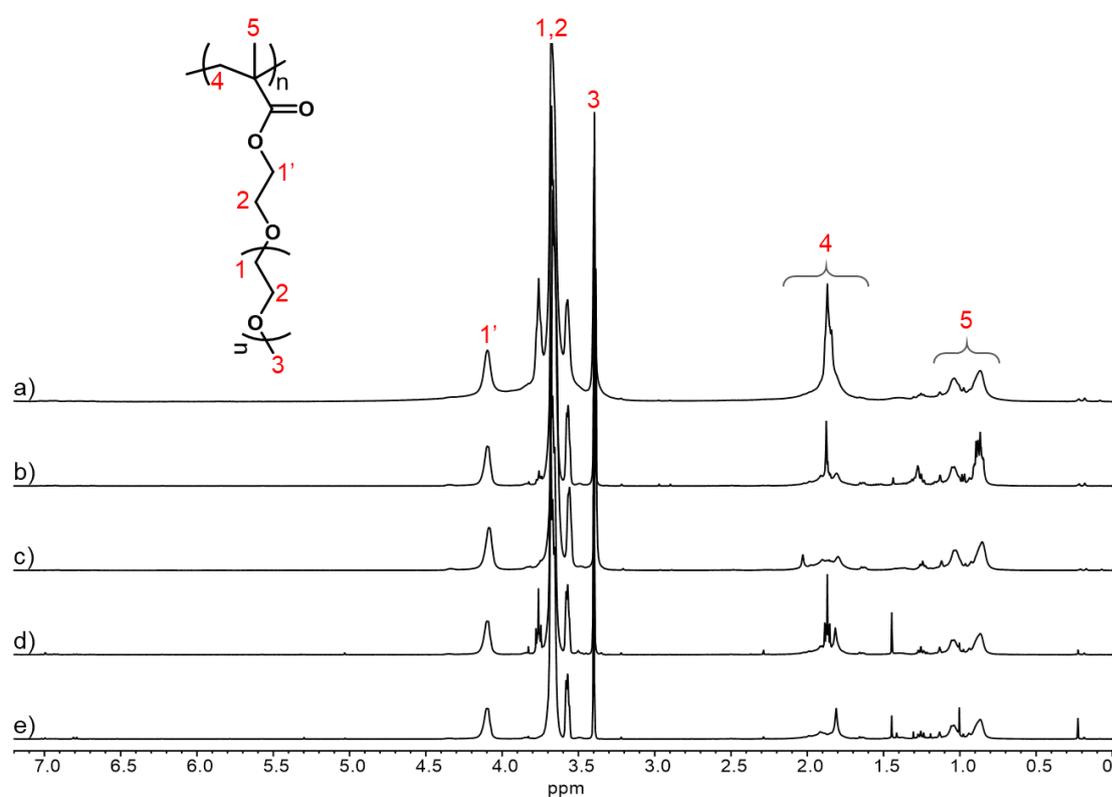
Figure 3.9 ^{1}H NMR spectra (CDCl$_3$, 400 MHz) of a) iPolyPEGMEM, b) ePolyPEGMEM1, c) ePolyPEGMEM2, d) ePolyPEGMEM3A and e) ePolyPEGMEM3B.

The region between 7.0 and 6.6 ppm should show two peaks of the aromatic protons of DPE-OSi, while at 1.0 and 0.1 ppm the signals of *t*-butyl and methyl groups of the silyl ether protecting group should appear, but no evidence of these peaks can be detected.

As explained above, the initiating procedure should not give any propagation at all once the radical resulting from the attack of the initiator onto DPE-OSi is

formed, because it is a very stable bis-benzyl radical which cannot propagate. However, the NMR spectrum of the final product (Figure 3.9a) shows the typical peaks of PolyPEGMEM. Given the very low yield (6%), it is possible that such a small amount of polymer could have been produced by a very low concentration of initiator, which can start the propagation of monomer.

The disappointing results obtained from the two different end-capping approaches were rather surprising, given the discussion about the role of DPE in radical polymerisation described above. A possible explanation can be the presence of the electron donating -OTBDMS group in para position on the aromatic rings of DPE-OSi, which partially destabilises the radical in the benzyl position. Moreover, it is possible that, at high conversions (97% in our case), the macroinitiator might have undergone significant radical termination reaction, meaning that many of the chains were no longer end-capped with the bromide needed for reaction with DPE-OSi, to yield a successful end-capping. Therefore, the presence of a deactivating group in para position, together with the probable termination reactions at high conversion, prevented the success of the end-capping approaches.

3.3.2.2   Synthesis of a novel bisphenol functionalised ATRP initiator (BP-Br)

The use of DPE-OSi as monomer proved to be ineffective in the functionalisation of a macromonomer by ATRP, thus the synthesis of a novel initiator, derived from the same molecule and suitable for ATRP, was designed, in order to introduce the desired bisphenol functionality at one chain end of the PolyPEGMEM chains. The novel ATRP initiator was synthesised in three steps (Scheme 3.8).
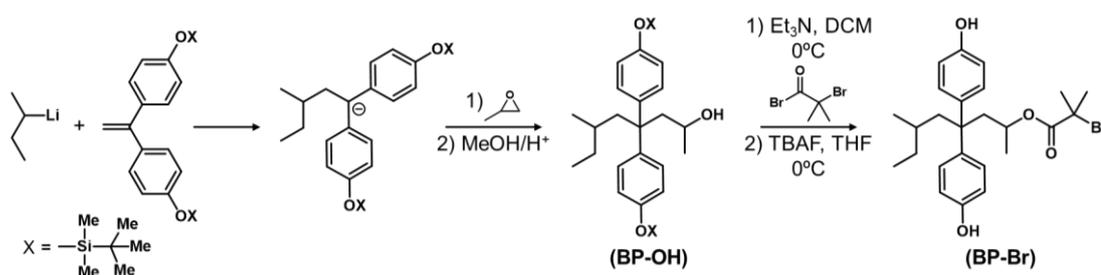
Scheme 3.8 Synthesis of DPE-OSi derived initiator, BP-Br, for ATRP.

The first step proceeded through an anionic polymerisation-like mechanism, exploiting the double bond of DPE-OSi, which can be attacked by *sec*-BuLi but is unable to propagate. An excess, with respect to DPE-OSi, of propylene oxide (PO) was then added to the 'living' adduct of BuLi and DPE-OSi, resulting in ring opening of the epoxide ring.

The excess of PO ensures a complete hydroxyl functionalisation of the adduct (BP-OH), and the presence of lithium as counterion prevents the propagation upon ring opening. This is due to the strong Li-O bond, which has a high covalent nature, because of the high density of charge on the small lithium ion. The same does not happen, for example, with potassium, in presence of which ethylene oxide has been polymerised by ring opening.[3] Previous literature is mainly focused on ethylene oxide, however the reaction of polystyryl lithium with PO has also been studied by Quirk *et al.*[16] It was demonstrated that the attack of the polystyryl carbanion happens mainly on the least hindered site of the PO epoxide ring and that there is no propagation of PO.[16] Based on this study, the regiospecificity of the attack on PO was confirmed and also no evidence of propagation was detected. The ^{1}H NMR spectra is reported in Figure 3.10.
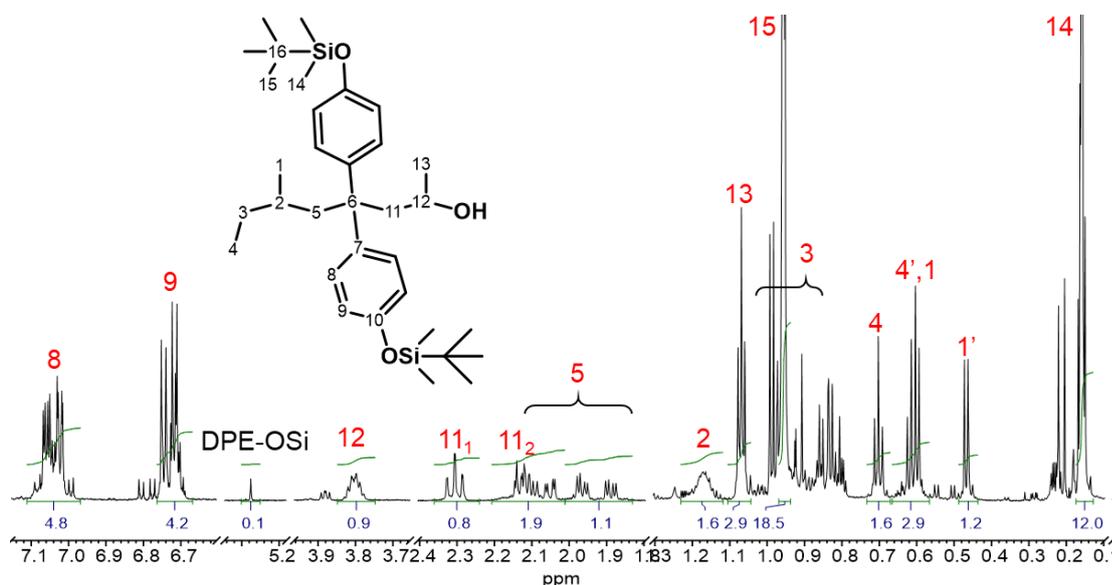
Figure 3.10 ^{1}H NMR (CDCl$_3$, 700 MHz) spectra of BP-OH.

A comprehensive NMR characterisation is reported in Appendix A. It is worth noting that the product has 2 stereo centres (C2 and C12), thus being

synthesised as 2 pairs of enantiomers (PO was purchased as a racemic mixture, thus giving 2 configurations in 1:1 ratio of C12) (Figure 3.11).
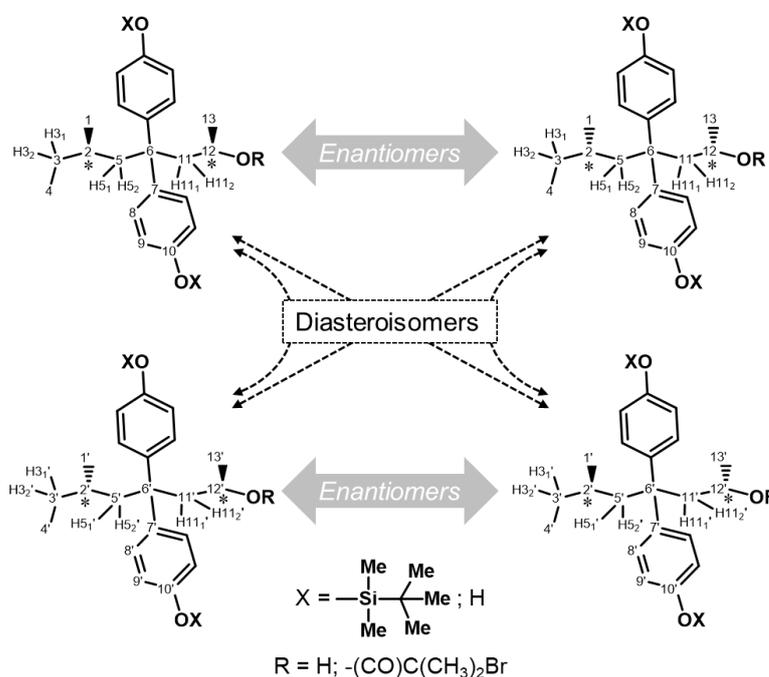
Figure 3.11 Structure of the 4 isomers (2 couples of enantiomers) obtained from the synthesis of BP-OH and BP-Br.

Some protons and carbons related to the 2 different pairs of enantiomers show different chemical shift and have been labelled as X and X' (as is the case, for example, of protons 1 and 4). Moreover, there are 3 diasterotopic protons (3, 5 and 11), which have been labelled X_1 and X_2.

Of primary importance in the NMR is the presence of the aromatic protons and the TBDMS protons, together with the almost complete disappearance of the vinyl peaks of DPE-OSi at 5.3 ppm, proving the success of BuLi attack. Moreover, the presence of the peaks ascribable to the PO moiety (11, 12, 13) proves the effectiveness of the addition, and the relative integral values (1 for peak 12, 1 for each diasterotopic proton 11, 3 for peak 13, compared to the aromatic protons peaks 8 and 9, with an integral of about 4 each, as expected) in the proton NMR spectrum suggest that the addition was quantitative and that there was no propagation of PO.

The final steps in the synthesis of the bisphenol functionalised ATRP initiator (BP-Br) involved i) an esterification reaction between the –OH introduced by

ring-opening of PO and α-bromoisobutyryl bromide, which was performed in DCM in presence of Et₃N, followed by ii) the deprotection of the phenol groups by TBAF in THF.

The final product, BP-Br, was purified by column chromatography using hexane/ethyl acetate (30:70) and characterised by NMR and mass spectrometry. The comprehensive NMR characterisation is reported in Appendix A. Figure 3.12 shows a comparison of the proton NMR spectra of BP-OH, the product of step 1, and BP-Br, the final product of the synthesis.
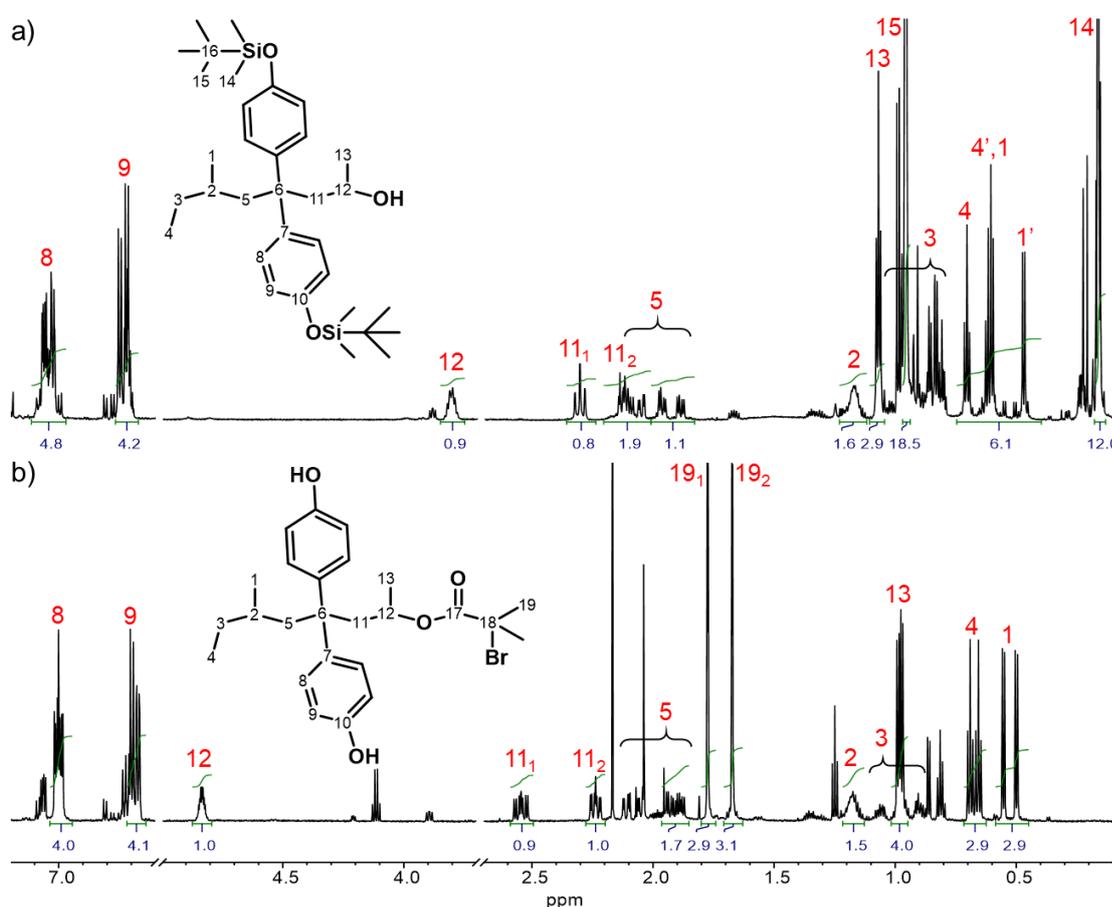
Figure 3.12 ¹H NMR (CDCl₃, 700 MHz) spectra of a) BP-OH and b) BP-Br.

The esterification reaction was confirmed by the appearance of 2 peaks at 1.78 and 1.67 ppm ascribable to the diasterotopic methyl groups 19, and by the shift of the other peaks, especially of protons 11 and 12, downfield - from 2.1 and 2.3 to 2.2 and 2.5 ppm, for the two diasterotopic protons 11, and from 3.8 to 4.8 ppm for proton 12 - because of the conversion of the adjacent group from an alcohol

to an ester. Moreover, the complete deprotection of the phenol groups is confirmed by the disappearance of the peaks at 0.96 and 0.16 ppm for protons 15 and 14 of the TBDMS group.

The high-resolution mass spectrometry analysis of the $[M-H]^-$ peak of BP-Br (calculated m/z for $C_{25}H_{32}O_4Br$ is 475.1484, found 475.1497) confirms the formula of the desired product, with no propagation of PO. The presence of a peak of similar intensity at $[M-H+2]^-$ is a sign of the presence of a bromine atom, because of its two stable isotopes – ^{79}Br and ^{81}Br - with relative abundance of 50.7% and 49.3%, respectively.[17] The LR and HR-MS spectra are shown in Appendix A.

Once obtained and fully characterised, the novel ATRP initiator was used for the synthesis of PolyPEGMEM macromonomers, but also for the copolymerisation of PEGMEM and MMA, in a 1:1 mole ratio, and of styrene, the latter to obtain macromonomers which could be then analysed by NP-IIC, in order to evidence the presence of the bisphenol functionality. The reaction conditions used and molar mass data for the resulting polymers are summarised in Table 3.3.

Table 3.3 Reagents and polymerisation conditions, yields, molar mass and dispersity values of the polymers obtained using the bisphenol functionalised ATRP initiator.

	L[a]	S[b]	T(°C)	r[c]	Conv.	Yield[d]	M_n[e]	Đ
PolyPEGMEM-OH1	P	T	60	1:1:3:16	69%	82%	12.7	1.35
PolyPEGMEM-OH2	P	A	90	1:1:2:17	74%	52%	21.2	1.12
Poly(PEGMEM-*co*-PEMMA)-OH	bipy	A	90	1:1:2:13	83%	86%	15.3	1.22
PS-OH	P	B	130	1:1:2:11	71%	52%	29.7	1.86

a) Ligand. P = PMDTA, bipy = 2,2' bipyridyl.
b) Solvent: T = toluene, A = anisole, B = bulk.
c) Ratio among initiator, catalyst, ligand and monomer, respectively.
d) Calculated as ratio between the mass of the final product and the percentage of initial mass of monomer given by conversion.
e) Number average molecular weight measured by SEC, in kg·mol^{-1}.

3.3.2.3   Synthesis of bisphenol end-functionalised PolyPEGMEM-OH macromonomer using BP-Br as initiator

Two PolyPEGMEM-OH macromonomers (1 and 2) were synthesised using the bisphenol functionalised initiator BP-Br and with reaction conditions that had proved to be effective in previous polymerisation reactions of the same monomer with common initiators, such as ethyl 2-bromoisobutyrate. CuBr was used as catalyst and PMDETA as ligand (in 1:1:2 molar ratio respectively), the first reaction was carried out in toluene at 60ºC and the second in anisole at 90ºC. In both cases, after only 1 hour, the conversion (measured by NMR by comparing the integral value of PEGMEM vinyl protons peak with DMF peaks, added as internal standard) was above 60% and the reaction was quenched. In both cases, the NMR spectrum of the resulting macromonomer (as an example the spectrum of PolyPEGMEM-OH2 is reported in Figure 3.13) clearly shows the presence of the aromatic peaks of the initiator (7.0 and 6.7 ppm).
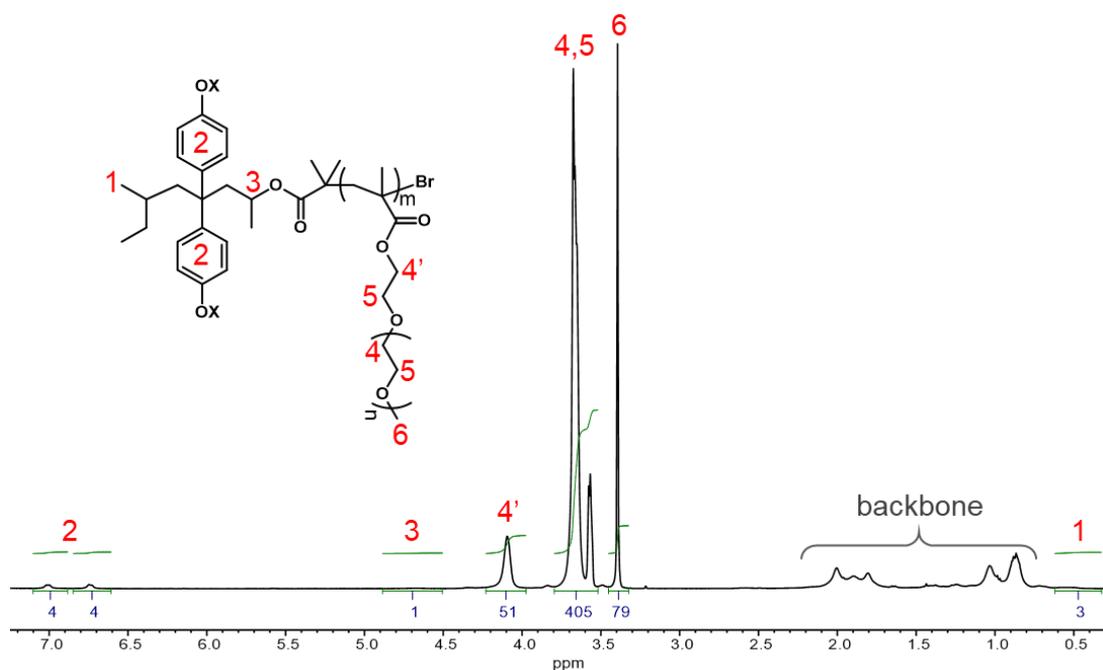
Figure 3.13 ^{1}H NMR spectrum (CDCl$_3$, 400 MHz) of PolyPEGMEM-OH2, synthesised by ATRP using BP-Br as initiator.

By comparing the integrals of peak 6 at 3.4 ppm (the terminal CH$_3$ of the PEO side chain of the PEGMEM repeat unit), to the aromatic protons introduced by

the initiator (peaks 2), it is possible to calculate a number of 26.3 monomer repeat units (each 300 g·mol^{-1}) per initiator (476 g·mol^{-1}), giving a M_n of 8,400 g·mol^{-1}. The same calculation for PolyPEGMEM-OH1 gave a M_n of 10,800 g·mol^{-1}. The number average molar mass obtained by NMR is not in good agreement with the number average molecular weight obtained by SEC (12,700 and 21,200 g·mol^{-1}, respectively), especially for the second attempt, in which the M_n measured by SEC is more than double that obtained by NMR. The dispersity for PolyPEGMEM-OH1 is quite high (1.35), while a good narrow distribution for PolyPEGMEM-OH2 (1.12) has been found. It should be underlined that the value obtained by NMR uses the signals of the aromatic protons on the initiator group. The intensity of these peaks is weak and the calculation is expected to be affected by an error. Moreover, and as explained earlier, in SEC analysis, there is a potential error in the calculation of dn/dc, because of the hygroscopic character of PolyPEGMEM, and the very low dn/dc value (0.069 ml·g^{-1}) for PolyPEGMEM means a weak response in the RALS detector, especially for lower MW chains (RALS detector response is proportional to MW). This can cause an overestimation of M_n by SEC and may contribute to the discrepancy between the M_n values obtained by the difference techniques. Nevertheless, in the case of PolyPEGMEM-OH1 the values obtained by NMR and SEC are reasonably close agreement.

Another possible contributing factor in this discrepancy could be the presence of chain termination by combination towards the end of the polymerisation, when conversion was above 70%. Combination would yield chains with bisphenol functionality at each chain ends and double the molecular weight. It is well known in literature that the preferred termination mechanism in radical polymerisation of methacrylate monomers is disproportionation,[18-20] however, it has been also shown that an increase in temperature, and the consequent decrease of viscosity of the reaction solution, favours combination over disproportionation.[21] This could have been the case for PolyPEGMEM-OH1 and 2, for which the polymerisation was performed at 60 and 90°C, respectively: the higher temperature for attempt 2 might have caused a higher occurrence of termination by combination, thus giving an M_n by SEC double than the one calculated by NMR. It is worth

underlining, though, that despite the issue of imperfect control of the obtained molecular weight, which could be partially solved by stopping the reaction at lower conversion, the functional initiator derived from DPE-OSi appears to have successfully initiated the polymerisation by ATRP of PEGMEM monomers.

3.3.2.4   Synthesis of bisphenol end-functionalised Poly(PEGMEM-*co*-MMA)-OH macromonomer using BP-Br as initiator

The copolymerisation of PEGMEM and MMA in 1:1 mole ratio, using the novel bisphenol functionalised initiator, CuBr as catalyst and bipy as ligand, in anisole at 90ºC (see Table 3.3), was followed by NMR (Figure 3.14). The inset expansion shows the disappearance of the peaks corresponding to the vinyl protons of both the monomers over time. After 2 hours the total conversion was above 70% and the polymerisation was quenched.
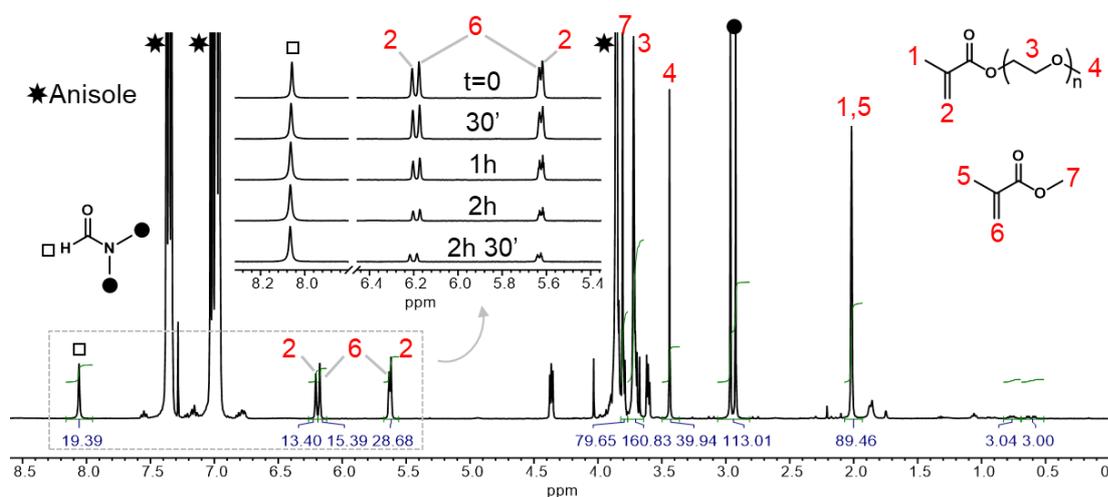
Figure 3.14 ^{1}H NMR spectra of the reaction solution of Poly(PEGMEM-*co*-PMMA)-OH at time 0 and, in the insert, the evolution of the vinyl peaks of PEGMEM (2) and MMA (6) monomers over time.

The presence of an internal standard (DMF) allows a calculation of monomer conversion vs time and the results are plotted in Figure 3.15. The monomers are consumed at almost an identical rate throughout the reaction, which is not unexpected based on previously published results from our group, which showed that the free radical copolymerisation of MMA and PEGMEM is almost random.[6]

Thus, we can expect the polymer sequence to have a nearly random distribution of monomers.
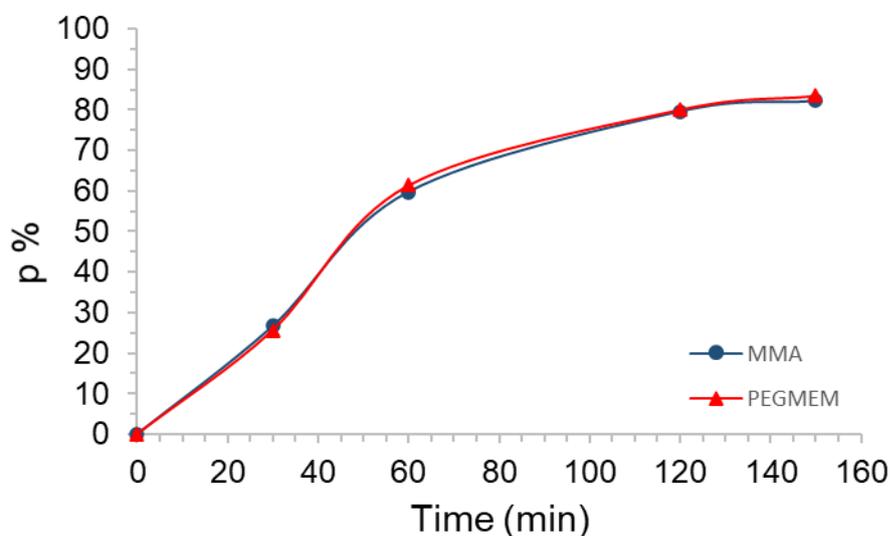
Figure 3.15 Percentage conversion (p%) vs time of PEGMEM (red trace) and MMA (black trace) in the ATRP copolymerisation using BP-Br as initiator.

The composition of the final product can be estimated from the NMR spectrum of the polymer (Figure 3.16).
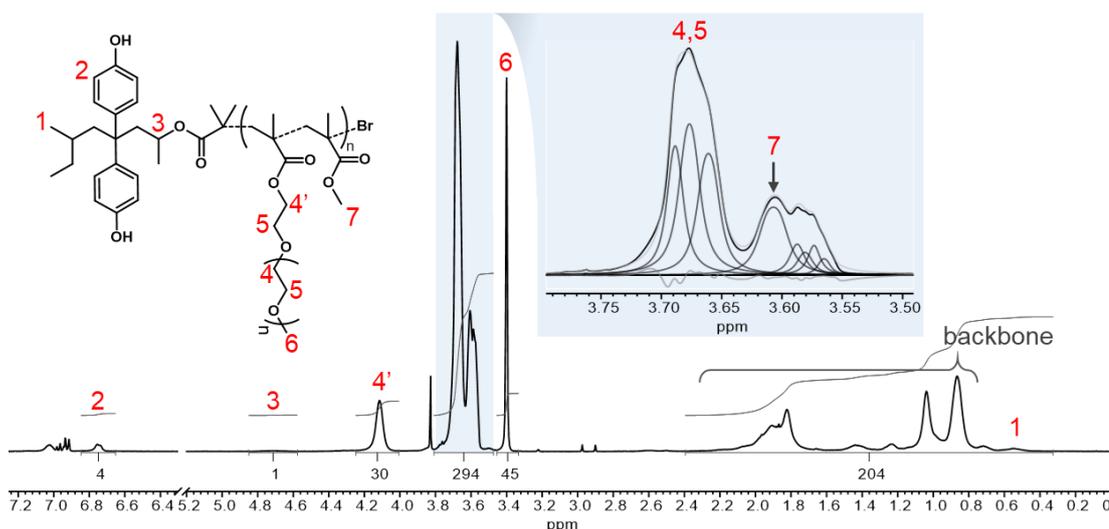
Figure 3.16 ^{1}H NMR spectrum (CDCl$_3$, 400 MHz) of Poly(PEGMEM-*co*-MMA)-OH synthesised by ATRP using BP-Br as initiator.

The broad group of peaks between 3.8 and 3.5 ppm (expansion in Figure 3.16) account for -CH$_2$ in the side PEO chain of PEGMEM (protons 4 and 5) and -CH$_3$

ester of MMA (7). Through deconvolution, achieved using the software MestReNova, it is possible to estimate the area under each peak which the broad peak is comprised of, and therefore estimate the ratio between the area under peak 7 (MMA methyl) and the area under the whole broad peak from 3.8 and 3.5 ppm. Knowing the ratio, it is possible to calculate the integral value of peak 7, as fraction of the whole integral (294), obtaining a value of 44. Comparing this value with the peak at 3.4 ppm, accounting for the terminal -CH_3 in the side PEO chain of PEGMEM (6), the final composition of the copolymer was determined: there are 45/3=15 PEGMEM units and 44/3=14.7 MMA units, for a composition of ca. 50% PEGMEM and 50% MMA, as expected.

As seen before for the ATRP of PEGMEM homopolymers using this novel initiator, the ATRP copolymerisation of PEGMEM with MMA gave a much higher value for the number average molar mass by SEC (15,300 g·mol^{-1}) than the one calculated by NMR (6,400 g·mol^{-1}), and with a dispersity of Đ=1.22. Taking into account the possible error derived from the use of the weak signals of the aromatic protons on the initiator group in the NMR calculation, and the overestimation of M_n by SEC caused by the low dn/dc value of the polymer, this discrepancy is still too large to be explained by an analytical error, but given the reaction conditions (high conversion and temperature), termination by coupling could be a reasonable explanation also in this case. However, if a significant amount of termination by combination had occurred, then the SEC trace should appear bimodal, with a second overlapping distribution derived from the chains with double the molecular weight. This is not the case for Poly(PEGMEM-co-MMA)-OH macromonomers obtained.

Despite the discrepancy between the data obtained by NMR and SEC, and the difficulty in explaining such evidence, the synthesised DPE-OSi-derived functional initiator proved to be effective also in the copolymerisation by ATRP mechanism of PEGMEM and MMA, to give a random copolymer. NMR was useful to clearly show the presence of initiator peaks. A further proof of the presence of the polar functional group carried by the initiator could be obtained by NP-IIC analysis, as performed for PS macromonomers in Chapter 2. However, to the best of our

knowledge, NP-IIC analysis of functionalised PolyPEGMEM or similar polar polymers has never been done, and we suspect that it would be extremely difficult to resolve chains which are already quite polar (PEG side chains) because of the interaction of a single bisphenol functional group with the polar stationary phase. Nevertheless, it would be an interesting analytical methodology to develop and optimise, but since this part of the project was performed in the last period of the PhD, not enough time was left to pursue this task. Therefore, PS was also synthesised by ATRP and initiated by BP-Br, in order to obtain a macromonomer which could be then analysed by NP-IIC to verify the presence of the bisphenol functionality.

3.3.2.5   Synthesis of bisphenol end-functionalised PS-OH macromonomer using a BP-Br as initiator

The ATRP of styrene initiated by BP-Br was performed in bulk, as commonly found in literature,[22] with CuBr as catalyst, PMDETA as ligand, at 130°C (see Table 3.3). After 2 hours the conversion – calculated by monitoring the decrease of NMR peaks arising due to the vinyl protons of styrene monomer at 5.8 and 5.3 ppm, compared to the peak of anisole, used as internal standard - was above 70% and the polymerisation was quenched.
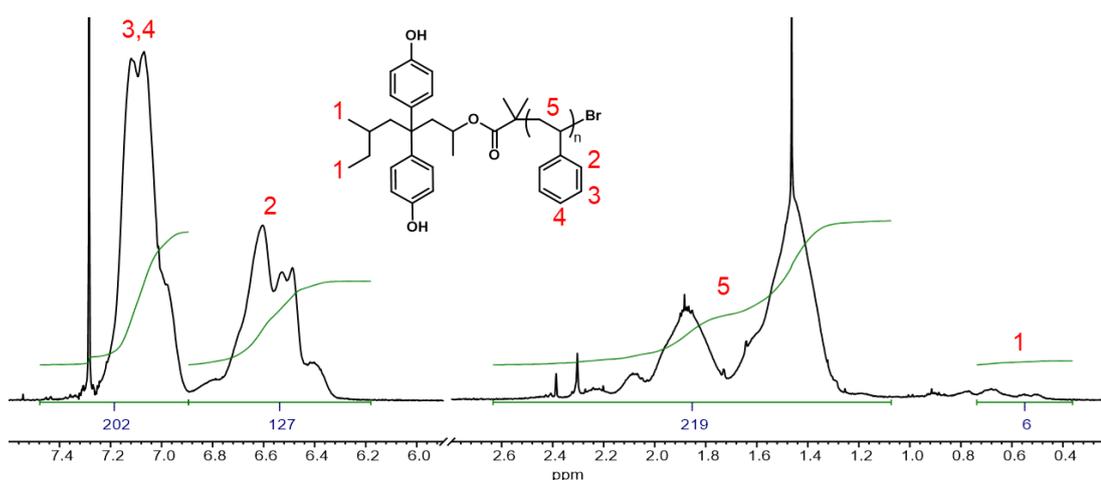
Figure 3.17 ^{1}H NMR spectrum (CDCl$_3$, 400 MHz) of PS synthesised by ATRP using BP-Br as initiator.

In this case, it is not easy to identify the presence of the bisphenol residue via NMR (Figure 3.17), because of the broad peaks of PS that cover large regions of the spectrum.

It is possible to estimate the M_n by comparing the integrals of polystyrene aromatic protons (2), between 6.89 - 6.18 ppm, with methyl groups of the initiator moiety (1), between 0.74 - 0.36 ppm. The error here is clearly significant, given the very weak and broad functional group signals available for the calculation. For each initiator (6 protons between 0.74 – 0.36 ppm) there are 127/2=63.5 styrene repeat units, which suggests a number average molar mass of 7,100 g·mol^{-1}. However, SEC analysis indicated a number average molar mass of 29,700 g·mol^{-1}, with a very broad dispersity (Đ=1.86). In this specific case, the calculation through NMR could be less reliable than before, because of the very small and broad peaks of the initiator that have been used in comparison with the polymer peaks. On the other hand, SEC should be much more accurate than for methacrylates macromonomers, because of the higher value of dn/dc of PS.

Looking at the SEC chromatogram recorded by RI detector in Figure 3.18, the trace appears to be bimodal, comprising at least two overlapping distributions, the main one with a peak maximum at almost 15 ml and a shoulder at higher retention volume.
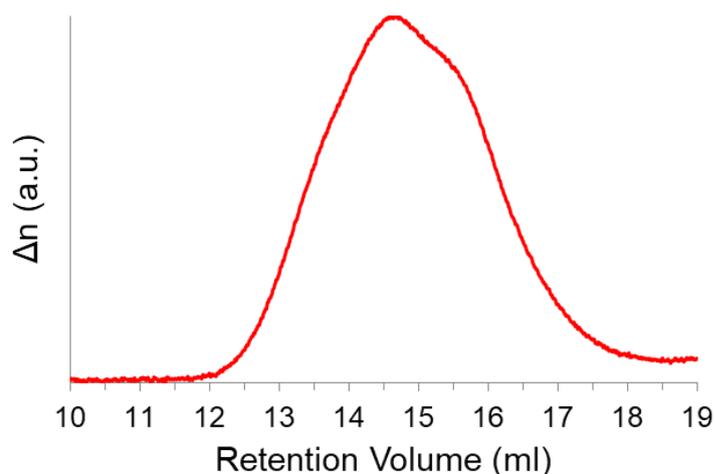
Figure 3.18 SEC chromatogram recorded by RI detector of PS-OH.

This evidence partly explains the high dispersity value (1.86). It has been reported previously that the preferred termination reaction for the radical polymerisation of

styrene is combination.[18,20,23] Moreover, Angot *et al.*[23] found that termination by combination during the ATRP of styrene is significant already at 20% monomer conversion, with the appearance of a shoulder at higher MW in the SEC chromatogram. It is, thus, reasonable to expect that, with a monomer conversion of 70% in this case, a significant amount of termination by combination will have occurred, resulting in a bimodal SEC trace and a high Đ.

A more complete understanding of the structure of the product can be obtained by analysis using NP-IIC, which can confirm the presence of the bisphenol functional group and explore the possibility of more than one bisphenol group per chain. The chromatography conditions (normal phase, eluent THF/isooctane in ratio 45/55 (v/v), flow rate 0.5 ml·min^{-1}, 15°C) were chosen according to a previous report.[24] For comparison, the chromatogram of a narrow molar mass polystyrene SEC standard – therefore un-functionalised - of similar M_n (30,230 g·mol^{-1}) was also recorded under the same conditions (Figure 3.19).
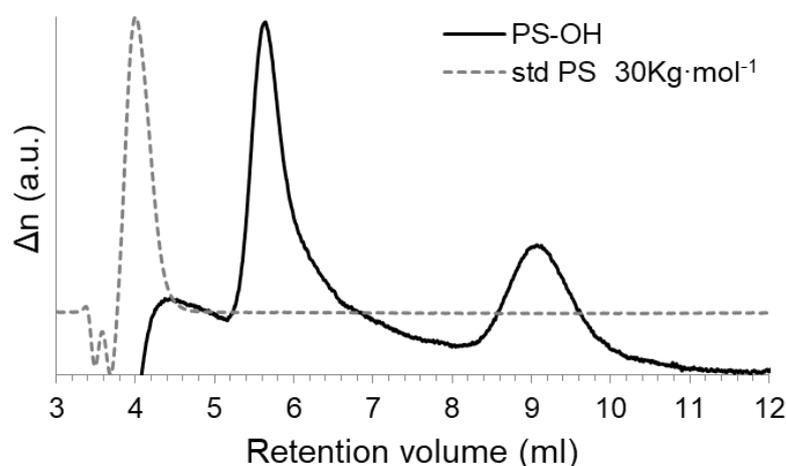
Figure 3.19 NP-IIC chromatograms of PS macromonomer synthesised by ATRP with BP-Br as initiator (solid trace) and un-functionalised standard PS with a comparable M_n (dashed trace). The detection is by RI.

The IC chromatogram of the PS-OH macromonomer (indicated by a solid line) synthesised by ATRP shows two peaks at about 5.8 and 9.2 ml retention volume, with a (similar) calculated M_n of 26.2 and 29.1 kg·mol^{-1}, whereas the un-functionalised polystyrene standard (indicated by a dashed line) is eluted at a lower elution volume (4.2 ml), with a calculated M_n of 26.1 kg·mol^{-1}.

The higher retention volumes measured for PS-OH macromonomer, compared to the standard PS peak, can only be caused by the presence of polar functional groups – the bisphenol functionality in this case – strongly interacting with the polar stationary phase. The presence of 2 peaks for the PS macromonomer, eluting separately with a similar molar mass, strongly suggests polymer chains with a different kind of functionalisation, with the later-eluting peak possibly arising due to the presence of polystyrene chains functionalised with 2 bisphenol moieties. As already mentioned, a previous report stated that for the polymerisation of styrene by ATRP, a significant amount of termination by combination occurs at relatively low monomer conversion (20%).[23] In this case two propagating chains, carrying one initiator group each, would be coupled together. Even if, hypothetically, it is to be expected that species with two bisphenol functional groups would elute at later retention volumes than species with only one functional group, it is worth noting that in the NP-IC analysis of PS macromonomers (section 2.3.1.1.2) no evidence of a later peak was ever seen, even when MALDI spectra clearly showed the presence of such di-functionalised species. We concluded that those chains are too polar to elute and probably remained adsorbed onto the stationary phase. To explain the presence of a second, later-eluting peak in Figure 3.19 one possibility is that, in the analysis performed in Chapter 2, the amount of di-functionalised chains was so low to not be actually detectable at later retention volumes. On the other hand, in this Chapter, the second peak might be caused by the presence of a different kind of functionalisation, besides the bisphenol carried by the initiator group. For example, it is well known that oxygen inhibits CLRPs by reacting with the carbon radicals to form peroxy radicals and finally hydroperoxides. The presence of such groups at the chain ends would explain an increase in polarity and therefore the higher retention volume.

Despite the poor control over M_n and Đ and the apparent presence of chains with different kind of functional groups, the polymerisation of PS initiated by BP-Br and the analysis by NP-IIC unequivocally proved that the initiator is able to initiate an ATRP reaction. The absence of un-functionalised chains confirms that the chains

were all initiated by the ATRP initiator and that a free radical mechanism can be excluded. This approach is thus a valid way to obtain the desired functionalisation of macromonomers by ATRP, provided that a suppression of chain combination reactions is achieved.

Considering also the polymerisation of the other monomers (PEGMEM and MMA), it is clear that further optimisation is needed, starting from stopping the reaction at much lower conversion, especially for PS, to improve the control of the radical mechanism and reduce termination reactions.

For the final purpose of this project - the synthesis of complex branched architectures with step-growth polymers - the PolyPEGMEM-OH macromonomers obtained by ATRP through the use of a functionalised initiator (BP-Br) were considered suitable to take forward for use in the polycondensation reaction with a view to synthesising branched block copolymers, as reported in the next Chapters.

3.4   CONCLUSIONS

After the extended study, described in Chapter 2, of the synthesis of PS macromonomers with a bisphenol moiety at one chain end, by different approaches exploiting anionic polymerisation and DPE-OSi, another monomer was chosen (PEGMEM), carrying a PEG side chain, with a view to synthesising macromonomers with hydrophilic properties. DPE-OSi was once again exploited to synthesise PolyPEGMEM macromonomers via a controlled radical mechanism, ATRP, because of the challenges encountered with the anionic polymerisation of PEGMEM. The PEGMEM monomer is, indeed, very difficult to purify, because of his high boiling point and hygroscopic nature.

After a few unsuccessful attempts to use DPE-OSi as monomer in an ATRP mechanism, to end-cap or initiate the chains, a synthetic strategy was designed to obtain a novel initiator derived from DPE-OSi, thus carrying the desired bisphenol functionality. The new species, labelled BP-Br, proved effective for the initiation of PEGMEM by an ATRP mechanism, but also PEGMEM and MMA in a 1:1 mole ratio random copolymerisation. NMR analysis showed the typical peaks

of the initiator as evidence of the presence of the bisphenol functionality. However, especially in the second of the two attempts made, a large discrepancy was found between the number average molar mass obtained by NMR and SEC, the latter being double the former. Even taking into account a potential error in the calculation of dn/dc, and a possible overestimation of M_n by SEC because of a low value of dn/dc and for methacrylate polymers, such a discrepancy may not be due only to analytical errors and the hypothesis of a degree of termination by combination has been suggested. Although it has been demonstrated in previous works that the termination of radical polymerisation of methacrylates usually favours disproportionation rather than combination it has also been found that a higher reaction temperature can increase the combination reaction.

The use of the same novel initiator did allow the polymerisation of styrene by an ATRP mechanism, but with considerably less control than seen with PEGMEM and PEGMEM/MMA. The PS macromonomer synthesised in this work also gave a high value of M_n by SEC. It was analysed by NP-IIC and compared with a standard (unfunctionalised) PS with a similar M_n. Analysis of the PS macromonomer revealed that no peak was eluted at similar retention volume as unfunctionalised standard PS. Instead two peaks were observed at higher retention volumes. The higher retention volume measured for PS macromonomer is compatible with the presence of the bisphenol functionality, that causes the higher retention of the macromonomer by the polar stationary phase, compared to the unfunctionalised standard PS. The absence of any unfunctionalised chains confirm the effectiveness of BP-Br as initiator, however the high M_n calculated by SEC, in relation to the one calculated by NMR, and the presence of a second peak at higher retention volume in the NP-IIC trace of PS suggests the presence of species with more than one bisphenol functionality per chain. An explanation for this could be the combination of two propagating chains, each one carrying the functionalised bisphenol moiety. However, since no evidence of di-functionalised chains was detected in previous NP-IIC analysis (Chapter 2), the possibility of a different kind of functionalisation, derived from impurities during the polymerisation, cannot be ruled out.

Although the ATRP of PEGMEM using the novel functionalised initiator, designed and synthesised in this study, was not fully optimised, there is no doubt that the resulting PolyPEGMEM macromonomers are functionalised as required. Therefore, they were used in a step-growth polycondensation reaction to obtain grafted copolymers, as described in the following Chapters.

REFERENCES

1. Baskaran, D., *Progress in Polymer Science*, **2003,** *28* (4), 521-581.
2. Quirk, R.P.; Wang, Y., *Polymer International*, **1993,** *31* (1), 51-59.
3. Hsieh, H., Quirk, R. P., *Anionic Polymerization: Principles and Practical Applications*. Marcel Dekker, Inc., **1996**.
4. Graham, R.K.; Dunkelberger, D.L*., et al.*, *Journal of the American Chemical Society*, **1960,** *82* (2), 400-403.
5. Greene, T.W.; Wuts, P.G.M., *Protective Groups In Organic Synthesis*. John Wiley & Sons, New York, **1999**.
6. Boulding, N.A.; Millican, J.M*., et al.*, *Polymer Chemistry*, **2019,** *10* (41), 5665-5675.
7. Kleine, A.; Altan, C.L*., et al.*, *Polymer Chemistry*, **2014,** *5* (2), 524-534.
8. Wang, X.S.; Armes, S.P., *Macromolecules*, **2000,** *33* (18), 6640-6647.
9. Wang, X.S.; F. Lascelles, S*., et al.*, *Chemical Communications*, **1999**. (18), 1817-1818.
10. Oh, J.K.; Min, K*., et al.*, *Macromolecules*, **2006,** *39* (9), 3161-3167.
11. Lee, B.S.; Lee, J.K*., et al.*, *Biomacromolecules*, **2007,** *8* (2), 744-749.
12. Yamamoto, S.-i.; Pietrasik, J*., et al.*, *Macromolecules*, **2007,** *40* (26), 9348-9353.
13. Neugebauer, D.; Zhang, Y*., et al.*, *Macromolecules*, **2003,** *36* (18), 6746-6755.
14. Tao, L.; Mantovani, G*., et al.*, *Journal of the American Chemical Society*, **2004,** *126* (41), 13220-13221.
15. Wieland, P.C.; Raether, B*., et al.*, *Macromolecular Rapid Communications*, **2001,** *22* (9), 700-703.
16. Quirk, R.P.; Lizárraga, G.M., *Macromolecules*, **1998,** *31* (11), 3424-3430.
17. Meija, J.; Coplen Tyler, B*., et al.*, *Pure and Applied Chemistry*, **2016,** *88* (3), 265.
18. Bamford, C.H.; Jenkins, A.D., *Nature*, **1955,** *176* (4471), 78-78.
19. Buback, M.; Günzler, F*., et al.*, *Macromolecules*, **2009,** *42* (3), 652-662.
20. Nakamura, Y.; Ogihara, T*., et al.*, *ACS Macro Letters*, **2016,** *5* (2), 248-252.
21. Nakamura, Y.; Ogihara, T*., et al.*, *Chemistry – A European Journal*, **2017,** *23* (6), 1299-1305.
22. https://www.cmu.edu/maty/index.html.
23. Angot, S.; Murthy, K.S*., et al.*, *Macromolecules*, **1998,** *31* (21), 7218-7225.
24. Hutchings, L.R.; Agostini, S*., et al.*, *European Polymer Journal*, **2015,** *73*, 105-115.

CHAPTER 4

SYNTHESIS OF
POLY(ETHYLENE ISOPHTHALATE) GRAFT
COPOLYMERS BY SOLUTION
POLYCONDENSATION

4.1 INTRODUCTION

Because of their excellent mechanical, thermal and electrical properties and the ease with which that can be processed into fibres, moulded products or film at relatively low cost, aromatic polyesters find applications in fields, such as blow-moulded bottles, textile fibres and biaxially oriented films. Poly(ethylene terephthalate) (PET) is the most widespread polyester, being employed in the textile and packaging industries as fibres (Mylar, Dacron, and Terylene) or as films (BOPET) and blow-moulded bottles for carbonated soft drinks. Other uses of PET include handles and housings for appliances (cookers, toasters, shower heads, industrial pump housings etc.).[1]

The mechanism for the synthesis of polyesters comprises chain-growth ring-opening polymerisation for some aliphatic polyesters (i.e. polycaprolactone, polylactic acid, polyhydroxybutyrate, polyglycolic acid) and step-growth polycondensation for most aromatic and semi-aromatic polyesters (i.e. poly(ethylene terephthalate), poly(butylene terephthalate), poly(ethylene naphthalate)). Step-growth polycondensation involves a reaction between two mutually reactive functional groups, with the loss of a small molecule condensate. Indeed, the typical esterification reaction for the synthesis of polyesters between diol and dicarboxylic acid involves the production of water as a by-product

(Scheme 4.1a), even if, on an industrial scale a transesterification reaction is usually employed, in which alcohol or glycol are produced (Scheme 4.1b).[2-3]

Scheme 4.1 Synthesis of polyesters by polycondensation mechanism, through a) esterification or b) transesterification. R_1 and R_2 can be either aliphatic or aromatic groups.[2]

The most common synthetic procedure for PET on an industrial scale is a melt-polycondensation reaction of bis(2-hydroxyethyl)terephthalate (BHET), performed under vacuum (<1 mbar) and at high temperatures (up to 290°C), to ensure the concurrent removal of ethylene glycol (EG) by distillation (Scheme 4.2). The most commonly used catalyst is antimony trioxide (Sb_2O_3).[4]
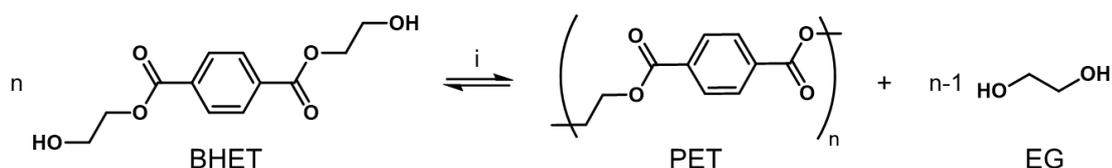
Scheme 4.2 Industrial synthesis of PET by melt polycondensation. Experimental conditions: i) 270-290°C, 1-3h, Sb_2O_3.[4]

The properties of a polymer may be tuned by copolymerisation, since the addition of a second monomer can alter the characteristics of the resulting copolymer.

Within the synthetic route for polyesters, it is possible to form copolymers, if comonomers with the same reactive groups, but different chemical structures, are used. In order to be incorporated within the polyester backbone during polycondensation step, any potential comonomer requires either di-acid (in the form of ester) or diol functionalities (Figure 4.1).
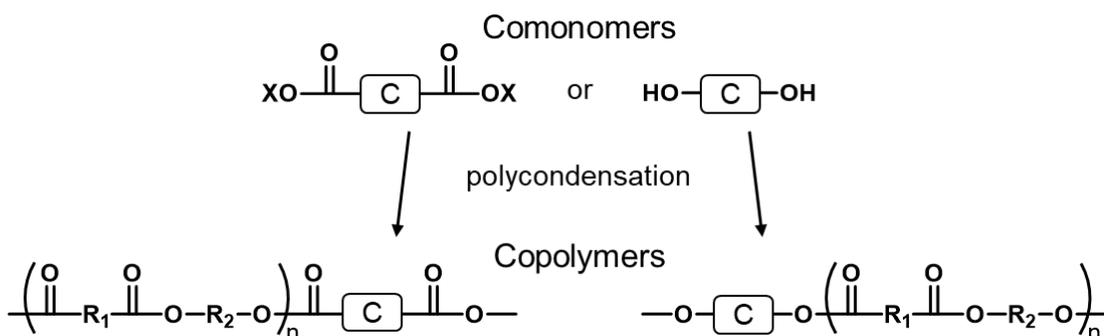
Figure 4.1 Possible structures of comonomers to be incorporated into a growing chain during a polycondensation reaction.
X=H: esterification reaction. X=R: transesterification.

In this chapter, the synthesis of graft block copolymers with a polyester backbone is described, by the incorporation of macromonomers carrying suitable functional groups to enable reaction as a comonomer in the polycondensation between a diacid and a diol (Figure 4.2).
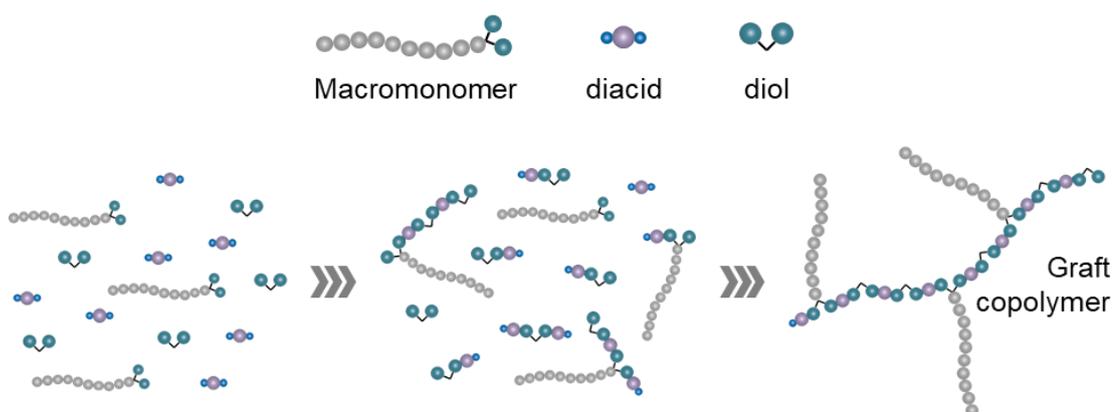
Figure 4.2 General approach to obtain grafted copolymers with a polyester backbone.

In particular, bisphenol functionalised macromonomers of polystyrene (PS) and poly(poly(ethylene glycol) methyl ether methacrylate (PolyPEGMEM), synthesised by controlled chain-growth polymerisation (discussed in Chapter 2 and 3), have been used.

Despite melt polycondensation being the most widely used industrial process for the synthesis of semi-aromatic polyesters such as PET, miscibility issues between two different polymers (e.g. PET and PS) in the blend would have inhibited the incorporation of PS macromonomer as comonomer into the PET growing chain, as previously reported in the literature.[5] Therefore, in order to obtain good mixing

of the reactants, it was decided to opt for a solution polycondensation approach. There are in literature many examples of polyesters prepared by solution or interfacial polyesterification. In general, those procedures involve the reaction of diacid chlorides and glycols, with the inherent advantage that reaction with the acid chloride is non-reversible. The diacid chloride and the glycol are usually mixed in equimolar proportions, and the mixture is warmed gradually to high temperatures. In some cases, reaction is carried out in the presence of an organic base, most commonly pyridine, to neutralize the hydrogen chloride formed.[6-9]

Since PET is insoluble in common organic solvents, and requires hazardous and/or expensive chemicals as solvents - such as nitrobenzene, phenol, o-chlorophenol, and 1,1,1,3,3,3, hexafluoro-2-propanol[10] - the meta isomer of phthalic acid (isophthalic) has been chosen instead, giving poly(ethylene isophthalate) chains (PEI), which are more readily soluble, both during the polycondensation reaction and for analysis via common analytical techniques (NMR and SEC). Thus, PS and PolyPEGMEM macromonomers could be added to the solution polymerisation of PEI, to take part into the polycondensation reaction. Initially, PS macromonomers of differing molecular weights (2,900, 6,400 and 9,300 g·mol^{-1}) were incorporated into the growing chain as a comonomer. PEI graft block copolymers with PEO brushes as grafts were also produced through the incorporation of PolyPEGMEM macromonomers into the polyester backbone.

4.2   EXPERIMENTAL

4.2.1   MATERIALS

Isophthaloyl chloride (IPCl, TCI UK Fine Chemicals) was stored in a desiccator and handled under an inert atmosphere of nitrogen. Chloroform (for HPLC, stabilised with amylene, ACROS Organics™) was filtered over alumina before use. Ethylene glycol (EG, anhydrous, 99.8%, Sigma-Aldrich), pyridine (anhydrous, 99.8%, Sigma-Aldrich), hexane (SLR, Fisher Chemical) and methanol (AR grade, Fischer Scientific), were all used as received.

Polystyrene macromonomers (ePS2.9K, M_n = 2,900 g·mol^{-1}, Đ=1.03; ePS6.4K, M_n = 6,400 g·mol^{-1}, Đ=1.05; ePS9.1K, M_n = 9,100 g·mol^{-1}, Đ=1.07) and poly(poly(ethylene glycol) methyl ether methacrylate) macromonomer (PolyPEGMEM-OH1, M_n = 12,700 g·mol^{-1}, Đ = 1.35) were synthesised according to procedures reported in Chapter 2 and 3, respectively.

4.2.2 CHARACTERISATION

^{1}H NMR spectra were measured on a Bruker DRX-400 MHz spectrometer and on a Varian VNMRS-700 spectrometer, using CDCl$_3$ as solvent. DOSY NMR was performed on a Varian VNMRS-600 spectrometer with CDCl$_3$ as solvent.

Triple detection size exclusion chromatography (SEC) with refractive index (RI), viscosity, and right angle light scattering (RALS) detectors was used for the analysis of molar mass and molar mass distribution of the copolymers, using a Viscotek TDA 302. Chloroform was used as the eluent, at a flow rate of 1.0 ml min^{-1} and at a temperature of 35°C. Separation was achieved using 2×300 mm PLgel 5 µm mixed C columns. A value of 0.16 ml·g^{-1} was used as the dn/dc of polystyrene, while a value of 0.098 ml·g^{-1} and 0.03 ml·g^{-1} (both measured in house) was used as the dn/dc of PEI and PolyPEGMEM macromonomer, respectively. For the analysis of the grafted copolymer, dn/dc has been calculated as a weighted average of the values of the macromonomer (PS or PolyPEGMEM) and PEI, according to the following equation:

$$dn/dc = dn/dc^M \times w.f.^M + 0.098 \text{ ml·g}^{-1} \times w.f.^{PEI}$$

where w.f. is the weight fraction of (M) the macromonomer and (PEI) poly(ethylene isophthalate), calculated using NMR data.

Isothermal interaction chromatography analysis was performed under normal phase conditions (NP-IIC) using a diol modified silica column (Nucleosil 100 Å pore, 250×4.6 mm I.D., 5 µm). A mixture of THF/isooctane (Fisher, GPC and HPLC grade respectively) was used in a ratio 45/55 (v/v) with a flow rate of 0.5 ml·min^{-1}. The temperature of the column was regulated using a ThermoScientific circulating bath and thermostat. Samples were prepared with a

concentration of 2.5 mg·ml^{-1} in the eluent mixture and the injection volume was 100 μl. The analysis was performed using a modified Viscotek TDA 301, mainly using the RI, the RALS and a Viscotek UV2600 detector, set to a wavelength of 260 nm.

Differential Scanning Calorimetry (DSC) was performed using a Perkin Elmer DSC 8500 under a nitrogen atmosphere and with heating/cooling cycles of: room temperature to 300°C at 10°C·min^{-1}, 300°C to 10°C at 20°C·min^{-1}, and 10°C to 300°C at 50°C·min^{-1}. Between each temperature a 2-minute isothermal period was applied. T$_g$ was obtained from the 2nd heating scan.

4.2.3 SYNTHESIS OF sp-PEI-*g*-PS COPOLYMERS BY SOLUTION POLYCONDENSATION

4.2.3.1   sp-PEI-*g*-PS$_{2.9K}$

IPCl (2.98 g, 15 mmol) was dissolved in ~20 ml of chloroform in a 2-neck round bottom flask and the solution was heated to reflux at 70°C. A solution of ePS2.9k (1.46 g, 0.5 mmol) and pyridine (4.85 ml, 60 mmol) in the same solvent (~15 ml) was added dropwise through a rubber septum, via a syringe pump. The solution was maintained at reflux and stirred for 1h. After this time, a sample was taken, precipitated in MeOH and collected upon filtration for analysis by ^{1}H NMR and NP-IIC, in order to confirm the formation of the isophthaloyl-functionalised PS macromonomer.

EG (0.85 ml, 15 mmol) was added dropwise to the reaction mixture through a rubber septum, via a syringe pump, and the solution was stirred for 24 hours to reflux at 70°C. All the steps were performed in an inert atmosphere of N$_2$. After this time, the solution was cooled down to room temperature, the product was precipitated in excess methanol, recovered by filtration and dried under vacuum. Yield 65%

M$_n$ 5,500 g·mol^{-1}, M$_w$ 6,600 g·mol^{-1}, Đ 1.20.
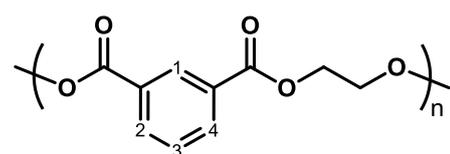
^{1}H NMR (400 MHz, CDCl$_3$, δ): 8.80 - 8.65 (1H, PEI H1), 8.30 – 8.10 (2H, PEI H2 H4), 7.60 – 7.40 (1H, PEI H3), 7.35 - 6.30 (PS Ar H), 4.80 – 4.60 (4H, PEI -OCH$_2$CH$_2$O-), 4.50 (4H, PEI -OCH$_2$CH$_2$OH), 4.00 (4H, PEI -OCH$_2$CH$_2$OH), 2.50 – 1.00 (PS Aliphatic H), 0.80 - 0.50 (3H, PS *sec*-Butyl CH$_3$CH$_2$), 0.80 - 0.50 (3H, PS *sec*-Butyl CHCH$_3$).

4.2.3.2 sp-PEI-*g*-PS$_{6.4K}$

The same procedure was followed, with IPCl (3.04 g, 15 mmol) in ~30 ml of chloroform, a solution of PS6.4k (3.20 g, 0.5 mmol) and pyridine (4.85 ml, 60 mmol) in the same solvent (~30 ml), and EG (0.85 ml, 15 mmol). Yield 82%.

M$_n$ 12,400 g·mol^{-1}, M$_w$ 14,400 g·mol^{-1}, Đ 1.16.
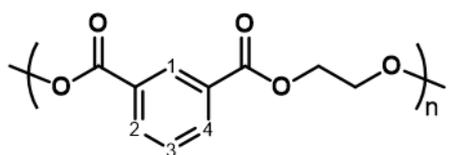
^{1}H NMR (400 MHz, CDCl$_3$, δ): 8.80 - 8.65 (1H, PEI H1), 8.30 – 8.15 (2H, PEI H2 H4), 7.60 – 7.40 (1H, PEI H3), 7.35 - 6.30 (PS Ar H), 4.85 – 4.60 (4H, PEI -OCH$_2$CH$_2$O-), 4.50 (4H, PEI -OCH$_2$CH$_2$OH), 4.00 (4H, PEI -OCH$_2$CH$_2$OH), 2.40 – 1.00 (PS Aliphatic H), 0.80 - 0.50 (3H, PS *sec*-Butyl CH$_3$CH$_2$), 0.80 - 0.50 (3H, PS *sec*-Butyl CHCH$_3$).

4.2.4 SYNTHESIS OF IPCl END-CAPPED PEI BY SOLUTION POLYCONDENSATION – PEI-IPCl

IPCl (3.01 g, 15 mmol) was dissolved in ~30 ml of chloroform in a 2-neck round bottom flask, and the solution was heated to reflux at 70°C. A solution of EG (0.85 ml, 15 mmol) and pyridine (4 ml, 50 mmol) in the same solvent (~20 ml) was added dropwise through a rubber septum, via a syringe pump. The solution was maintained at reflux and stirred for 24h, at which point a sample was collected for analysis by NMR and SEC.

A further amount of IPCl (548 mg, 3 mmol) was dissolved in chloroform (~3 ml) and added dropwise to the reaction mixture. The reaction was stirred at 70°C overnight and then cooled to room temperature. All the steps were performed in

an inert atmosphere of N_2. The product was precipitated in excess methanol, recovered by filtration and dried under vacuum. Yield: 90%

M_n 5,300 g·mol^{-1}, M_w 8,200 g·mol^{-1}, Đ 1.55.

^{1}H NMR (400 MHz, CDCl$_3$, δ): 8.75 - 8.65 (1H, PEI H1), 8.30 – 8.15 (2H, PEI H2 H4), 7.60 – 7.45 (1H, PEI H3), 4.76 – 4.60 (4H, PEI -OCH$_2$CH$_2$O-), 3.92 (3H, PEI -OCH$_3$).

4.2.5   SYNTHESIS OF cc-PEI-*g*-PS COPOLYMERS BY CHAIN COUPLING: PEI-IPCl + ePS

For the synthesis of cc-PEI-*g*-PS$_{6.4K}$, the diacid end-capped PEI-IPCl (2.37 g, 0.4 mmol) was dissolved in chloroform (~20 ml) in a three-necked round bottomed flask. An equimolar amount of ePS6.4k (2.56 g, 0.4 mmol) and pyridine (250 μl, 3.1 mmol) in chloroform (~20 ml) was added dropwise through a rubber septum, via a syringe pump. The solution was refluxed at 70°C and stirred for 24h. All the steps were performed in an inert atmosphere of N_2. After cooling to room temperature, the product was precipitated in excess methanol, recovered by filtration and dried under vacuum. Yield: 89%

M_n 5,300 g·mol^{-1}, M_w 8,200 g·mol^{-1}, Đ 1.55.

^{1}H NMR (400 MHz, CDCl$_3$, δ): 8.80 - 8.60 (1H, PEI H1), 8.30 – 8.15 (2H, PEI H2 H4), 7.60 – 7.45 (1H, PEI H3), 7.35 - 6.25 (PS Ar H), 4.80 – 4.65 (4H, PEI -OCH$_2$CH$_2$O-), 3.96 (3H, PEI -OCH$_3$), 2.45 – 1.00 (PS Aliphatic H), 0.80 - 0.50 (3H, PS *sec*-Butyl CH$_3$CH$_2$), 0.80 - 0.50 (3H, PS *sec*-Butyl CHCH$_3$).

4.2.6 SYNTHESIS OF EG END-CAPPED PEI BY SOLUTION POLYCONDENSATION – PEI-OH

4.2.6.1 PEI-OH1

IPCl (3.02 g, 15 mmol) was dissolved in ~20 ml of chloroform in a 2-neck round bottom flask, and the solution was heated to reflux at 70°C. A solution of EG (0.85 ml, 15 mmol) and pyridine (5 ml, 62 mmol) in chloroform (~30 ml) was added dropwise through a rubber septum, via a syringe pump. The solution was maintained at reflux and stirred for 24h, at which point a sample was collected for analysis by NMR and SEC.

A further quantity of EG (280 μl, 5 mmol) was then added dropwise to the reaction mixture and the reaction mixture was stirred at 70°C overnight. All the steps were performed in an inert atmosphere of N_2. The solution was then cooled to room temperature and the product precipitated in excess methanol, recovered by filtration and dried under vacuum. Yield: 73%

M_n 8,900 g·mol^{-1}, M_w 11,800 g·mol^{-1}, Đ 1.33.

^{1}H NMR (400 MHz, CDCl$_3$, δ): 8.76 - 8.64 (1H, PEI H1), 8.28 – 8.16 (2H, PEI H2 H4), 7.58 – 7.42 (1H, PEI H3), 4.78 – 4.60 (4H, PEI -OC$\underline{H}_2$C$\underline{H}_2$O-), 4.50 (4H, PEI -OC$\underline{H}_2$CH$_2$OH), 4.00 (4H, PEI -OCH$_2$C$\underline{H}_2$OH).
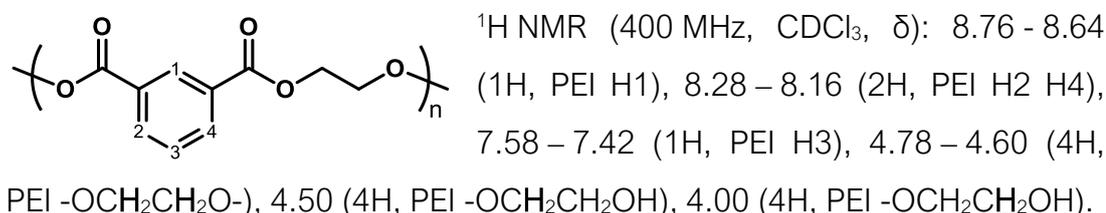
4.2.6.2 PEI-OH2

The procedure described above (Section 4.2.6.1) was repeated with IPCl (3.02 g, 15 mmol) in ~30 ml of chloroform and a solution of EG (0.85 ml, 15 mmol) and pyridine (5.0 ml, 64 mmol) in chloroform (~30 ml). In the second step EG (280 μl, 5 mmol) was added dropwise. Yield 73%.

M_n 9,100 g·mol^{-1}, M_w 14,600 g·mol^{-1}, Đ 1.60.

^{1}H NMR (400 MHz, CDCl$_3$, δ): 8.72 - 8.65 (1H, PEI H1), 8.26 – 8.18 (2H, PEI H2 H4),
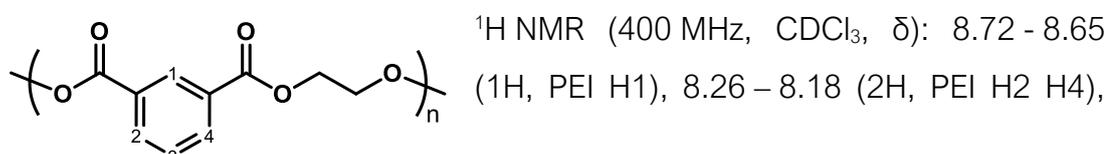
7.55 – 7.45 (1H, PEI H3), 4.80 – 4.65 (4H, PEI -OC$\underline{H}_2$C$\underline{H}_2$O-), 4.50 (4H, PEI -OC$\underline{H}_2$CH$_2$OH), 4.00 (4H, PEI -OCH$_2$C$\underline{H}_2$OH).

4.2.6.3   PEI-OH3

The procedure described above (Section 4.2.6.1) was repeated with IPCl (100.1 g, 0.49 mol) in ~300 ml of chloroform and a solution of EG (27.5 ml, 0.49 mol) and pyridine (168.6 ml, 2 mol) in chloroform (~400 ml). In the second step EG (7.5 ml, 0.13 mol) was added dropwise. Yield 58%.

M_n 17,200 g·mol^{-1}, M_w 25,200 g·mol^{-1}, Đ 1.47.
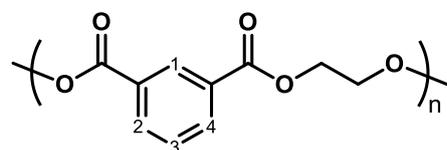
^{1}H NMR (400 MHz, CDCl$_3$, δ): 8.72 - 8.65 (1H, PEI H1), 8.26 – 8.18 (2H, PEI H2 H4), 7.55 – 7.45 (1H, PEI H3), 4.80 – 4.65 (4H, PEI -OC$\underline{H}_2$C$\underline{H}_2$O-), 4.50 (4H, PEI -OC$\underline{H}_2$CH$_2$OH), 4.00 (4H, PEI -OCH$_2$C$\underline{H}_2$OH).

4.2.7   SYNTHESIS OF cc-PEI-*g*-PS COPOLYMERS BY CHAIN COUPLING: PEI-OH + ePS-IPCl

4.2.7.1   cc-PEI$_1$-*g*-PS$_{2.9K}$

IPCl (34 mg, 0.17 mmol) was dissolved in ~3 ml of chloroform in a 2-neck round bottom flask, and the solution was heated to reflux at 70°C. A solution of ePS2.9k (181 mg, 0.06 mmol) and pyridine (100 µl, 1.2 mmol) in chloroform (~10 ml) was added dropwise through a rubber septum, via a syringe pump. The solution was maintained at reflux and stirred for 1h at which point a sample was collected for analysis by ^{1}H NMR and NP-IIC.

An equimolar (with respect to PS macromonomer) amount of PEI-OH1 (532 mg, 0.06 mmol) in chloroform (~6 ml) was added dropwise through a rubber septum, via a syringe pump, and the solution was stirred for 24 hours at reflux at 70°C. All the steps were performed in an inert atmosphere of N$_2$. The solution was cooled to room temperature, and the product was precipitated in excess methanol, recovered by filtration and dried under vacuum. Yield 75%

R.V 15.00 ml, M_n 24,000 g·mol^{-1}, M_w 29,300 g·mol^{-1}, Đ 1.22.

R.V 15.72 ml, M_n 8,800 g·mol^{-1}, M_w 9,600 g·mol^{-1}, Đ 1.09.
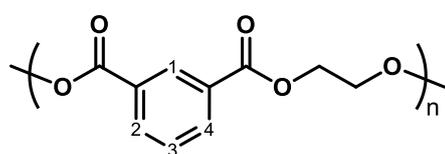
^{1}H NMR (400 MHz, CDCl$_3$, δ): 8.75 - 8.65 (1H, PEI H1), 8.30 – 8.15 (2H, PEI H2 H4), 7.60 – 7.45 (1H, PEI H3), 7.35 - 6.25 (PS Ar H), 4.80 – 4.55 (4H, PEI -OCH$_2$CH$_2$O-), 4.50 (4H, PEI -OCH$_2$CH$_2$OH), 4.00 (4H, PEI -OCH$_2$CH$_2$OH), 2.50 – 1.00 (PS Aliphatic H), 0.80 - 0.50 (3H, PS *sec*-Butyl CH$_3$CH$_2$), 0.80 - 0.50 (3H, PS *sec*-Butyl CHCH$_3$).

4.2.7.2 cc-PEI$_1$-*g*-PS$_{6.4K}$

The procedure described above (Section 4.2.7.1) was repeated with IPCl (30 mg, 0.15 mmol) in ~3 ml of chloroform, a solution of ePS6.4k (322 mg, 0.05 mmol) and pyridine (80 µl, 1.0 mmol) in chloroform(~5 ml), and a solution of PEI-OH1 (447 mg, 0.05 mmol) in chloroform (~10 ml). Yield 61%.

R.V 15.01 ml, M_n 32,700 g·mol^{-1}, M_w 37,300 g·mol^{-1}, Đ 1.14.

R.V 15.33 ml, M_n 14,500 g·mol^{-1}, M_w 16,500 g·mol^{-1}, Đ 1.14.
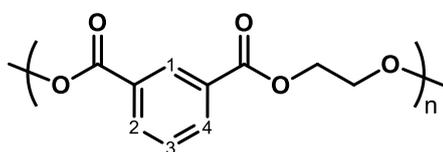
^{1}H NMR (400 MHz, CDCl$_3$, δ): 8.80 - 8.65 (1H, PEI H1), 8.30 – 8.15 (2H, PEI H2 H4), 7.60 – 7.45 (1H, PEI H3), 7.35 - 6.30 (PS Ar H), 4.85 – 4.60 (4H, PEI -OCH$_2$CH$_2$O-), 2.40 – 1.00 (PS Aliphatic H), 0.80 - 0.50 (3H, PS *sec*-Butyl CH$_3$CH$_2$), 0.80 - 0.50 (3H, PS *sec*-Butyl CHCH$_3$).

4.2.7.3 cc-PEI$_2$-*g*-PS$_{9.1K}$

The procedure described above (Section 4.2.7.1) was repeated with IPCl (24 mg, 0.12 mmol) in ~5 ml of chloroform, a solution of ePS9.1k (465 mg, 0.05 mmol) and pyridine (100 µl, 1.2 mmol) in chloroform (~5 ml), and PEI-OH2 (453 mg, 0.05 mmol) in chloroform (~20 ml). Yield 78%.

R.V 14.38 ml, M_n 37,900 g·mol^{-1}, M_w 40,300 g·mol^{-1}, Đ 1.06.

R.V 15.02 ml, M_n 21,700 g·mol^{-1}, M_w 22,500 g·mol^{-1}, Đ 1.04.

^{1}H NMR (400 MHz, CDCl$_3$, δ): 8.76 - 8.65 (1H, PEI H1), 8.30 – 8.15 (2H, PEI H2 H4), 7.60 – 7.45 (1H, PEI H3), 7.35 - 6.30 (PS Ar H), 4.75 – 4.60 (4H, PEI -OC**H**$_2$CH$_2$O-), 4.50 (4H, PEI -OC**H**$_2$CH$_2$OH), 4.00 (4H, PEI -OCH$_2$C**H**$_2$OH), 2.40 – 1.00 (PS Aliphatic **H**), 0.80 - 0.50 (3H, PS *sec*-Butyl C**H**$_3$CH$_2$), 0.80 - 0.50 (3H, PS *sec*-Butyl CHC**H**$_3$).
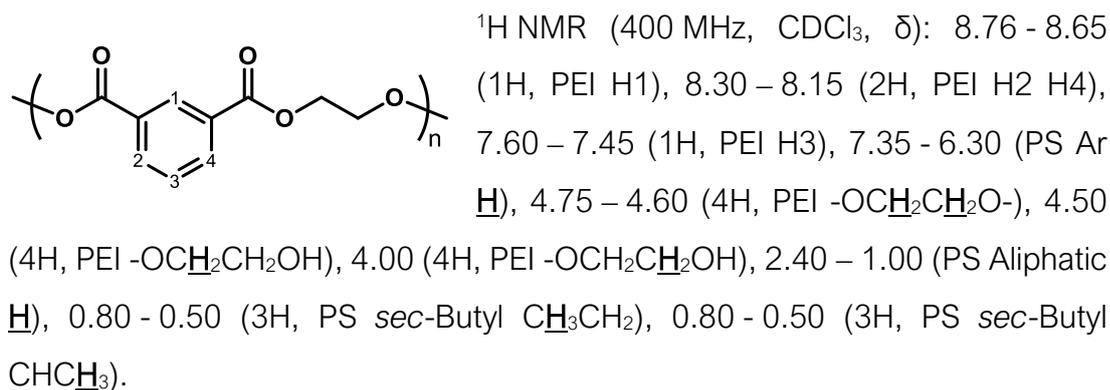
4.2.8 SYNTHESIS OF PEI-*g*-POLYPEGMEM COPOLYMERS BY CHAIN COUPLING

IPCl (22 mg, 0.11 mmol) was dissolved in ~2 ml of chloroform in a 2-neck round bottom flask, and the solution was heated to reflux at 70°C. PolyPEGMEM-OH1 (397 mg, 0.03 mmol) was azeotropically dried three times with dry benzene and then dissolved in dry chloroform (~6 ml). After the addition of pyridine (48 μl, 0.6 mmol), the solution was added dropwise through a rubber septum, via a syringe pump to the 2-neck round bottom flask. The solution was maintained under reflux and stirred for 1h at which point a sample was collected for analysis by ^{1}H NMR.

An equimolar amount of EG end-capped PEI-OH3 (320 mg, 0.03 mmol) in chloroform (~4 ml) was added dropwise through a rubber septum, via a syringe pump, and the solution stirred for 24 hours at reflux. All the steps were performed in an inert atmosphere of N$_2$. The reaction mixture was then cooled to room temperature and the product precipitated in hexane, recovered by filtration and dried under vacuum. Yield 65%

M$_n$ 51,900 g·mol^{-1}, M$_w$ 149,000 g·mol^{-1}, Đ 2.87.

^{1}H NMR (400 MHz, CDCl$_3$, δ): 8.75 - 8.65 (1H, PEI H1), 8.30 – 8.18 (2H, PEI H2 H4), 7.55 – 7.45 (1H, PEI H3), 4.75 – 4.65 (4H, PEI -OC**H**$_2$C**H**$_2$O-), 4.15 – 4.05 (2H, PolyPEGMEM COOC**H**$_2$CH$_2$O), 3.80 – 3.55 (18H, PolyPEGMEM COOCH$_2$C**H**$_2$O (C**H**$_2$C**H**$_2$O)$_4$CH$_3$), 3.40 – 3.35 (3H,
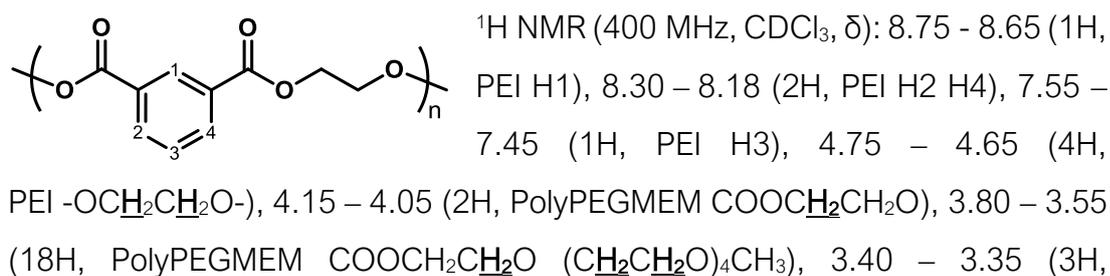
PolyPEGMEM COOC$\underline{H_2}$C$\underline{H_2}$O(C$\underline{H_2}$C$\underline{H_2}$O)$_4$C$\underline{H_3}$), 2.10 – 0.55 (5H, PolyPEGMEM backbone C$\underline{H_2}$CC$\underline{H_3}$).

4.3 RESULTS AND DISCUSSION

In Chapter 2 and 3, the synthesis of PS and PolyPEGMEM bisphenol functionalised macromonomers (Figure 4.3), respectively, was designed and optimised to allow the incorporation of the macromonomer as a comonomer in a polycondensation reaction.
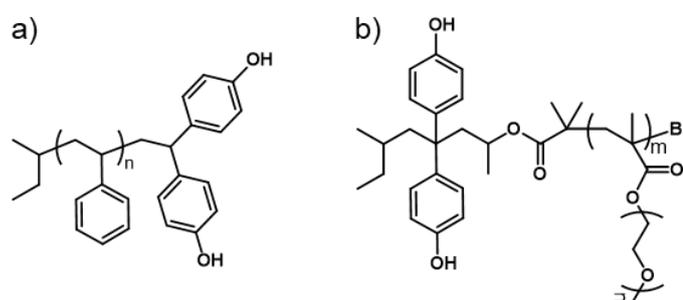
Figure 4.3 Structure of bisphenol functionalised macromonomers: a) PS, synthesised via end-capping procedure by anionic polymerisation, and b) PolyPEGMEM synthesised with a functionalised initiator by ATRP.

In this Chapter, the copolymerisation of PS and PolyPEGMEM macromonomers in the polycondensation of poly(ethylene isophthalate) to produce graft block copolymers is described. Initially, 2 PS macromonomers with different molar mass (2,900 and 6,400 g·mol^{-1}) were added to a solution polycondensation reaction, reacting first with isophthaloyl chloride, and then, upon addition of ethylene glycol (EG), being incorporated into the growing chain as a comonomer (Scheme 4.3). Subsequently, a modified approach was attempted, in which EG end-capped PEI chains were synthesised before coupling with isophthaloyl bis-functionalised PS macromonomers (Scheme 4.5). In this way, it was possible to know the PEI chain length between two grafted PS arms, thanks to the SEC characterisation of the PEI block before the coupling reaction. Different PS macromonomers were used also in this case, with molar masses of 2,900, 6,400 and 9,300 g·mol^{-1}. The same coupling approach was chosen for the synthesis of

a graft copolymer of PEI-*g*-PolyPEGMEM through the incorporation of a polyPEGMEM macromonomer into the polyester backbone.

4.3.1   sp-PEI-*g*-PS COPOLYMERS BY SOLUTION POLYCONDENSATION

In an initial attempt to introduce the bisphenol end-functionalised PS macromonomer into a polycondensation reaction between isophthaloyl chloride (IPCl) and ethylene glycol (EG), a solution of the macromonomer in chloroform was added dropwise to a solution of IPCl in the same solvent, in the presence of pyridine (Scheme 4.3). The presence of a base is crucial to neutralise the HCl released from the esterification reaction between the alcohol (OH groups on PS macromonomer and EG) and the acid chloride (IPCl).
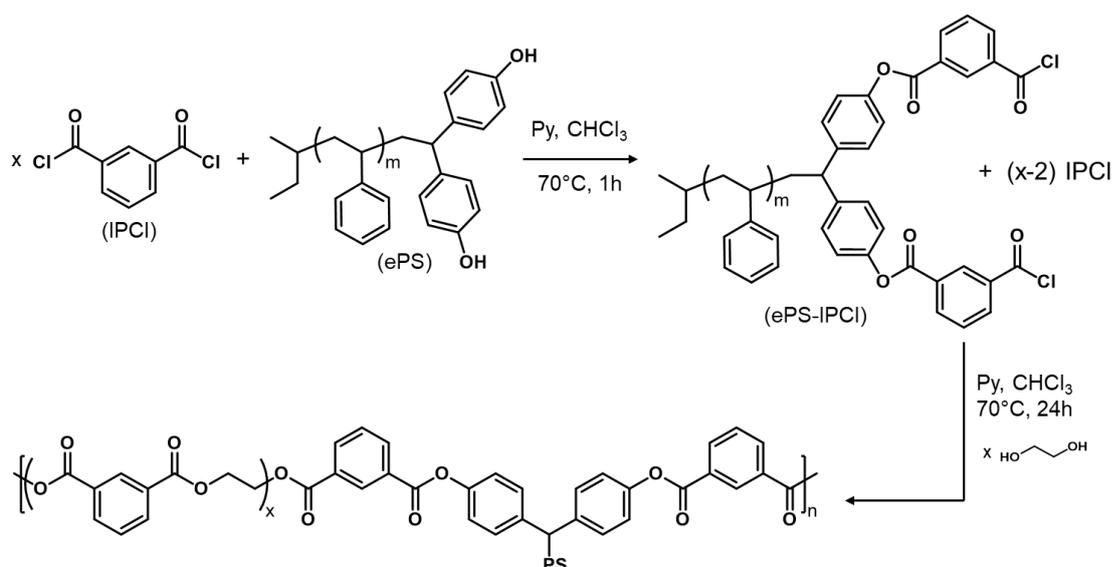
Scheme 4.3 Synthesis of sp-PEI-*g*-PS copolymers by solution polycondensation.

It is also necessary that an excess of IPCl, with respect to PS, is always present. Therefore, even if IPCl was in excess compared to PS (30:1 molar ratio), the solution of PS was added dropwise with vigorous stirring, in order to prevent the formation of local high concentration of PS. The presence of an excess of IPCl ensures that each macromonomer reacts with 2 IPCl to give the ePS-IPCl species in Scheme 4.3. Otherwise, given the bis-functionalisation of each PS, 2 macromonomers could be bonded together through one IPCl molecule. The molar ratio between the ethylene glycol (EG) and the diacid chloride was chosen

to be 1:1, in order to obtain high MW, according to the theory of polycondensation kinetics.[11] The reaction was performed under an inert atmosphere and with dry reagents and solvents, in order to avoid hydrolysis of the IPCl to isophthalic acid, that would prevent the esterification. Two copolymerisations were performed, each using a different macromonomer (ePS2.9k and ePS6.4k) to yield sp-PEI-*g*-PS$_{2.9K}$ and sp-PEI-*g*-PS$_{6.4K}$, respectively. The quantities of reagents are summarised in Table 4.1.

Table 4.1 Amount of reagents (in mmol) and yields for the sp-PEI-*g*-PS graft copolymers obtained by solution polycondensation.

	IPCl	EG	ePS	Py	Yield
sp-PEI-*g*-PS$_{2.9K}$	15	15	0.5	60	65%
sp-PEI-*g*-PS$_{6.4K}$	15	15	0.5	60	82%

After 1 hour of reaction between the PS macromonomer and IPCl, a sample was collected and recovered by precipitation into excess MeOH, for analysis by NMR and NP-IIC, in order to verify the isophthaloyl functionalisation of the macromonomer.

In both experiments, the NMR spectrum (see for example ePS6.4k-IPOMe in Figure 4.4b) confirm the appearance of peaks, between 9 and 7.5 ppm, which can be assigned to the aromatic protons of the isophthaloyl groups, while the peak corresponding to the OH peak of the macromonomer (4.5 ppm in Figure 4.4a) completely disappears. In the same aromatic region, the sharp peaks of residual unreacted IPCl, following esterification to the methyl ester once exposed to an excess MeOH, are visible (8.73, 8.27 and 7.57 ppm). The precipitation in MeOH causes the esperification of ePS-IPCl sample too, as proven by the appearance of a sharp peak at 4.0 ppm, which can be assigned to the methyl ester of the isophthaloyl groups.
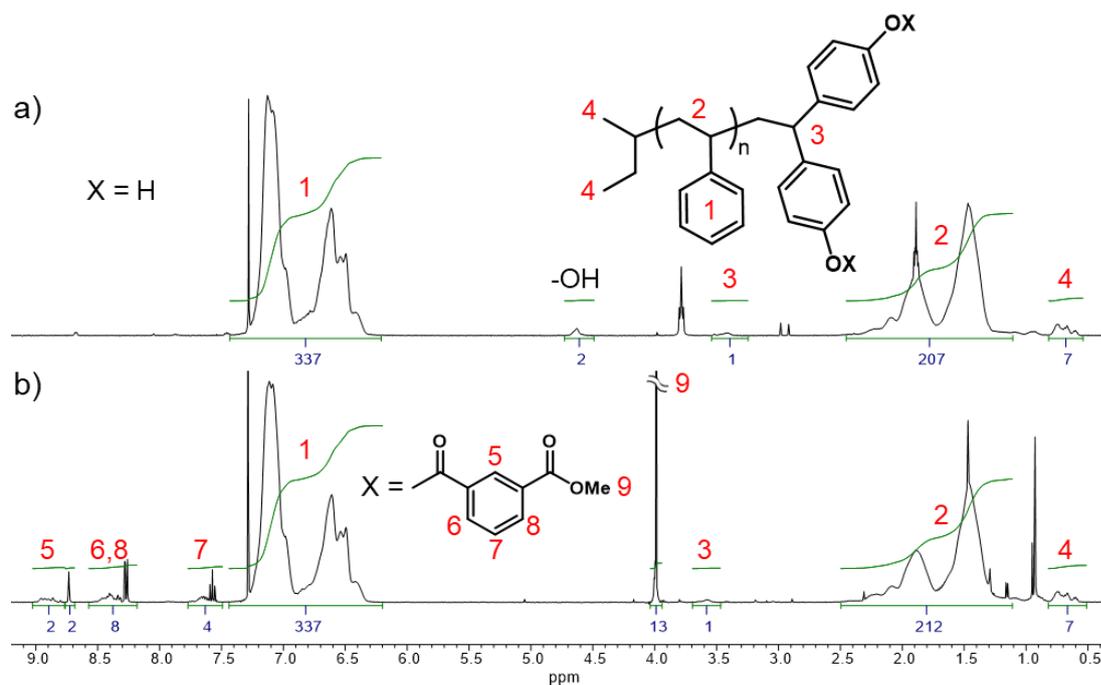
Figure 4.4 ^{1}H NMR (CDCl$_3$, 400 MHz) spectra of a) ePS6.4k and b) the methyl ester of ePS6.4k-IPCl (ePS6.4k-IPOMe).

The NMR analysis alone is not enough to be sure that the reaction reached completion in these conditions, thus NP-IIC was added as analytical technique to further prove the effectiveness of the reaction. If the reaction between the macromonomer and IPCl was successful, the change from hydroxyl groups of the original ePS, to -COOMe group, after the reaction with IPCl and precipitation into excess MeOH would result in a change in interaction of the polymer with the stationary phase and a related change in retention volume. The chromatograms for the samples after step 1 in the case of each of the two copolymerisations are presented in Figure 4.5 (ePS2.9k-IPOMe and ePS6.4k-IPOMe, solid lines). For comparison, the chromatograms of the bisphenol functionalised macromonomers (ePS2.9k and ePS6.4k, dashed lines) before the reaction with IPCl are also reported in the same figure.

As discussed in Chapter 2, with normal phase interaction chromatography, the separation of polymers is achieved by partition between a polar stationary phase and a less polar mobile phase, thus obtaining resolution primarily in terms of functionality.[12-13] In this case in particular, we expect to see a difference of retention volume between the polar OH functionalised ePS and the isophthaloyl

methyl ester group – which is less polar and therefore less strongly retained - after the reaction with IPCl and precipitation in excess MeOH.
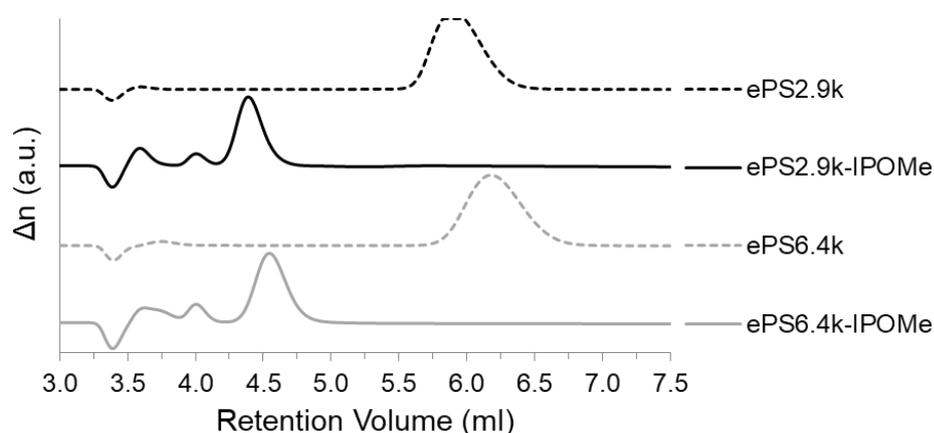
Figure 4.5 NP-IIC chromatograms, recorded by RI detector, of PS macromonomers ePS2.9k and ePS6.4k (dashed lines) compared with the traces of the respective -COOMe functionalised PS (solid lines), ePS2.9k-IPOMe and ePS6.4k-IPOH.

Looking at Figure 4.5, is evident that the peak of bisphenol ePS2.9k and ePS6.4k at around 6 and 6.2 ml has completely shifted to lower retention volume (ca. 4.3 and 4.5 ml, respectively) in both ePS-IPOMe traces, proving that the reaction reached completion. It is worth mentioning that the small difference in retention volume between ePS2.9k and ePS6.4k and between ePS2.9k-IPOMe and ePS6.4k-IPOMe is due to the difference in M_n. Even if the separation in NP-IC is primarily due to functionality, with equal functional groups higher molar mass chains will be eluted later, in comparison to smaller chains. This explains why the peaks of ePS6.4k polymers are eluted slightly later than the ePS2.9k polymers.

Once the PS macromonomers were functionalised with isophthaloyl chloride in step 1, the addition of EG started the proper polycondensation reaction in which ePS-IPCl could act as comonomer to be incorporated into the PEI chain (Scheme 4.3). Figure 4.6 shows an example of the NMR spectrum of the final copolymer, in this case sp-PEI-*g*-PS$_{2.9K}$, compared with the spectrum of a PEI homopolymer (PEI-OH3, synthesised via the same solution polycondensation procedure and used for the synthesis of grafted copolymers by chain coupling,

as discussed later in Section 4.3.4), in order to identify the peaks of the PEI block in the copolymer.

The NMR spectrum of the copolymer (Figure 4.6b), which is similar to that of the second attempt sp-PEI-*g*-PS$_{6.4K}$, shows the broad peaks of PS macromonomers (the aromatic protons between 7.3 and 6.3 ppm, and the aliphatic protons of the PS backbone between 2.5 and 1.1 ppm, together with the butyl protons of the initiator, between 0.8 and 0.5 ppm) and peaks ascribable to PEI, as proven by the comparison with the spectrum of PEI homopolymer in Figure 4.6a.
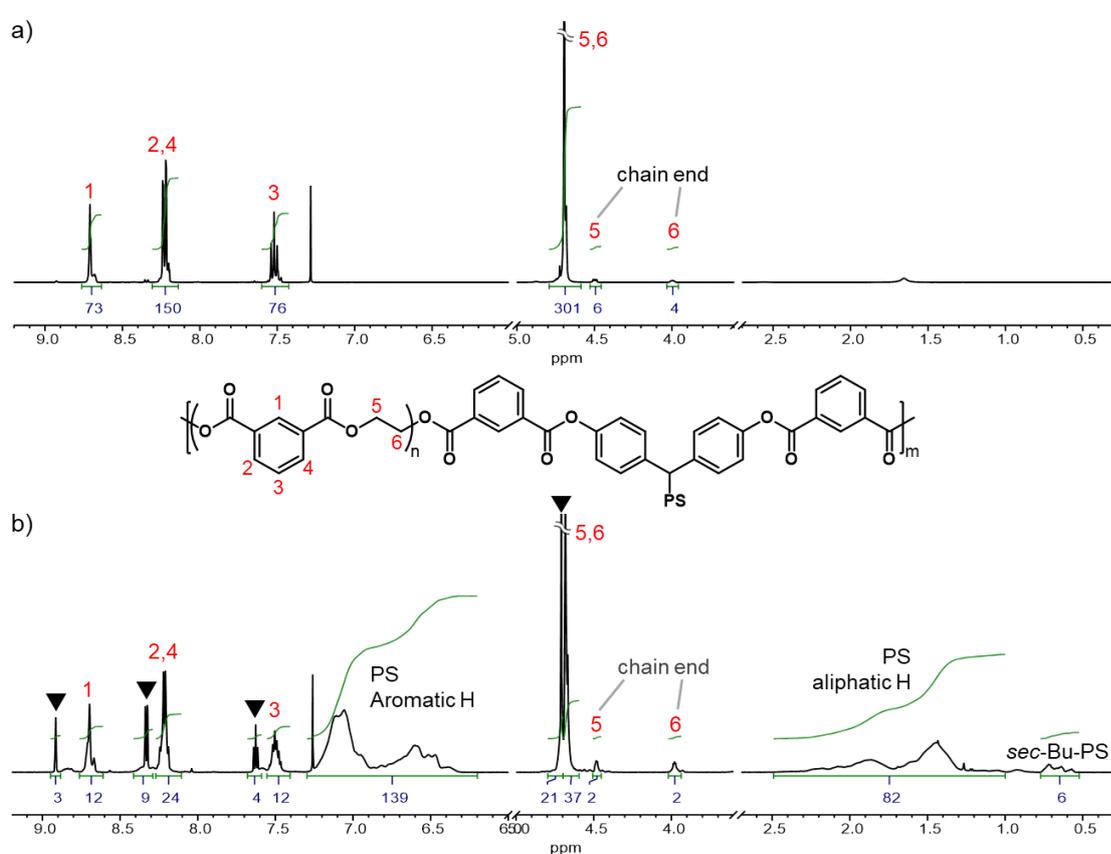
Figure 4.6 ^{1}H NMR (CDCl$_3$, 400 MHz) of a) PEI-OH3 homopolymer and b) sp-PEI-*g*-PS$_{2.9K}$.

There are, however, some additional peaks close to the main PEI peaks (highlighted with triangles in Figure 4.6b). These peaks are actually present after every solution polycondensation reaction, be it the synthesis of PEI homopolymers or copolymerisation with macromonomers, e.g. Figure 4.7a, which shows the NMR spectrum of PEI-OH3 following recovery by precipitation in MeOH. It was noticed that during the polycondensation, the reaction solution

turned gradually cloudy white, meaning that there was probably some species forming, which was not completely soluble. It was decided, therefore, to filter the reaction mixture, resulting in a clear solution which was added into excess MeOH, in order to precipitate the product. The NMR spectra of PEI-OH3 after this additional filtration step is presented in Figure 4.7b. The NMR spectrum of the product obtained following filtration of the reaction mixture reveals the complete disappearance of the peaks previously indicated by triangles in Figure 4.7a, which can therefore be ascribed to the partially unsoluble species, removed by filtering the cloudy solution.
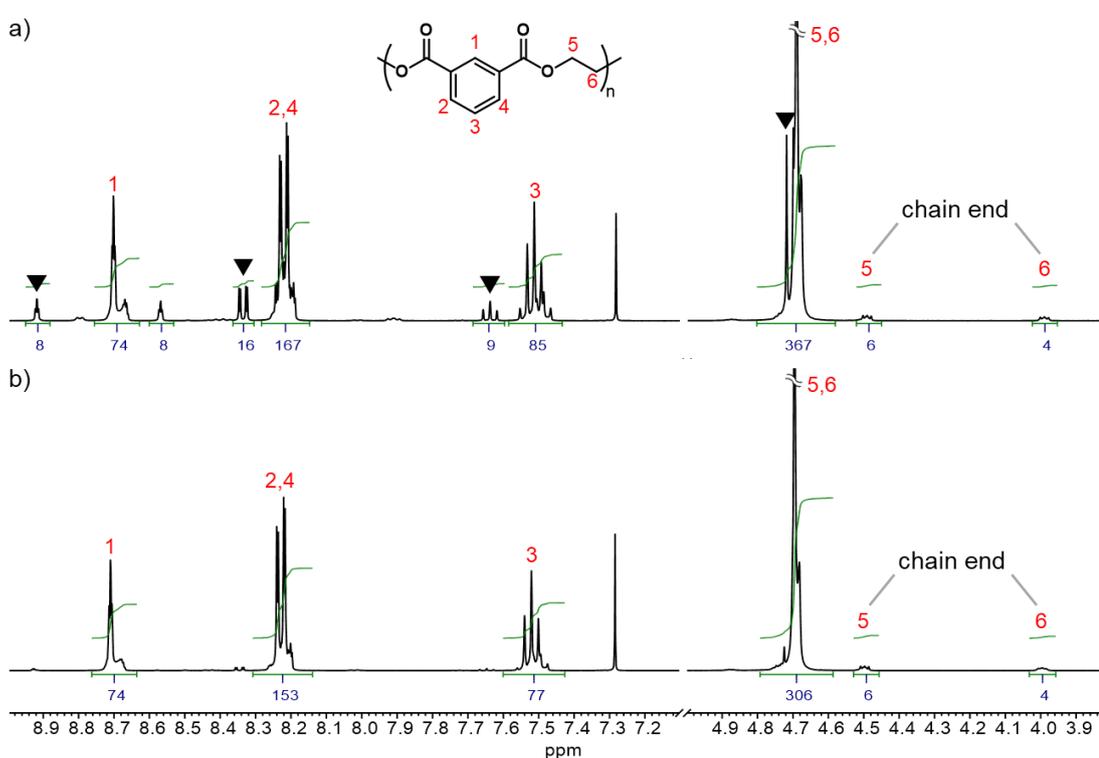
Figure 4.7 ^{1}H NMR (CDCl$_3$, 400 MHz) of a) PEI-OH3 and b) PEI-OH3 after being resolubilised in chloroform, filtered and precipitated in MeOH.

Additional evidence that can help in identifying the nature of these species can be found in SEC chromatograms of PEI-OH3 before and after filtration, shown in Figure 4.8. The clear difference is the disappearance of the sharp peak at ca. 18.5 ml, which corresponds to species with a low molecular weight of about 200 g·mol^{-1} (calculated by conventional calibration with PS standards). Given the

very low MW, these peaks could reasonably comprise solvents, unreacted IPOMe, or perhaps PEI oligomers composed of one or two repeat units.
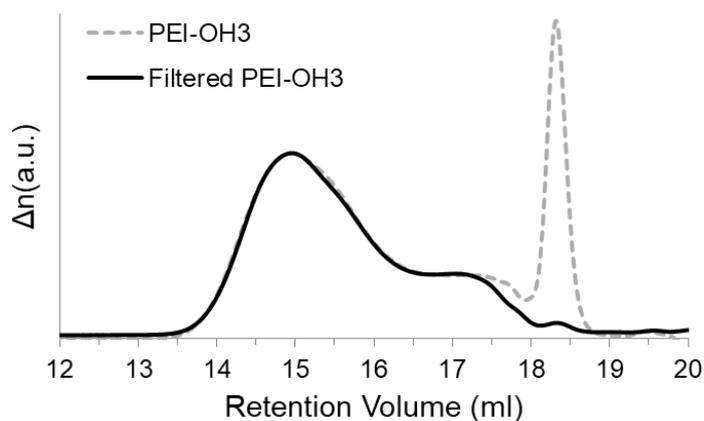
Figure 4.8 SEC chromatograms of PEI-OH3 (dashed trace) and PEI-OH3 after being resolubilised in chloroform, filtered and precipitated in MeOH (solid trace).

Since the acid chloride is very easily hydrolysed by traces of water, either during storage or in the reaction solution, the presence of partially hydrolysed IPCl can stop the polycondensation, which is not expected to proceed via the esterification of a (less reactive) carboxylic acid, and which usually requires much higher temperatures.[14-16] The result of such hydrolysis is likely to be PEI oligomers with 1 or 2 repeat units. These species would contain carboxylic acid groups, which make the species partially insoluble in the reaction solvent, chloroform. Therefore, they can be filtered off the solution in chloroform, but can be still analysed by NMR in the same solvent, giving the peaks identified earlier in the NMR spectra.

Going back to the discussion about the synthesis of grafted copolymers by solution polycondensation, the NMR analysis (Figure 4.6b) suggests that the polycondensation copolymerisation reaction worked, resulting in the successful formation of the sp-PEI-*g*-PS. However, the presence of peaks in the NMR spectrum of the product which can be assigned to both polystyrene and polyester, is not evidence enough to prove that PS macromonomers actually took part in the polycondensation reaction and were incorporated into the PEI chain. In this sense, a comparison of the SEC chromatograms - in chloroform - of the copolymers and the macromonomers before the polycondensation reaction, can

give more evidence of the copolymerisation. The SEC traces for both the copolymers, along with the respective PS macromonomers, are presented in Figure 4.9. It is clear that in both cases, the peak of the ePS macromonomer (dashed traces) has completely disappeared, with the peak of the copolymer shifting to lower retention volumes (solid traces), proving that the macromonomer took part in the polycondensation reaction and was incorporated into the PEI chain.
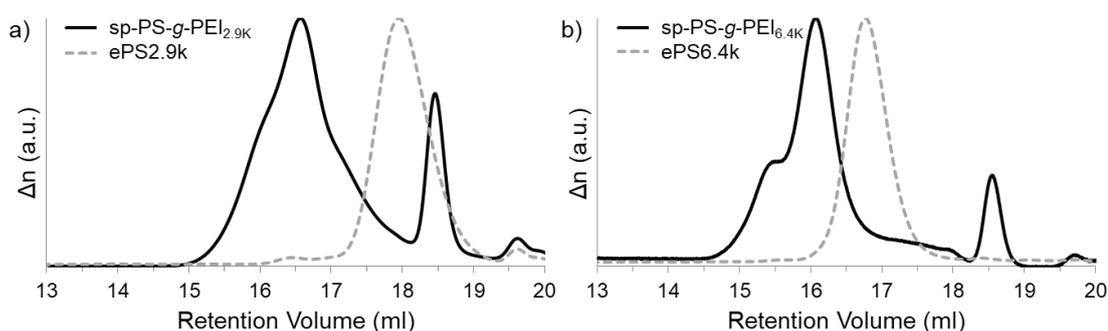
Figure 4.9 SEC chromatograms of a) sp-PEI-g-PS$_{2.9K}$ and b) sp-PEI-g-PS$_{6.4K}$, compared with the respective PS macromonomer traces (ePS2.9k and ePS6.4k, respectively).

In both cases, the reaction solution at the end of the synthesis was not filtered before precipitation in MeOH. Therefore, the peak at ca. 18.5 ml, corresponding to low MW PEI oligomers, is still present in both chromatograms.

The M_n and dispersity of the copolymers were calculated by triple detection, using as dn/dc a weighted average of the dn/dc values of PS (0.16 ml·g^{-1}) and PEI (0.098 ml·g^{-1}), as shown in the following equation:

$$dn/dc^{PEI\text{-}g\text{-}PS} = 0.16 \text{ ml·g}^{-1} \times \text{w.f.}^{PS} + 0.098 \text{ ml·g}^{-1} \times \text{w.f.}^{PEI}$$

where w.f. is the percentage weight fraction of the macromonomer (PS) or of the polyester (PEI), calculated as:

$$\text{w.f.}^{x} = \frac{\chi_x \cdot MW^x}{\chi_{PEI} \cdot MW^{PEI} + \chi_{PS} \cdot MW^{PS}}$$

where x can indicate either PS or PEI, MW^{PEI} is the molar mass of the PEI repeat unit (192.17 g·mol^{-1}) and MW^{PS} is the molecular weight of the PS repeat unit

(104.15 g·mol^{-1}). χ is the mole fraction, calculated by NMR using the integrals of the peaks of PS and PEI in the aromatic region (example for sp-PEI-*g*-PS$_{2.9K}$ in Figure 4.10).

For each PEI repeat unit, peaks 1 and 3 (Figure 4.10) have integrals equal to 1 (1H) and the overlapping peaks 2 and 4 have a combined integral, arising due to 2H.
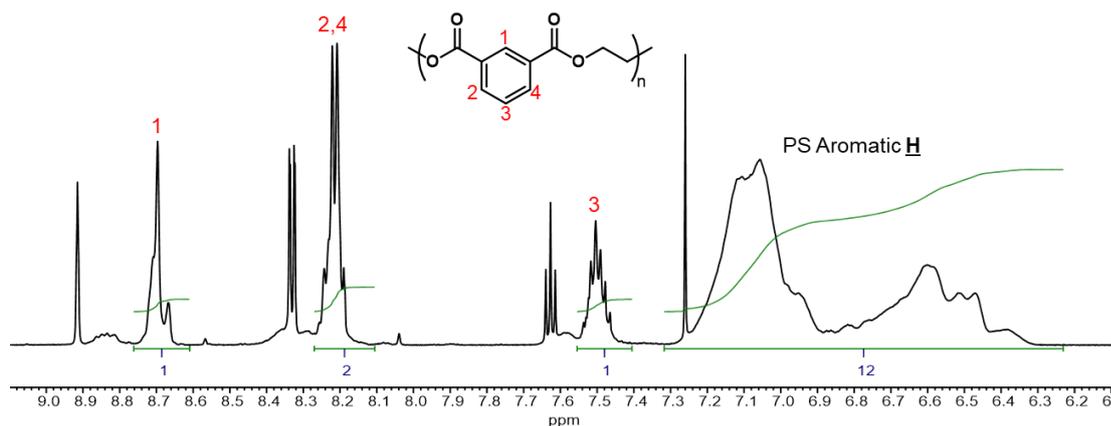
Figure 4.10 Aromatic region of ^{1}H NMR (CDCl$_3$, 700 MHz) spectra of sp-PEI-*g*-PS$_{2.9K}$ copolymer.

By comparison the 5 aromatic protons of polystyrene have a combined integral of 12, indicating there are in this case 2.4 PS repeat units for each PEI repeat unit. The mole fraction of PS can be calculated as χ_{PS} = 2.4/(1+2.4) = 0.71, thus giving a PEI mole fraction of 0.29. The same calculation has been done for sp-PEI-*g*-PS$_{6.4K}$, giving a value of 4.4 PS repeat units per PEI repeat unit, and therefore χ_{PS} = 0.81 and χ_{PEI} = 0.19.

The SEC data resulting from the calculations by triple detection, gave M$_n$ 5,500 g·mol^{-1} with Đ 1.20 for sp-PEI-*g*-PS$_{2.9K}$, and M$_n$ 12,400 g·mol^{-1} with Đ 1.16 for sp-PEI-*g*-PS$_{6.4K}$. Comparing these numbers with the M$_n$ of the PS macromonomers used in the 2 copolymerisations (2.9 and 6.4 kg·mol^{-1}), it can be concluded that PS macromonomers were successfully incorporated into the growing PEI chain, but copolymers with only 1 grafted PS and a few repeat units of PEI were obtained, with the M$_n$ growing from 2.9 to 5.5 kg·mol^{-1} for sp-PEI-*g*-PS$_{2.9K}$, and from 6.4 to 12.4 kg·mol^{-1} for sp-PEI-*g*-PS$_{6.4K}$. These results can explain the copolymer dispersities, which are quite narrow (<1.2) in both

cases, for a step-growth polymerisation mechanism. Carothers equation predicts that as, a step-growth polymerisation approaches full monomer conversion, the dispersity tends to 2.0, in case the molar mass of the monomers is negligible with respect to the final polymer. However, in the current reactions one of the comonomers is a macromonomer, with relatively high value of M_n and a low Đ, and it is plausible that the dispersity of the final copolymer is mainly due to the macromonomer, obtained by anionic polymerisation and thus very narrow, while the polycondensation reaction only slightly contributed to broaden the dispersity, from less than 1.05 for ePS to around 1.20 for the copolymers.

To complete the characterisation, the copolymers were analysed by Diffusion-Ordered NMR Spectroscopy (DOSY-NMR). DOSY-NMR analysis has been successfully used before to provide evidence of graft copolymer formation.[17-20] This technique correlates the NMR signals to the diffusion coefficient D by measuring the rate of attenuation of NMR peaks caused by diffusion. Any signal from nuclei on the same molecule will diffuse at the same rate and, as a result, should appear in the spectrum at the same value of D. Signals belonging to small molecules will have a higher diffusion coefficient compared to larger molecules, which will diffuse more slowly and hence show a lower diffusion coefficient. Applying this theory to a graft copolymer, we expect to see peaks of different, covalently connected blocks with similar D values, if they are in the same copolymer macromolecule, since the side chains have the same translational mobility as the backbone.[20]

Figure 4.11 and 4.12 show the DOSY NMR spectra of the copolymers, sp-PEI-*g*-PS$_{2.9K}$ and sp-PEI-*g*-PS$_{6.4K}$ respectively, obtained by solution polycondensation. The attribution made earlier (Figure 4.7) of the sharp NMR peaks, appearing immediately adjacent to the main PEI peaks (8.9, 8.3 and 7.6 ppm) to low molar mass PEI homopolymers, is also supported by DOSY: in both cases the diffusion coefficient value for these peaks (between 6×10^{-6} and 7×10^{-6} cm^2·sec^{-1}) is significantly higher than the other signals, meaning that they are ascribable to smaller species, also in accordance with the SEC analysis (peak at 18.5 ml in Figure 4.9, ca. 200 g·mol^{-1}).

The diffusion coefficients (D) associated with the other PEI NMR peaks are spread over a wide range of values, suggesting that there are distribution of species containing PEI repeat units. In the DOSY spectra of sp-PEI-*g*-PS$_{2.9K}$ (Figure 4.11), there are PEI NMR peaks (D~1.8×10^{-6} cm^2·sec^{-1}) in close proximity with PS signals (D=1.75×10^{-6} cm^2·sec^{-1}), which are ascribable to the PEI blocks in the copolymer.
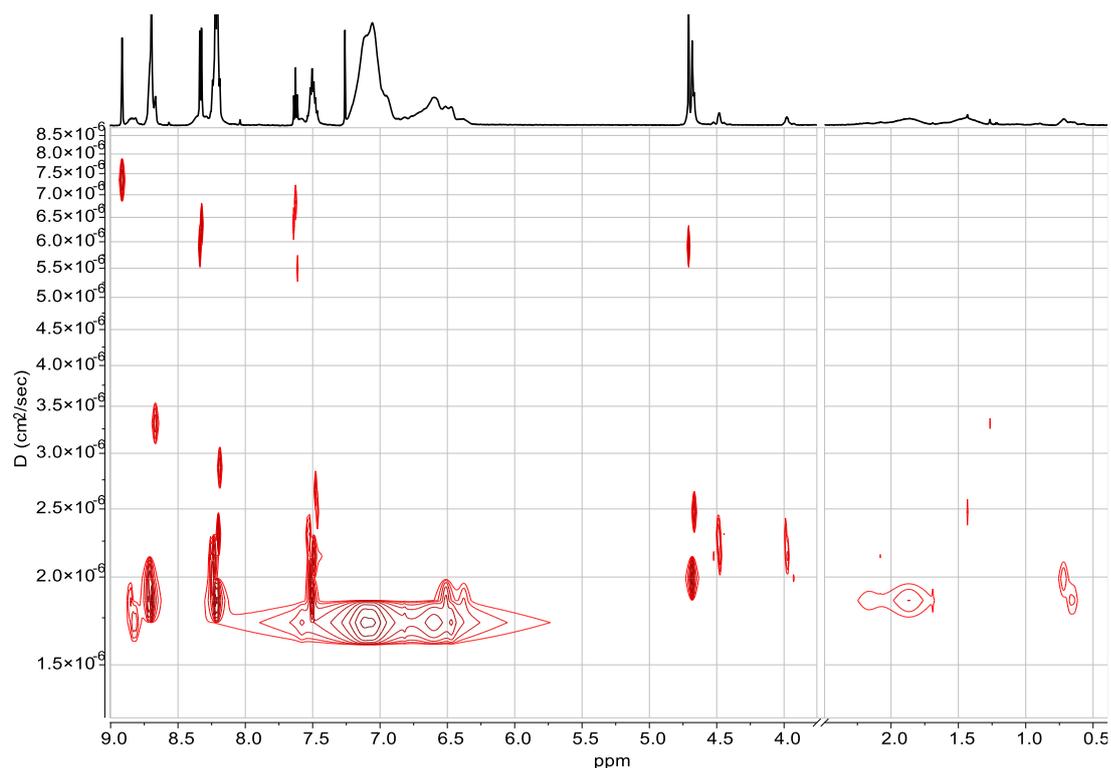
Figure 4.11 DOSY-NMR (CDCl$_3$, 600 MHz) of sp-PEI-*g*-PS$_{2.9K}$.

Most of PEI NMR signals are in the same D range as the PS NMR signals, below 2.0×10^{-6} cm^2·sec^{-1} – indicating that the two polymers are indeed part of the same molecule. There are also PEI NMR peaks with D values between 3.5 and 2.5×10^{-6} cm^2·sec^{-1}, due to smaller PEI homopolymers that probably did not incorporate the macromonomers. It is interesting to notice that the signals of -CH$_2$CH$_2$OH (PEI) chain ends (at 4.5 and 4.0 ppm) show a D value (2.3×10^{-6} cm^2·sec^{-1}), which is slightly higher than the main PEI chain (D=2.0×10^{-6} cm^2·sec^{-1}), possibly because of the greater freedom of movement that the chain-ends experience, compared to EG segments within the chain (peak at 4.7 ppm).

The DOSY spectra of sp-PEI-*g*-PS$_{6.4K}$ (Figure 4.12) also shows PEI NMR peaks with similar D values (1.4×10^{-6} cm^2·sec^{-1}) compared to the D values for the PS signals (1.3×10^{-6} cm^2·sec^{-1}). In this case, though, these signals are not the PEI main peaks (8.7, 8.2 and 7.5 ppm), but weaker and broader peaks in the same spectral region (8.9-8.8, 8.4-8.3 and 7.65-7.55 ppm). The assignment of these peaks is not clear, but they could be related with the first isophthaloyl groups that react with PS macromonomer. Similar peaks are also seen in the NMR spectra of the macromonomer after step 1 (see for instance Figure 4.4b).
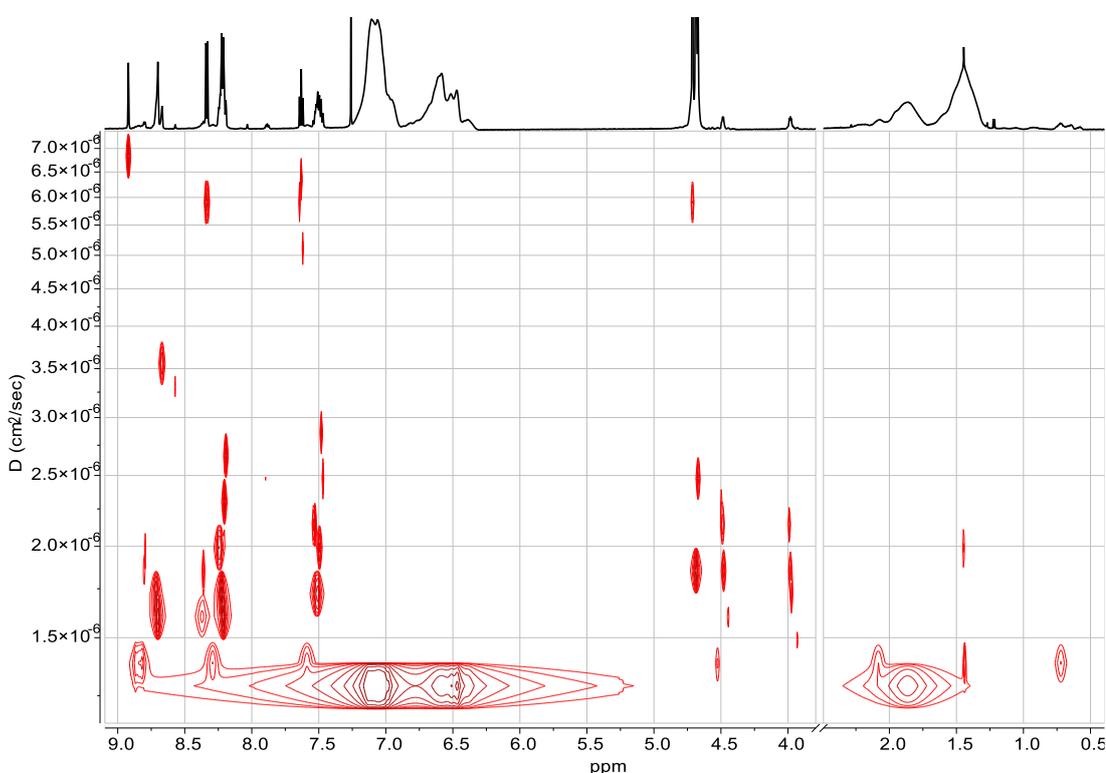
Figure 4.12 DOSY NMR (CDCl$_3$, 600 MHz) of sp-PEI-*g*-PS$_{6.4K}$.

Further PEI NMR signals appear, with a wide distribution of D values (between 1.5 and 3.0×10^{-6} cm^2·sec^{-1}), suggesting that only the weak PEI NMR peaks with D similar to PS chains can be attributed to PEI units which are part of a copolymer, and that the majority of the PEI signals with higher D values (at 1.7×10^{-6} cm^2·sec^{-1}) corresponds to PEI which is actually not in the same molecule (the copolymer), but constitutes a PEI homopolymer.

The same argument made before about the EG end-group signals (at 4.5 and 4.0 ppm) with slightly higher D values because of the greater freedom of

movement, might be also valid here for PEI signals with a higher D value than the PS blocks. In this case, given the graft architecture of the copolymer, the PEI backbone comprises of blocks which are 'trapped' between two PS macromonomers and blocks of PEI at the copolymer ends, with a free chain end. This could be a reason for the appearance of PEI signals with D values in line with the PS ones ('trapped' blocks) and with slightly higher D values between 1.5 and 3.0×10^{-6} $cm^2 \cdot sec^{-1}$ (free PEI backbone ends). Probably, a more detailed DOSY investigation of copolymers with this kind of structure could be useful to better assign the different signals.

To conclude the DOSY discussion, the presence of signals from PEI and PS with similar D values does not necessarily prove that the 2 blocks are in the same copolymer molecule, because they might have similar M_n (as in the case of sp-PEI-*g*-PS$_{2.9K}$ in which PEI is 2,300 $g \cdot mol^{-1}$ and ePS$_{2.9k}$ 2,900 $g \cdot mol^{-1}$) and thus similar D. In this sense, SEC analysis discussed before is a better confirmation of copolymerisation, with the macromonomer peaks that completely shifted to lower retention volumes (Figure 4.9). On the other hand, DOSY-NMR offered some supporting evidence that, despite the fact that PS macromonomers were effectively incorporated into PEI chains, the polycondensation reaction also occurred without PS incorporation, thus producing a significant amount of PEI homopolymers.

4.3.2   cc-PEI-*g*-PS COPOLYMERS BY CHAIN COUPLING

By simply adding the PS macromonomer into the solution polycondensation reaction, we demonstrated (and described above) that it is possible for the PS macromonomer to be incorporated into the polyester chain as a comonomer. However, it seems that, on an average, one PS macromonomer per PEI chain was incorporated, yielding something more similar to a three-arm star-shaped copolymer than a graft copolymer. In an attempt to improve the outcome, a modified approach has been explored in which PEI chains were synthesised by solution polycondensation, and then coupled with the PS macromonomer. The procedures and relative results are discussed in the following sections.

4.3.2.1 Diacid chloride end-capped PEI + bisphenol functionalised ePS (cc-PEI-*g*-PS)

In order to have chain coupling, each species must carry 2 mutually reactive functional groups. The first attempt involved reaction between the bisphenol-functionalised PS macromonomer and diacid chloride end-capped PEI chains (Scheme 4.4).
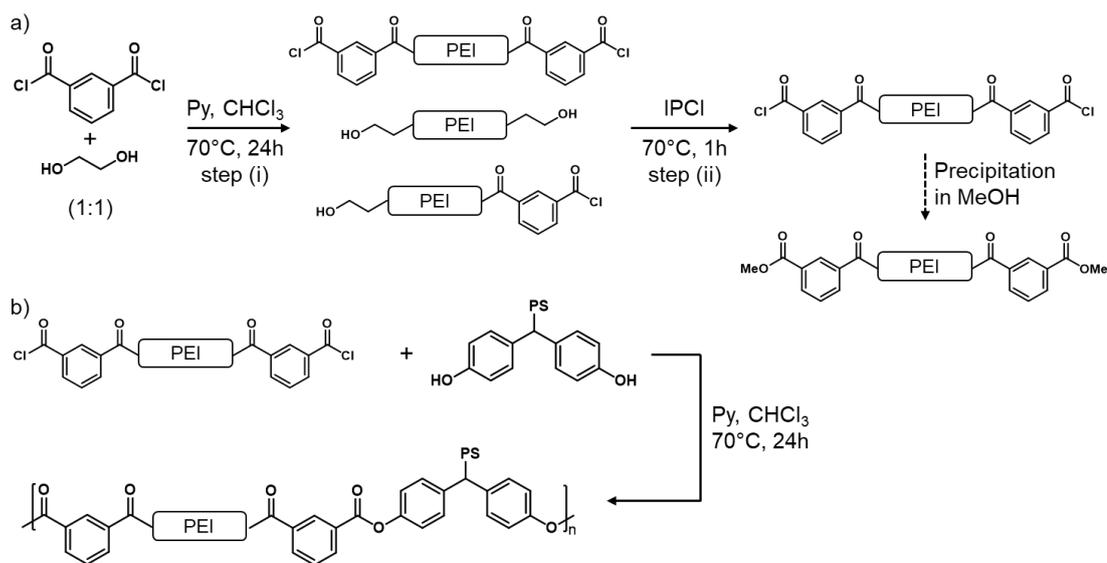
Scheme 4.4 Synthesis of a) a diacid chloride end-capped PEI and b) subsequent coupling with ePS macromonomers, to yield cc-PEI-*g*-PS copolymers.

IPCl end-capped PEI was synthesised in two steps (Scheme 4.4a) by (i) solution polycondensation between IPCl and EG in 1:1 molar ratio, followed by (ii) the addition of a slight excess of IPCl in order to end-cap any EG chain-end. A sample was collected upon precipitation in excess MeOH after step (i) for analysis, and to compare with the final product, collected after step (ii), to ensure complete end-capping with IPCl. The PEI chains formed after step (ii) need to be collected by precipitation in MeOH, in order to remove any excess IPCl that can be present in the reaction solution, which could react with PS macromonomer and in turn prevent coupling of the PS macromonomer with PEI-IPCl in the following step of the procedure (Scheme 4.4b).

The NMR spectrum of a sample taken after step (i) of the synthesis of PEI blocks (Figure 4.13a) shows all the expected peaks of PEI, and also peaks at 4.5 and

4.0 ppm which can be assigned to EG chain ends. This suggest that, even if the reaction in step (i) was performed in a 1:1 ratio of the comonomers, there was probably a slight excess of EG hydroxyl groups, with respect to acid chloride groups, possibly caused by the hydrolysis of IPCl during storage. An excess of hydroxyl groups naturally resulting in most of the chains being end-capped by EG.
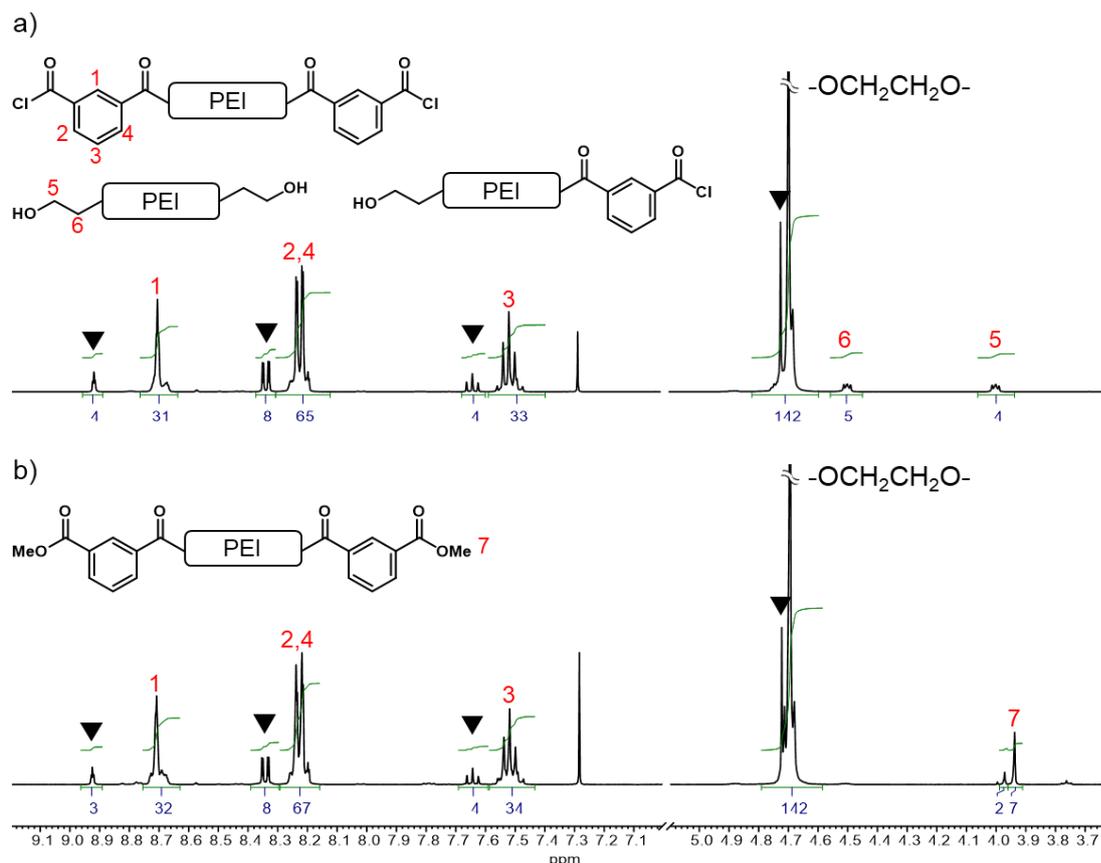
Figure 4.13 ^{1}H NMR (CDCl$_3$, 400 MHz) spectra of PEI after a) step (i) and b) step (ii), in the synthesis of diacid end-capped PEI.

As seen already in Section 4.3.1, the peaks of low molecular weight PEI oligomer, indicated by triangles, are also present, both after step (i) and (ii). After an excess of IPCl was added in step (ii), all the chains were successfully end-capped, as evidenced by the disappearance in Figure 4.13b of the peaks at 4.5 and 4.0 ppm (EG chain ends) and the appearance of a new peak at 3.94 ppm, which is consistent with the formation of a methyl ester.[21] It is almost certain that the acid chloride functionality at the chain ends of PEI underwent esterification when the

solution was poured into excess methanol to precipitate the polymer, giving the methyl ester peak in the NMR spectrum.

Assuming that was the case, then subsequent coupling with ePS would not be possible, because the transesterification reaction (methyl ester with bisphenol moieties on ePS) cannot happen under these reaction conditions.[14-16] Instead, the bisphenol end-capped PS macromonomer has suitable functionalisation to undergo an esterification reaction with acid chloride moieties to give a polyester graft copolymer (Scheme 4.4b).

The coupling step was attempted regardless, using a 1:1 molar ratio between PEI and the macromonomer, in order to obtain a graft block copolymer.[11] The SEC analysis (Figure 4.14) confirmed that no coupling had occurred.
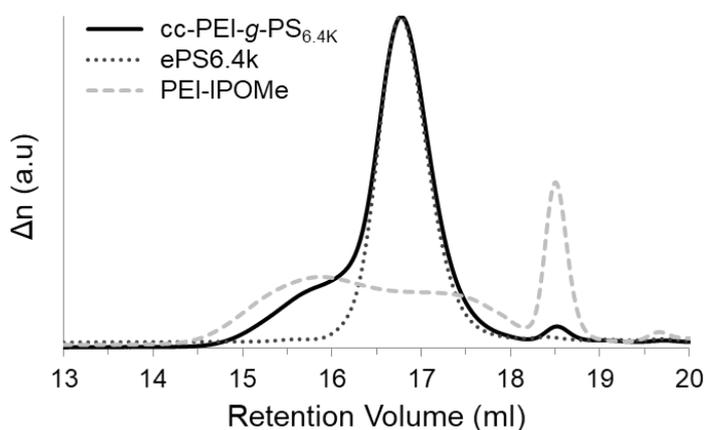
Figure 4.14 SEC chromatograms of cc-PEI-*g*-PS$_{6.4K}$, compared with ePS6.4k macromonomer and PEI-IPOMe traces.

The copolymer trace (solid line), is basically the sum of the traces of the 2 precursor chains - PS and PEI - that did not react with each other. In particular, the ePS peak (dotted line) remained exactly unchanged, in terms of both retention volume and dispersity, while the shoulder at ca. 15.5 ml is due to the PEI chain. It can be concluded that this approach to coupling is not feasible, because the excess IPCl used to end-cap PEI chains in step (ii) needs to be removed by collecting the product as precipitate in MeOH. However, this process results in the esterification of the acid chloride group on PEI chain-end. Even if PEI was precipitated into a solvent that cannot give esterification, the chloride chain ends could undergo hydrolysis very easily, because of moisture, during the

storage or the handling of the polymer, making the coupling with bisphenol functionalised PS impossible. A different coupling strategy was, therefore, necessary, in which PEI was end-capped with the more stable EG, enabling the purification of the PEI before coupling with diacid chloride functionalised PS macromonomers.

4.3.2.2 EG end-capped PEI + diacid chloride functionalised ePS (cc-PEI-*g*-PS)

Since the acid chloride moiety cannot be on the PEI block, because of its sensitivity to water and to MeOH used for precipitation end purification, in the second coupling strategy EG end-capped PEI was synthesised by adding an excess of EG to a solution in which PEI was previously obtained via the polycondensation between EG and IPCl in 1:1 ratio (Scheme 4.5a). The polycondensation was performed with a 1:1 ratio of the reagents in order to obtain high MW. If either EG or IPCl was used in excess in this initial step, a significant reduction of the final MW would be expected.[11]
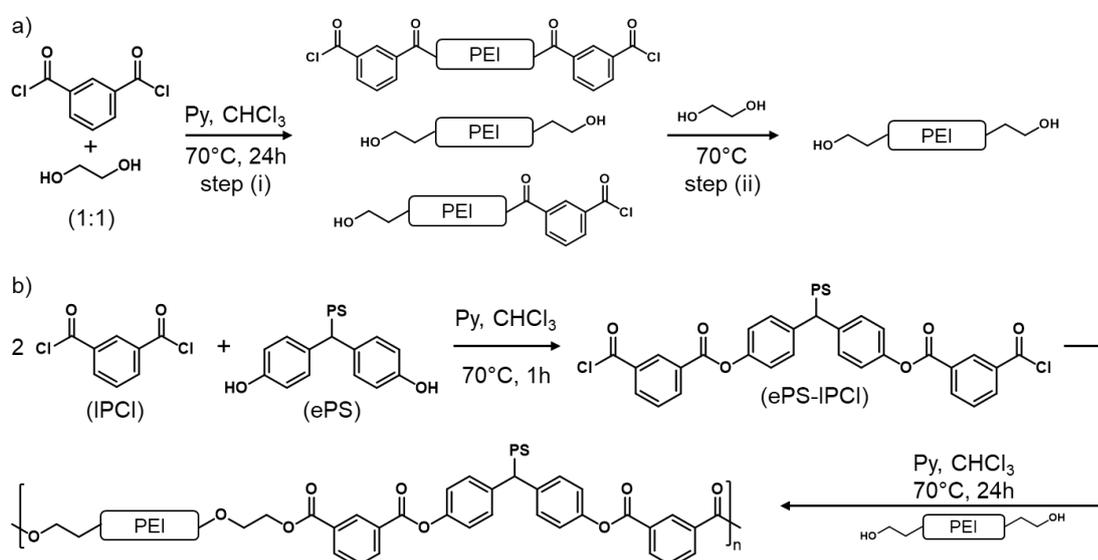
Scheme 4.5 Synthesis of a) an EG end-capped PEI and b) subsequent coupling with diacid functionalised ePS macromonomers, to yield cc-PEI-*g*-PS copolymers.

In the second step of the procedure (Scheme 4.5b), ePS underwent reaction with an equivalent amount of IPCl (2:1 IPCl-PS molar ratio), to yield the diacid chloride species ePS-IPCl, ideally with no excess IPCl left. The acid chloride functionalised

PS macromonomer (ePS-IPCl) did not have to be precipitated and isolated before the following step, thus preserving the reactive acid chloride moiety from hydrolysis or esterification. Afterwards, in the same solution, EG end-capped PEI was added, to give the coupling.

The NMR spectrum of EG end-capped PEI (example for PEI-OH2 in Figure 4.15) shows the peaks of the aromatic protons (1-4) between 8.7 and 7.5 ppm, and of CH$_2$ (5 and 6) at 4.7 ppm, together with peaks at 4.0 and 4.5 ppm for the -CH$_2$CH$_2$OH chain ends, each accounting for 4 protons. Actually, the integral value of peak at 4.5 ppm is higher (5.6), but this is due to a partial overlapping with the tail of the much bigger peak at 4.7 ppm, as more clearly shown in the insert of Figure 4.15.
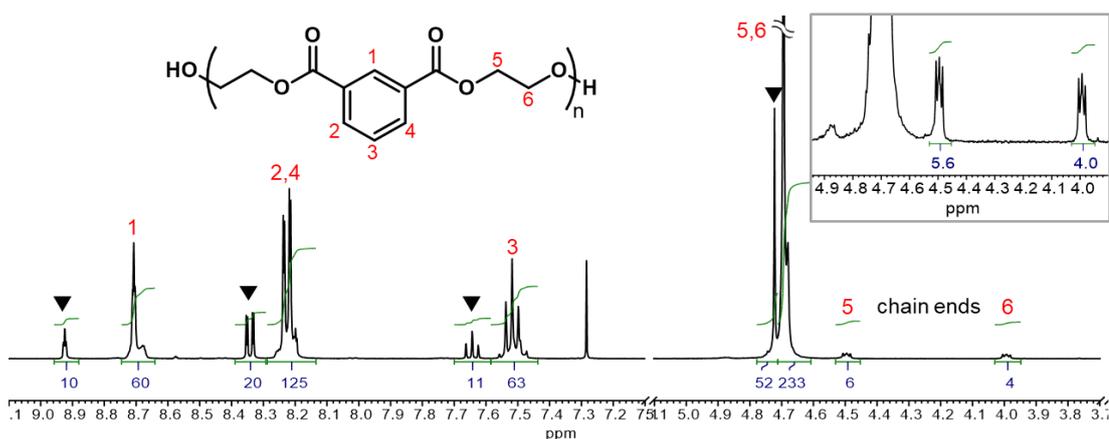
Figure 4.15 ^{1}H NMR (CDCl$_3$, 400 MHz) spectrum of EG end-capped PEI-OH2.

As seen previously in Section 4.3.1 for the copolymers obtained by solution polycondensation, the homopolymerisation of PEI here also results in the formation of oligomers (indicated by triangles in the NMR spectrum) caused by the presence of unreactive, partially hydrolysed IPCl. The relevant peak at high retention volume (ca. 18.5 ml) is also present in the SEC chromatogram (Figure 4.16). A comparison of the SEC traces before and after the end-capping with EG (dashed and solid traces in Figure 4.16, respectively), revealed no significant change in the traces, with M$_n$ measuring 9.8 before and 9.1 kg·mol^{-1} after EG end-capping. In addition, each of the two SEC chromatograms shows a

bimodal distribution which is consistent with the other PEI homopolymers synthesised in this Chapter.
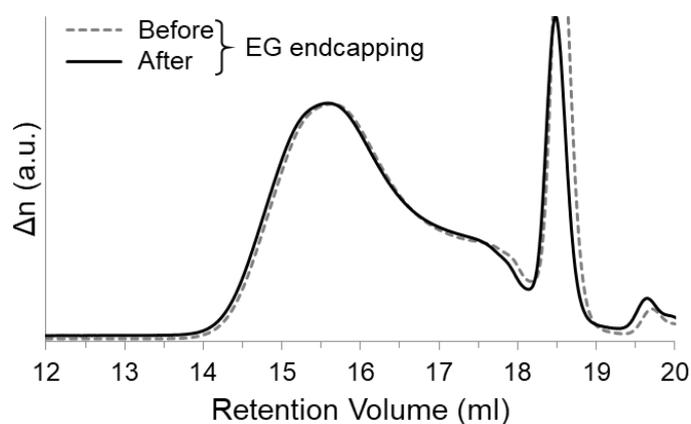
Figure 4.16 SEC chromatograms of EG end-capped PEI-OH2, before (dashed trace), and after (solid trace) the end-capping with EG.

The reason for this is not entirely clear but the less intense peak/shoulder at lower MW (retention volume ca. 17.5 ml in Figure 4.16) could be due to shorter chains obtained when a partially hydrolysed, thus unreactive, IPCl is incorporated into the chain, or if a cyclical species is formed. In both cases propagation is prevented and, moreover, the resulting PEI would not be reactive in the following coupling reaction with PS. The fact that, in the SEC chromatograms of the copolymers obtained by coupling (Figure 4.20 discussed later), this peak at higher retention volume remains almost unchanged, provides further support for this hypothesis. Therefore, SEC calculations to define the M_n of PEI-OH were performed by fixing the integration limits to exclude the part related to the unreactive chains at higher retention volume (for instance, in the case of the chromatogram shown in Figure 4.16, the integration limits were set at 13.7 ml and 16.9 ml). The aim was to obtain a more representative value of the reactive chains (peak with maximum at 15.5 ml in Figure 4.16), which was considered important to get a more accurate valuation of the number of moles to be used in the subsequent coupling reaction with PS macromonomers.

The EG end-capped PEI was subsequently used in coupling reactions with IPCl-functionalised PS of differing chain length (2.9, 6.4 and 9.1 kg·mol^{-1}). The copolymers are labelled cc-PEI$_x$-*g*-PS$_{yK}$, where *x* is related to the PEI-OH used (1

or 2, in this case) and y is the M_n of PS macromonomer, in kg·mol^{-1}. The amount of reagents in moles and the yields are summarised in Table 4.2.

Table 4.2 Amount of reagents (in mmol) and yields for the cc-PEI-*g*-PS graft copolymers obtained by coupling.

	IPCl	ePS	Py	PEI-OH	Yield
cc-PEI$_1$-*g*-PS$_{2.9K}$	0.17	0.06	1.2	0.06	75%
cc-PEI$_1$-*g*-PS$_{6.4K}$	0.15	0.05	1.0	0.05	61%
cc-PEI$_2$-*g*-PS$_{9.1K}$	0.12	0.05	1.2	0.05	78%

The amount of IPCl used to functionalise the PS macromonomers represented a slight molar excess with respect to the number of OH groups, in order to compensate for the potential loss of any acid chloride groups by hydrolysis during storage and/or handling. It is important, though, that during the subsequent coupling step the amount of unreacted IPCl is minimised, to avoid any reaction with the PEI-OH, which could prevent the desired coupling with ePS-IPCl.

After the reaction with IPCl, a sample of the macromonomer was collected for analysis to verify the successful functionalisation of ePS, yielding ePS-IPCl. Actually, the precipitation in excess MeOH to collect the sample causes the esterification of the acid chloride to methyl ester, as seen before in the procedure involving solution polycondensation (Paragraph 4.3.1), and as shown by the presence of the methyl ester peak at 4.0 ppm in the NMR spectra, as for example, for ePS2.9k-IPOMe in Figure 4.17.
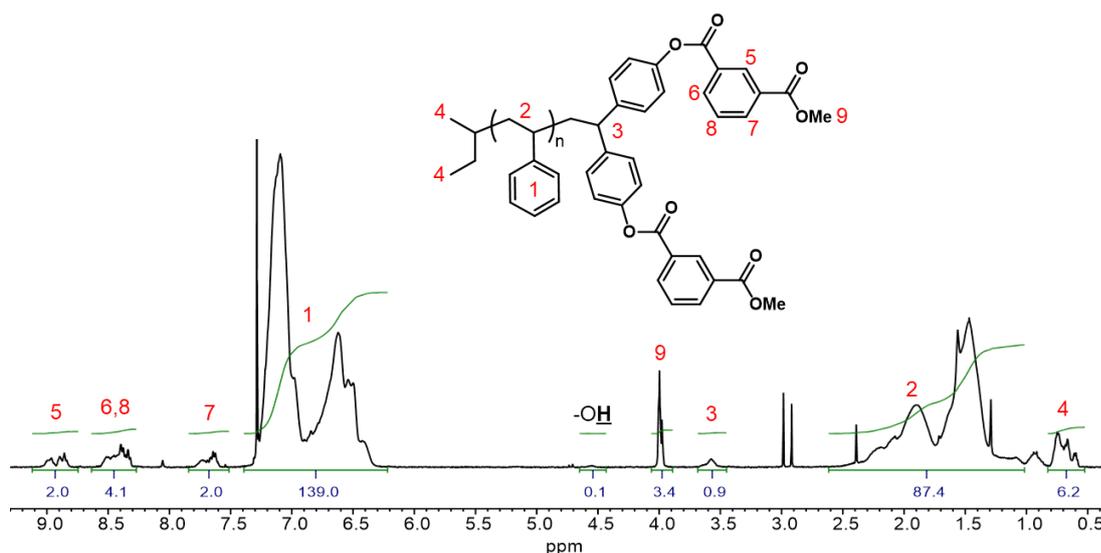
Figure 4.17 ^{1}H NMR (CDCl$_3$, 400 MHz) spectrum of a sample of ePS2.9k-IPOMe, obtained after reaction with IPCl, in the chain coupling procedure to obtain cc-PEI$_1$-*g*-PS$_{2.9k}$.

NP-IIC is very useful for the analysis of such reaction, because of the difference of retention induced by OH groups on the original ePS and the ester groups after the reaction with IPCl and precipitation in MeOH. In Figure 4.18, the NP-IIC chromatograms of the macromonomers before (dashed traces) and after (solid traces) reaction with IPCl are reported.

It is worth remembering that the PS macromonomers differ in M$_n$, increasing from 2.9, 6.4 to 9.3 kg·mol^{-1}. The effect of M$_n$ is visible in samples of ePS2.9k and ePS6.4k, where the peaks relative to the latter macromonomer are eluted slightly later than the respective species of the former. The peaks of ePS9.1k, though, do not obey this trend, with both ePS9.1k and ePS9.1k-IPOMe being eluted before the respective species for macromonomer ePS2.9k and 6.4k. The explanation might be in a sort of 'dilution effect' of the polar functional group in a longer non-polar chain, which results in a weaker retention by the stationary phase. This behaviour has been noticed in a previous NP-IIC analysis of functionalised polybutadiene of different chain length.[13] On the other hand, it is worth mentioning that NP-IIC as a technique is extremely sensitive to minor changes in solvent polarity and temperature,[22] so much that, in order to be truly comparable, samples should be analysed on the same day and each day of analysis requires a new calibration. Samples of ePS9.1k and ePS9.1k-IPOMe

were run the same day, but not together with samples ePS2.9k and 6.4k. This might also have affected the retention volumes slightly. Regardless, the impact of the change of functionality is still clearly evident.
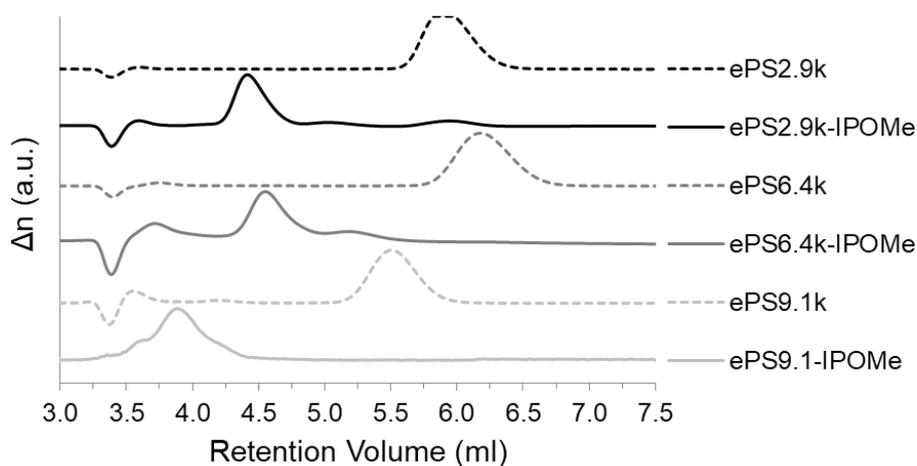
Figure 4.18 NP-IIC chromatograms recorded by RI detector of PS macromonomers ePS2.9k, ePS6.4k and ePS9.1k (dashed lines) compared with the traces of ePS2.9k-IPOMe, ePS6.4k-IPOMe and ePS9.1k-IPOMe (solid lines), obtained in the first step of the chain coupling reaction.

For each macromonomer, the peak of bisphenol functionalised ePS (dashed lines) elutes at a significantly higher retention volume compared to the ePS-IPOMe macromonomer (solid lines), proving that the reaction with IPCl was successful. However, the chromatograms of both ePS2.9k-IPOMe and ePS6.4k-IPOMe also show additional weak peaks. ePS2.9k-IPOMe shows a peak at the same retention volume as the bisphenol PS peak, at ca. 6 ml. It can be assumed that a small quantity of PS macromonomers did not react, as also suggested by the NMR spectrum (Figure 4.17), which shows a peak of residual -OH group at 4.5 ppm. The presence of traces of unreacted ePS is probably due to the presence of hydrolysed IPCl. The chromatogram of the same sample (ePS2.9k-IPOMe) shows another weak peak in between the peaks of ePS and ePS-IPOMe, at around 5.2 ml. This peak could be ascribable to macromonomers with only 1 of the 2 OH groups reacted with IPCl, and thus with an intermediate polarity between the fully reacted and unreacted macromonomers.

Once the PS macromonomers were functionalised with isophthaloyl chloride, an equimolar solution of EG end-capped PEI was added into the reaction solution, in order to enable the coupling and yielding the desired grafted copolymer. The NMR spectrum of the final product, in this case cc-PEI$_1$-g-PS$_{6.4K}$ and (for comparison) PEI-OH1 before the coupling, are shown in Figure 4.19.
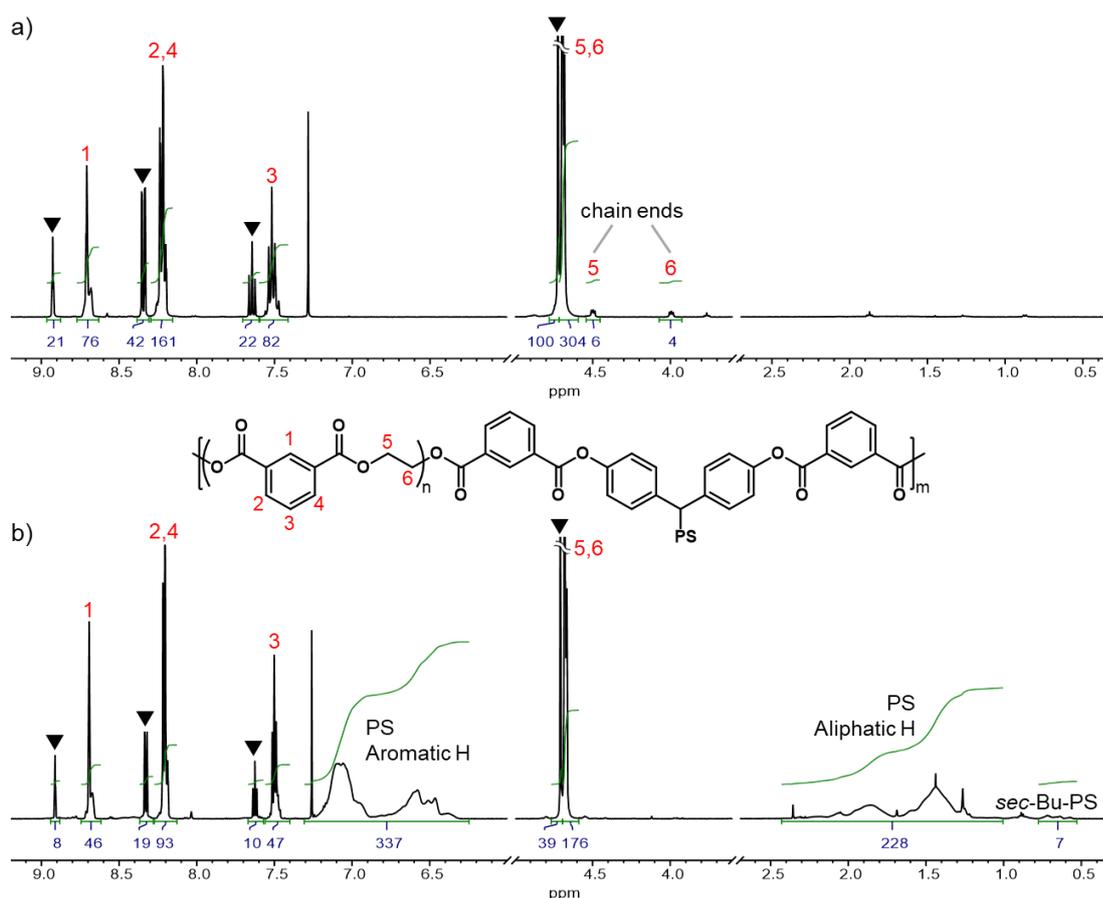
Figure 4.19 ^{1}H NMR (CDCl$_3$, 700 MHz) of a) PEI-OH1 and b) cc-PEI$_1$-g-PS$_{6.4K}$.

For each copolymer (exemplified by cc-PEI$_1$-g-PS$_{6.4K}$ in Figure 4.19), the NMR spectra show the broad peaks arising from PS blocks (the aromatic protons between 7.3 and 6.2 ppm, and the aliphatic protons of the backbone between 2.5 and 1.1 ppm, together with the butyl protons of the initiator, between 0.8 and 0.5 ppm) and the peaks of PEI backbone, including the additional peaks close to the main PEI peaks (highlighted by triangles) due to small PEI oligomers. The disappearance of the peaks of the EG chain ends (4.5 and 4.0 ppm) of PEI-OH suggests that the chain ends completely reacted with the IPCl functionalised PS macromonomers. However, the SEC chromatograms (Figure 4.20) of each

copolymer, compared with chromatograms of PS macromonomers and the PEI-OH starting materials can give more detail about the outcome of the copolymerisation.
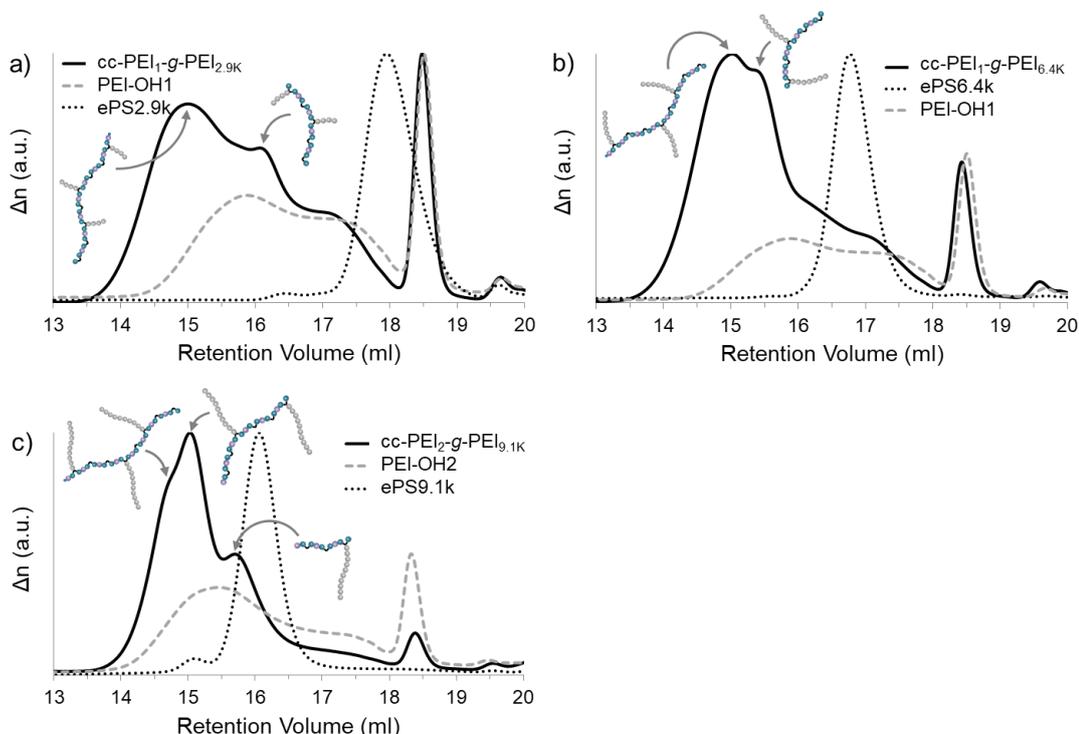
Figure 4.20 SEC chromatograms of copolymers a) cc-PEI$_1$-g-PS$_{2.9K}$, b) cc-PEI$_1$-g-PS$_{6.4K}$ and c) cc-PEI$_2$-g-PS$_{9.1K}$ (solid lines), compared with the respective EG end-capped PEI (dashed grey lines) and PS macromonomers (dotted lines).

For each copolymer, the main peak of ePS macromonomer (dotted line) has shifted to lower retention volumes, proving that the coupling was effective. Another evident feature, common to all, is the presence of a peak at ca. 18.5 ml, accounting for a MW of about 200 g·mol^{-1}, related to small PEI oligomers, whose peaks are also visible in the NMR spectra (see related discussion in Paragraph 4.3.1). Another feature which is evident in each case (to a greater or lesser extent) is a broad shoulder at ca. 17-17.5 ml, which can be correlated to an equivalent feature in the bimodal distribution of the PEI-OH homopolymers (Figure 4.16 and relative discussion) before the coupling. The fact that this feature seems to remain almost unchanged after the coupling reaction is consistent with the suggestion that it corresponds to unreactive PEI chains,

produced by the incorporation of partially hydrolysed IPCl or by the formation of cyclical species during the synthesis of PEI-OH.

The M_n and dispersity of the copolymers were calculated by triple detection, using as dn/dc a weighted average of the values of PS (0.16 $ml\cdot g^{-1}$) and PEI (0.098 $ml\cdot g^{-1}$), according to the weight fraction composition of the copolymer calculated by the NMR integral values of the aromatic protons peak of both PEI and PS, as described in Section 4.2.3 for the graft copolymers obtained by solution polycondensation. The SEC data resulting from the calculations by triple detection are summarised in Table 4.3.

Table 4.3 SEC data of cc-PEI-*g*-PS copolymers obtained by chain coupling.

	R.V. (ml)	M_n (g·mol⁻¹)	M_w (g·mol⁻¹)	Đ
cc-PEI$_1$-*g*-PS$_{2.9K}$	15.00	15,300	23,000	1.50
cc-PEI$_1$-*g*-PS$_{6.4K}$	15.01	20,900	27,000	1.29
cc-PEI$_2$-*g*-PS$_{9.1K}$	15.02	17,700	24,600	1.39

It is worth mentioning that, even though the SEC trace for each copolymer is not monomodal peak, but shows two or more overlapping peaks, the SEC calculation was performed without separating the peaks, but considering the whole distribution , apart from the shoulder between 17 and 17.5 ml discussed above. This decision was made because the calculated dn/dc for each copolymer depends on a composition which was extrapolated from the NMR analysis, and which is, therefore, an average estimation. Since clearly the product of each coupling is a mixture of species with different PEI-PS composition, and also the peaks are significantly overlapping, any attempt to define the exact molecular weight for each peak would be futile. Nonetheless, the shape of each chromatogram can be discussed qualitatively, since the different peaks comprising the traces show a quite narrow distribution that make them distinguishable from each other. Only the presence of ePS, with its Đ<1.1 thanks to the anionic polymerisation synthesis, can explain such narrow distributions of the peaks after coupling with much broader PEI-OH. Therefore, it is right to assume that the different peaks, making up the chromatograms of each

copolymer, are ascribable to species with different number of PS grafts on the PEI backbone. Figure 4.20a clearly shows, for the copolymer cc-PEI$_1$-g-PS$_{2.9K}$, two overlapping peaks: the main one, with a maximum at ca. 15 ml, and a second peak at 16.2 ml. It is reasonable to assume that the peak at 16.2 ml could be related to a structure (as indicated) comprising two ePS chains grafted to a PEI backbone, given the significant shift from the original PS macromonomer peak at 18 ml, while the main peak at 15 ml (higher M_n) might comprise a copolymer with 3 PS grafts. Similarly, in Figure 4.20b for copolymer cc-PEI$_1$-g-PS$_{6.4K}$ it is possible to identify two peaks at ca. 15 and 15.5 ml, ascribable to species with different number of graft PS, probably 2 and 3. In Figure 4.20c for cc-PEI$_2$-g-PS$_{9.1K}$ there is a peak at 15.6 ml, close to the PS macromonomer peak at 16 ml, which could be ascribed to one PS macromonomer plus 1 - or maybe 2 – PEI chain, and then a main peak at 15 ml and a shoulder at slightly lower retention volume, suggesting the presence of species with 2 and 3 PS grafted chains.

To complete the characterisation, the copolymers were analysed by DOSY-NMR, to establish if the peaks of different blocks show similar diffusion coefficients D, which would indicate that the coupling was successful in yielding copolymers. Figure 4.21 shows the DOSY-NMR spectra of cc-PEI$_1$-g-PS$_{2.9K}$. As seen before in Paragraph 4.3.1, the sharp peaks close to the main PEI peaks show significantly higher D values than the other signals (6×10^{-6} cm$^2 \cdot$sec^{-1}), as expected for low molar mass PEI homopolymers (peak at 18.5 ml in Figure 4.20, ca. 200 g$\cdot$mol^{-1}). Further PEI D values can be seen in a wide range (between 1.5×10^{-6} and 3×10^{-6} cm$^2 \cdot$sec^{-1}), which are higher values than seen for the peaks associated with the PS grafts (9×10^{-7} cm$^2 \cdot$sec^{-1}), meaning that there are PEI species present that did not couple to the PS macromonomers. Moreover, it is clear from the SEC analysis of EG end-capped PEI (Figure 4.16) and of the copolymers (Figure 4.20) that there are some PEI species – cyclic or hydrolysed - that seem not to take part in the coupling reaction (shoulder at 17.5 ml). It is reasonable to assume, then, that these PEI species show D values different from the copolymer. Significantly, there are PEI signals with D values in line with D values attributed to the key peak of PS (9×10^{-7} cm^{2}sec^{-1}), which can be ascribed to PEI blocks in the

copolymer. In the case of the copolymers obtained by solution polycondensation discussed before (Figure 4.11 and 4.12), the NMR signals of the $-CH_2CH_2OH$ chain ends (at 4.5 and 4.0 ppm) have a D value (1×10^{-6} $cm^2\cdot sec^{-1}$) which is slightly higher than that of the PEI chain in the copolymer.
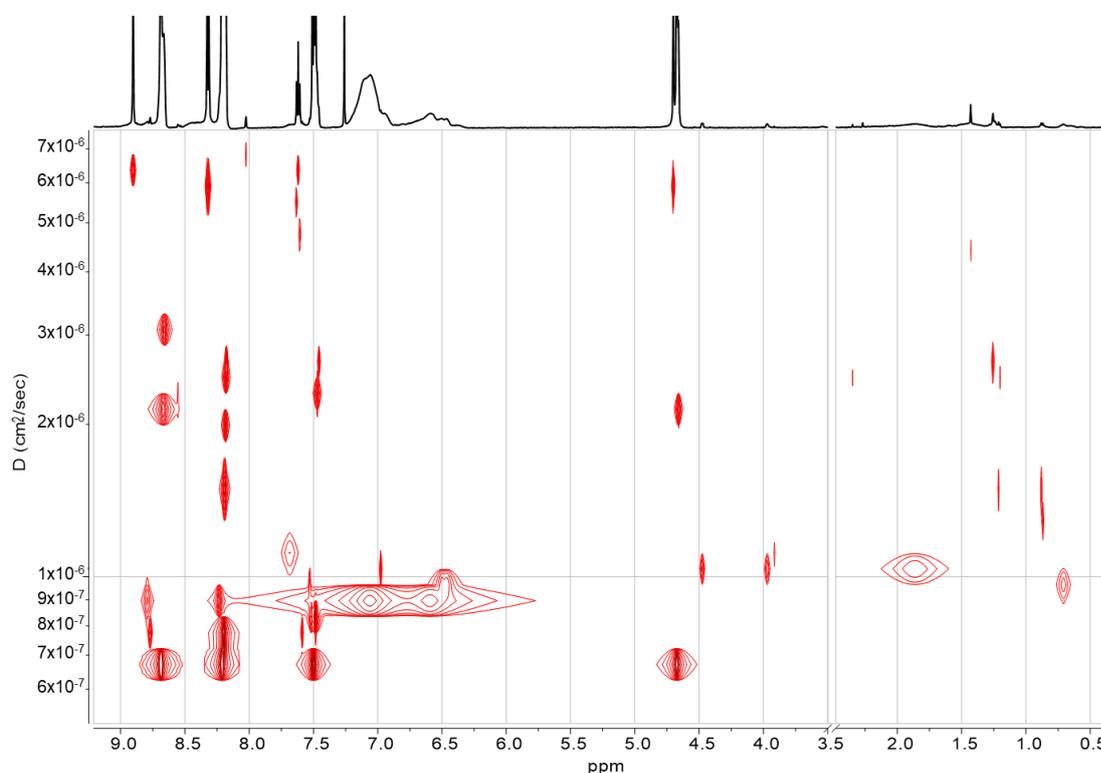
Figure 4.21 DOSY-NMR ($CDCl_3$, 600 MHz) of cc-PEI$_1$-g-PS$_{2.9K}$.

It was suggested that the reason for this difference in D values arises due to the fact that chain-ends have more freedom of movement compared to the main chain, and thus have a high diffusion coefficient. Coming back now to the copolymers prepared by chain coupling, and in particular cc-PEI$_1$-g-PS$_{2.9K}$ in Figure 4.21, intense signals for PEI peaks with D values which are lower than anything else in the spectrum (7×10^{-7} $cm^2\cdot sec^{-1}$) are observed. According to the DOSY theory, based on a lower diffusion coefficient, this species should be expected to have a MW which is higher than that of the copolymer. However, PEI-OH1 homopolymer used for the coupling has a M_n calculated by SEC of 8.9 kg·mol^{-1}, lower than the copolymer (M_n of 15.3 kg·mol^{-1}). An explanation for the unexpectedly low diffusion coefficient could be that, in contrast to EG chain ends, which are believed to have an unexpectedly higher diffusion coefficient, as

a result of being freer to move, the PEI blocks sandwiched in between two PS macromonomers in the same copolymer are less free to move and to diffuse, thus showing a lower value of D.

The DOSY-NMR spectrum of copolymer cc-PEI$_1$-g-PS$_{6.4K}$ is reported in Figure 4.22.
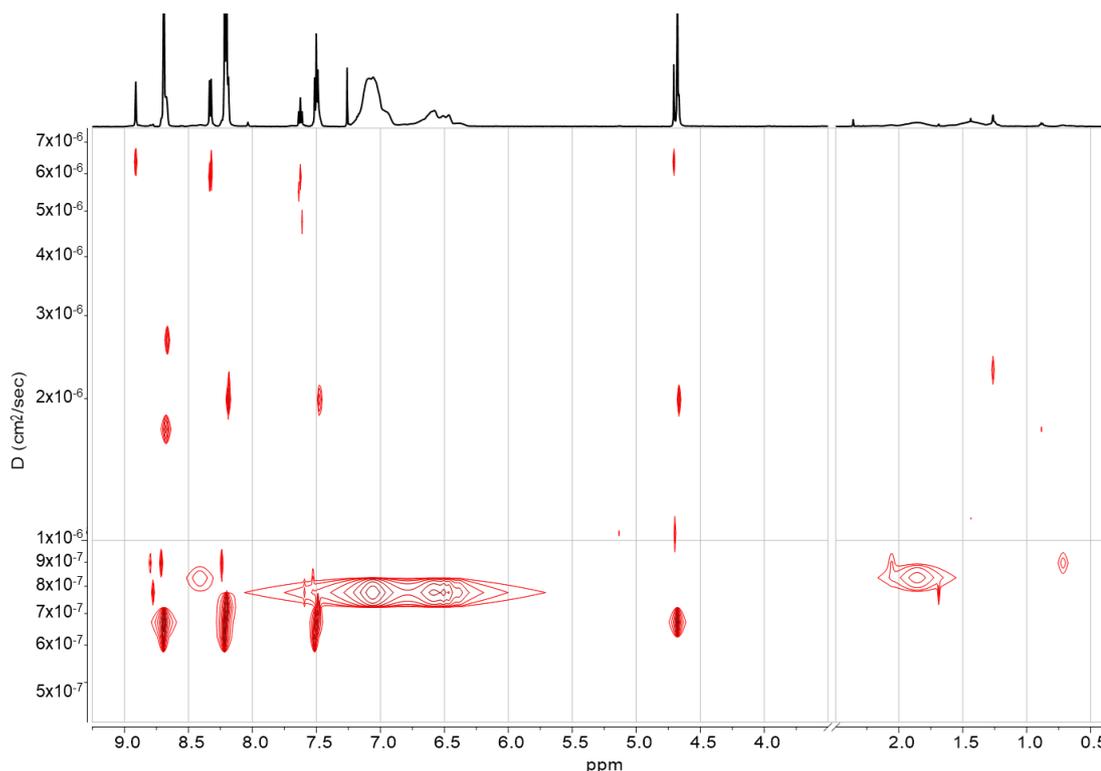
Figure 4.22 DOSY-NMR (CDCl$_3$, 600 MHz) of cc-PEI$_1$-g-PS$_{6.4K}$.

In common with the previous spectra, the PEI low molecular weight homopolymers (D=6×10^{-6} cm^2·sec^{-1}), the unreactive PEI species (with D between 1.8×10^{-6} and 3×10^{-6} cm^2·sec^{-1}) and the copolymer (with D values between 8×10^{-7} cm^2·sec^{-1} and 6×10^{-7} cm^2·sec^{-1}) can be identified, with the lower D value caused by PEI blocks in between two PS grafts, with less freedom to move and to diffuse. However, the most intense PEI peaks are not exactly in line with PS signal, but show a slightly lower D value (6-7×10^{-7} cm^{2}sec^{-1}). If the hypothesis above is correct, this might be related to the formation of a graft copolymer with no free PEI chains at the sides, but only with PEI blocks in between PS graft arms.

The absence of NMR signals for EG chain end of PEI (4.0 and 4.5 ppm) provides further support for this proposal.

Moving to the last copolymer, cc-PEI$_2$-*g*-PS$_{9.1K}$, the DOSY analysis (Figure 4.23) shows a much cleaner spectrum, in which the PEI low molecular weight homopolymers (2.5×10^{-5} cm^2·sec^{-1}) can still be seen, but where unreactive PEI species seem to be almost completely absent. The most intense peaks for PEI and PS are directly in line at D=1.2×10^{-6} cm^2·sec^{-1} and can be ascribed to the successful formation of a graft block copolymer.
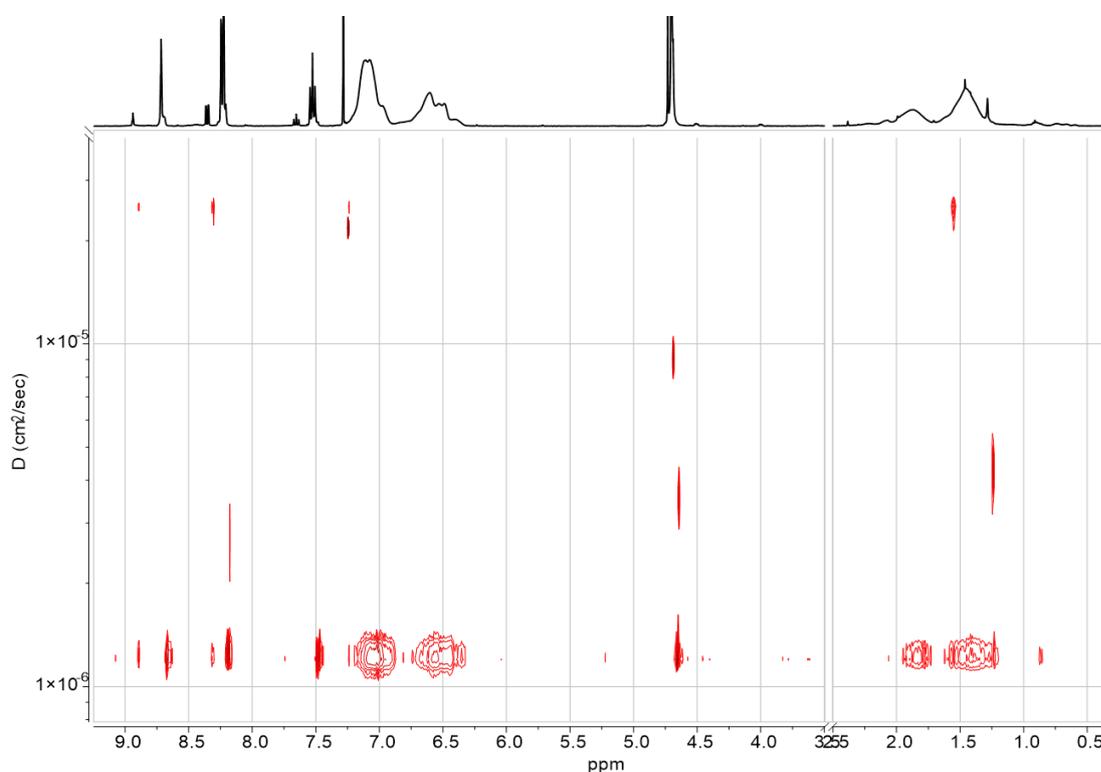
Figure 4.23 DOSY-NMR (CDCl$_3$, 600 MHz) of cc-PEI$_2$-*g*-PS$_{9.1K}$.

In conclusion, the DOSY analysis supports the conclusions drawn from SEC data discussed above, with the presence of signals from PEI and PS with similar D values as a further proof of copolymerisation. Moreover, two of the copolymers show PEI signals with very low diffusion coefficient values and which are believed to arise due to the inhibited diffusions of a PEI block in between PS graft arms. To the best of our knowledge, such behaviour has not previously been observed in the DOSY spectra of graft copolymers[17-20] and it might be worth a more detailed

investigation in future. For the purposes of this project, the SEC chromatograms are an irrefutable evidence that the PS macromonomers reacted in the coupling, resulting in a complex mixture of species with different number of grafted PS into the PEI backbone.

4.3.3   DSC ANALYSIS OF PEI-*g*-PS COPOLYMERS

The 5 copolymers described above were analysed by DSC, together with the PS macromonomers and PEI-OH2 as an example of a PEI homopolymer, in order to measure the T_g of each sample. An exemplifying thermogram for each of the copolymer synthetic approaches is reported in Figure 4.24, for the solution polycondensation synthesis, and 4.25, for the chain coupling approach.
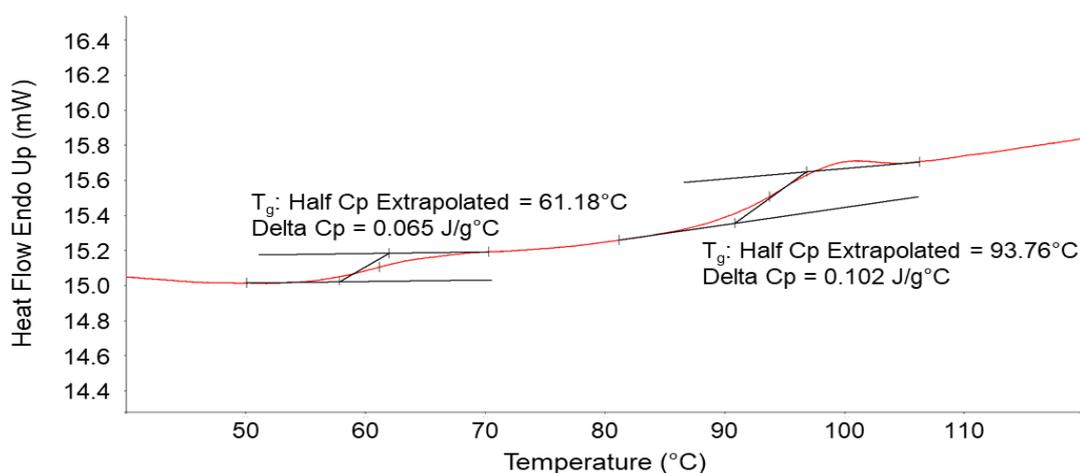
Figure 4.24 DSC second heating scan of sp-PEI-*g*-PS$_{6.4K}$.
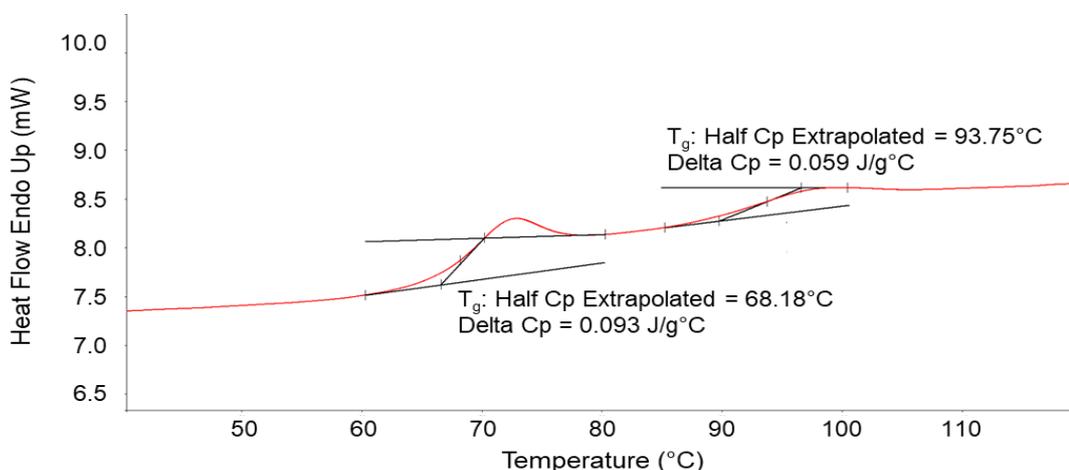
Figure 4.25 DSC second heating scan of cc-PEI$_1$-*g*-PS$_{6.4K}$.

The obtained data for each sample analysed are summarised in Table 4.4.

Table 4.4 T_g obtained by DSC of the PS macromonomers, the EG end-capped PEI-OH2 and the PEI-*g*-PS copolymers, synthesised by either solution polycondensation (sp) or chain coupling (cc) approaches.

Sample	T_g (°C)	
ePS2.9k	90.1	
ePS6.4k	95.1	
ePS9.1k	101.3	
PEI-OH2	64.5	
sp-PEI-*g*-PS$_{2.9K}$	65.8	83.5
sp-PEI-*g*-PS$_{6.4K}$	61.2	93.8
cc-PEI$_1$-*g*-PS$_{2.9K}$	68.1	94.9
cc-PEI$_1$-*g*-PS$_{6.4K}$	67.5	91.1
cc-PEI$_2$-*g*-PS$_{9.1K}$	67.5	91.2

The first observation is that the T_g of the PS macromonomers increases with molecular weight, in line with the Flory-Fox equation,[23] from 90.1°C for ePS2.9k to 101.3°C for ePS9.1k. The T_g measured for PEI-OH2 is in the range expected for PEI (T_g 50-65°C).[24-25]

All the copolymers show 2 distinct T_g values, one around the value expected for PEI and the other in the range expected for PS (around 100°C).[10] The fact that two distinct T_g values were observed for each copolymer suggests microphase separation of the two segments, as in the case of blends or block copolymers, while a completely homogeneous system, such as compatible polymers or random copolymers, would show a single T_g, intermediate between the two constituents.[26-27] In a blend of 2 polymers, without any bond between them, the two measured T_g would be the same of the single polymers. In this case, almost all the copolymers show two T_g with the values shifted towards each other, when compared with the values of the homopolymer precursors, especially for copolymers with ePS6.4k and ePS9.1k (sp-PEI-*g*-PS$_{6.4K}$, cc-PEI$_1$-*g*-PS$_{6.4K}$ and cc-PEI$_2$-*g*-PS$_{9.1K}$). This behaviour has been seen in previous studies on block

copolymers,[27] and is due to a better cohesion of the 2 polymers, caused by the coexistence in the same copolymer structure. The softer block, PEI in this case, is in contact with the harder component, PS, and the rigidity of the PS block prevents the mobility of the PEI chains, giving a higher T_g. On the other hand, the mobility of PEI chains of the soft microphase affects the PS domain, causing a decrease in T_g.[28-29]

4.3.4   SYNTHESIS OF PEI-*g*-POLYPEGMEM COPOLYMERS BY CHAIN COUPLING

After having investigated two different synthetic approaches to obtain a copolymer with a PEI backbone and PS grafted blocks, a different macromonomer derived from poly(ethylene glycol) methyl ether methacrylate (PEGMEM) was used and the coupling approach chosen to form a copolymer with EG end-capped PEI. The synthesis of the PolyPEGMEM-OH macromonomer by ATRP, using a novel DPE-OSi derivative as an ATRP initiator (BP-Br), is described in Chapter 3, and yielded a macromonomer with the desired bisphenol functionality at one chain end (Figure 4.26).
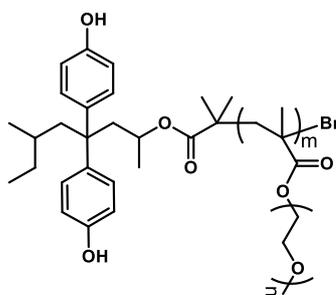
Figure 4.26 Structure of PolyPEGMEM macromonomer synthesised by ATRP using a DPE-OSi derived initiator (BP-Br).

PolyPEGMEM-OH1 macromonomer was introduced in the same way as the PS macromonomers, except that in this case an additional purification step was required. The PEG side chains of this macromonomer are very hygroscopic, therefore, before reacting with IPCl, the macromonomer was azeotropically dried 3 times with benzene, then dissolved in dry chloroform and added dropwise to the solution of IPCl, in presence of pyridine. Upon reaction with IPCl, EG

end-capped PEI-OH3 was added, in order to perform the coupling reaction to yield the desired copolymer.

The final product was soluble in methanol and was therefore recovered by precipitation into hexane instead and collected by filtration. Since PEI is not soluble in methanol and the product of this reaction was soluble and did not precipitate upon addition to methanol, this is a first sign that the copolymerisation worked.

The NMR spectrum of the resulting copolymer (Figure 4.27b) shows the expected proton signals of both PEI and PolyPEGMEM, assigned according to the inset copolymer structure.
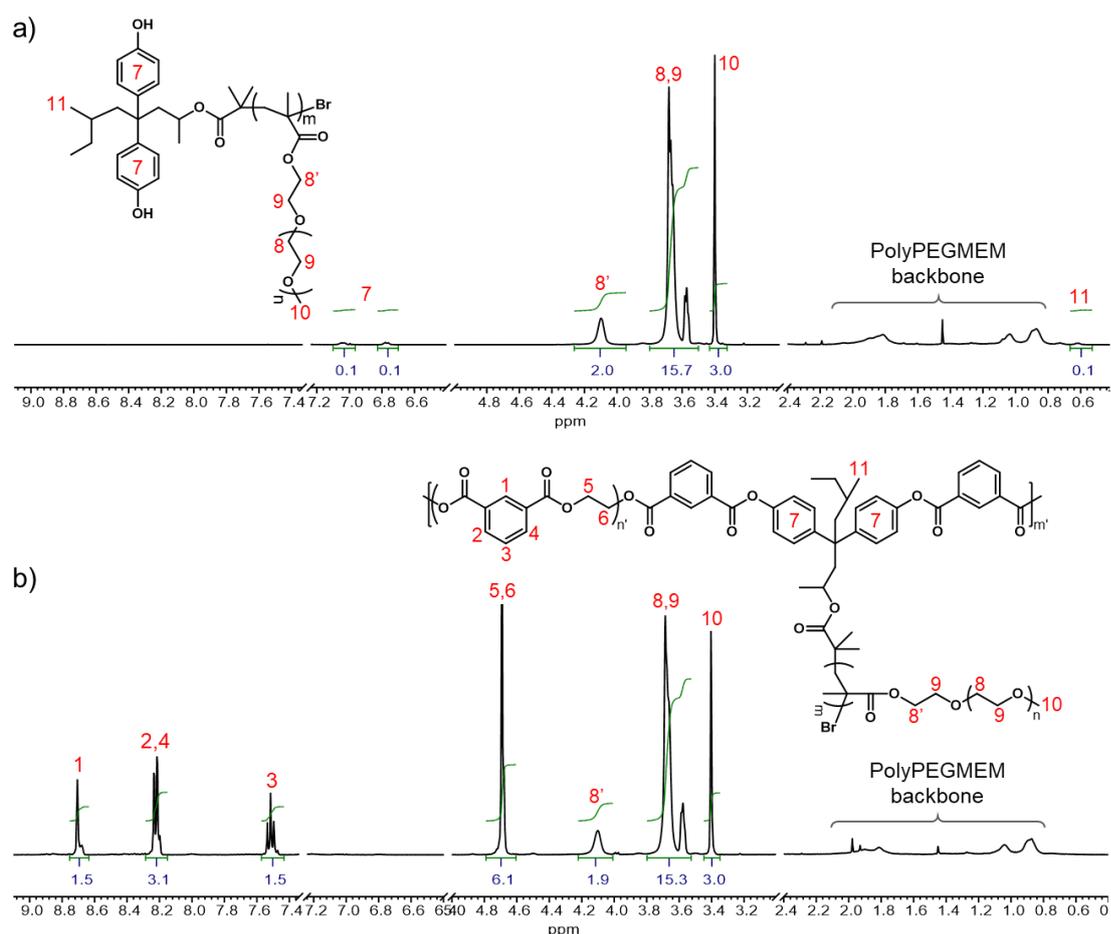
Figure 4.27 ^{1}H NMR (CDCl$_3$, 400 MHz) spectra of a) PolyPEGMEM-OH1 macromonomer and b) PEI-*g*-PolyPEGMEM copolymer.

It is worth mentioning that, at the end of the reaction and before precipitation in hexane, the reaction solution in chloroform was filtered, in order to remove the

partially insoluble low molecular weight PEI species, which are usually visible in the NMR spectrum as small sharper peaks close to the main PEI peaks, and in the SEC trace, as a peak at high retention volume. Effectively, the NMR spectrum (Figure 4.27b) and the SEC chromatogram (green trace in Figure 4.28) of PEI-*g*-PolyPEGMEM copolymer do not show evidence of the presence of these PEI species.

As seen before, such an NMR spectrum provides the opportunity to calculate the weight fractions of PEI and PolyPEGMEM in the resulting copolymer. The PolyPEGMEM peak at 3.4 ppm (10 in Figure 4.27b) was fixed to a value of 3, as it accounts for 3 protons per repeat unit, while the value of the integrals of PEI peaks between 8.8 and 7.4 ppm (4 aromatic protons per repeat unit) gives the number of PEI r.u., in this case 1.5, per PolyPEGMEM r.u. The mole fraction of PolyPEGMEM can be calculated as $\chi_{PolyPEGMEM} = 1/(1+1.5) = 0.4$, thus giving a PEI mole fraction of 0.6.

The weight fraction of PolyPEGMEM and PEI in the copolymer, and the dn/dc of the copolymer are calculated according to the following equations:

$$\text{w.f.}^{x} = \frac{\chi_{x} \times MW^{x}}{\chi_{PEI} \times MW^{PEI} + \chi_{PolyPEGMEM} \times MW^{PolyPEGMEM}}$$

$$\text{dn/dc} = 0.03 \text{ ml·g}^{-1} \times \text{w.f.}^{PolyPEGMEM} + 0.098 \text{ ml·g}^{-1} \times \text{w.f.}^{PEI}$$

where w.f.^{x} is the weight fraction of the macromonomer (x = PolyPEGMEM) or of the polyester (x = PEI), MW^{PEI} is the molecular weight of the PEI repeat unit (192.17 g·mol^{-1}) and MW^{PolyPEGMEM} is the molecular weight of the PolyPEGMEM repeat unit (300 g·mol^{-1}). χ is the mole fraction, calculated by NMR as explained before.

The triple detection SEC analysis of the graft block copolymer gave a M_n of 51,900 g·mol^{-1} and a dispersity of Đ 2.87. The chromatograms of the copolymer and starting materials are compared in Figure 4.28, showing that the peak of the copolymer at ca. 15 ml (green line), is slightly shifted towards higher molecular weight, in comparison to the PolyPEGMEM-OH1 macromonomer peak (blue

dashed line) at 15.5 ml. However, the dispersity of the copolymer distribution is significantly increased to 2.87 from 1.35 for the macromonomer.
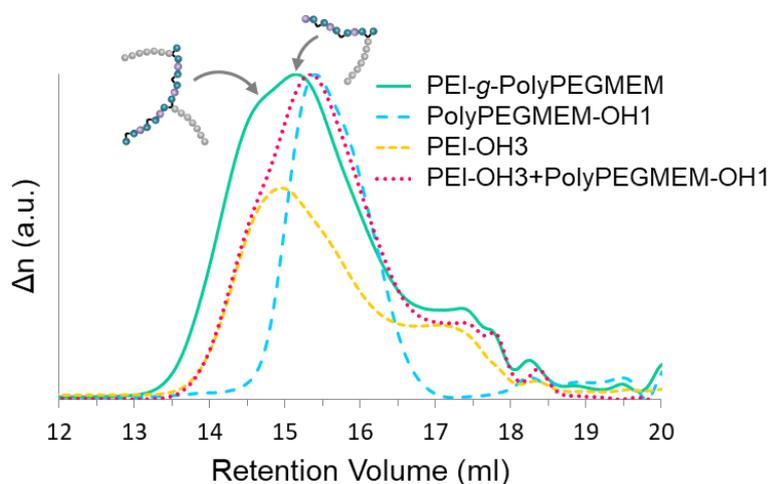
Figure 4.28 SEC chromatograms of PEI-*g*-PolyPEGMEM (green line), compared with the EG end-capped PEI-OH3 (yellow dashed lines) and PolyPEGMEM-OH1 macromonomer (blue dashed lines), and with the trace of the solution of the two blocks (pink dotted line).

Since the SEC trace of the copolymer might appear similar to the sum of the two polymer starting materials, a sample was prepared for SEC analysis which consisted of a simple mixture of PolyPEGMEM-OH1 and PEI-OH3, in the same molar ratio as used for the coupling reaction (1:1). The SEC trace of this physical mixture is presented as the pink dotted line in Figure 4.28 and is clearly different from the trace of the copolymer, confirming that the coupling reaction had worked to some extent. As seen for the samples prepared by coupling with PS, there is a broad shoulder at ca. 17.5 ml, which can be correlated to the second peak in the bimodal distribution of the PEI-OH3 homopolymer starting material (yellow dashed line in Figure 4.28). This peak remains almost unchanged after the coupling reaction, because, as discussed before, it can be ascribed to unreactive PEI chains, produced by the incorporation of partially hydrolysed IPCl or by the formation of cyclical species, during the synthesis of PEI-OH. The main peak of the chromatogram at ca. 15.1 ml actually shows a shoulder at lower retention volume, suggesting the presence of species with different number of grafted PolyPEGMEM onto the PEI backbone. However, given the significant overlap with

the original peak of PolyPEGMEM macromonomer, it is reasonable to assume that copolymers with 1 and 2 grafted arms were obtained.

Figure 4.29 shows the DOSY-NMR spectra of PEI-*g*-PolyPEGMEM. All the PolyPEGMEM signals (green diamonds) have diffusion coefficients in line with PEI peaks (blue triangles) at ca. 1×10^{-6} $cm^2 \cdot sec^{-1}$, confirming that the two blocks are in the same copolymer macromolecule.
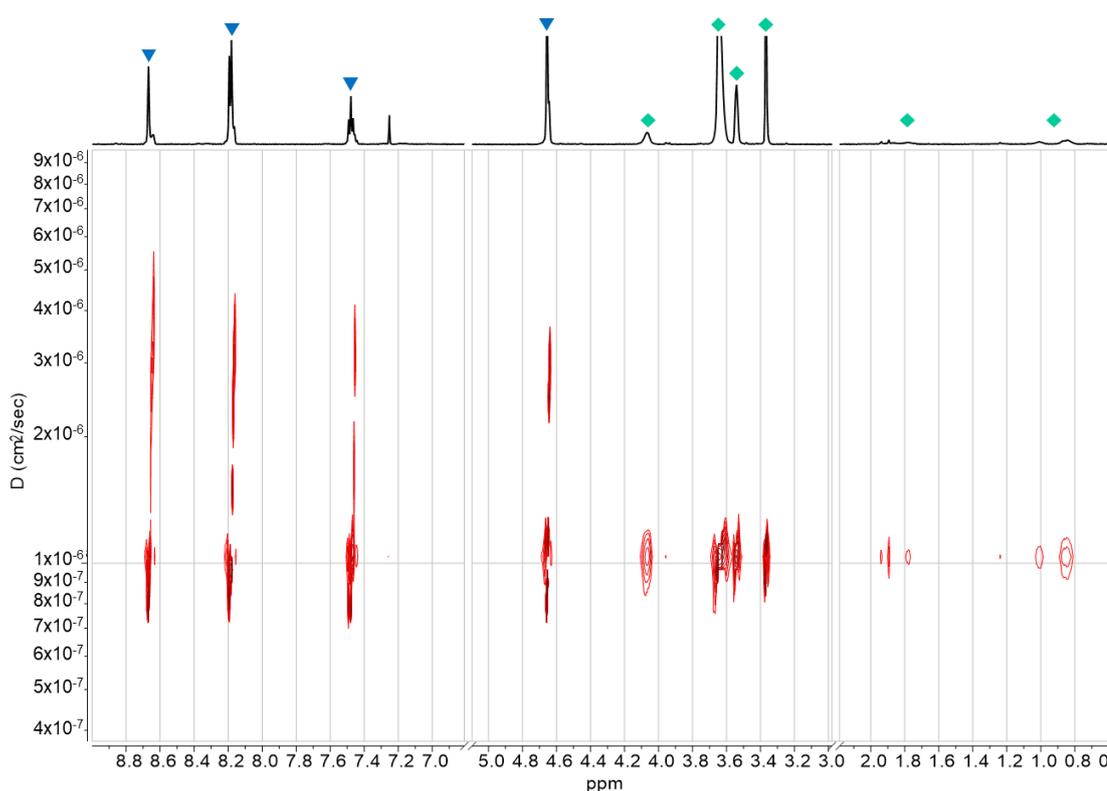
Figure 4.29 DOSY-NMR (CDCl$_3$, 600 MHz) of PEI-*g*-PolyPEGMEM. (▼) Signals of PEI backbone; (◆) signals of PolyPEGMEM blocks.

It might be argued that a similar D value can also derive from a similar molecular weight, and not necessarily from the fact that the two blocks are bond in the same molecule. The M_n of the two polymers are slightly different (12.7 kg·mol^{-1} for PolyPEGMEM and 17.2 kg·mol^{-1} for PEI) and a difference in diffusion coefficients can be expected. In this sense, the DOSY analysis of a simple mixture of PolyPEGMEM1 and PEI-OH3 in the same molar ratio as used for the coupling reaction (1:1), as done before for the SEC analysis, might have helped in confirming or refuting the hypothesis of homopolymers with similar D.

Besides the signals at $D=1\times10^{-6}$ cm^2·sec^{-1}, there are other PEI signals with a diffusion coefficient between 5.0 and 1.5×10^{-6} cm^2·sec^{-1}, due to PEI homopolymers that did not react with the macromonomers in the coupling reaction. Apart from PEI-OH blocks that did not couple with PolyPEGMEM macromonomer, these PEI species can also account for unreactive – cyclic or hydrolysed - PEI in the second peak of the bimodal distribution of PEI-OH3 homopolymer before the coupling, which is still visible in the copolymer chromatogram as a shoulder at ca. 17.5 ml.

In the case of PEI-*g*-PolyPEGMEM copolymer, SEC analysis does not show a decisive shift in retention volume of the copolymer peak after the coupling, as seen for PEI-*g*-PS copolymers in Section 4.3.2. Nevertheless, it is clear that the copolymer trace is significantly different from the one of a simple mixture of the two components. Moreover, there is other evidence that support the actual success of the coupling reaction between PEI-OH and PolyPEGMEM macromonomer. First, at the end of the reaction, the product was soluble in MeOH, whereas homopolymer PEI is not. This is only possible if the insoluble PEI chains are bonded to the soluble PolyPEGMEM chains in the copolymer. Secondly, the DOSY-NMR clearly evidences the presence of PEI signals with the same D value as signals of PolyPEGMEM, and probably in the same copolymer molecule, even if further analysis would be necessary to exclude the hypothesis of disconnected homopolymers with similar D.

Finally, looking back at the discussion related to the synthesis of bisphenol functionalised PolyPEGMEM macromonomers in Chapter 3, the effective coupling with PEI-OH is a further proof of the successful synthesis of a macromonomer with PEG brush and with the desired bisphenol functional moiety at one chain end.

4.4 CONCLUSIONS

In this Chapter we have reported the addition of functionalised macromonomers, synthesised by controlled chain-growth polymerisation, into a step-growth

mechanism, in order to obtain a grafted block copolymer. In particular, we demonstrated that PS macromonomers, carrying a bisphenol functionality at one chain end, can be successfully incorporated as a comonomer into the polycondensation reaction between IPCl and EG to yield PEI, even if copolymers with only 1 grafted PS and a few repeat units of PEI were obtained, using either 2.9 or 6.4 kg·mol^{-1} PS macromonomers, to yield sp-PEI-*g*-PS$_{2.9K}$ and sp-PEI-*g*-PS$_{6.4K}$, respectively.

In order to improve the final outcome, a different approach was investigated in which PEI blocks were synthesised by solution polycondensation, and then coupled with the macromonomer. There are two possibilities to do so: either coupling the bisphenol functionalised PS with acid chloride end-capped PEI or, vice versa, synthesising an EG end-capped PEI to couple with IPCl functionalised PS. The former approach turned out to be unfeasible, because during the work up the acid chloride chain ends of PEI underwent esterification or hydrolysis, thus becoming unreactive. The latter strategy, on the other hand, proved to be very effective, yielding copolymers with up to 3 PS grafts on the PEI backbone, using PS macromonomers of 2.9, 6.4 and 9.1 kg·mol^{-1} (cc-PEI$_1$-*g*-PS$_{2.9K}$, cc-PEI$_1$-*g*-PS$_{6.4K}$ and cc-PEI$_1$-*g*-PS$_{9.1K}$, respectively). The samples were analysed by NMR, SEC, DOSY-NMR and DSC, all techniques that collectively contributed to prove the successful copolymerisation and also to identify the presence of different PEI species, apart from the copolymer, such as small PEI oligomers (ca. 200 g·mol^{-1}) and unreactive PEI homopolymers, probably due to the incorporation of partly hydrolysed IPCl or to the formation of cyclic chains.

Finally, the coupling procedure was exploited also with a different kind of macromonomer, carrying hydrophilic PEG brushes, obtained by the polymerisation of poly(ethylene glycol) methyl ether methacrylate by ATRP. Even if SEC analysis did not show a decisive shift in retention volume of the copolymer peak after the coupling, it is clear that successful coupling happened to some extent, since the copolymer trace is significantly different from a simple blend of the 2 components. Moreover, DOSY-NMR also confirmed that the two blocks were part of the same copolymer macromolecule, with the same diffusion

coefficient, even if further analysis would be necessary to exclude the hypothesis of homopolymers with similar D.

Given the positive results obtained in either modifying the molar mass or the nature of macromonomer introduced into the coupling reaction with EG end-capped PEI, this approach represents a versatile strategy to obtain grafted block copolymers with a PEI backbone and a variety of grafted blocks, provided that the reaction procedure is slightly adjusted to take into account the macromonomers characteristics. In the case of PolyPEGMEM, for example, a further purification step had to be added, because of the highly hygroscopic nature of the PEG chains.

REFERENCES

1. http://polymerdatabase.com/polymer%20classes/Polyester%20type.html.
2. http://www.polymerdatabase.com/polymer%20chemistry/Stepgrowth%20 Polymerization.html.
3. Higashihara, T.M.U., *Polycondensation*, in *Encyclopedia of Polymer Science and Technology*, John Wiley & Sons, **2013**.
4. Al Luhaidan, K.; Bashir, Z.*, et al.*, EP1593702A1, **2005**.
5. Yoshida, M.; Ma, J.J.*, et al.*, *Polymer Engineering & Science*, **1990,** *30* (1), 30-43.
6. Conix, A., *Industrial & Engineering Chemistry*, **1959,** *51* (2), 147-150.
7. Gomes, M.; Gandini, A.*, et al.*, *Journal of Polymer Science Part A: Polymer Chemistry*, **2011,** *49* (17), 3759-3768.
8. June, S.M.; Suga, T.*, et al.*, *The Journal of Adhesion*, **2013,** *89* (7), 548-558.
9. Liaw, D.-J.; Liaw, B.-Y.*, et al.*, *Journal of Polymer Science Part A: Polymer Chemistry*, **2000,** *38* (24), 4451-4456.
10. Brandrup, J.; Immergut, E.H.*, et al.*, *Polymer Handbook (4th Edition)*. John Wiley & Sons, **2017**.
11. Saunders, J.H.; Dobinson, F., *Chapter 7 The Kinetics of Polycondensation Reactions*, in *Comprehensive Chemical Kinetics*, Elsevier, **1976**; Vol. 15, pp 473-581.
12. Lee, W.; Cho, D.*, et al.*, *Journal of Chromatography A*, **2001,** *910* (1), 51-60.
13. Hutchings, L.R.; Agostini, S.*, et al.*, *European Polymer Journal*, **2015,** *73*, 105-115.
14. Rieckmann, T.; Völker, S., *Chemical Engineering Science*, **2001,** *56* (3), 945-953.
15. http://www.hitachi.com/businesses/infrastructure/product_site/ip/process/pet.html.
16. http://guichon-valves.com/faqs/pet-manufacturing-process-of-polyethylene-terephtalate-pet/.
17. Ohkawa, H.; Ligthart, G.B.W.L.*, et al.*, *Macromolecules*, **2007,** *40* (5), 1453-1459.
18. Pan, X.; Chen, C.*, et al.*, *Chemical Communications*, **2012,** *48* (76), 9510-9512.
19. Moreira, G.; Fedeli, E.*, et al.*, *Polymer Chemistry*, **2015,** *6* (29), 5244-5253.
20. Phiri, M.M.; Hadasha, W.*, et al.*, *European Polymer Journal*, **2018,** *102*, 178-186.
21. Silverstein, R.M.; Webster, F.X.*, et al.*, *Spectrometric Identification of Organic Compounds, 8th Edition*. Wiley, **2014**.
22. Chang, T.; Lee, H.C.*, et al.*, *Macromolecular Chemistry and Physics*, **1999,** *200* (10), 2188-2204.
23. Jr., T.G.F.; Flory, P.J., *J. Appl. Phys.*, **1950,** *21* (6), 581-591.
24. Karayiannis, N.C.; Mavrantzas, V.G.*, et al.*, *Macromolecules*, **2004,** *37* (8), 2978-2995.
25. http://polymerdatabase.com/polymers/polyethyleneisophthalate.html.
26. Ting, Y.-P.R.; Hancock, L.F., *Macromolecules*, **1996,** *29* (23), 7619-7621.
27. Morese-Seguela, B.; St-Jacques, M.*, et al.*, *Macromolecules*, **1980,** *13* (1), 100-106.
28. Chevallier, C.; Becquart, F.*, et al.*, *Materials Chemistry and Physics*, **2013,** *139* (2-3), 616-622.
29. Shieh, Y.-T.; Liao, T.-N.*, et al.*, *Journal of Applied Polymer Science*, **2001,** *79* (12), 2272-2285.

CHAPTER 5

PREPARATION AND CHARACTERISATION OF COMPATIBILIZED PET-PS BLENDS

5.1 INTRODUCTION

Blends of different polymers are very interesting from a commercial point of view, because of the great potential to combine in one material the properties of each component. Usually, though, the blend components are immiscible and interfacial adhesion between the polymer phases is poor, leading to unstable morphologies, poor processability, low impact strength and mechanical properties. In an ideal blend, realising the desired properties will critically depend on the improvement of compatibility, with stronger interfacial adhesion and lower interfacial tension. This often results in stabilised morphologies with finer dispersion of the minor component.[1]

Polymer miscibility is determined by thermodynamics.[2] In a general blend system, the free energy of mixing is given by:

$$\Delta G_m = \Delta H_m - T\Delta S_m$$

where ΔH_m and ΔS_m are the enthalpy and entropy of mixing, respectively. For two polymers to be miscible, ΔG_m must be negative. The enthalpic term for most polymer mixture is slightly positive (endothermic), while entropy favours mixing ($\Delta S_m>0$). However, for polymers it is small and decreases with degree of polymerisation. The result is $\Delta G_m>0$ in most cases of polymer blends.

The thermodynamic behaviour of polymer blends can be treated theoretically with the Flory-Huggins theory, considering the blend as a lattice in which every cell,

all identical in size, is occupied by a repeat unit of a polymer chain. The *Flory-Huggins equation for the Gibbs free energy of mixing* of polymer blends is:

$$\Delta G_m = RT \, (n_1 \, \ln\varphi_1 + n_2 \, \ln\varphi_2 + x_1 n_1 \varphi_2 X)$$

where n_1 and n_2 represent the number of moles of polymer 1 and 2, x_1 is the number of continuous cells occupied by polymer 1 (degree of polymerisation), φ_1 and φ_2 are the volume fractions of the components, and X is the *Flory-Huggins polymer-polymer interaction parameter*. The first two terms represent the combinational entropy of mixing and the last is the enthalpy term. The latter term is the one dominating the thermodynamics of mixing. It has been demonstrated that X is inversely proportional to temperature, meaning that an increase in temperature causes an overall increase of ΔG_m, decreasing the miscibility of polymer blends.

Even if most polymer mixtures are immiscible, it is possible to make the components more compatible by modifying the interface between them, in order to obtain good dispersion of one into the other. Among many different potential applications, block copolymers have been the subject of considerable research activity because of their use as compatibilizer for polymer blends. The choice of a block – linear or graft - copolymer as a compatibilizer is based on the miscibility of its segments with each of the blend components. Therefore, such a block copolymer tends ideally to concentrate at the interface and acts as emulsifier (Figure 5.1), often resulting in stabilised morphology, with a finer dispersion of the minor phase and an improvement of the blend macroscopic properties.
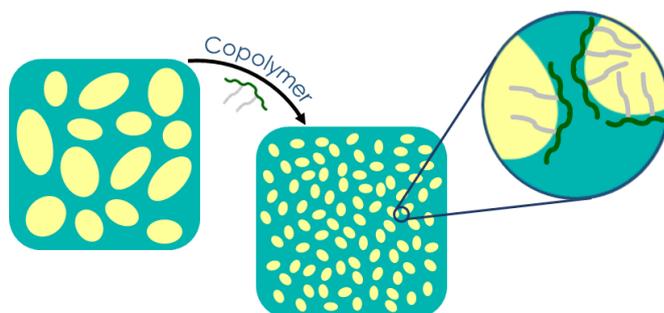
Figure 5.1 Schematic illustration of the compatibilizing effect of a block copolymer into a blend of immiscible polymers.

An alternative to the use of specifically designed copolymers is the so-called reactive compatibilization, in which a functionalised polymeric additive, which is miscible or partially miscible with one component of the blend, can undergo a chemical reaction with the other component, under normal blending conditions. As a result, a hybrid graft or linear block copolymer is formed in situ, at the interface, which has the ability to reduce the domain size of the dispersed phase and promote adhesion between the dispersed polymer and matrix polymer phases.[3-6]

Many attempts to compatibilize PET and polystyrene are reported in the literature, because of the great commercial potential that a blend of these two commodity polymers would have. The outcome could be, for example, to improve the properties of commodity thermoplastics and to lower the cost of high-performance polymers. Of particular interest nowadays, an effective compatibilization would upgrade recycled polymer waste, which often comprise more than one polymer.[1] One of the most widely-investigated routes exploits reactive epoxy functional groups or anhydrides on polystyrene chains, which can react with polyester end groups (-OH and -COOH), under melt conditions to form polyester-polystyrene grafted copolymers. An example is the use of styrene-glycidyl methacrylate copolymers (GMA) (see Figure 5.2a).[4,7] A report by Papke *et al.* described the use of GMA as a compatibilizer in blends containing PET or PBT and various rubbers, such as ethylene/propylene copolymer (EPR), ethylene/propylene/diene terpolymer (EPDM) and styrene/butadiene rubber (SBR).[8] The effectiveness of a polystyrene-co-maleic anhydride copolymer (SMA) (Figure 5.2b) as a reactive compatibilizer in blends with PET has also been tested.[9]

Another reported strategy uses reactive styrene-ethylene/butylene-styrene (SEBS) triblock copolymers, with the aim of improving, in particular, the toughness of the PET-PS blends. For example, SEBS can been functionalised with either maleic anhydride (Figure 5.2c), or glycidyl methacrylate, in order to act as reactive compatibilizer.[10]

Finally, a dual compatibilizer, composed of a mixture of SMA random copolymer and poly[methylene(phenylene isocyanate)] (PMPI) (Figure 5.2d), has been shown to effectively compatibilize immiscible blends of PET and polystyrene.
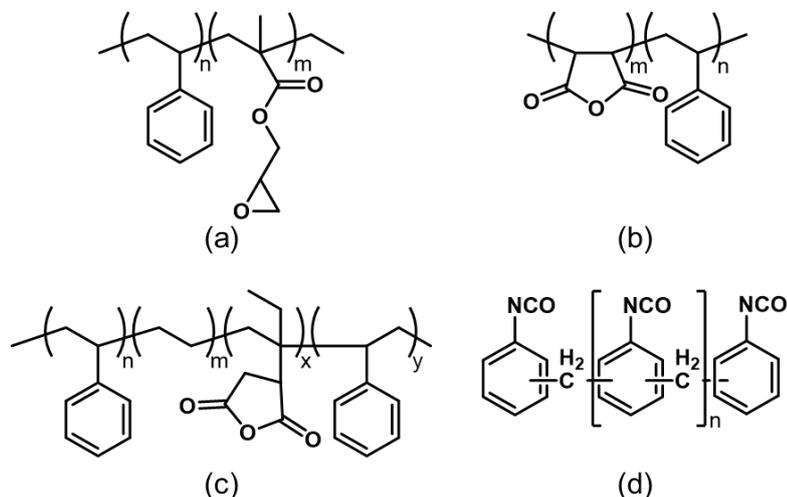
Figure 5.2 Structure of copolymers used as reactive compatibilizers: a) styrene-glycidyl methacrylate copolymer (GMA); b) styrene-maleic anhydride copolymer (SMA); c) styrene-ethylene/butylene-styrene (SEBS) triblock copolymer maleic anhydride; d) poly[methylene(phenylene isocyanate)] (PMPI).

The isocyanate group reacts rapidly - at the high temperature of the melt blending procedure - with carboxyl and hydroxyl groups of PET, as summarised in Scheme 5.1.
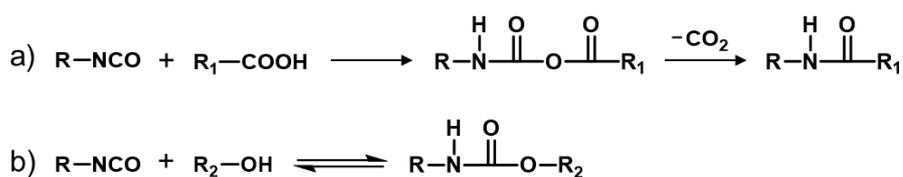
Scheme 5.1 Chemistry of isocyanate group: typical reaction with a) carboxyl and b) hydroxyl groups.

The isocyanate groups of PMPI can react with the terminal groups of PET (–OH and –COOH) and the hydroxyl groups of the ring-opened SMA simultaneously, to form the desired PET-co-PMPI-co-SMA copolymers at the interface, which serves as an effective compatibilizer. Certainly, not all the added PMPI is expected to undergo reactions simultaneously with both and, if part of PMPI

reacts with only one blend component, such a product is unable to serve as a compatibilizer.[11]

In this Chapter, we report the results of investigations into the use of graft block copolymers, comprising of a polyester backbone and PS grafts, as a compatibilizing agent for PET/PS blends. The aim of this study is to verify if these copolymers can effectively improve the miscibility of PET and PS in a blend, by comparing the domain size of the minor component (PS) with the PS domains in a non-compatibilized blend and in blends with previously reported compatibilizers. The synthesis and characterisation of the graft block copolymers have been reported in Chapter 4. For each copolymer, an increasing percentage weight fraction (0.5, 2.5 and 5 wt.%) was added to PET/PS (75/25 by mass) blends, and the mean diameter of the minor phase – PS – domains was compared with the same in uncompatibilized blends by SEM imaging. A reduction in PS droplet size would indicate a better dispersion of it in the matrix of PET, and therefore it would prove the effectiveness of PEI-*g*-PS copolymers as blend compatibilizer.

Finally, the compatibilizing effect of these novel copolymers has been compared, under the same conditions and wt.%, with a styrene-glycidyl methacrylate copolymer (GMA) and a dual compatibilizer (styrene-maleic anhydride random copolymer (SMA) and poly[methylene(phenylene isocyanate)] (PMPI)), commercially available materials which have previously been studied for this application.

5.2 EXPERIMENTAL

5.2.1 MATERIALS

PET grade E333 (standard IV), polystyrene (Xarec 142ZE, Idemitsu Kosan Co., Ltd.), styrene-glycidyl methacrylate copolymer (GMA), and styrene-maleic anhydride random copolymer (SMA, 8% maleic anhydride), were kindly provided by DuPont Teijin Films. Before use, they were all dried under vacuum at 50°C for 24 hours. Polystyrene (PS-192, average M_w ~192,000 g·mol^{-1}, Sigma-Aldrich)

was dried under vacuum at 50°C for 24 hours before use. Poly[methylene(phenylene isocyanate)] (PMPI, average M_n ~340 g·mol^{-1}, Sigma Aldrich) was used as received.

PEI-*g*-PS graft copolymers were dried under vacuum at 50°C for 24 hours before use. Their synthesis and characterisation are reported in Chapter 4. The graft copolymers differ in length of PS grafted chains (specified in the subscript), and in the strategy employed for their synthesis (solution polycondensation, sp-, or chain coupling, cc-). The SEC data are listed below:

sp-PEI-*g*-PS$_{2.9K}$	M_n 5,500 g·mol^{-1}, M_w 6,600 g·mol^{-1}, Đ 1.20
sp-PEI-*g*-PS$_{6.4K}$	M_n 12,400 g·mol^{-1}, M_w 14,400 g·mol^{-1}, Đ 1.16
cc-PEI$_1$-*g*-PS$_{2.9K}$	M_n 15,300 g·mol^{-1}, M_w 23,000 g·mol^{-1}, Đ 1.50
cc-PEI$_1$-*g*-PS$_{6.4K}$	M_n 20,900 g·mol^{-1}, M_w 27,000 g·mol^{-1}, Đ 1.29
cc-PEI$_2$-*g*-PS$_{9.1K}$	M_n 17,700 g·mol^{-1}, M_w 24,600 g·mol^{-1}, Đ 1.39

Another graft copolymer (cc-PEI$_3$-*g*-PS$_{6.4K}$) was synthesised by coupling of ePS6.4K (M_n 6,400 g·mol^{-1}, Đ 1.05) and PEI-OH3 (M_n 17,200 g·mol^{-1}, Đ 1.47), as described in Chapter 4. It was only used as example to test the stability of the copolymers upon extrusion in the same conditions of the blends.

cc-PEI$_3$-*g*-PS$_{6.4K}$ $\quad$ M_n 12,900 g·mol^{-1}, M_w 17,600 g·mol^{-1}, Đ 1.36

5.2.2 CHARACTERISATION

^{1}H NMR spectra were measured on a Bruker DRX-400 MHz spectrometer using CDCl$_3$ as solvent.

Triple detection size exclusion chromatography (SEC) with refractive index (RI), viscosity, and right angle light scattering (RALS) detectors was used for the analysis of molar mass and molar mass distribution of a sample of PS-192 and cc-PEI$_3$-*g*-PS$_{6.4K}$ after extrusion, using a Viscotek TDA 302. THF was used as eluent for PS-192 and chloroform for the copolymer, both at a flow rate of 1.0 ml·min^{-1} and at a temperature of 35°C. Separation was achieved using 2×300 mm PLgel 5 µm mixed C-columns. A value of 0.185 ml·g^{-1} was used as

the dn/dc of polystyrene (in THF) and 0.123 ml·g^{-1} for the copolymer cc-PEI$_3$-*g*-PS$_{6.4K}$ (in CHCl$_3$).

SEM imaging was performed in low vacuum mode, using a FEI Quanta FEG 250 Environmental SEM. Randomly selected sections from each of the blends were immersed in liquid nitrogen and cryofractured. The resulting fracture surfaces were mounted for SEM imaging using conductive carbon tabs. A thin conductive gold/palladium coating (<20 nm) was applied to the samples to help eliminate charging issues. The PS domains diameter distribution was analysed by ImageJ, measuring the diameter of a minimum of 200 domains per sample.

5.2.3 BLENDING PROCEDURE

Melt extrusion was performed at 270°C and 125 rpm in a ThermoFischer Scientific MiniLab II HAAKE Rheomex CTW5 counter-rotating twin-screw extruder. Commercial polystyrene (PS-192) and cc-PEI$_3$-*g*-PS$_{6.4K}$ copolymer were extruded first to test their thermal stability under the chosen extrusion conditions, in either air or inert atmosphere (argon) and after 5 or 10-minute mixing by the screws, before the extrusion.

PET and PS (both Xarec 142ZE and PS-192) underwent a grinding stage before the blending, in order to improve the mixing of the powders. The copolymers were already in powder form and were used as synthesised. All the polymers were dried under vacuum at 50°C for 24 hours before use.

The extrudates were cooled down in air.

5.3 RESULTS AND DISCUSSION

PET/PS blends were prepared in 75/25 weight ratio composition by melt extrusion with the addition of the PEI-*g*-PS copolymers in different amounts, in order to investigate their effectiveness as blend compatibilizers. Effectiveness was assessed by measuring the domain dimensions by SEM of the dispersed component (PS) in the matrix of PET. The total mass of PET/PS blend was 5 g, plus a 5, 2.5 and 0.5 wt.% of copolymer. The graft copolymers differ in length of PS grafted chains, and in the strategy employed for their synthesis (solution

polycondensation or chain coupling), that resulted in a different number of PS side grafts in the PEI backbone. The ones synthesised by solution polycondensation (sp-PEI-*g*-PS$_{2.9K}$ and sp-PEI-*g*-PS$_{6.4K}$) resulted in being comprised of only one PS chain per backbone of PEI, while with the coupling approach (cc-PEI$_1$-*g*-PS$_{2.9K}$, cc-PEI$_1$-*g*-PS$_{6.4K}$ and cc-PEI$_2$-*g*-PS$_{9.1K}$) we demonstrated that a mixture of species were obtained, among which copolymers with up to 3 PS grafts per chain can reasonably be expected.

Before proceeding with the compatibilized blends, the whole melt extrusion procedure needed to be optimised. Starting from the typical conditions used for melt extruding PET (270-290°C, 125 rpm), it was first necessary to establish whether PS and the PEI-*g*-PS copolymers were thermally and mechanically stable during the melt blending and extrusion procedure. Moreover, PET/PS blend (75/25 w/w) was produced without any copolymer compatibiliser, in order to have a reference sample.

5.3.1   OPTIMISATION OF THE BLENDING PROCEDURE

The instrument used for the preparation of the blends is a ThermoFischer Scientific MiniLab II HAAKE Rheomex CTW5 counter-rotating twin-screw extruder, shown in Figure 5.3.
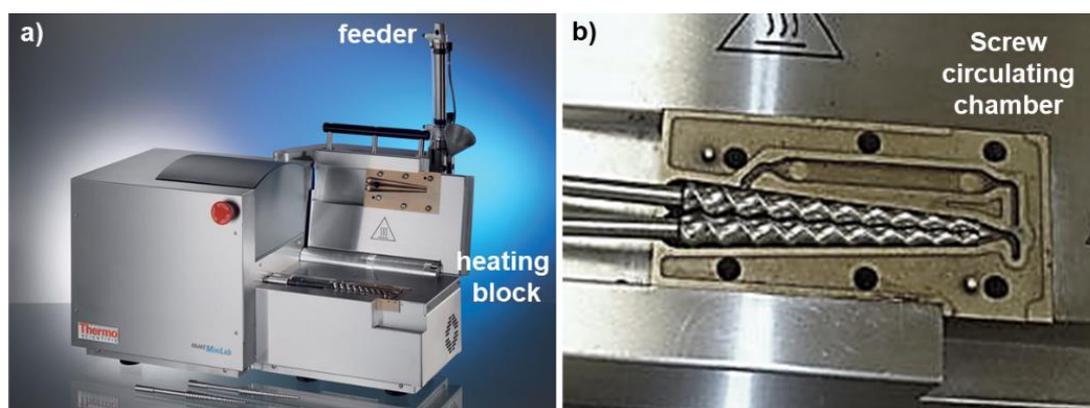
Figure 5.3 a) ThermoFischer Scientific MiniLab II HAAKE Rheomex CTW5 counter-rotating twin-screw extruder. b) Zoom in on the counter-rotating twin-screw circulating chamber.

In Figure 5.3b, the counter-rotating twin-screw circulating chamber is shown, in which the melt material can be recirculated and, in the case of a blend, mixed for different amount of time and with a controlled screw speed. The feeder, on the top of the instrument, also allows the whole extrusion process to be carried out under an inert gas.

In order to confirm the stability of PS and the PEI-*g*-PS copolymers during the blending process, a mass of 5 g of PS-192 and 5 g of cc-PEI$_3$-*g*-PS$_{6.4K}$ were each subjected to melt extrusion individually at 270°C and 125 rpm, with different time of cycling through the screw chamber before the actual extrusion, and comparing the effect of having or not an inert atmosphere of argon. PS-192 was used in these preliminary tests, instead of Xarec 142ZE which was used in the melt blends, because the latter is syndiotactic PS, with a high degree of crystallinity, and thus not soluble in common organic solvents. This would have prevented the post-processing analysis by SEC and NMR. NMR analysis of the extruded PS and cc-PEI$_3$-*g*-PS$_{6.4K}$ samples showed no significant changes in comparison to the original polymer, however SEC analysis was more helpful in highlighting some differences. Figure 5.4 compares the chromatograms of PS-192 before processing and after being melt-processed for 5 and 10 minutes.
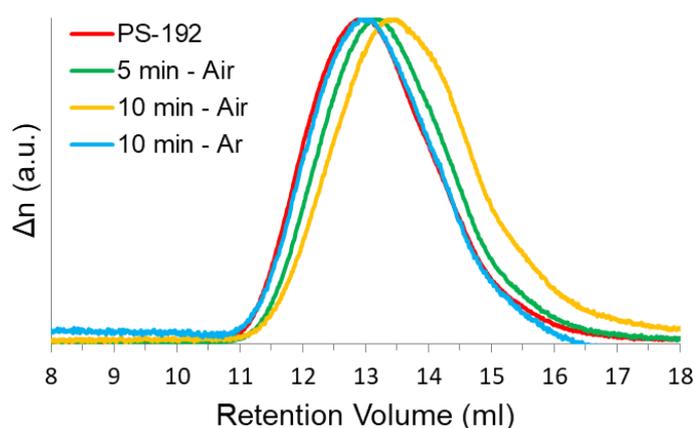
Figure 5.4 SEC chromatogram of PS-192 compared with the same polymer after extrusion under different atmospheres and for different processing times.

SEC analysis was also used to compare the impact of processing in the presence and absence of air. When processing was not carried out under an inert atmosphere (green and yellow lines in Figure 5.4), the SEC analysis of PS-192

shows a shift to greater retention volume (lower molar mass) and a broadening of the peak. The SEC data are summarised in Table 5.1.

Table 5.1 SEC data of PS-192 before processing and after being melt-processed for 5 and 10 minutes, in air or argon.

	M_n (kg·mol^{-1})	M_w (kg·mol^{-1})	Đ
PS-192	103.3	215.1	2.1
5 min - air	92.1	175.3	1.9
10 min - air	57.0	139.1	2.4
10 min - argon	99.6	194.1	2.0

M_n gradually shifts from 103 kg·mol^{-1} to 92 and 57 kg·mol^{-1} as the processing time increases from 5 to 10 minutes in air, respectively. An increase in Đ from 2.1 to 2.4 with increasing processing time was also observed. This evidence clearly demonstrates that PS undergoes (thermo-oxidative) degradation under these conditions, and clearly the extent of degradation increases, as the processing time in the extruder increases. Significantly though, when processing was carried out under an inert atmosphere of argon, even after 10 minutes, the SEC chromatogram shows that PS 192 was largely unaffected by processing, with a M_n that stays around 100 kg·mol^{-1} and Đ 2.0. Thus, the SEC peak (blue line in Figure 5.4) retains the same retention volume and dispersity as the original sample. Perhaps unsurprisingly, we can conclude that an inert atmosphere is crucial to prevent thermo-oxidation of polystyrene polymer.

Subsequently, cc-PEI$_3$-*g*-PS$_{6.4K}$ was also processed in the recirculating extruder at 270°C and 125 rpm, in an inert atmosphere of argon, with process times of 5 and 10 minutes. The SEC traces are shown in Figure 5.5 and the data are summarised in Table 5.2.

The retention volumes, and therefore the calculated M_n, show little change, slightly shifting to higher molecular weights, while the dispersity remains around

1.4. It is possible to notice, though, in Figure 5.5 small differences in the relativeintensity of the peaks at 15 ml and 16.2 ml.
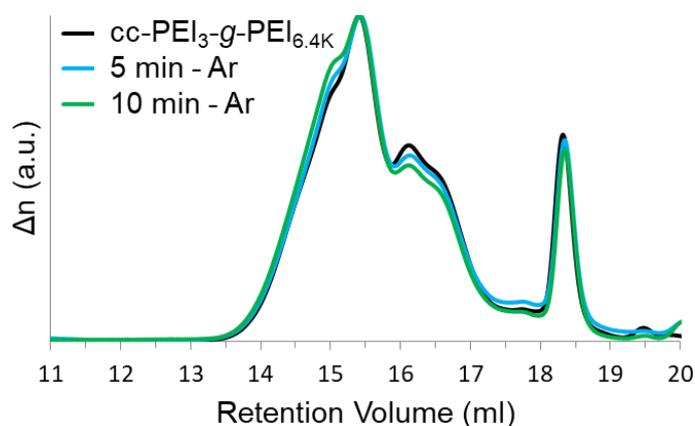
Figure 5.5 SEC chromatogram of cc-PEI$_3$-*g*-PS$_{6.4K}$ compared with the same polymer after extrusion under different atmospheres and for different processing times.

Table 5.2 SEC data of cc-PEI$_3$-*g*-PS$_{6.4K}$ before processing and after being melt-processed for 5 and 10 minutes under argon.

	M$_n$ (kg·mol^{-1})	M$_w$ (kg·mol^{-1})	Đ
cc-PEI$_3$-*g*-PS$_{6.4K}$	12.9	17.6	1.36
5 min - argon	13.1	18.0	1.37
10 min - argon	13.5	18.9	1.40

At longer processing time, the latter peak slightly decreases in intensity, while the former increases. This evidence might suggest that the chain coupling reaction progresses under melt-processing conditions, causing the increase in intensities of the higher molecular weight species. Nevertheless, the main outcome of this analysis is the good thermal stability of the copolymer under these conditions, even after 10 minutes of processing. The chromatogram also shows the peak at 18.5 ml, which is ascribable to PEI oligomers, as seen before for the other copolymers and amply discussed in Chapter 4. This species also seems to be unaffected by the process conditions.

The result of these preliminary tests on PS and cc-PEI$_3$-*g*-PS$_{6.4K}$ copolymer show that the chosen conditions of temperature, screw rotation speed, processing time

and an inert atmosphere are compatible with the materials that will be used in the blends.

Finally, two reference blends were prepared (PET/PS 75/25 w/w, no copolymer) using the conditions mentioned above, to investigate the impact of processing time on the blend morphology, and in particular the dimensions of PS domains in the PET matrix. The SEM images of both reference blends are shown in Figure 5.6.
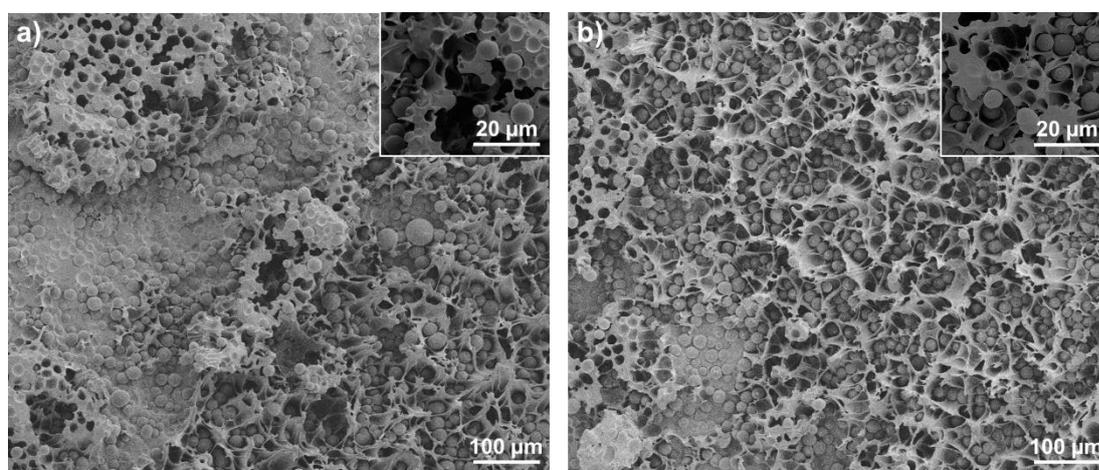
Figure 5.6 SEM images of PET/PS 75/25 w/w blends, extruded after a) 5 and b) 10-minute mixing.

The average diameter of PS spherical domains was measured as 5.6 ± 1.3 and 5.5 ± 0.7 µm for the blends formed after processing times of 5 and 10 minutes, respectively. This result suggests that the longer cycling time does not affect in any way the miscibility of the two components, giving the same average size of PS domains, but does improve the homogeneity of PS size distribution, which is significantly narrower after longer cycling.

In conclusion, considering the results of PS and copolymer degradation and PET/PS blending without compatibilisation, the conditions chosen for subsequent melt blending experiments were 270°C, 125 rpm screw speed, 10-minute cycling, under an inert atmosphere of argon. The data obtained from the extruded blend without copolymer after 10 minutes of processing were also used as a reference for comparison with the compatibilized blends.

5.3.2 PS DOMAINS SIZE DISTRIBUTION IN THE COMPATIBILIZED BLENDS

Once the processing conditions were optimised to minimize polymer degradation and to get the narrower size distribution of PS domains, 3 PET/PS blends were prepared with varying amounts of each PEI-*g*-PS copolymer. In each case the PET/PS ratio was fixed at 75/25 (by mass) for a total mass of 5 g, and an increasing amount of copolymer (0.5, 2.5 and 5 wt.% of the total mass) was added. The blends were named PET/PS-xy-z, where x refers to the copolymer synthesis approach (sp for solution polycondensation; cc for chain coupling), y refers to M_n of PS macromonomer in the copolymer (2.9, 6.4 and 9.1 kg·mol^{-1}), and z is the amount of copolymer in wt.% in the blend. So, for instance, the blend PET/PS-sp2.9K-2.5 comprises PET/PS in 75/25 ratio by mass, plus 2.5 wt.% of copolymer sp-PEI-g-PS$_{2.9K}$. After 10-minute mixing at 270°C, with a 125-rpm screw speed and under argon, the samples were extruded and subsequently cryo-fractured, the surface to be imaged by SEM.

The micrographs of the compatibilized blends are presented in Figure 5.7, together with the image of the reference blend without any additive, in the first column on the left. Going from left to right in each row, the amount of copolymer increases from 0 to 5 wt.% and the effect of its presence is quite evident, even without measuring the actual size of PS domains. Comparing especially the first two rows (0 and 0.5 wt.%) the difference in PS domain diameter is significant for each copolymer, meaning that as little as 0.5 wt.% copolymer is enough to improve the compatibility in PET/PS blends. The images in the remaining two rows (2.5 and 5 wt.%) also show a gradual reduction in PS domains size with increasing weight fraction of copolymer, but the differences are slightly less evident than from 0 to 0.5 wt.%.
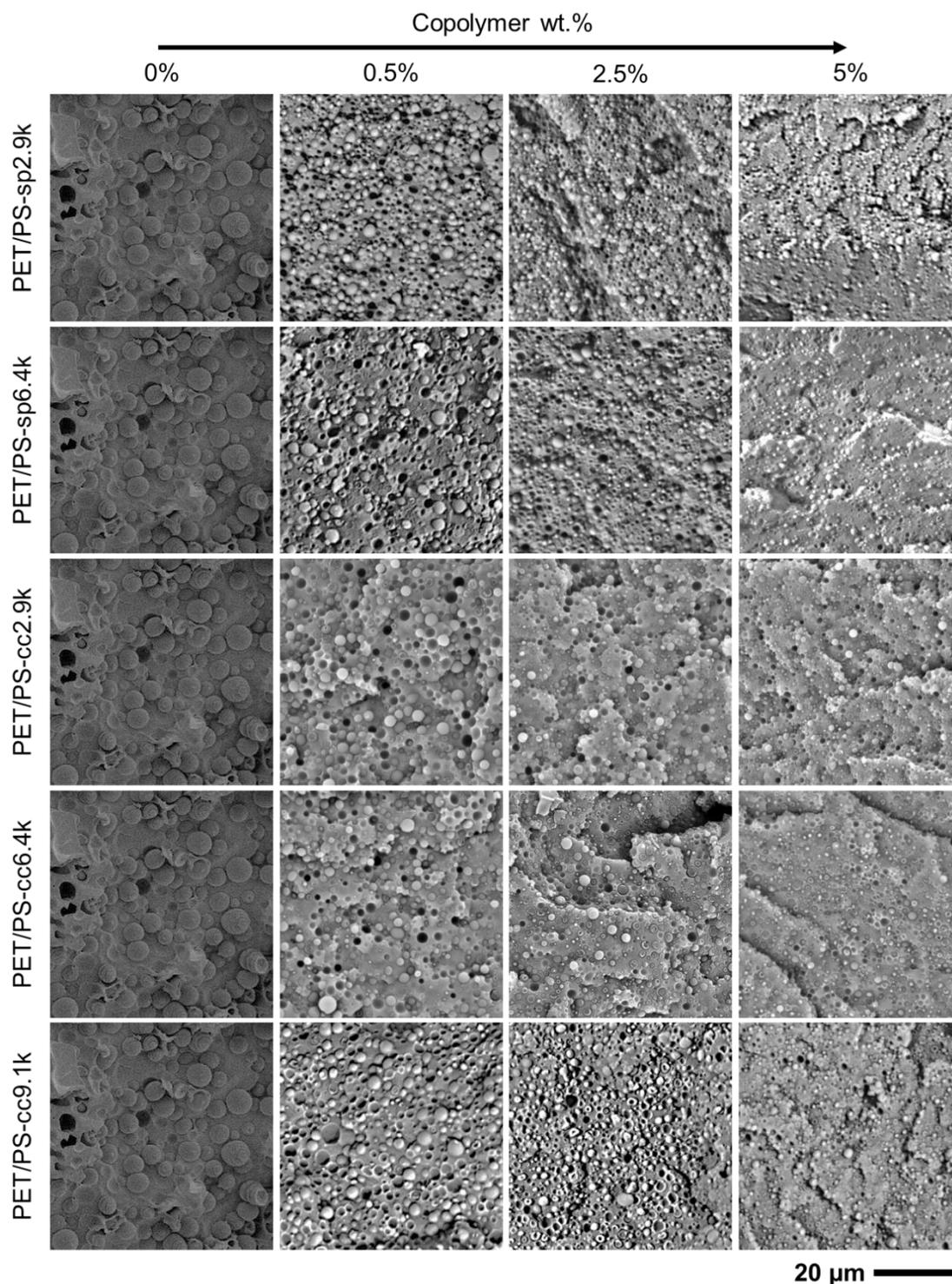
Figure 5.7 SEM images of PET/PS blends with 0, 0.5, 2.5 and 5 wt.% of copolymers.

In order to better quantify the effect of PEI-*g*-PS copolymers as compatibilizers, the diameter of PS domains was measured using ImageJ, with average values based on a distribution of dimensions from at least 200 measurements. The mean values obtained and their standard deviations (σ), reported as mean value $\pm \sigma$, are summarised in Figure 5.8.
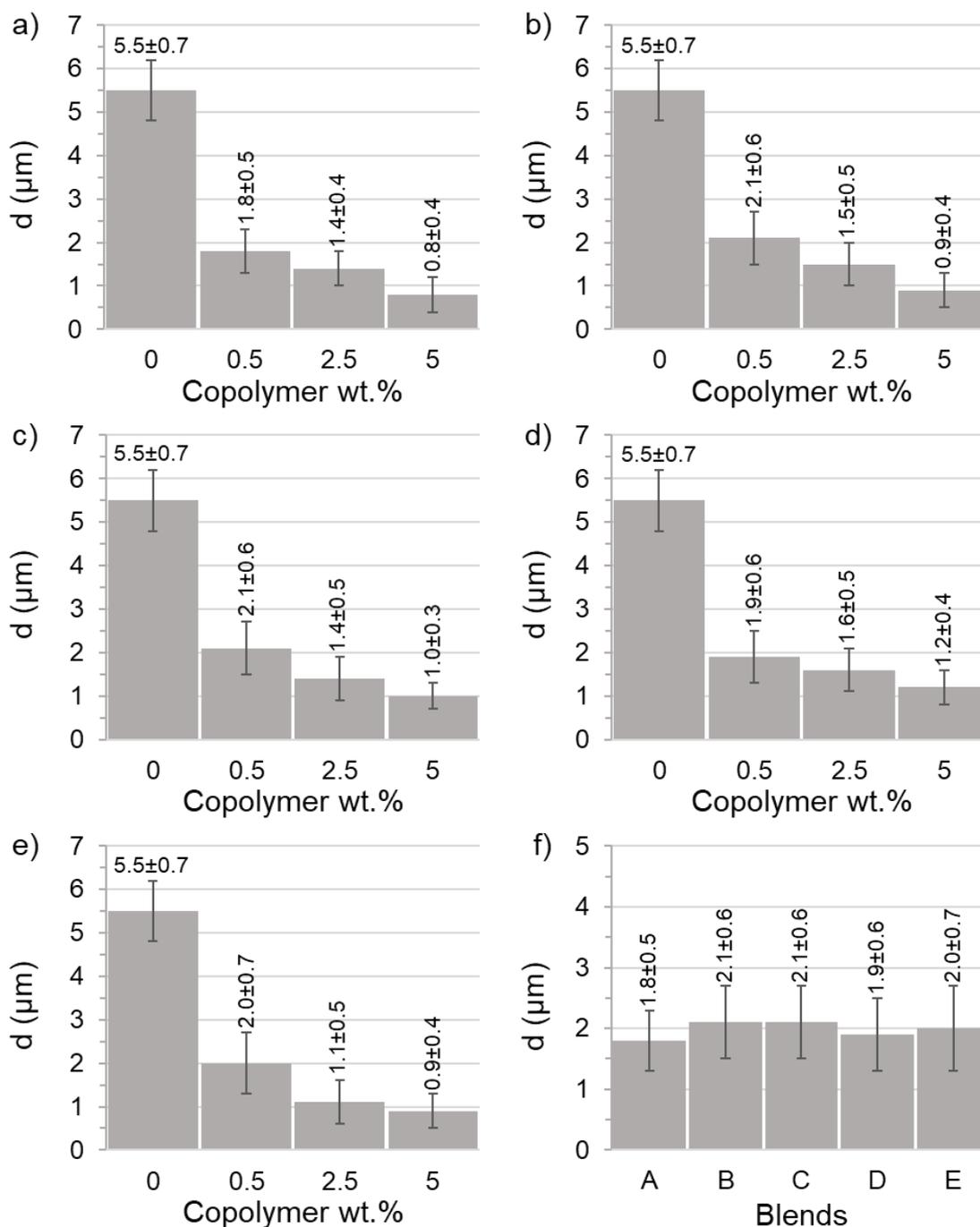
Figure 5.8 PS domains diameter in PET/PS blends prepared with varying weight percentage of the different PEI-*g*-PS copolymers: a) PET/PS-sp2.9K, b) PET/PS-sp6.4K, c) PET/PS-cc2.9K, d) PET/PS-cc6.4K, e) PET/PS-cc9.1K. f) PS domains diameter PET/PS compatibilized blends with 0.5 wt.% of PEI-*g*-PS copolymers (A = PET/PS-sp2.9k-0.5; B = PET/PS-sp6.4k-0.5; C = PET/PS-cc2.9k-0.5; D = PET/PS-cc6.4k-0.5; E = PET/PS-cc9.1k-0.5).

The addition of 0.5 wt.% of copolymer resulted in a ~65% reduction in average PS domains size for each copolymer, from 5.5±0.7 to values around 2.0 µm, with statistically no difference between the five copolymers.

Looking at each graph from a to e in Figure 5.8 individually, the use of a higher weight percentage of compatibilizer – 2.5 and 5 wt.% - caused a general and consistent trend of lowering domain sizes, even if the values cannot be considered statistically different. They are significantly different, though, if comparing 0.5 and 5 wt% of compatibilizer, except for the blend PET/PS-cc6.4K (Figure 5.8d), in which the uncertainty ranges slightly overlap.

When comparing the effect of the different copolymers, with equal amounts added in the blend (for instance, the average PS domains size measured in blends compatibilized with 0.5 wt.% of copolymers, shown in Figure 5.8f), the average PS domain size does not show any statistically significant difference.

5.3.3 COMPARISON WITH COMMERCIAL COMPATIBILIZERS

We have successfully proved that the PEI-*g*-PS graft copolymers described in Chapter 4 are effective compatibilizers for PET/PS blends, and significant reduction is PS domain size is observed when as little as 0.5 wt. % copolymer is added. However, because of the commercial interest in blends of these two polymers, many previous attempts to compatibilize PET/PS blends are reported in literature. Thus, a series of experiments to allow a direct comparison with previously reported compatibilizers under the same conditions was considered necessary. Here we present the SEM images and report the PS domain sizes of two PET/PS blends (75/25 by weight), compatibilized with 0.5 wt.% of i) styrene-glycidyl methacrylate copolymer (GMA) and ii) a dual compatibilizer composed of styrene-maleic anhydride random copolymer (0.5 wt.%) and poly[methylene(phenylene isocyanate)] (PMPI) (0.01 wt.%).

Figure 5.9 shows the SEM images of the blends compatibilized with 0.5 wt.% of each PEI-*g*-PS copolymer, and the same wt.% of commercial compatibilizers GMA and SMA/PMPI.

The size of the PS domains in the blends compatibilized with both commercial systems (Figure 5.9f and g), visually, are clearly larger than the blends compatibilized with the PEI-*g*-PS copolymers prepared in the current project (Figure 5.9a-e).
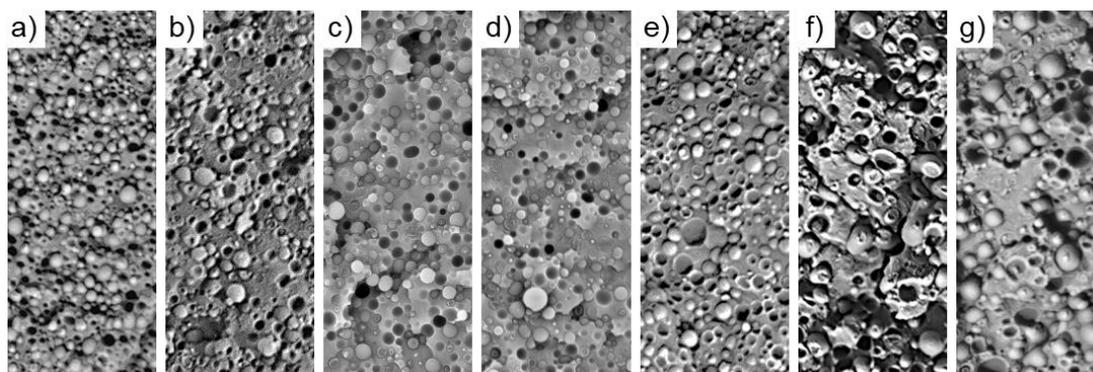
Figure 5.9 SEM images of PET/PS blends, each with 0.5 wt.% of a different PEI-*g*-PS copolymer or commercial compatibilizers, GMA and SMA/PMPI. In particular: a) PET/PS-sp2.9k-0.5; b) PET/PS-sp6.4k-0.5; c) PET/PS-cc2.9k-0.5; d) PET/PS-cc6.4k-0.5; e) PET/PS-cc9.1k-0.5; f) PET/PS-GMA and g) PET/PS-SMA/PMPI.

The mean values, obtained by the measurement of over 200 domains via ImageJ, quantify the data and these data are reported in Figure 5.10.
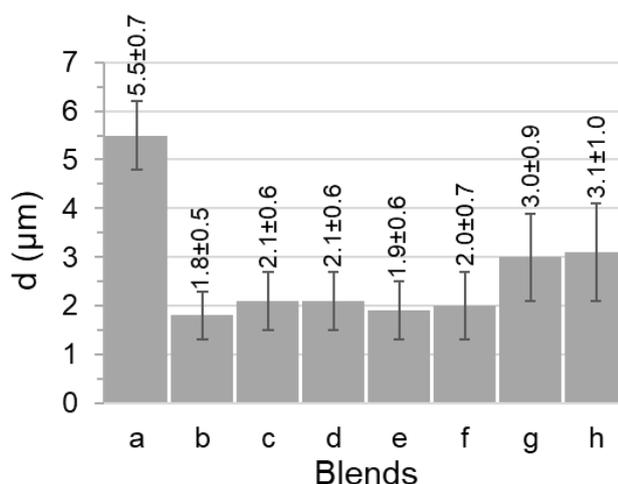
Figure 5.10 PS domains diameter in PET/PS blends compatibilized with 0.5 wt.% PEI-*g*-PS copolymers (b = PET/PS-sp2.9k-0.5; c = PET/PS-sp6.4k-0.5; d = PET/PS-cc2.9k-0.5; e = PET/PS-cc6.4k-0.5; f = PET/PS-cc9.1k-0.5) compared with uncompatibilized blend (a = PET/PS) and identical blends prepared with the same amount of commercial compatibilizers GMA and SMA/PMPI (g = PET/PS-GMA and f = PET/PS-SMA/PMPI).

The last two bars on the right of the graph, related to the blends with GMA and SMA/PMPI compatibilizers, clearly show a smaller impact on the PS domains diameter in the blend, if compared with PEI-*g*-PS copolymers, even if also in this case the error bars overlap. Nevertheless, considering the mean values, the

reduction in size with commercial additives is about 45%, while ~65% reduction was obtained with the synthesised copolymers.

5.4 CONCLUSIONS

In this Chapter the PEI-*g*-PS graft copolymers, described in Chapter 4, have been tested as compatibilizers for blends of PET and PS. The PEI-PS copolymers differ in PS chain length (2.9, 6.4 and 9.1 kg·mol^{-1}) and number of PS graft arms (1 for the copolymers obtained by solution polycondensation; mixture of species with up to 3 PS grafted chains, with the chain coupling approach). The blends were prepared by melt blending and extrusion of PET/PS in weight ratio 75/25 plus each copolymer in increasing amount, from 0.5 wt% to 2.5 and 5 wt.% of the total mass.

Before proceeding, some tests were performed, in order to verify the stability of the materials – especially PS and the copolymers – in the extrusion conditions, and to optimize the procedure. The SEC analysis of commercial PS, extruded at 270°C, with a 125 rpm screw speed, varying the time of cycling in the screw chamber and the presence or not of an inert atmosphere of argon, proved that the process in air causes significant PS degradation, reducing M_n and increasing Đ, and that an inert atmosphere is crucial to eliminate degradation. Subsequently, the extrusion of a PEI-*g*-PS copolymer in the same conditions and under argon, proved not to affect the material, with no significant changes in SEC traces, as for both retention volume and Đ.

To optimise the procedure, PET/PS blends were extruded at 270°C, with a 125 rpm screw speed and under argon, testing the effect of different time of cycling (5 and 10 minutes). Little difference in the mean values of PS domains diameter was detected, however, the distributions in domain size were significantly narrower for longer cycling times, meaning that longer time of cycling does not affect the miscibility of the two components – same average domain size of the minor one - but only the distribution of the values.

The optimised conditions (270°C, 125 rpm screw speed, 10-minute mixing, and argon) were chosen to extrude the blends with PEI-*g*-PS copolymers as a

compatibiliser. The SEM images and the mean value of PS domains diameter, calculated from measuring at least 200 domains per each sample, showed that the addition of 0.5 wt.% of copolymer resulted in a ~65% reduction of PS domains diameters for each copolymer, with little differences among them. When more compatibilizer was added, a consistent trend of reducing the domain size was observed, even if the difference is not statistically significant. No significant changes were detected among the different copolymers, with equal amount in the blend.

Finally, the compatibilizing effect was compared with previously studied commercial blend compatibilizers, under the same conditions and using the lower amount of additive (0.5 wt.%). Both GMA and the dual compatibilizer SMA/PMPI did improve the dispersion of PS into the PET matrix, however only a 45% reduction of the mean PS domains diameter was detected.

In conclusion, we have demonstrated that the graft block copolymers, comprising a polyester backbone and grafted PS arms, are suitable to be used in common blending processes as compatibilizing agents. Moreover, their effectiveness proved to be superior than other commercial copolymers, previously used for the same purpose, meaning that, using these copolymers, less material would be necessary to obtain the same degree of compatibilization.

REFERENCES

1. Heino, M.; Kirjava, J*., et al.*, *Journal of Applied Polymer Science*, **1997,** *65* (2), 241-249.
2. Young, R.J.; Lovell, P.A., *Introduction to Polymers*. 3rd Edition; Taylor and Francis, **2011**.
3. Todd, A.D.; McEneany, R.J*., et al.*, *Macromolecules*, **2016,** *49* (23), 8988-8994.
4. Huang, J.-M., *Journal of Applied Polymer Science*, **2003,** *88* (9), 2247-2252.
5. Patel, A.C.; Brahmbhatt, R.B*., et al.*, *Journal of Applied Polymer Science*, **2003,** *88* (1), 72-78.
6. Joseph, S.; Focke, W.W*., et al.*, *Composite Interfaces*, **2012,** *17* (2-3), 175-196.
7. Maa, C.-T.; Chang, F.-C., *Journal of Applied Polymer Science*, **1993,** *49* (5), 913-924.
8. Papke, N.; Karger-Kocsis, J., *Polymer*, **2001,** *42* (3), 1109-1120.
9. Yoon, K.H.; Lee, H.W*., et al.*, *Polymer*, **2000,** *41* (12), 4445-4449.
10. Heino, M.; Kirjava, J*., et al.*, *Journal of Applied Polymer Science*, **1997,** *65* (2), 241-249.
11. Ju, M.Y.; Chang, F.C., *Polymer*, **2000,** *41* (5), 1719-1730.

CHAPTER 6

SYNTHESIS OF POLYSULFONE GRAFT COPOLYMERS BY POLYCONDENSATION

6.1 INTRODUCTION

Aromatic polysulfones - poly(ether sulfone)s and poly(phenyl sulfone)s (Figure 6.1) - are high-temperature (HT) thermoplastics, with high glass transition temperature, high strength, toughness and stiffness at elevated temperatures, good chemical stability (resistance to hydrolysis as well as to acids and bases), good film forming properties, transparency and biocompatibility.[1]
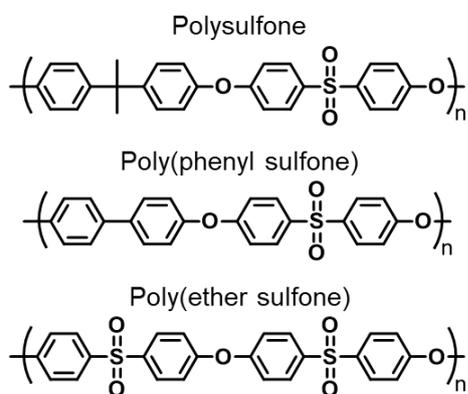
Figure 6.1 Structure of the most common aromatic polysulfones.[2]

The most widely used method for the commercial production of this class of polymers is by polyetherification, based on a nucleophilic aromatic substitution reaction of a bisphenolate with an aromatic sulfone dihalide to produce a diaryl ether linkage (Scheme 6.1b). The synthetic procedure requires the formation of a bisphenolate anion using dry potassium carbonate (weak base approach) in polar aprotic solvents (Scheme 6.1a). Finally, the generated bisphenolate anions react with the aromatic activated dihalides (the sulfones) to yield the polymer.[2]

a)

b)
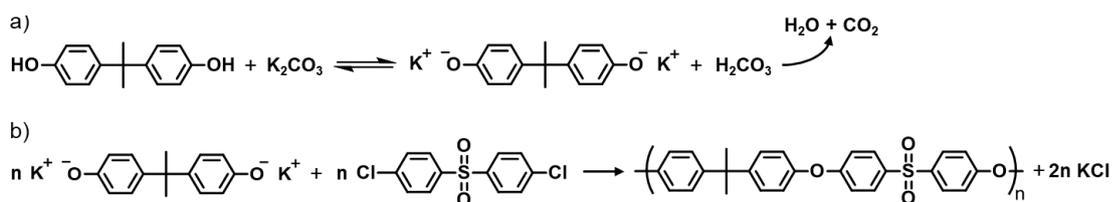
Scheme 6.1 Synthesis of polysulfone via polyetherification: a) formation of bisphenolate anion and b) poly-condensation with aromatic sulfone dihalide.

Thanks to their remarkable properties, these materials find many applications in a wide range of fields: from automotive and aerospace to medical devices and food processing applications, especially as membranes for filtration,[3-4] biomaterials[5-7] and fuel cells.[8-10]

In order to improve the performance of these materials and to tune their characteristics for an extended range of applications, many efforts have been made to functionalise the polysulfone backbone or to combine polysulfones with other homopolymers, mechanically in a blend or by chemically linking them into block or graft copolymers.[2]

Blending polysulfones (PSf) with other homo- or copolymers has been principally employed for the fabrication of membranes. The blend of immiscible polymers allows the formation and control of porosity for filtration,[11-13] while the synthesis of PSf block copolymers or functionalised PSf can improve the original material in terms of hydrophilicity[14-16] and ion condictivity.[17-18]

While blending can result in poor mechanical stability, because of the immiscibility of the blended polymers, the introduction of functional groups allows for the chemical modification of the polymer backbone itself and/or the introduction of a stable chemical bond with other homopolymers.

There are two main approaches to accomplish the functionalisation of PSf: the incorporation of functional monomers during the polycondensation stage, and the post-polymerisation transformation of polymers.[2]

Both components of the polysulfone chain - the unit derived from bisphenol and the phenyl sulfone unit (Figure 6.2) - can be easily functionalised, either before or after the polymerisation, by electrophilic or nucleophilic aromatic substitution

reactions, or be substituted with a derivative to introduce the functionality during the polymerisation stage.

Bisphenol part
Electron rich

Sulfone part
Electron poor

Aromatic
Electrophilic
Substitutions

Aromatic
Nucleophilic
Substitutions
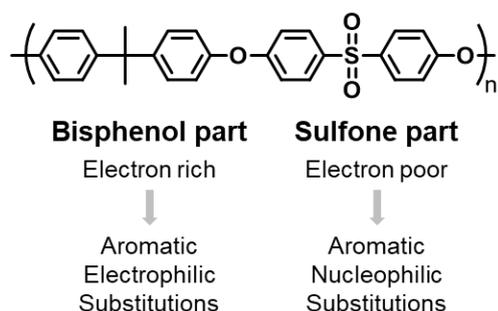
Figure 6.2 Chemical reactivity of the two units of polysulfones.[2]

6.1.1 INCORPORATION OF A FUNCTIONAL MONOMER IN THE POLYCONDENSATION REACTION

For the approaches that imply the substitution of one of the components of the polysulfone chain by a functional monomer, it is necessary that the functional group should not react with any other species in the reaction and should be stable under the reaction conditions. A comprehensive review summarising the range of functional groups which have been introduced to a polysulfone backbone through this approach has been previously reported.[2]
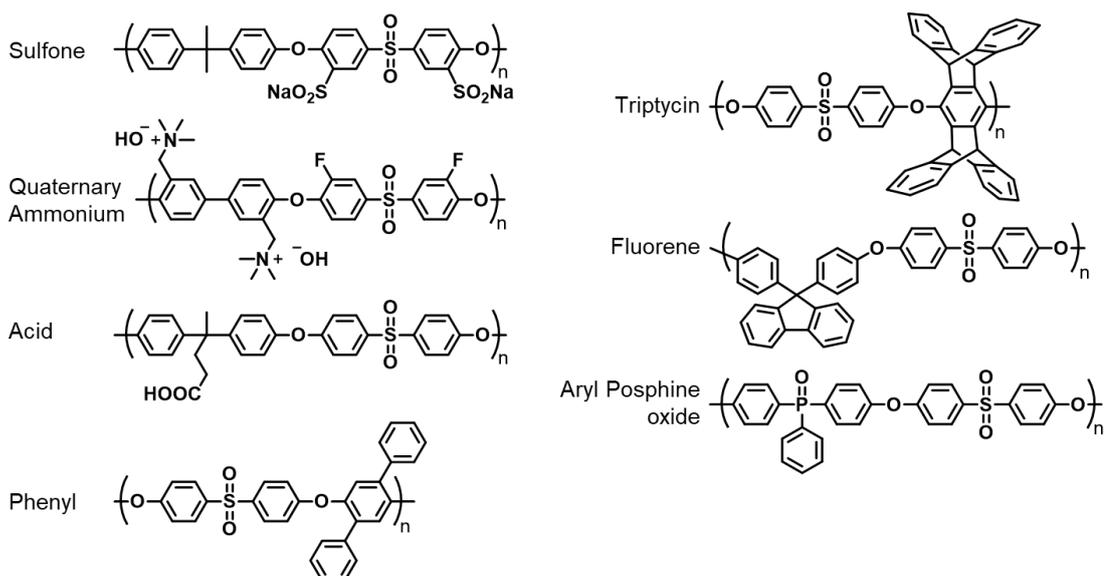
Figure 6.3 Examples of polysulfones prepared by incorporation of a functional monomer.[2]

To cite some of the main examples in Figure 6.3, polycondensation of sulfonated aromatic dihalide sulfones, with various bisphenols, yields sulfonated polysulfones, commonly used in proton exchange membranes for fuel cell applications.[19-24] For the same purpose, quaternary ammonium functionalised polysulfones[25-27] or with pendant carboxylic acid groups[28] have been synthesised by the insertion of functional bisphenols in the polycondensation reaction. Various bulky and/or rigid groups, such as phenyl, triptycene, fluorene, naphthalene and aryl phosphine oxide, have been incorporated in the polymer backbone as bisphenol derivatives, to improve the flame retardancy or to gain high glass transition temperatures, high thermal decomposition temperatures and very attractive gas transport properties.[29-34]

The incorporation of multifunctional monomers (examples in Figure 6.4) in the growing backbone allows the synthesis of hyperbranched polysulfones, characterised by low viscosity, excellent solubility, multifunctionality, and the possibility of acting as molecular encapsulants.[2]
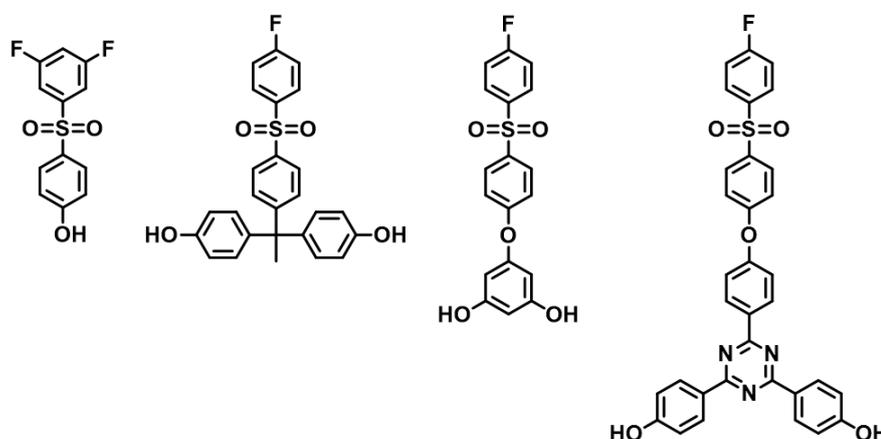
Figure 6.4 Examples of types of multifunctional monomers for the synthesis of hyperbranched polysulfones.[2]

6.1.2   POST-POLYMERISATION TRANSFORMATIONS

In cases where the desired functionality is not compatible with the polysulfone polymerisation conditions, the post-polymerisation approach can be exploited. Both electrophilic and nucleophilic substitutions on the aromatic rings of the backbone are suitable for the introduction of various functional groups onto the

polymer backbone, with the range of possible reactions recently reviewed.[2,35] Among these reactions, the halomethylation and lithiation are of particular interest because both the halomethyl group and the lithiated polysulfone can be further transformed into various functional groups (Figure 6.5).[2,35]
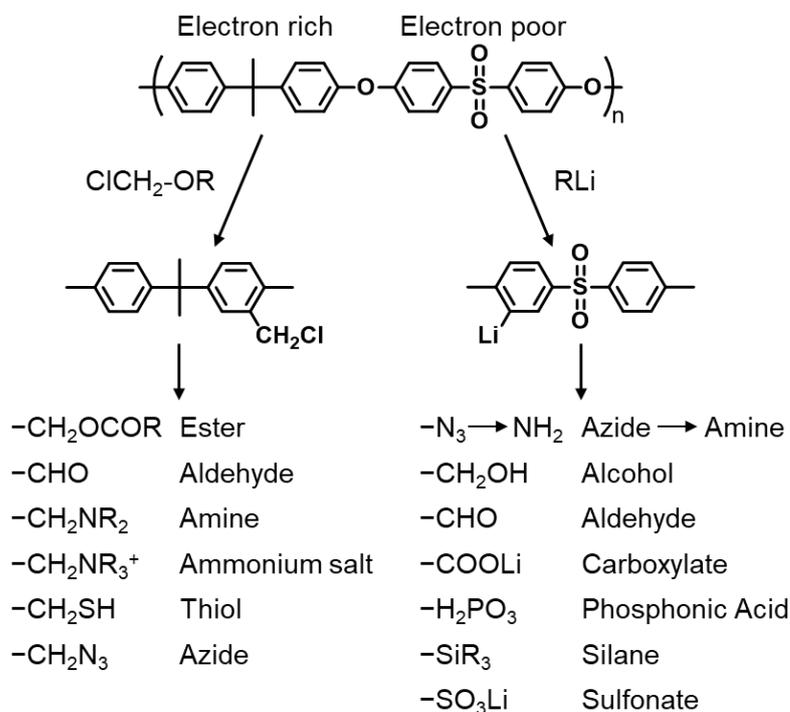
Figure 6.5 Examples of post-polymerisation transformation from halomethylated (left) and lithiated (right) polysulfones.[2]

The halomethylation is performed by electrophilic aromatic substitution onto the electron rich bisphenol aromatic rings with a halomethyl alkylether ($ClCH_2$-OR) in the presence of a Lewis acid catalyst ($SnCl_4$ or $ZnCl_2$). The lithiation is simply achieved using organo-lithium reagents, which remove a proton at the ortho position of the electron-poor sulfone aromatic rings of the polymer.

In addition to side-chain functionalisation, chain-end functionalisation of polysulfones can also be achieved by stoichiometric imbalance of one of the two comonomer. If one of the comonomers is present in slight excess, the polymerisation will proceed to a point at which the other comonomer is completely consumed and all the chain ends possess the same functional group of the comonomer in excess. Further polymerisation is not possible, and the polymer is stable to subsequent molecular weight changes. Thus, an excess of

bisphenol-A (BPA) with respect to bis chlorophenyl sulfone (BCPS) would result in hydroxy-terminated telechelic polysulfones (Scheme 6.2).
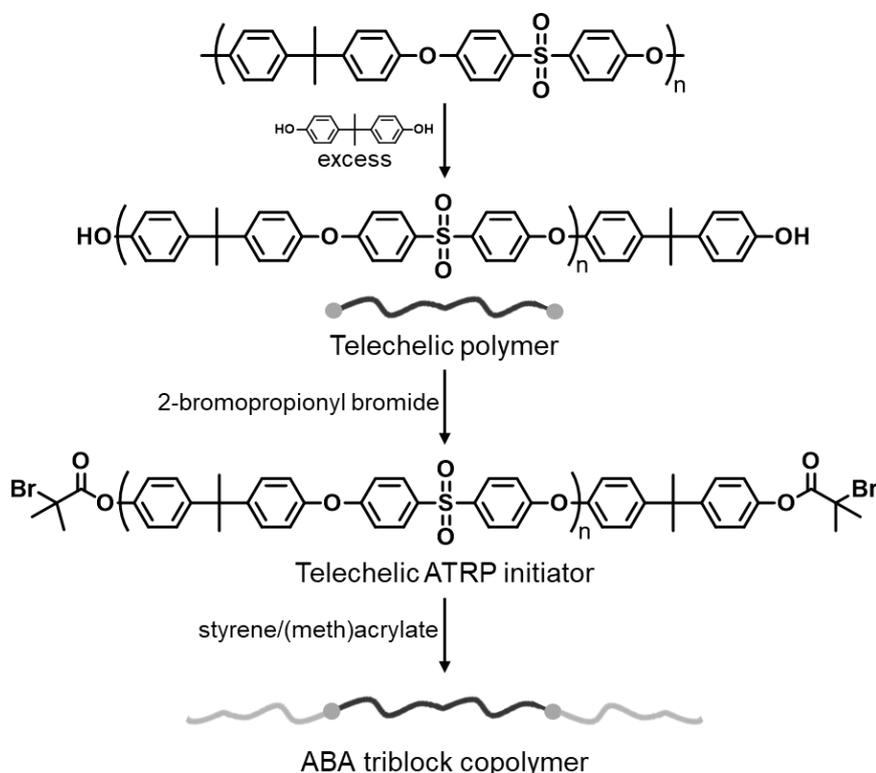
Scheme 6.2 Telechelic polymer prepared using a stoichiometric imbalance in a step-growth polymerisation and subsequent post-polymerisation reaction to obtain a telechelic ATRP initiator and, finally, a ABA triblock copolymer.[2]

An interesting consequence of both side-chain and chain-end functionalisation is the possibility to transform the polysulfone backbone into a macroinitiator for (controlled) radical polymerisation, in a so-called mechanistic transformation. Thus telechelic polysulfone can be used as a precursor for the synthesis of ABA triblock or AB multiblock copolymers.[36-39] The hydroxyl-terminal groups, for example, can react with 2-bromopropionyl bromide to yield an ATRP macroinitiator,[40-41] as shown in Scheme 6.2, or with a suitably designed RAFT agent,[14,42] leading to the controlled radical polymerisation of styrene or (meth)acrylates.

If an initiating functional group is introduced within the chain of the polymer backbone (see Scheme 6.3), then the polymerisation of a second monomer

results in the formation of a graft copolymer, through what is called a 'grafting from' approach.[43-45]

Side-chain functionalisation
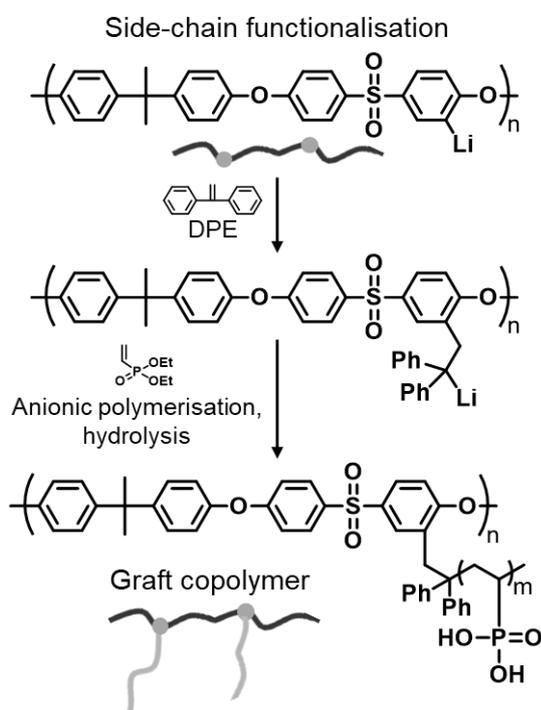
Scheme 6.3 Synthesis of graft copolymer from a side-chain functionalised polysulfone.[2]

In this chapter, the synthesis of grafted copolymers with a polysulfone backbone via a 'grafting through' approach is described. This method involves the copolymerisation of monomers with macromonomers carrying suitable functionalisation (Figure 6.6).[46]
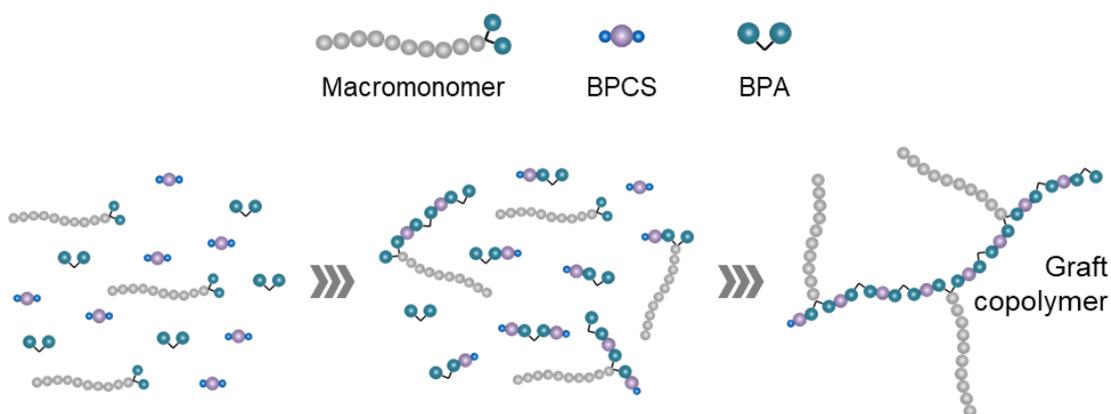
Figure 6.6 'Grafting through' approach to obtain grafted copolymers with a polysulfone backbone.

In particular, bisphenol end-functionalised macromonomers, synthesised by controlled chain growth polymerisation mechanisms (anionic or ATRP), are used in a polycondensation reaction to copolymerise together with the components of polysulfones, namely bisphenol A (BPA) and bis(4-chlorophenyl) sulfone (BCPS). The target is a grafted block copolymer with a PSf backbone and in which the macromonomers constitute the grafted branches. To the best of our knowledge, there are no previous reports on the synthesis of polysulfone-based graft copolymers obtained by the 'grafting through' approach.

6.2 EXPERIMENTAL

6.2.1 MATERIALS

Bisphenol A (BPA, ≥99%), bis(4-chlorophenyl) sulfone (BCPS, 98%) and potassium carbonate (BioXtra, ≥99%) (all Sigma-Aldrich) were used as received. Tetrahydrofuran (AR grade), methanol (AR grade), hydrochloric acid (37 wt.%) and toluene (CHROMASOLV™, for HPLC, 99.9%) (all Fischer Scientific) were used as received. 1-Methyl-2-pyrrolidinone (NMP, anhydrous, 99.5%, Alfa Aesar) was used as received.

Polystyrene (ePS6.2k, M_n 6,200 g·mol^{-1}, Đ 1.08) and poly(poly(ethylene glycol) methyl ether methacrylate) (PolyPEGMEM-OH2, M_n 21,200 g·mol^{-1}, Đ 1.12) macromonomers synthesis and characterisation are reported in Chapter 2 and 3.

6.2.2 CHARACTERISATION

Size exclusion chromatography was performed using tetrahydrofuran as eluent at a flow rate of 1.0 ml·min^{-1} and at a temperature of 35°C. Separation was achieved using 2×300 mm PLgel 5 µm mixed C-columns. For the final copolymer, triple detection SEC with refractive index (RI), viscosity, and right-angle light scattering (RALS) detectors was performed using a Viscotek TDA 302. A value of 0.185 ml·g^{-1} was used as the dn/dc of PS, 0.069 ml·g^{-1} for PolyPEGMEM (measured in house) and 0.2026 ml·g^{-1} for PSf (measured in house). For each

grafted copolymer, dn/dc has been calculated as a weighted average of the values of the macromonomer (PS or PolyPEGMEM) and PSf, according to the following equation:

$$dn/dc = dn/dc^M \times w.f.^M + 0.2026 \; ml \cdot g^{-1} \times w.f.^{PSf}$$

where w.f. is the weight fraction of (M) the macromonomer and (PSf) polysulfone, calculated by NMR. For the analysis of PSf-*g*-PS samples throughout the reaction, conventional calibration based on PS standard was used.

^{1}H NMR spectra were measured on Bruker DRX-400 MHz using $CDCl_3$ as solvent.

6.2.3   SYNTHESIS OF PSf HOMOPOLYMER

BPA (573 mg, 2.50 mmol), BCPS (720 mg, 2.50 mmol), and K_2CO_3 (1.037 g, 7.50 mmol) were put in a 2-neck round bottom flask equipped with a Dean-Stark trap, under a N_2 atmosphere. The solvents, NMP (7.5 ml) and toluene (2.5 ml), were injected by a syringe through a rubber septum in the second neck of the flask. The reaction mixture was heated in an oil bath to 160°C and stirred through a magnetic stirrer. Water was distilled out as an azeotrope with toluene and collected in the side arm of the Dean-Stark trap. After 4 hours at 160°C, the temperature was raised to 190°C to complete the polymerisation and to distil out the rest of toluene. The progress of the polymerisation reaction was monitored over time by periodically removing samples for analysis by SEC. After a total of 9 hours, the reaction was stopped by cooling the solution down to room temperature. The viscous solution was then diluted with roughly twice as much THF, poured dropwise into 5 times the volume of MeOH, made acidic with HCl in order to neutralise K_2CO_3. The precipitated polymer was collected by filtration and dried under vacuum. Yield 88%.

Triple detection: M_n 11,200 $g \cdot mol^{-1}$, M_w 13,100 $g \cdot mol^{-1}$, Đ 1.17
Conventional calibration: M_n 4,300 $g \cdot mol^{-1}$, M_w 10,200 $g \cdot mol^{-1}$, Đ 2.37

^{1}H NMR (400 MHz, CDCl$_3$, δ): 7.85 (4H, Sulfone Ar H̲), 7.25 (4H, BPA Ar H̲), 7.00 (4H, Sulfone Ar H̲), 6.95 (4H, BPA Ar H̲), 1.70 (6H, (CH̲$_3$)$_2$-BPA).

6.2.4   SYNTHESIS OF PSf-*g*-PS COPOLYMERS

The graft copolymers were synthesised according to the procedure described above for the synthesis of PSf homopolymers, with PS macromonomers added in the reaction flask together with the other reagents, before injecting the solvents. The reactions were monitored over time by the periodic collection of samples for analysis by SEC.

^{1}H NMR (400 MHz, CDCl$_3$, δ): 7.85 (4H, sulfone Ar H̲), 7.4 – 6.3 (overlapping, ePS6.2k Ar H̲), 7.25 (4H, overlapping, BPA Ar H), 7.00 (4H, overlapping, sulfone Ar H̲), 6.95 (4H, overlapping, BPA Ar H), 2.3 – 1.2 (overlapping, ePS6.2k aliphatic H̲), 1.70 (6H, overlapping, (CH̲$_3$)$_2$-BPA), 0.8–0.5 (3H, ePS6.2k sec-Butyl CH̲$_3$CH$_2$), 0.8–0.5 (3H, ePS6.2k sec-butyl CHCH̲$_3$).

6.2.4.1   PSf-*g*-PS1

BPA (549 mg, 2.40 mmol), BCPS (719 mg, 2.50 mmol), ePS6.2k (623 mg, 0.10 mmol) and K$_2$CO$_3$ (1.037 g, 7.50 mmol) were dissolved in NMP (7.5 ml) and toluene (2.5 ml). Yield 73%.

Triple detection: M$_n$ 32,100 g·mol^{-1}, M$_w$ 36,600 g·mol^{-1}, Đ 1.14
Conventional calibration: M$_n$ 11,500 g·mol^{-1}, M$_w$ 20,700 g·mol^{-1}, Đ 1.80

6.2.4.2   PSf-*g*-PS2

BPA (526 mg, 2.30 mmol), BCPS (719 mg, 2.50 mmol), ePS6.2k (1.176 g, 0.19 mmol) and K$_2$CO$_3$ (1.037 g, 7.50 mmol) are dissolved in NMP (7.5 ml) and toluene (2.5 ml). Yield 78%.

Triple detection: M$_n$ 32,800 g·mol^{-1}, M$_w$ 41,700 g·mol^{-1}, Đ 1.27
Conventional calibration: M$_n$ 16,000 g·mol^{-1}, M$_w$ 30,600 g·mol^{-1}, Đ 1.91

6.2.4.3   PSf-*g*-PS3

BPA (507 mg, 2.22 mmol), BCPS (720 mg, 2.50 mmol), ePS6.2k (1.740 mg, 0.28 mmol) and K_2CO_3 (1.037 g, 7.50 mmol) are dissolved in NMP (7.5 ml) and toluene (2.5 ml). Yield 89%.

Triple detection: M_n 32,200 g·mol^{-1}, M_w 40,900 g·mol^{-1}, Đ 1.27
Conventional calibration: M_n 14,800 g·mol^{-1}, M_w 28,000 g·mol^{-1}, Đ 1.89

6.2.4.4   PSf-*g*-PS4

BPA (526 mg, 2.31 mmol), BCPS (720 mg, 2.50 mmol), ePS6.2k (1.178 mg, 0.19 mmol) and K_2CO_3 (1.037 g, 7.50 mmol) are dissolved in NMP (9.6 ml) and toluene (3.2 ml). Yield 95%.

Triple detection: M_n 26,600 g·mol^{-1}, M_w 31,900 g·mol^{-1}, Đ 1.20
Conventional calibration: M_n 12,200 g·mol^{-1}, M_w 22,100 g·mol^{-1}, Đ 1.81

6.2.4.5   PSf-*g*-PS5

BPA (529 mg, 2.31 mmol), BCPS (721 mg, 2.50 mmol), ePS6.2k (1.179 mg, 0.19 mmol) and K_2CO_3 (1.037 g, 7.50 mmol) are dissolved in NMP (6.2 ml) and toluene (2.0 ml). Yield 98%.

Triple detection: M_n 39,100 g·mol^{-1}, M_w 51,600 g·mol^{-1}, Đ 1.32
Conventional calibration: M_n 19,300 g·mol^{-1}, M_w 37,600 g·mol^{-1}, Đ 1.95

6.2.5   SYNTHESIS OF PSf-*g*-POLYPEGMEM GRAFT COPOLYMERS

The PSf-*g*-PolyPEGMEM block copolymer was synthesised according to the same procedure described above for the synthesis of PSf-*g*-PS copolymers, with PolyPEGMEM macromonomer added in the reaction flask together with the other reagents, before injecting the solvents. The polymer was precipitated in excess hexane as a viscous liquid, allowed to settle to the bottom of the beaker, and the supernatant liquor was decanted away. The polymer was, finally, dried under vacuum.

BPA (539 mg, 2.36 mmol), BCPS (684 mg, 2.38 mmol), PolyPEGMEM (1.052 g, 0.05 mmol) and K_2CO_3 (993 mg, 7.19 mmol) were dissolved in NMP (13.0 ml) and toluene (4.3 ml). Yield 57%.

Triple detection: M_n 38,300 g·mol^{-1}, M_w 57,300 g·mol^{-1}, Đ 1.09
Conventional calibration: M_n 3,700 g·mol^{-1}, M_w 9,600 g·mol^{-1}, Đ 2.59

^{1}H NMR (400 MHz, CDCl$_3$, δ): 7.85 (4H, Sulfone Ar <u>H</u>), 7.25 (4H, BPA Ar H), 7.05 (4H, Sulfone Ar <u>H</u>), 6.95 (4H, BPA Ar <u>H</u>), 4.10 (2H, PolyPEGMEM side chain -COOC<u>H</u>$_2$CH$_2$O-); 3.65 (PolyPEGMEM side chain -OC<u>H</u>$_2$CH$_2$O-); 3.55 (PolyPEGMEM side chain -OC<u>H</u>$_2$CH$_2$O-); 3.55 (PolyPEGMEM side chain -OCH$_2$CH$_2$O-C<u>H</u>$_3$); 2.10 – 0.80 (PolyPEGMEM backbone); 1.70 (6H, (C<u>H</u>$_3$)$_2$-BPA); 0.60, 0.40 (6H, initiator *sec*-Butyl C<u>H</u>$_3$).

6.3 RESULTS AND DISCUSSION

The PS and PolyPEGMEM bisphenol functionalised macromonomers (Figure 6.7), whose synthesis has been described in Chapter 2 and 3, are designed to react as a comonomer in the polycondensation reaction used to synthesise polysulfones.
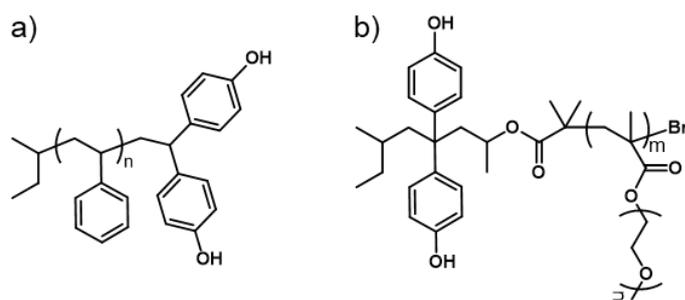
Figure 6.7 Structure of bisphenol functionalised macromonomers: a) PS (ePS6.2k), synthesised via end-capping procedure by anionic polymerisation, and b) PolyPEGMEM synthesised with a functionalised initiator by ATRP.

Being incorporated into the polysulfone backbone, the macromonomer chains constitute the side arms of a grafted block copolymer. In the case of polysulfones, the usual reactions conditions (NMP and toluene as solvents, 160°C and 190°C)[2] are compatible with the use of PS and PolyPEGMEM macromonomers: in

particular, the solvents are also good solvents for both, thus the macromonomers could be added the step growth polycondensation reaction without any particular changes to the procedure.

6.3.1 SYNTHESIS OF PSf HOMOPOLYMER AND PSf-*g*-PS BLOCK COPOLYMERS BY SOLUTION POLYCONDENSATION

The bisphenol end-functionalised PS macromonomer (ePS6.2k, M_n 6200 g·mol^{-1}, Đ 1.08) was added into the step-growth polycondensation synthesis of polysulfone in order to obtain the desired grafted copolymer, as shown in Scheme 6.4.
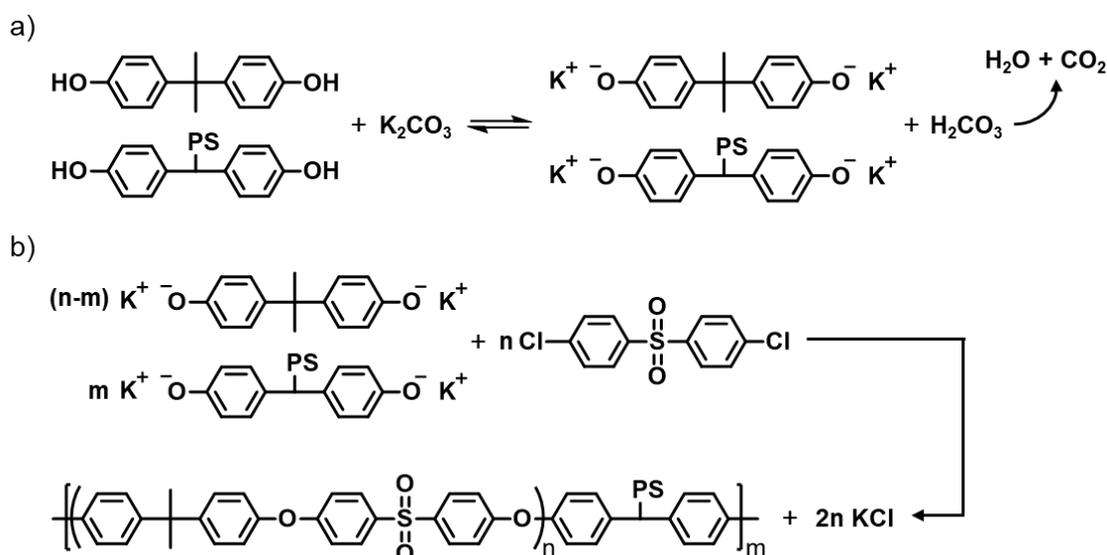
Scheme 6.4 Synthesis of PSf-*g*-PS graft copolymers by polycondensation in 2 steps.

In the first step (Scheme 6.4a), carried out at 160°C, the reaction of the aromatic bisphenols (BPA and PS macromonomer) with a weak base (K_2CO_3) forms bisphenolate anions with potassium counter ion, and resulting in the formation of H_2CO_3. At this stage water - distilled out as an azeotrope with toluene and collected in the Dean-Stark trap - and carbon dioxide, both from the equilibrium with carbonic acid, are removed to push the deprotonation to completion. After 4 hours, when the temperature is increased at 190°C in step 2 (Scheme 6.4b), the bisphenolate anions, both from BPA and macromonomers, react with

aromatic sulfone dihalides to produce the diaryl ether linkage that leads to the formation of the polymer backbone, with grafted PS chains.

Three polycondensation copolymerisation reactions were performed, keeping the overall bisphenol:sulfone ratio fixed (1:1) but varying ratio of bisphenol-A (BPA) to PS macromonomer such that BPA:PS macromonomer ratio was 24:1, 12:1 and 8:1. Since the total solvent volume is also unchanged, the molar concentration of functional groups was always the same – calculated as total number of moles of reagents (BPA + PS + BCPS) at the beginning of the reaction over the total volume of solvents (NMP + toluene). However, the concentration of reactants in terms of $g \cdot ml^{-1}$ varied a lot, increasing significantly as the mole fraction of PS macromonomer increases. An increase in the amount of PS macromonomer used resulted in an increase in the solution viscosity. To investigate the potential impact of the concentration in $mg \cdot ml^{-1}$, and thus the viscosity of the reaction solution on the outcome of the reaction, two further copolycondensation reactions were performed. In these cases an identical amount of reagents was used (BPA:PS 12:1, total bisphenols:sulfone 1:1) but the total volume of solvent was varied. Finally, a polysulfone homopolymer, without PS, was also prepared for comparison and to aid characterisation. The amounts of reagent used in each polymerisation are summarised in Table 6.1.

Table 6.1 Amount (in mmol) of reagents used for the synthesis of PSf-*g*-PS copolymers.

	BPA	ePS6.2k	BCPS	K_2CO_3	BPA:ePS6.2k	Conc. $(M)^{a)}$	Conc. $(mg \cdot ml^{-1})^{a)}$
PSf	2.50	/	2.50	7.50	/	0.5	129
PSf-*g*-PS1	2.40	0.10	2.50	7.50	24:1	0.5	189
PSf-*g*-PS2	2.31	0.19	2.50	7.50	12:1	0.5	242
PSf-*g*-PS3	2.22	0.28	2.50	7.50	8:1	0.5	296
PSf-*g*-PS4	2.31	0.19	2.50	7.50	12:1	0.4	189
PSf-*g*-PS5	2.31	0.19	2.50	7.50	12:1	0.6	296

a) The concentration is calculated as number of moles or mg of reagents (BPA + ePS6.2k + BCPS) over the total volume of solvents (NMP+toluene).

The NMR spectrum of PSf homopolymer is shown in Figure 6.8a and contains peaks assigned to all of the expected protons.
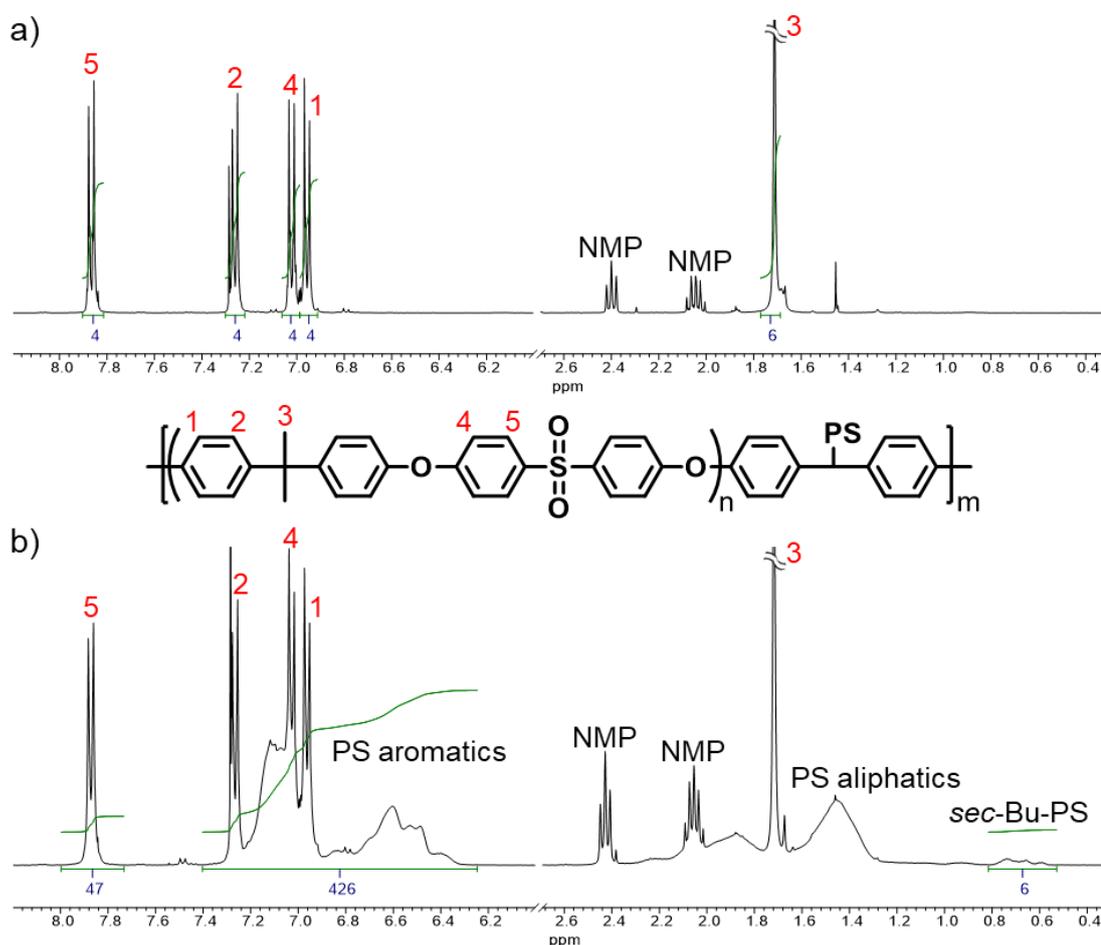
Figure 6.8 ^{1}H NMR (CDCl$_3$, 400 MHz) spectra of a) PSf homopolymer and b) PSf-*g*-PS4 copolymer.

The NMR spectra of each copolymer, exemplified by PSf-*g*-PS4 in Figure 6.8b, show the broad peaks of PS macromonomers (the aromatic protons between 7.4 and 6.2 ppm, and the aliphatic protons of the backbone between 2.5 and 1.1 ppm, together with the butyl protons of the initiator, between 0.8 and 0.5 ppm) and all the expected protons of PSf, suggesting that the polycondensation reaction worked. However, the presence of peaks in the NMR spectrum which can be assigned to both polystyrene and polysulfone is not evidence enough to prove that PS macromonomers actually took part in the polycondensation reaction and were incorporated into the PSf chain. The NMR spectrum could simply be indicating a blend of the two polymers. In this context

SEC analysis is more useful, in so much that it is possible to follow by SEC analysis any shift and/or broadening of the PS macromonomer peak during the reaction. Thus, samples were collected at various times during each polymerisation reaction, both during the first step at 160°C and in the second step, after raising the temperature to 190°C. The chromatograms recorded by RI detector for each copolymerisation are shown in Figure 6.9 (step 1) and 6.10 (step 2). The SEC analysis was performed by conventional calibration, using PS standards. The data are listed in Table 6.2.

The chromatograms throughout the homopolymerisation reaction (Figure 6.9a and 6.10a) help us to understand the mechanism of the reaction found in literature.[2] At time 0 (grey trace in Figure 6.9a), the peaks at retention volume 19 and 19.5 ml can be ascribed to monomers and solvent respectively. It is right to assume that the peak at around 19.5 ml is solvent, particularly NMP, since a similar peak, with different intensities, is also visible in all the other chromatograms in Figure 6.9 and 6.10. NMP is very difficult to be washed away by precipitation in MeOH and its presence is confirmed also by NMR spectra (see peaks at 2.4 and 2.1 ppm in Figure 6.8). Repeated re-dissolution in THF and precipitation in MeOH could improve the purity of the polymer, but for the samples collected at intermediate reaction times especially, this would have caused a loss of mass too big to allow the subsequent required analysis.

At these very low MW and using the conventional calibration based on PS standards, the error on the calculated MW can be quite high. Nevertheless, a qualitative comparison between the two peaks and their retention volume is still reliable. The SEC peak at 19.5 ml gives a MW of about 140 $g \cdot mol^{-1}$ by conventional calibration with standard PS in all the chromatograms, while NMP has a MW of 99.13 $g \cdot mol^{-1}$. However, the other peak visible at ca. 19 ml corresponds to higher MW (lower retention volume) of about 220 $g \cdot mol^{-1}$, approximately in line with the molar mass of the monomers, (BPA 228.28 $g \cdot mol^{-1}$ and BCPS 287.16 $g \cdot mol^{-1}$).

Figure 6.9 Evolution of SEC chromatograms, recorded by RI detector, of a) PSf homopolymer and b)-f) PSf-*g*-PS graft copolymers, during step 1 at 160°C.

Moving to the traces at 2 and 4 hours (see Figure 6.9a and data in Table 6.2), the appearance of peaks at lower retention volume (higher MW), shifting gradually from 500 to 600 g·mol^{-1}, suggests not more than two repeat units of PSf (442.52 g·mol^{-1}). This evidence is consistent with the mechanism described above (Scheme 6.1 and 6.4) during Step 1, in which bisphenols are deprotonated by K$_2$CO$_3$, and only the formation of small PSf oligomers is expected, before the actual polycondensation, which takes place at higher temperature in Step 2.

Table 6.2 SEC data obtained by conventional calibration with PS standards for PSf homopolymer and PSf-*g*-PS copolymers.

	M_n (g mol^{-1})	M_w (g mol^{-1})	Đ		M_n (g mol^{-1})	M_w (g mol^{-1})	Đ
PSf				**PSf-g-PS3**			
0	220	224	1.02	0	5,100	5,600	1.09
2h	500	560	1.12	2h	5,600	6,000	1.07
4h	600	730	1.21	4h	5,700	6,300	1.11
5h	1,500	2,200	1.47	5h	7,000	8,500	1.22
6h	2,200	3,800	1.67	6h	7,900	12,600	1.60
7h	3,000	5,800	1.94	7h	10,500	17,500	1.67
8h	3,600	7,800	2.16	8h	12,700	22,500	1.77
9h	4,300	10,100	2.36	9h	14,800	28,000	1.89
PSf-*g*-PS1				**PSf-*g*-PS4**			
0	5,100	5,600	1.09	0	5,100	5,600	1.09
2h	5,300	5,800	1.09	2h	5,500	6,000	1.09
4h	5,800	6,200	1.07	4h	5,600	6,200	1.10
5h	6,600	7,900	1.20	5h	6,500	7,500	1.15
6h	6,500	10,700	1.64	6h	5,900	9,500	1.61
7h	8,800	15,200	1.73	7h	9,400	15300	1.63
8h	10,400	18,700	1.80	8h	11,200	18,700	1.67
9h	11,500	20,700	1.80	9h	12,200	22,100	1.81
PSf-*g*-PS2				**PSf-*g*-PS5**			
0	5,100	5,600	1.09	0	5,100	5,600	1.09
2h	5,600	6,200	1.11	2h	5,600	6,000	1.08
4h	6,300	7,200	1.14	4h	5,700	6,300	1.10
5h	7,100	12,100	1.70	5h	7,800	9,800	1.26
6h	8,200	15,900	1.94	6h	11,100	17,300	1.56
7h	10,600	20,000	1.89	7h	15,300	26,900	1.76
8h	14,600	27,400	1.88	8h	18,600	33,100	1.78
9h	16,000	30,600	1.91	9h	19,300	37,600	1.95

Looking at the chromatograms of samples collected during step 2 for PSf homopolymer (Figure 6.10a), there is the sudden appearance of a broad and intense peak at lower retention volume (17.3 ml) with a higher MW (M_n 1,500 g·mol^{-1}, Đ 1.47) after 1 hour at 190°C (5 hours of reaction from time 0, light blue trace), which then gradually shifts to higher MW and broadens in dispersity throughout the reaction to give a final molar mass after 9 hours of M_n 4,300 g·mol^{-1} and Đ 2.37. Contextually, the small peaks at high retention volumes (between 17.5 and 19 ml) seen at 4 hours gradually decrease in intensity.
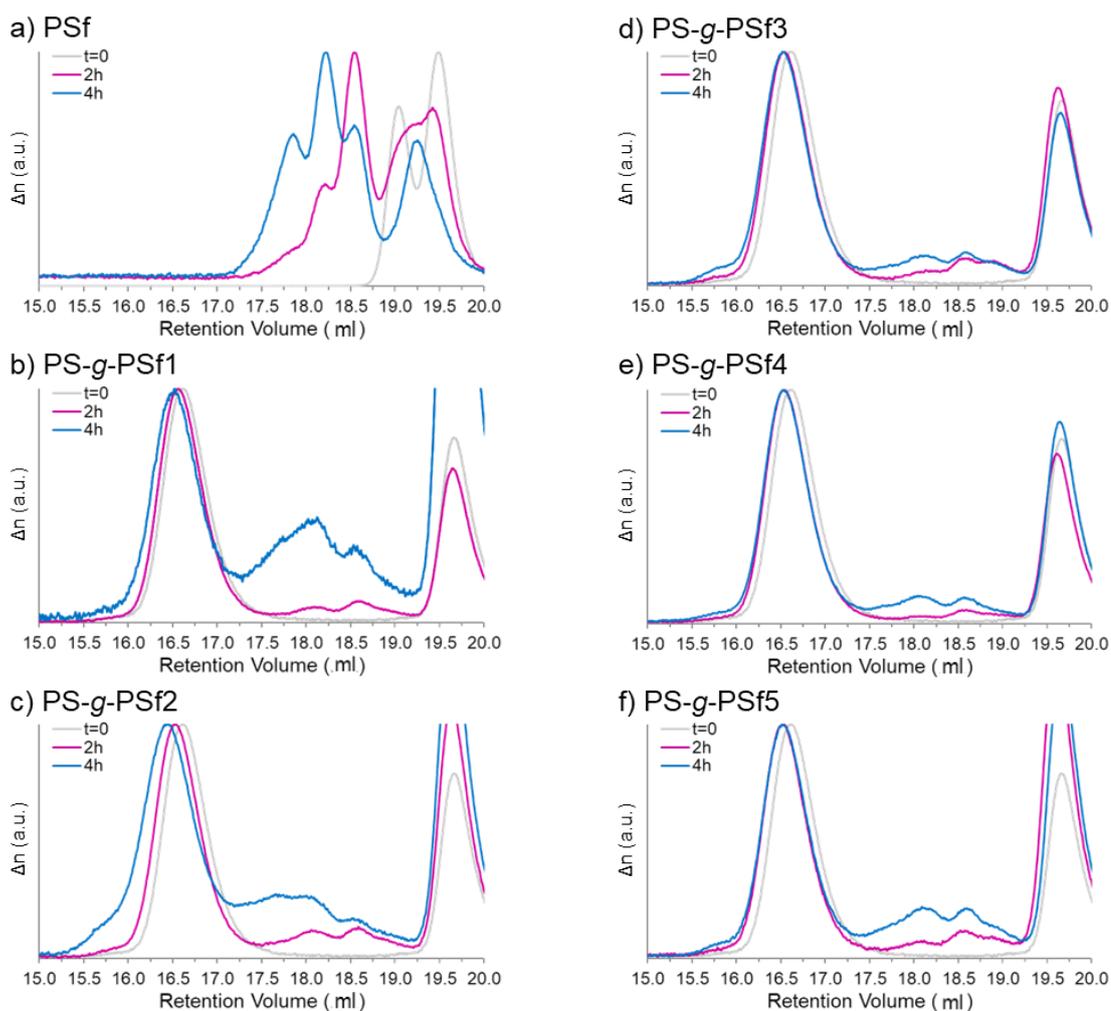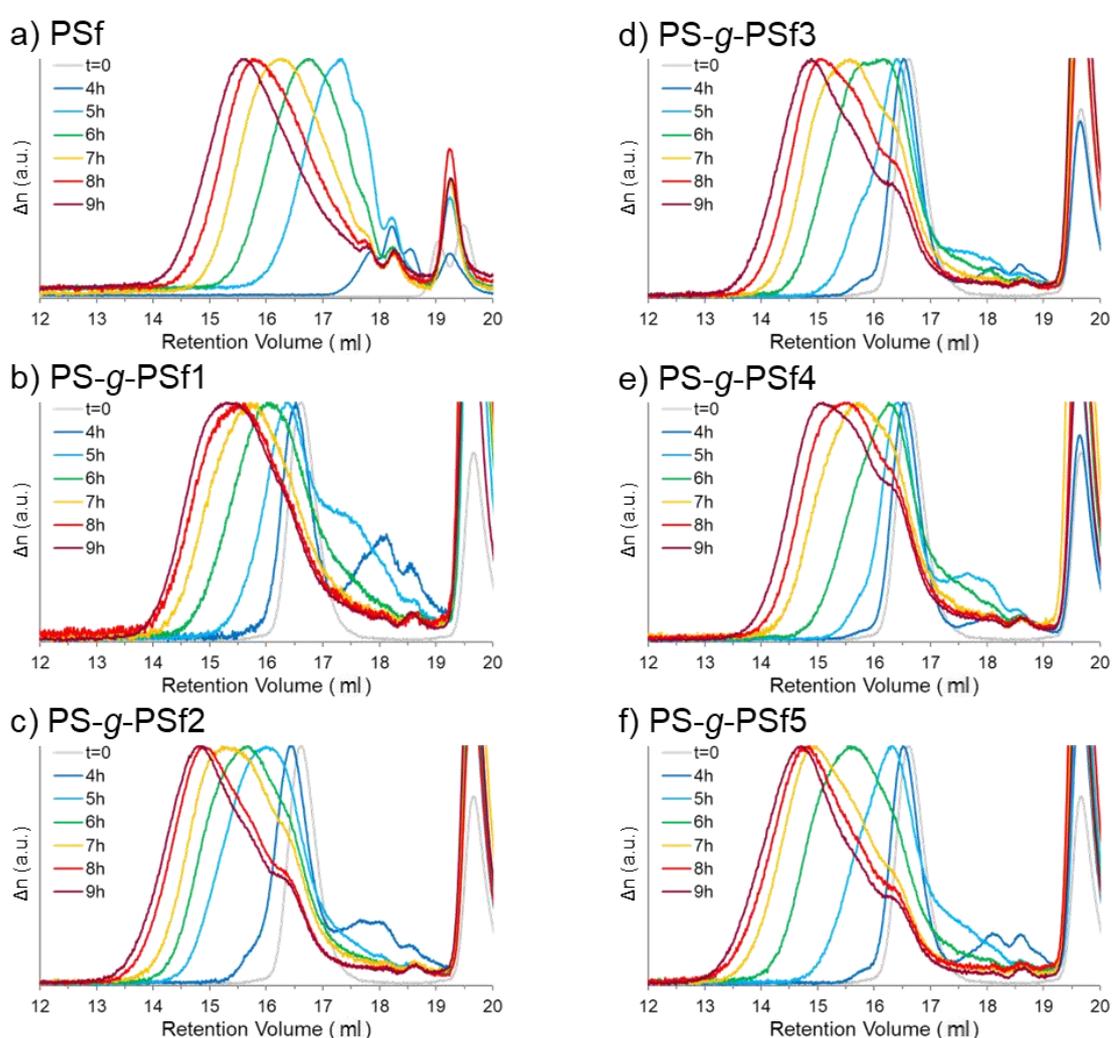

Figure 6.10 Evolution of SEC chromatograms, recorded by RI detector, of a) PSf homopolymer and b)-f) PSf g PS graft copolymers, during step 2 at 190°C.

When PS macromonomers are added into the reaction to synthesise the copolymers, the trends are not dissimilar from the homopolymerisation reaction.

The appearance of small peaks between 17.25 and 19.25 ml (M_n between 800 and 1000 g·mol^{-1}) during step 1 (Figure 6.9b-f) can be observed, which increase in intensity up to 4 hours and then gradually disappear in step 2 (Figure 6.10b-f). The peak due to the PS macromonomer at about 16.5 ml, remains almost unchanged during step 1, while an evident change in retention volume and dispersity is shown during step 2. It is easy to assume that during step 1 small PSf oligomers are formed while the PS macromonomer is only slightly affected. To be precice, in each reaction during step 1, and most clearly in PSf-*g*-PS2 (Figure 6.9c), a slight shift of the PS macromonomer peak to lower retention volume is seen, giving, in this case, an increasing M_n value, from 5.1 to 6.3 kg·mol^{-1}, suggesting that perhaps a few repeat units of PSf are added to the macromonomer too, during this step. Evidently, during step 2 (Figure 6.10b-f), PS macromonomers participate in the polycondensation reaction, being incorporated into the growing PSf chain, to give a copolymer with increasing M_n and Đ.

In order to better compare and discuss the chromatograms of Figure 6.9 and 6.10, the relative SEC data calculated by conventional calibration with PS standards for the final copolymer, collected after 9 hours, have been reported in the following graphs, comparing the three copolymers produced with a decreasing (see Table 6.1) BPA to ePS6.2k ratio (PSf-*g*-PS1 to PSf-*g*-PS3 in Figure 6.11) and separately the copolymers with same BPA:ePS6.2k, but increasing concentration of the reaction solution (PSf-*g*-PS2, 4 and 5 in Figure 6.12). Even if the M_n values calculated using a conventional calibration are not as accurate as those absolute values obtained by triple detection with light scattering, this method is a good way to qualitatively compare the different copolymerisation reactions.

In Figure 6.11, the ratio of BPA:ePS6.2k is reported in the legend as $\chi_{ePS6.2k}$, the mole fraction of PS macromonomer with respect to BPA in the reaction feed. For instance, for PSf-*g*-PS1 with a BPA:ePS6.2k ratio of 24:1, $\chi_{ePS6.2k}$= 1/25 = 0.04. The dashed line in Figure 6.11a and b indicates the switch from step 1 to step 2 at 4 hours. After this point, for all the copolymers there is a significant increase in

both M_n and $Đ$, although the trends of increasing molar mass and dispersity vary with different mole fraction of PS macromonomer (increasing from PSf-*g*-PS1 to 3, from 0.04 to 0.08 and 0.11).
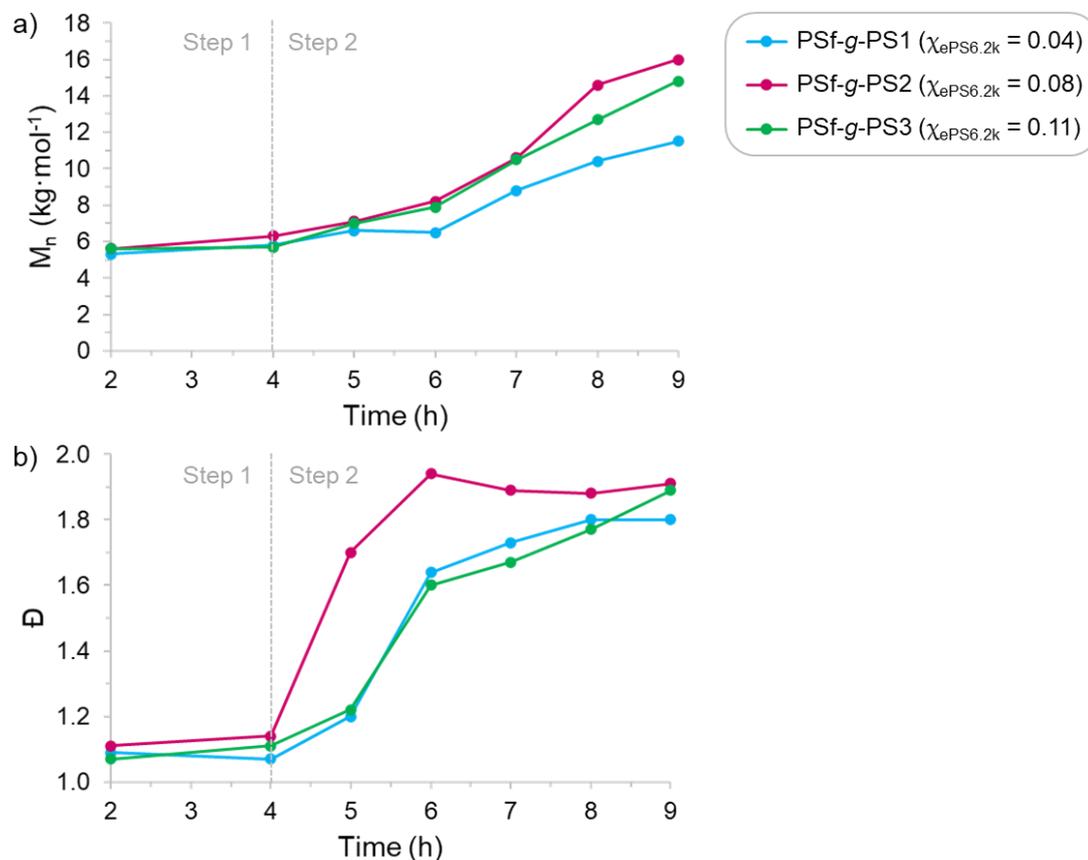
Figure 6.11 a) M_n and b) $Đ$ data for the copolymers obtained with different mole fraction ($\chi_{ePS6.2k}$) of PS macromonomer with respect to BPA in the feed, measured throughout the polycondensation reaction by SEC conventional calibration, using standard PS.

For the sample with the lowest $\chi_{ePS6.2k}$, PSf-*g*-PS1 (blue trace in Figure 6.11), M_n and $Đ$ increase steadily to give a final M_n of 11.5 kg·mol^{-1} and $Đ$ of 1.80. PSf-*g*-PS2 (pink trace in Figure 6.11) shows a significantly faster growth to give final values of M_n and $Đ$ of 16.0 kg·mol^{-1} and 1.91 respectively. This is most certainly due to the higher mole fraction of PS macromonomer in the feed. When one macromonomer molecule is added as a comonomer in the PSf chain in place of one BPA molecule, the MW increases a lot more, and this will account for the difference in M_n between PSf-*g*-PS1 and PSf-*g*-PS2. However, this behaviour seems to be contradicted by the trend seen for PSf-*g*-PS3 (green trace in

Figure 6.11), the sample obtained with the highest molar fraction of PS macromonomer. Even if M_n increases similarly to PSf-*g*-PS2 up to 7 hours of reaction, the final value is lower than PS-g-PSf2 (14.8 kg·mol^{-1} with a Đ of 1.89), but this may be due to the limiting factor of viscosity on progress of the reaction. Varying the BPA:PS ratio whilst keeping all the other variables constant (i.e. the bisphenol:sulfone ratio (1:1), the amount of solvent and base) also significantly affects the concentration in mg·ml^{-1} of starting materials, resulting in a much more viscous reaction solution, as the mass of PS macromonomer increases, giving a concentration that increases from 189 to 242 and finally 296 mg·ml^{-1}. To investigate this effect, independently the variation of BPA:ePS6.2k in the feed, copolymers 2, 4, and 5 were synthesised, for which the BPA:ePSe6.2k ratio was kept constant (12:1) while the volume of solvents was changed, thus varying the concentration and viscosity.
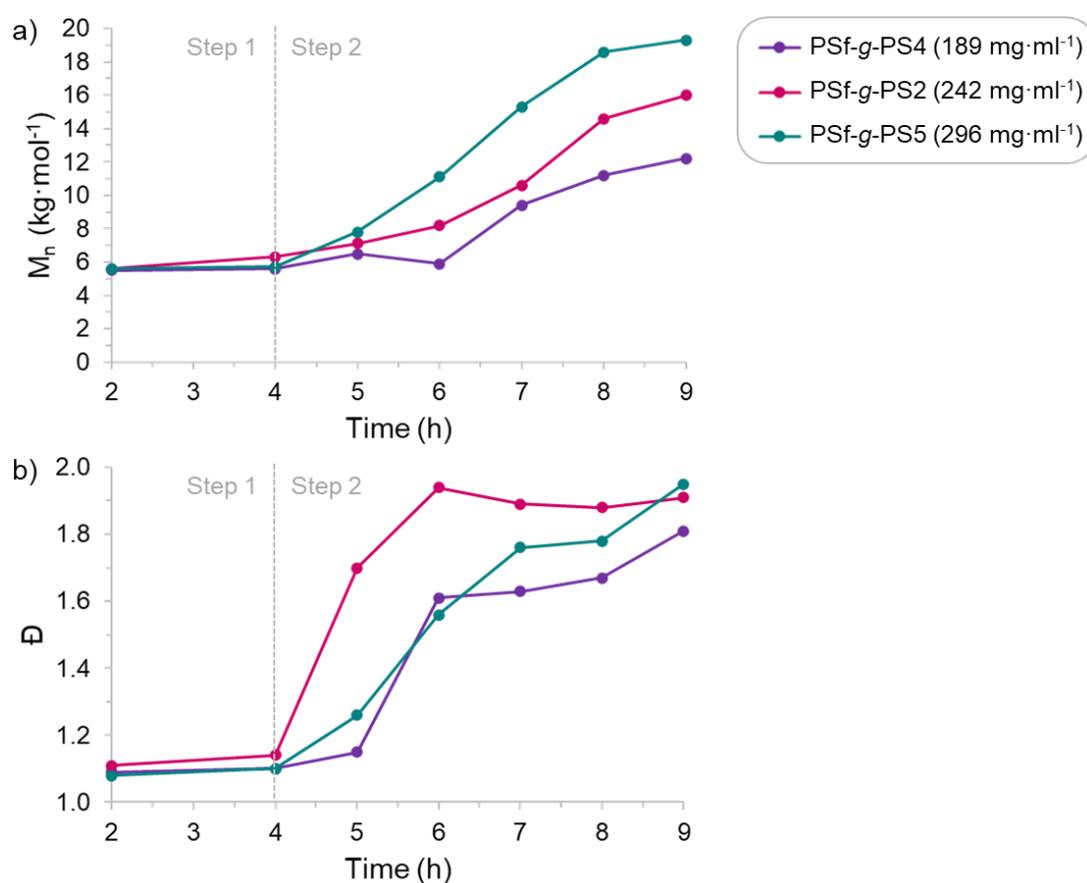
Figure 6.12 a) M_n and b) Đ data for the copolymers with same feed ratio of reagents, but increasing concentration (expressed in mg·ml^{-1}), measured throughout the polycondensation reaction by SEC conventional calibration, using standard PS.

Figure 6.12 shows how M_n and Đ evolved in each of these copolymerisation reactions.

Now that the feed ratio of reagents is constant, any difference in the evolution of M_n will be related to the viscosity of the solution. As seen before in Figure 6.11, also for this series of samples there is a significant increase in both M_n and Đ after 4 hours of reaction (dotted lines), when the switch from step 1 to step 2 happens. However, the trends of the three samples differ and it seems that an increase in concentration (from PSf-*g*-PS4 to 2 and 5) actually results in a higher M_n (and to some extent dispersity) at each hour of step 2, up to the end of the reaction after 9 hours, with final products with increasing M_n (12.2, 16.0 and 19.3 kg·mol^{-1}, as the concentration of reactants increases from 189 to 242 and 296 mg·ml^{-1}). It is almost certain that an increase in solution concentration, instead of inhibiting the reaction due to increasing viscosity, and therefore a decreasing diffusion coefficient, actually accelerated the reaction because of an increase of the molar concentration of reactants (0.4, 0.5, and 0.6M for PSf-*g*-PS4, 2 and 5, respectively), which resulted in higher frequency of collision, thus faster and more effective polycondensation reaction.

One might think that an increase in viscosity should affect the diffusion of reactive species involved in the polycondensation reaction, thus resulting in a slowing down of the frequency of collision and, therefore, of the rate of reaction. Previous studies,[47-48] however, show that the collision rate of functional group must not be confused with the diffusion rate of the polymer as a whole. The mobility of the terminal functional group is much greater and can diffuse readily via a rearrangement in chain conformation of nearby chain segments.[48] Moreover, a large molecule can also act as a 'cage', reducing the ease with which reacting groups diffuse away from each other.[47] In conclusion, therefore, the rate of polycondensation reactions in solution are controlled primarily by the kinetics of the reactions between the functional groups involved, rather than by diffusion. A certain limiting effect of diffusion might be expected at high degree of polymerisation, when the concentration of reactive groups driving the condensation reaction is low. This could explain why after 7 hours of reaction (Figure 6.11a), the polycondensation for the synthesis of PSf-*g*-PS3 (higher

ePS6.2k mole fraction, but also higher viscosity) gave samples with lower M_n than PSf-*g*-PS2, with a lower mole fraction of PS macromonomer in the feed. It could be that, in those conditions of viscosity and at the degree of polymerisation reached after 7 hours, the reaction became diffusion controlled.

The final product of each polycondensation was analysed by triple detection SEC, using as dn/dc a weighted average of the values of PS (0.185 ml·g^{-1}) and PSf (0.2026 ml·g^{-1}), as shown in the following equation:

$$\text{dn/dc}^{\text{PSf-}g\text{-PS}} = 0.185 \text{ ml·g}^{-1} \times \text{w.f.}^{\text{PS}} + 0.2026 \text{ ml·g}^{-1} \times \text{w.f.}^{\text{PSf}}$$

where w.f. is the weight fraction of styrene (PS) or of sulfone (PSf), calculated as:

$$\text{w.f.}^{x} = \frac{\chi_x \cdot \text{MW}^x}{\chi_{\text{PSf}} \cdot \text{MW}^{\text{PSf}} + \chi_{\text{PS}} \text{MW}^{\text{PS}}}$$

Where x can either be PS or PSf, MW$^{\text{PS}}$ is the molecular weight of polystyrene repeat unit (104.15 g·mol^{-1}) and MW$^{\text{PSf}}$ is the molecular weight of the PSf repeat unit (442.54 g·mol^{-1}). χ_x is the mole fraction of styrene or sulfone in the copolymer, calculated by NMR using the integrals of the peaks of PS and PSf in the aromatic region (example for PSf-*g*-PS4 in Figure 6.13).
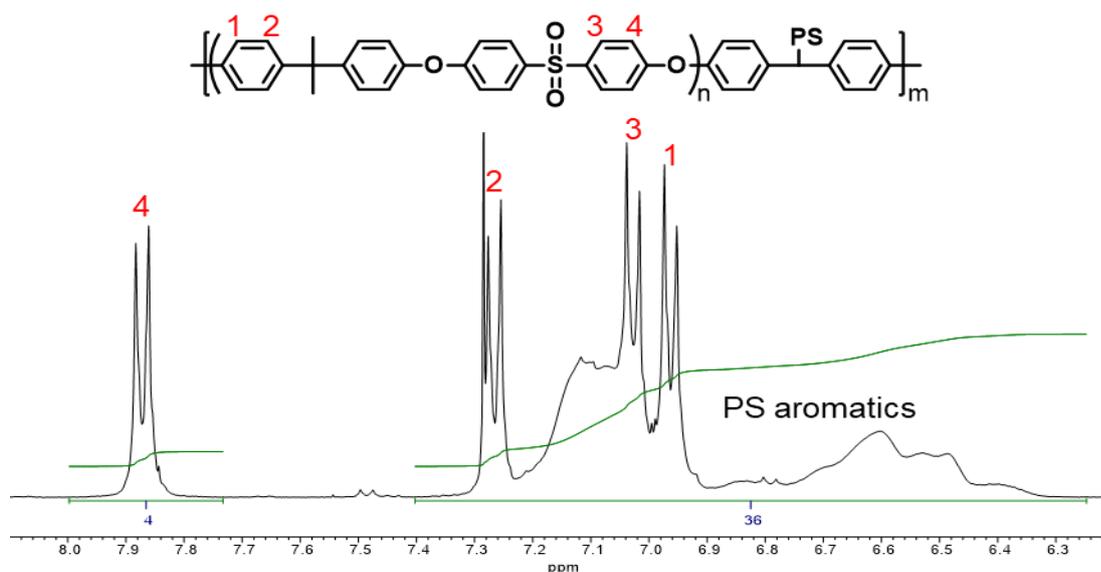
Figure 6.13 Aromatic region of ^{1}H NMR (CDCl$_3$, 400 MHz) spectrum of PSf-*g*-PS4 copolymer.

For each PSf repeat unit in which peak 4 arises due to 4 protons, there are in this case (36-(3x4))/5 aromatic protons of PS, which is equivalent to 4.8 PS repeat units, where the integral value between 7.4 and 6.2 ppm has been corrected by subtracting the integral values due to PSf peaks 1, 2 and 3 (corresponding to 4 protons each). The mole fraction of PS in the collected product can be calculated as χ_{PS} = 4.8/(1+4.8) = 0.83, thus giving a PSf mole fraction of 0.17. The same calculation has been done for the other copolymers, giving the values listed in Table 6.3.

Table 6.3 BPA-ePS6.2k feed composition, expressed as BPA:ePS6.2k ratio and weight fraction of ePS6.2k (w.f.$^{ePS6.2k}$), mole (χ_{PS}) and weight fractions (w.f.^{PS}) of PS in the final copolymer calculated by NMR, SEC data, through triple detection calibration, and number of PS graft macromonomers per copolymer (n) of the final product of the polycondensation reactions.

	BPA:ePS6.2k	w.f.$^{ePS6.2k}$	χ_{St}	w.f.St	MW$_{PSf-PS}$	M$_n$ (g·mol^{-1})	n
PScoPSf1	24:1	0.36	0.72	0.38	16,300	32,100	2.0
PScoPSf2	12:1	0.54	0.83	0.53	11,700	32,800	2.8
PScoPSf3	8:1	0.64	0.88	0.63	9,800	32,200	3.3
PScoPSf4	12:1	0.54	0.83	0.53	11,700	26,600	2.3
PScoPSf5	12:1	0.54	0.83	0.53	11,700	39,100	3.3

This calculation is clearly an approximation, since we are assuming that there are equal numbers of BPCS and BPA units in the copolymer, but we know that this is not true because part of the BPA has been replaced by PS macromonomer, in order to keep the bisphenol:BCPS ratio constant at 1:1. Nevertheless, looking at Table 6.3, it should be noted that the composition of each copolymer, given by the weight fraction of styrene (w.f.^{PS}) is in good agreement with the BPA-ePS6.2k composition in the original feed, expressed as weight fraction of ePS6.2k (w.f.$^{ePS6.2k}$). For example, for PScoPSf1, a BPA:ePS6.2k original feed ratio of 24:1 corresponds to:

$$\text{w.f.}^{ePS6.2k} = 6{,}200 \text{ g·mol}^{-1}/((24 \times 442.52 \text{ g·mol}^{-1}) + 6{,}200 \text{ g·mol}^{-1}) = 0.36$$

where w.f.$^{ePS6.2k}$ is the weight fraction of ePS6.2k macromonomer, effectively the weight fraction of styrene with respect to BPA+BCPS units in the reaction feed. Thus a value of w.f.$^{ePS6.2k}$=0.36 (in the feed) is in excellent agreement with a value of w.f.^{PS}=0.38 (in the copolymer). This suggests that, in good approximation, each PSf repeat unit in the resulting copolymer corresponds to a BPA in the feed at time 0, while the excess BCPS does not contribute significantly to the number of PSf repeat unit in the final copolymer.

In order to estimate the average number of PS grafts per copolymer, it is possible to calculate the average molecular weight of a unit comprising one PS graft and one PSf block (MW$_{PSf-PS}$) from the weight fractions calculated above. In the case of PSf-*g*-PS4, for instance:

$$MW_{PSf-PS} = M_n^{ePS6.2k} / w.f.^{PS} = 6,200 \text{ g·mol}^{-1} / 0.53 = 11,700 \text{ g·mol}^{-1}$$

Now dividing M$_n$ obtained from SEC triple detection by MW$_{PSf-PS}$, we can estimate the average number of PSf-PS units - and thus of PS grafts (n) - per copolymer chain as being, for PSf-*g*-PS4, 26,600 g·mol^{-1} / 11,700 g·mol^{-1} = 2.3. The values calculated for the other copolymers are shown in Table 6.3.

In order to better compare and discuss the data listed in Table 6.3, in particular the M$_n$ of each copolymer (calculated by triple detection SEC) and n have been reported in the following figures. The data for the series of copolymers prepared with a decreasing BPA:ePS6.2k in the feed (PSf-*g*-PS1 to 3) are shown in Figure 6.14, and the series of copolymers prepared with the same BPA:ePS6.2k ratio, but increasing solution concentration (PSf-*g*-PS2, 4 and 5), are shown in Figure 6.15.

Looking firstly at M$_n$ (Figure 6.14a), it seems that the M$_n$ of the final copolymer is hardly affected by the ratio of BPA:ePS6.2k, with values between 32 and 33 kg·mol^{-1}. Figure 6.14b, however, shows that there is an increase in the average number of PS grafts (n) in the resulting copolymer, as the feed ratio of BPA:ePS6.2k decreases from 24:1 to 8:1 ($\chi_{ePS6.2k}$ increases from 0.04 to 0.11).
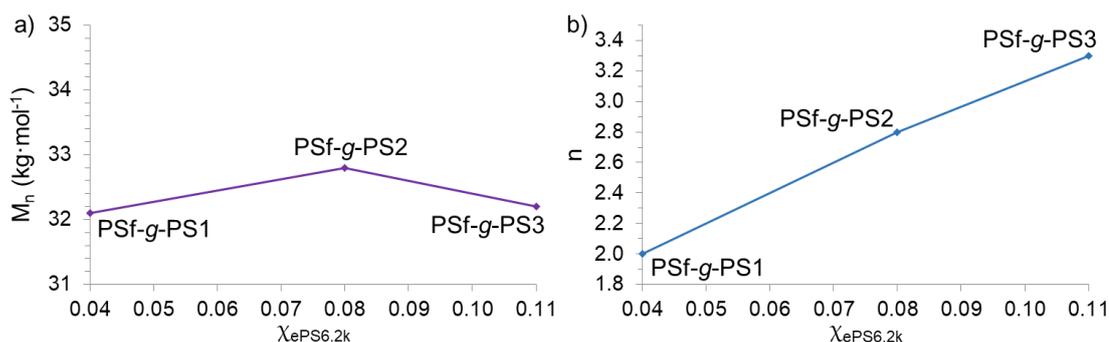
Figure 6.14 Impact of PS content, expressed as $\chi_{ePS6.2k}$, on a) M_n and b) *n*, average number of PS graft per copolymer chain.

These 2 graphs are not in disagreement, even if it is easy to assume that a higher number of PS grafts per chain should cause a significant increase in the molar mass of the resulting copolymer. However, the data above suggests that, as the ratio of BPA:ePS6.2k decreases from 24:1 to 8:1, indicating an increase of the amount of PS macromonomer in the feed with respect to BPA, there is an apparent decrease of the degree of polymerisation of the PSf backbone, which could account for the lack of increase in molar mass of the resulting copolymer, despite an increase in the average number of PS grafts per chain. Thus, the 2 effects, in this case, seem to neutralise each other. Despite the different BPA:ePS6.2k ratio, the overall concentration of reactive functionalities in solution is constant (0.5M), but the reaction solution gets more viscous, going from PSf-*g*-PS1 to PSf-*g*-PS3, as the mass of PS macromonomer increases, resulting probably in a limiting effect of diffusion on the progress of polycondensation. As seen before in Figure 6.11, this limiting effect of diffusion is particularly evident for PSf-*g*-PS3, obtained with the higher viscosity, at high degree of polymerisation. The apparent discrepancy between Figure 6.14a and b, with a similar M_n for the final products but increasing PS graft per copolymer, seems to confirm this balancing effect between the increasing amount of ePS6.2k in the feed and the increasing influence of diffusion.

The data obtained by triple detection for the copolymers prepared with same ratio of BPA:ePS6.2k but different volumes of reaction solution, to test the effect of solution viscosity on the extent of polymerisation, are summarised in Figure 6.15.

As was seen for the samples collected at intermediate reaction times (Figure 6.12), triple detection SEC confirms that the M_n of the final copolymer increases with the concentration of the reaction solution, in spite of an increase in viscosity, as does the number of PS chains incorporated into the backbone. Therefore, it seems that the increase in concentration (and viscosity) does not appear to significantly inhibit the progress of the polycondensation, which actually seems to be more effective, with a higher number of PS macromonomers incorporated into the backbone.
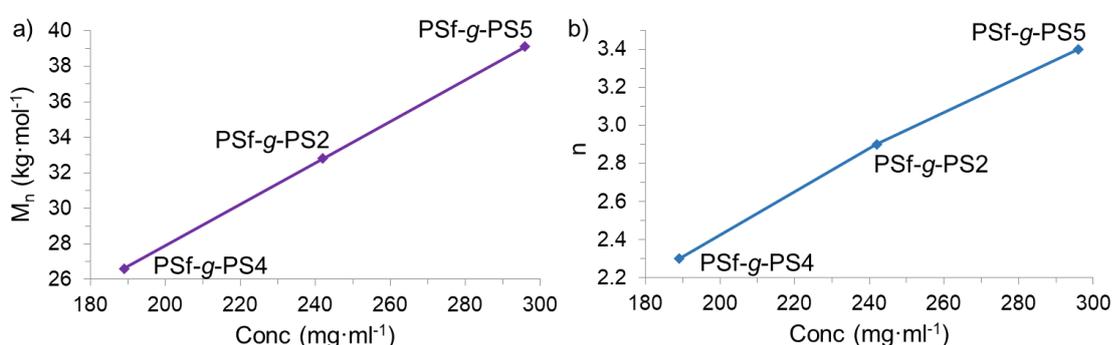
Figure 6.15 Impact of solution viscosity, expressed as conc. of reactants in mg·ml^{-1}, on a) M_n and b) n, average number of PS graft per copolymer chain.

In conclusion, the study of the incorporation of PS macromonomers into a PSf backbone showed that, by varying the BPA:ePS6.2k ratio in the feed (in particular increasing the fraction of PS macromonomer), and keeping all the other variables constant, including the total bisphenol:BCPS ratio at 1:1, it is possible to increase the number of PS grafts incorporated into the chain, but with little change in the total M_n. It would seem that the effect of increasing the amount of macromonomer in the feed is to reduce the molar mass of the PSf backbone, resulting in copolymers with similar final M_n but different average number of grafts per chain. This suggests a reduced extent of polycondensation reaction, that is the polycondensation reaction is less effective at a higher fraction of macromonomers, possibly due to a limiting effect of viscosity/diffusion on the progress of polycondensation at high degrees of polymerisation.

On the other hand, it is possible to enhance the polycondensation reaction, and in this way increase the average number of PS graft incorporated into the

backbone, by keeping the same BPA:ePS6.2k ratio and increasing the solution concentration of the species. Since, in general, the extent of solution polycondensation is controlled by the rate constant of the reaction between the mutual reactive groups and only marginally by diffusion, even if a higher molar concentration also cause a slower diffusion rate of the species - because of an higher viscosity of the solution - the actual result is a higher frequency of collisions, thus faster and more effective polycondensation reaction, yielding polymers with higher M_n and number of PS grafts per chain. Nevertheless, it must be pointed out that, after a certain threshold, viscosity seems to significantly affect the rate of polycondensation, especially at high degree of polymerisation, when the concentration of reactive groups is low, and the reaction appears to become diffusion controlled.

6.3.2 SYNTHESIS OF PSf-*g*-POLYPEGMEM GRAFT COPOLYMERS BY SOLUTION POLYCONDENSATION
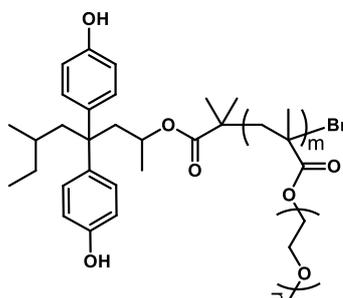
Figure 6.16 Structure of PEGMEM macromonomer synthesised by ATRP using a DPE-OSi derived initiator (BP-Br).

After having investigated the effect of different reaction conditions on the incorporation of a bisphenol-functionalised polystyrene macromonomer in a PSf polycondensation reaction, a different macromonomer prepared from a different monomer (poly(ethylene glycol) methyl ether methacrylate, PEGMEM) was reacted using the same synthetic strategy. This macromonomer was synthesised by ATRP of PEGMEM using a novel DPE-OSi derivative as initiator (see Chapter 3), to give a macromonomer with the desired bisphenol functionality at one chain end, and with grafted side PEG chains along the methacrylate backbone (Figure 6.16).

The procedure used for the synthesis of the graft copolymer was exactly the same as described for the copolymers prepared with a PS macromonomer, with two steps, at 160°C and 190°C, and using the same solvents (NMP and toluene). The total bisphenol:BCPS was kept constant at 1:1, while a ratio of BPA:PolyPEGMEM of 47:1 was chosen because of the high molar mass of the PolyPEGMEM-OH2 macromonomer (M_n 21,200 g·mol⁻¹, Đ 1.12). In this way the NMR signals of PSf would be of comparable intensity with respect to the PolyPEGMEM ones, and the calculations by NMR would be more accurate. The solution concentration was 0.3M or 412 mg·ml⁻¹.

There is, however, a difference in the procedure in the work-up step: the final product was soluble in methanol, therefore the reaction solution was poured into hexane and the product collected as a viscous gel on the bottom of the beaker, after having decanted away the supernatant liquor. PSf is not soluble in methanol and is expected to precipitate if poured into methanol. The fact that the presumed copolymer, containing PolyPEGMEM - a polymer which is soluble in methanol - did not precipitate is a first sign that the copolymerisation was successful.
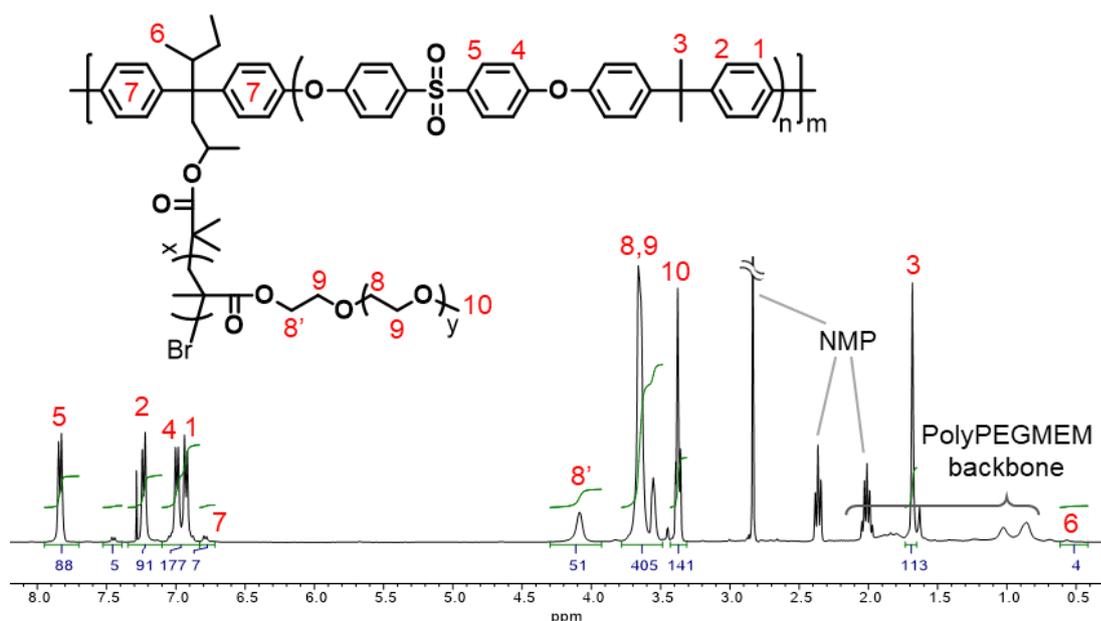
Figure 6.17 ¹H NMR (CDCl₃, 400 MHz) spectra of PSf-*g*-PolyPEGMEM copolymer.

The NMR spectrum of the resulting copolymer (Figure 6.17) shows the expected

proton signals of both PSf and PolyPEGMEM, assigned according to the inset copolymer structure. As seen before, such an NMR spectrum provides an opportunity to calculate the weight fractions of PSf and PolyPEGMEM in the resulting copolymer. The peak at 4.1 ppm (8') accounts for 2 protons in each PEGMEM unit, while the peak at 7.8 ppm (5) is ascribable to 4 protons per PSf repeat unit. The integral values of these peaks were used to calculate the mole and weight fractions of PolyPEGMEM and PSf in the copolymer, as described for PSf-*g*-PS copolymers in Section 6.3.1. The weight fraction of PolyPEGMEM and PSf were also used to calculate the dn/dc of the copolymer, according equations seen in Section 6.2.2.

SEC analysis of the resulting copolymer and the PolyPEGMEM macromonomer in THF (Figure 6.18) shows a solvent peak at ca. 19.7 ml (as seen in previous SEC traces), while the main peak of the copolymer (purple trace) shows a significant increase of Đ (2.59), and a slight shift towards lower retention volume compared to the macromonomer trace (grey), confirming the success of the step-growth polycondensation reaction.

Figure 6.18 SEC chromatograms in THF PolyPEGMEM-OH2 macromonomer (grey trace) and PSf-*g*-PolyPEGMEM graft copolymer (purple trace).

The resulting copolymer has a M_n of 38,300 g·mol^{-1}. It must be pointed out that the broadening of the peak to higher retention volume than the macromonomer peak, also suggests the presence of polymer chains with a lower molar mass that

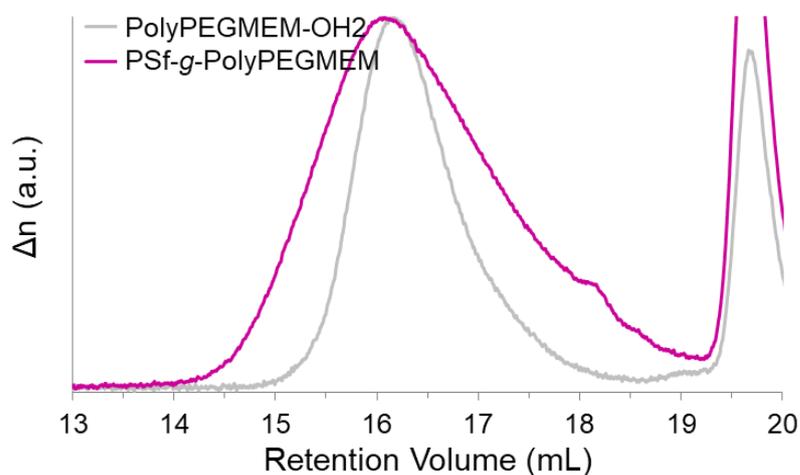the macromonomer, probably PSf homopolymers without incorporation of PolyPEGMEM macromonomers.

It is possible to estimate the average number of PolyPEGMEM grafts per copolymer, by calculating the average molecular weight of a unit comprising one PolyPEGMEM graft and one PSf block ($MW_{PSf-PolyPEGMEM}$) from the weight fractions calculated before:

$$MW_{PSf-PolyPEGMEM} = M_n^{PolyPEGMEM} / w.f.^{PolyPEGMEM} = 21{,}200 \text{ g·mol}^{-1} / 0.43 = 49{,}300 \text{ g·mol}^{-1}$$

Now dividing M_n obtained from SEC triple detection (38,300 g·mol^{-1}) by $MW_{PSf-PolyPEGMEM}$, we can estimate the average number of PSf-PolyPEGMEM units - and thus of PolyPEGMEM grafts - per copolymer chain as being 0.8. The incorporation of PolyPEGMEM grafts in the PSf backbone seems to be less effective than for PS macromonomers, for which copolymers with an average of up to 3 PS grafts were obtained. However, these results must also be considered in the context of the BPA:macromonomer ratio and molar concentration of reactive groups, especially in light of what has been concluded after the study of the analogous copolymerisation with PS macromonomers. The high molar mass of the PolyPEGMEM macromonomer resulted in a decision to use a high ratio of BPA:PEGMEM (47:1) to make the subsequent NMR analysis and related calculations more accurate and reliable. However, this also resulted in a reaction solution with a low molar concentration of reactive groups (0.3M) and quite high mass concentration (calculated from the total mass of reactants, BPA, BCPS and PolyPEGMEM) - 412 mg·ml^{-1}, compared to 296 mg·ml^{-1}, which is the highest value for PSf-*g*-PS copolymers - which will have resulted in a high solution viscosity. If the viscosity, in general, should not affect too much the rate of a polycondensation reaction,[47-48] in this case the high molar mass of the macromonomer leads to a high mass concentration of reactants, and consequently high solution viscosity, but a low molar concentration of reactive functionalities, factors that collectively might have been the reason for a less effective/efficient reaction. This, though, does not exclude the possibility that the use of a smaller macromonomer, a lower BPA: PolyPEGMEM ratio and an overall

higher molar concentration could contribute to make the copolymerisation more effective and to incorporate more PolyPEGMEM grafts into the PSf backbone.

6.4 CONCLUSIONS

Controlled chain growth polymerisation mechanisms (anionic and ATRP) were exploited to synthesise bisphenol functionalised macromonomers, which were then added into a polycondensation reaction as a comonomer, in order to obtain grafted copolymers with a polysulfone backbone via a 'grafting through' approach.

The copolymerisation with PS macromonomer was extensively investigated, varying the amount of PS and the mass concentration of the reaction solution, and following the reaction over time by SEC chromatograms. All the reactions performed showed a qualitatively similar behaviour in the 2 steps of the procedure, also in comparison with a polysulfone homopolymerisation reaction. Namely, in the first step at 160ºC, almost no polymerisation is observed in line with the expectation that this first step sees only the deprotonation of the bisphenol species. The peak in the SEC due to the PS macromonomer remains almost unchanged, however the appearance of small peaks at longer retention volume (lower molar mass) can be ascribed to PSf oligomers. In the second step, performed at 190ºC, the polycondensation takes place and the macromonomer is gradually incorporated into the PSf backbone, as evidenced by a steady shift to higher MW and an increase of Đ of the peak in the chromatogram over time, occurring at the same time as the disappearance of the small oligomer peaks at higher retention volumes.

It was found that, increasing the mole fraction of ePS6.2k macromonomer by decreasing the ratio of BPA:ePS6.2k in the feed, but keeping all the other variables constant, resulted in a decrease in the degree of polymerisation of the PSf backbone, but with an increasing number of PS grafts incorporated per copolymers, resulting in copolymers with a similar final M_n but different number of grafted arms. It is suggested that this is probably because of the effect of a higher

viscosity and lower diffusion rate on the progress of polycondensation at high degree of polymerisation.

A study of the effect of increasing mass concentration on the copolymerisation actually demonstrated that the resulting higher viscosity of the reaction solution has little apparent effect on the polycondensation reaction, and it is rather the related higher molar concentration that increases the frequency of collisions, giving a more effective polycondensation reaction and yielding copolymers with higher M_n and number of PS grafts per chain. Therefore, by keeping the same BPA:ePS6.2k ratio and changing the molar concentration of the functional groups by varying the volume of solvents used, it is possible to enhance the effectiveness of the polycondensation reaction, and therefore increase the number of PS incorporated into the backbone. The maximum average number of PS macromonomers incorporated in a single copolymer (n) has been reached either by increasing the fraction of PS macromonomer with respect to BPA ($\chi_{ePS6.2k}$) in the feed (PSf-*g*-PS1, $\chi_{ePS6.2k}$=0.04, n=2.0; PSf-*g*-PS2, $\chi_{ePS6.2k}$=0.08, n=2.8; PSf-*g*-PS3, $\chi_{ePS6.2k}$=0.11, n=3.3), or the molar concentration, with a lower amount of PS (PSf-*g*-PS4, 0.4M, n=2.3; PSf-*g*-PS2, 0.5M, n=2.8; PSf-*g*-PS5, 0.6M, n=3.3).

Another bisphenol functionalised macromonomer, PolyPEGMEM, with completely different characteristics, was tested in the same co-polycondensation reaction with PSf, giving a copolymer with an average ca. 0.8 macromonomers incorporated in the backbone. Even if the incorporation of PolyPEGMEM seems to be less effective than PS, it must be considered that the amount of PolyPEGMEM used, in comparison with BPA, and the overall molar concentration were much lower than used in the copolymerisation reaction with PS macromonomers. This seems to confirm that the molar concentration could account for the less effective polycondensation and that the use of a smaller PolyPEGMEM macromonomer, a lower BPA: PolyPEGMEM ratio and an overall higher molar concentration could contribute to make the copolymerisation more effective and to incorporate more macromonomers into the PSf backbone.

REFERENCES

1. Olabisi, O., *Handbook of thermoplastics*. Marcel Dekker, New York, **1997**.
2. Dizman, C.; Tasdelen, M.A.*, et al.*, *Polymer International*, **2013**, *62* (7), 991-1007.
3. Zhao, C.; Xue, J.*, et al.*, *Progress in Materials Science*, **2013**, *58* (1), 76-150.
4. Aryanti, P.; Sianipar, M.*, et al.*, *Membrane Water Treatment*, **2017**, *8* (5), 463-481.
5. Wenten, I.G.; Aryanti, P.T.P.*, et al.*, *Journal of Membrane Science and Research*, **2016**, *2* (2), 78-89.
6. Xiang, T.; Lu, T.*, et al.*, *Acta biomaterialia*, **2016**, *40*, 162-171.
7. Teotia, R.S.; Kalita, D.*, et al.*, *ACS Biomaterials Science & Engineering*, **2015**, *1* (6), 372-381.
8. Liu, L.; Tong, C.*, et al.*, *Journal of membrane science*, **2015**, *487*, 99-108.
9. Albu, R.M.; Avram, E.*, et al.*, *Polymer Composites*, **2011**, *32* (10), 1661-1670.
10. Ozden, A.; Ercelik, M.*, et al.*, *Electrochimica Acta*, **2017**, *256*, 196-210.
11. Oyanguren, P.; Galante, M.*, et al.*, *Polymer*, **1999**, *40* (19), 5249-5255.
12. Yoo, J.E.; Kim, J.H.*, et al.*, *Journal of Membrane Science*, **2003**, *216* (1), 95-106.
13. Richard Bowen, W.; Doneva, T.A.*, et al.*, *Journal of Membrane Science*, **2001**, *181* (2), 253-263.
14. Yi, Z.; Zhu, L.-P.*, et al.*, *Journal of Membrane Science*, **2012**, *390-391*, 48-57.
15. Park, J.Y.; Acar, M.H.*, et al.*, *Biomaterials*, **2006**, *27* (6), 856-865.
16. Sivakumar, M.; Mohan, D.R.*, et al.*, *Journal of Membrane Science*, **2006**, *268* (2), 208-219.
17. Hasiotis, C.; Qingfeng, L.*, et al.*, *Journal of the electrochemical society*, **2001**, *148* (5), A513-A519.
18. Fu, Y.; Manthiram, A.*, et al.*, *Electrochemistry Communications*, **2006**, *8* (8), 1386-1390.
19. Choi, J.; Lee, K.M.*, et al.*, *Journal of The Electrochemical Society*, **2010**, *157* (6), B914-B919.
20. Sankir, M.; Bhanu, V.*, et al.*, *Journal of applied polymer science*, **2006**, *100* (6), 4595-4602.
21. Arnett, N.Y.; Harrison, W.L.*, et al.*, *Journal of Power Sources*, **2007**, *172* (1), 20-29.
22. Roy, A.; Hickner, M.A.*, et al.*, *Journal of Polymer Science Part A: Polymer Chemistry*, **2009**, *47* (2), 384-391.
23. Harrison, W.; Hickner, M.*, et al.*, *Fuel cells*, **2005**, *5* (2), 201-212.
24. Kim, Y.S.; Sumner, M.J.*, et al.*, *Journal of the Electrochemical Society*, **2004**, *151* (12), A2150-A2156.
25. Weiber, E.A.; Jannasch, P., *Journal of Membrane Science*, **2016**, *520*, 425-433.
26. Weiber, E.A.; Jannasch, P., *Journal of Membrane Science*, **2015**, *481*, 164-171.
27. Chen, W.; Hu, M.*, et al.*, *Journal of Materials Chemistry A*, **2017**, *5* (29), 15038-15047.
28. Ritter, H.; Rodewald, B., *Journal of Macromolecular Science, Part A*, **1996**, *33* (sup2), 103-115.
29. Aitkin, C.L.; Paul, D.R., *Journal of Polymer Science Part B: Polymer Physics*, **1993**, *31* (8), 1061-1065.
30. Camacho-Zuñiga, C.; Ruiz-Treviño, F.A.*, et al.*, *Journal of Membrane Science*, **2009**, *340* (1), 221-226.
31. Chen, D.; Wang, S.*, et al.*, *Energy Conversion and Management*, **2010**, *51* (12), 2816-2824.
32. Thankamony, R.L.; Hwang, J.-M.*, et al.*, *Journal of Membrane Science*, **2012**, *392-393*, 58-65.
33. Gong, F.; Mao, H.*, et al.*, *Polymer*, **2011**, *52* (8), 1738-1747.
34. Liu, B.; Robertson, G.P.*, et al.*, *Polymer*, **2010**, *51* (2), 403-413.

35. Williamson, J.B.; Lewis, S.E*., et al.*, *Angewandte Chemie International Edition*, **2019,** *58* (26), 8654-8668.
36. Yang, Y.; Shi, Z*., et al.*, *Macromolecules*, **2004,** *37* (5), 1678-1681.
37. Noshay, A.; Matzner, M*., et al.*, *Journal of Polymer Science Part A-1: Polymer Chemistry*, **1971,** *9* (11), 3147-3159.
38. Hancock, L.F.; Fagan, S.M*., et al.*, *Biomaterials*, **2000,** *21* (7), 725-733.
39. Hedrick, J.L.; Brown, H*., et al.*, *Macromolecules*, **1989,** *22* (5), 2048-2053.
40. Gaynor, S.G.; Matyjaszewski, K., *Macromolecules*, **1997,** *30* (14), 4241-4243.
41. Wang, J.; Xu, Y*., et al.*, *Polymer*, **2008,** *49* (15), 3256-3264.
42. Xie, Y.; Moreno, N*., et al.*, *Polymer Chemistry*, **2016,** *7* (18), 3076-3089.
43. Aktas Eken, G.; Acar, M.H., *Macromolecular Chemistry and Physics*, **2018,** *219* (20), 1800227.
44. Yi, Z.; Zhu, L.-P*., et al.*, *Journal of Membrane Science*, **2010,** *365* (1), 25-33.
45. Park, J.Y.; Acar, M.H*., et al.*, *Biomaterials*, **2006,** *27* (6), 856-865.
46. Matyjaszewski, K.; Beers, K.L*., et al.*, *Journal of Polymer Science Part A: Polymer Chemistry*, **1998,** *36* (5), 823-830.
47. Saunders, J.H.; Dobinson, F., *Chapter 7 The Kinetics of Polycondensation Reactions*, in *Comprehensive Chemical Kinetics*, Elsevier, **1976**; Vol. 15, pp 473-581.
48. Flory, P.J., *Principles of polymer chemistry*. Cornell University Press, **1953**.

CHAPTER 7

CONCLUDING REMARKS

7.1 CONCLUSIONS

The main aim of this PhD project was the synthesis of complex polymer architectures, namely grafted block copolymers, in which the graft backbone is an aromatic polyester, and to investigate the effectiveness of the copolymer as a compatibilizing additive in a blend of polymers, in order to obtain a better/controlled dispersion of the minor component. The long-term potential application is as an additive in the production of porous polyester (especially PET) membranes or films, with improved transport and/or barrier properties. One way to produce such porous films involves the biaxial stretching of thin films comprising blends of PET as major component and another incompatible polymer, such as polystyrene, polypropylene or polyethylene. Control of the domains size of the minor component, through the use of an effective blend compatinilizer, can also allow control of the porosity of the stretched film. In this perspective, given the variety of possible applications of PET-PS blends, the synthesis of polyester graft polystyrene block copolymers was pursued.

The general synthetic strategy firstly required the synthesis, by a chain-growth polymerisation mechanism, of macromonomers which are strictly functionalised at only one chain end, with a functional group which enables the macromonomer to be incorporated into a step-growth polymerisation reaction as a comonomer.

The first part of the work was dedicated to the design, synthesis and characterisation of macromonomers with a single functional group - a bisphenol functionality - selectively at one chain end.

For the synthesis of polystyrene macromonomers, the use of the functionalised monomer DPE-OSi in living anionic polymerisation (LAP) was investigated, comparing two approaches: the end-capping and the initiating procedures. Combining characterisation by NMR, SEC, MALDI ToF and NP-IIC allowed us to better understand the outcome in terms of number of functional DPE-OSi units per chain. MALDI and NP-IIC data proved particularly useful in showing that the initiating procedure gave only ~50% of the desired mono-functionalised product, along with both un-functionalised and di-functionalised polymer. The end-capping procedure, on the other hand, resulted >90% functionalisation and the absence of di-functionalised species, but required a much longer time of reaction (5 days instead of typically a few hours for the initiating procedure).

In order to overcome the intrinsic limitations of each approach with DPE-OSi, the introduction of the same bisphenol functionality to the chain end of polymers was attempted by the development of a functional initiator based on bisphenol F (BPF). In theory, the use of a functionalised initiator ensures 100% functionalisation, since each initiated chain will carry the functional group of the initiator. Moreover, this approach should exclude the possibility to add more than one functionalised unit per chain. However, despite the encouraging early results and potential for the use of the BPF initiator, this approach showed some issues during the synthesis of the initiator and the polymerisation step.

After all these considerations, we concluded that the end-capping approach using DPE-OSi is the most effective and reliable method to obtain the desired control over the functionalisation of the chains, despite the long reaction time. Therefore, the end-capping approach was used for the scaled-up synthesis of PS macromonomers with different chain length (2.9, 6.4 and 9.1 kg·mol^{-1}), to be subsequently added in step-growth polycondensation reactions.

A different monomer was chosen, poly(ethylene glycol) methyl ether methacrylate (PEGMEM), carrying a PEG side chain, with a view to synthesising macromonomers with hydrophilic properties. In this case, PolyPEGMEM macromonomers was synthesised via a controlled radical mechanism, ATRP, because of the challenges encountered with the anionic polymerisation of

PEGMEM. The PEGMEM monomer is, indeed, very difficult to purify, because of his high boiling point and hygroscopic nature.

After a few unsuccessful attempts to use DPE-OSi as monomer in an ATRP mechanism, to end-cap or initiate the chains, a synthetic strategy was designed to obtain a novel ATRP initiator derived from DPE-OSi, thus carrying the desired bisphenol functionality. The new initiator (BP-Br) proved effective for the polymerisation of PEGMEM by an ATRP mechanism, but also PEGMEM and MMA in a 1:1 mole ratio statistical copolymerisation. However, in most of these polymerisation reactions, a large discrepancy was found between the number average molar mass obtained by NMR and SEC, the latter being approximately double the former. Even taking into account analytical errors that can be significant, the hypothesis that a high degree of termination by both combination and disproportionation has been suggested to account for higher than expected molar mass. Although it has been demonstrated in previous works that the termination of radical polymerisation of methacrylates usually favours disproportionation rather than combination, it has also been found that a higher reaction temperature can increase the combination reaction.

Although the use of the same novel initiator, BP-Br, did also allow the successful polymerisation of styrene by an ATRP mechanism, considerably less control was observed than seen with the polymerisation of PEGMEM and PEGMEM/MMA. The obtained sample was analysed by NP-IIC and compared with a standard (un-functionalised) PS with a similar M_n. The absence of any peak eluting at the same retention volume of standard PS confirmed the presence of bisphenol functional group and, therefore, the effectiveness of BP-Br as initiator. However, the high M_n calculated by SEC, in relation to the one calculated by NMR, and the presence of two peaks in the NP-IIC trace of PS, clearly indicated the presence of species of unknown composition. A possibility could be PS with more than one bisphenol functionality per chain, maybe caused by the coupling of two propagating chains (termination by combination), each one carrying the functionalised bisphenol moiety, but the possibility of a different kind of functionalisation, derived from impurities during the polymerisation, cannot be ruled out.

Although the synthesis of macromonomers by ATRP using the novel functionalised initiator BP-Br was not fully optimised, the resulting PolyPEGMEM macromonomers with the required bisphenol functionalisation were used in a step-growth polycondensation reaction to obtain grafted copolymers.

In the second step of the project, the bisphenol functionalised macromonomers, obtained by controlled chain-growth polymerisation, were added into a step-growth reaction as comonomers, in order to obtain a grafted block copolymer.

PS macromonomers (prepared by LAP) were successfully incorporated as a comonomer into the polycondensation reaction between IPCl and EG to yield a poly(ethylene isophthalate) (PEI) backbone, even if it seemed that, on an average, copolymers with only 1 graft PS and a few repeat units of PEI were obtained, using either 2.9 or 6.4 kg·mol⁻¹ PS macromonomers.

In order to improve the final outcome, a different approach was investigated in which PEI blocks were synthesised by solution polycondensation first, and then coupled with the macromonomer. The first attempt to couple bisphenol functionalised PS with acid chloride end-capped PEI turned out to be unfeasible, because during the work-up the acid chloride chain ends of PEI underwent esterification or hydrolysis, thus becoming unreactive. The coupling of EG end-capped PEI with IPCl functionalised PS, on the other hand, proved to be very effective, yielding copolymers with up to 3 PS grafts on the PEI backbone, using PS macromonomers of 2.9, 6.4 and 9.1 kg·mol⁻¹. The samples were analysed by NMR, SEC, DOSY-NMR and DSC, all techniques that collectively contributed to prove the successful copolymerisation but also to identify the presence of different PEI species, apart from the copolymer.

The same coupling procedure was exploited also with PolyPEGMEM macromonomer. Even if SEC analysis did not show a dramatic shift in the retention volume of the copolymer peak after the coupling, as previously seen with PEI-*g*-PS copolymers, the fact that the copolymer trace was significantly different from a simple mixture of the 2 components, clearly proved that

successful coupling occurred to some extent. Moreover, DOSY-NMR also confirmed that the two blocks were part of the same copolymer macromolecule.

The final step in the project was to test the obtained PEI-*g*-PS copolymers as compatibilizers for blends of PET and PS, using graft copolymers that differ in PS chain length (2.9, 6.4 and 9.1 kg·mol^{-1}) and number of PS graft arms (1 for the copolymers obtained by solution polycondensation; mixture of species with up to 3 PS grafted chains, with the chain coupling approach). The blends were prepared by melt blending in a twin screw extruder, PET/PS in weight ratio 75/25 plus each copolymer in increasing amount, from 0.5 wt% to 2.5 and 5 wt.% of the total mass. The whole melt procedure was performed under argon, to avoid degradation of the polymers used.

The effect of the added copolymers was determined by measuring the mean diameter of the resulting PS domains from measuring at least 200 PS domains per sample in SEM images. A comparison with the mean diameter obtained for un-compatibilized PET/PS blend showed that the addition of 0.5 wt.% of graft block copolymer resulted in a ~65% reduction in the diameter of PS domains for each copolymer, with little differences among them. When more compatibilizer was added, a consistent trend of further reducing the domain size was observed, even if with not a statistically significant difference.

The compatibilizing effect was compared also with existing commercial blend compatibilizers, under the same conditions and using the lower amount of additive (0.5 wt.%). Both GMA and the dual compatibilizer SMA/PMPI did improve the dispersion of PS into the PET matrix, however only a 45% reduction of the mean PS domains diameter was detected, allowing us to conclude that, using the PEI-*g*-PS copolymers synthesised in this work, less compatibilizer material would be required to obtain the same degree of compatibilization.

The proposed macromonomer approach to obtain graft block copolymer with a step-growth backbone is inherently versatile, i.e. the well-controlled bisphenol functionalised macromonomers could, in theory, be incorporated into any polycondensation reaction comprising a bisphenol species as comonomers. In order to demonstrate this versatility, another commercially relevant step-growth

polymer system was tested. The same macromonomers used for the synthesis of a graft copolymer with PEI backbone, namely ePS and PolyPEGMEM-OH, were added into a polycondensation reaction as comonomer, in order to obtain grafted copolymers with a polysulfone backbone via a 'grafting through' approach.

The copolymerisation with PS macromonomers was extensively investigated, varying the amount of PS and the mass concentration of the reaction solution, and following the reaction over time by SEC chromatograms. All the reactions for the synthesis of graft copolymers were successful and showed qualitatively similar behaviour, confirming the mechanism found in literature for the two steps. Namely, in the first step at 160ºC, almost no polymerisation was observed, with the macromonomer peak remaining almost unchanged, since only the deprotonation of the bisphenol species happens. In the second step, performed at 190ºC, the polycondensation takes place and the macromonomer was gradually incorporated into the PSf backbone, as evidenced by a steady shift to lower retention volume and an increase of Đ of the peak in the chromatograms over time.

A first set of samples were synthesised with an increasing mole fraction of PS macromonomer, but keeping all the other variables constant. The effect was a decrease in the degree of polymerisation of the PSf backbone, but with an increase of number of PS grafts per copolymer, i.e. the three samples had similar final M_n but different number of grafted arms. It was proposed that after a certain threshold of solution viscosity and degree of polymerisation – when the concentration of monomers is low – the reaction becomes diffusion-controlled.

A second set of samples were synthesised to study the effect of increasing mass concentration, and therefore the viscosity of the reaction solution, while keeping the same mole composition of the reactants. It was found that apparently a higher solution concentration in $mg \cdot mol^{-1}$, and therefore in viscosity, has little effect on the progress of the polycondensation reaction, however it was concluded that the related higher molar concentration of reactive functionalities resulted in a more effective polycondensation reaction, yielding copolymers with higher M_n and number of PS grafts per chain.

By varying the reaction conditions, as for mole fraction of PS macromonomer and concentration of the reaction solution, copolymers with up to 3.3 PS graft arms were obtained.

The incorporation of PolyPEGMEM macromonomers into a PSf backbone gave a copolymer with an average of 0.8 graft per copolymer, proving that another macromonomer, with the same bisphenol functionalisation, but completely different characteristics, can take part in the polysulfone polycondensation reaction as comonomer. However, the outcome was less satisfying with regards to copolymerisation with PS macromonomers, but it must be considered that the mole ratio of PolyPEGMEM used and the overall molar concentration were much lower than used in the copolymerisation reaction with PS macromonomers, and therefore better results might be obtained by optimising the reaction conditions, in terms of macromonomer amount and solution concentration.

In conclusion, the macromonomer approach developed in this PhD work represents a versatile strategy to obtain grafted block copolymers with a step-growth backbone and different grafted blocks. Two macromonomers with different characteristics were successfully incorporated into PEI and PSf backbones, but of course the reaction conditions needed to be slightly adjusted, to take into account the macromonomers characteristics. In the case of PolyPEGMEM, for example, a further purification step had to be added, because of the high hygroscopicity of the PEG chains.

One kind of the copolymers synthesised, namely PEI-*g*-PS copolymers, were also tested as compatibilizers for blends of PET and PS, proving to be significantly effective, outperforming commercially available compatibilizers.

7.2 FUTURE WORK

The current work presented a few issues that could not be completely addressed and that could benefit from a few more experiments. At the same, a few hints for further research could be found.

The use of a functionalised initiator derived from bisphenol F for anionic polymerisation was attempted as a really promising strategy to obtain 100% functionalisation in a straightforward way, but gave polymers with unknown functional groups, besides the desired ones. It is believed that the main problem is in the presence of other initiating species, as result of the synthesis (metallic potassium and potassium naphthalenide), but also in some possible degradation mechanism of the initiator itself. To address the first issue, different stoichiometric ratio of reagents could be tried, in order to minimise the residual reactive species. To identify possible degradation paths, suitable analytical techniques should be identified to observe the evolution of the anionic initiator. Recently in our group, anionic polymerisations have been performed in NMR tubes and followed real-time by periodic NMR measurements, meaning that it is possible to observe and chararacterise a living anion in solution. Maybe the same can be used to take periodic NMR spectra of a solution of BPFK initiator, to verify any changes over time and identify possible degradation products.

An interesting further development, in terms of obtaining new hybrid materials with many potential applications, would be the incorporation of functionalised macromonomers into different step-growth systems. Polycarbonate, for example, is a kind of thermoplastic polymer which is widely used for numerous applications and which is synthesised using a bisphenol, BPA, as component. The incorporation of PS, though, might be tricky, since the most common synthesitic approach for polycarbonate is an interfacial polycondensation, including a bisphenol deprotonation step in water by a strong base. Clearly this is not suitable for PS, but it could be interesting in the case of the hydrophilic PolyPEGMEM macromonomer.

PolyPEGMEM itself is a very interesting polymer, due to the presence of PEG side chains, which is known to coordinate lithium and has been investigated for the development of solid polymer electrolytes. In this sense, the macromonomer approach developed in this project could be exploited to create an hybrid material that combines the conductivity of PEG with another polymer that gives mechanical stability. PEGMEM with different PEG length are available, therefore

the effect of different PEG chain lengths might be investigated, together with the effect of a different PEG side chain density, if random copolymerisation with MMA, for example, is performed.

DOSY-NMR is a powerful technique which was used to analyse the copolymers synthesised in this project. This technique was very useful in helping to prove the successful outcome of the copolymer synthesis, but it also raised many questions, with some results difficult to explain and never reported before in literature. A more detailed investigation - for example, the comparison of the data already recorded with DOSY spectra of homopolymers (PEI, PS, PolyPEGMEM), alone or in solution in the same tube - could help to clearly separate the copolymers signals from the unreacted homopolymers, and give interesting outcomes that can help in a better understanding of the use of this NMR experiment for the analysis of copolymers. Moreover, different branched (co)polymer architectures, such as mikto-arm stars or H-shaped copolymers, previously synthesised and characterised in our group, could be used as model samples to verify the possibility that different segments of the same (co)polymer structure, for instance the chain ends and the blocks in between two arms, might have different diffusion coefficients, due to a different degree of spacial freedom.

Finally, the interesting results obtained with PEI-*g*-PS used as compatibilizers can be integrated with a complete test of the properties (calorimetric measurements, rheology, mechanical testing) of the compatibilized blends, to verify the effect of the compatibilization on the macroscopic properties of the material.

APPENDIX A

NMR AND MS CHARACTERISATION OF A NOVEL BISPHENOL FUNCTIONALISED ATRP INITIATOR (BP-BR)

1. NMR CHARACTERISATION OF BP-OH
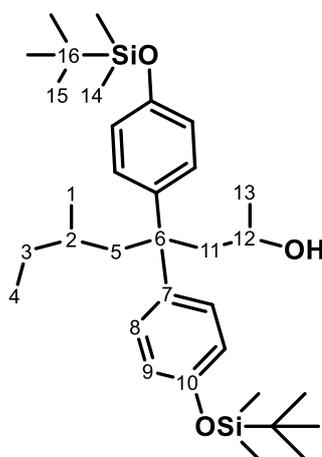
Figure A.1 Molecular structure of BP-OH.
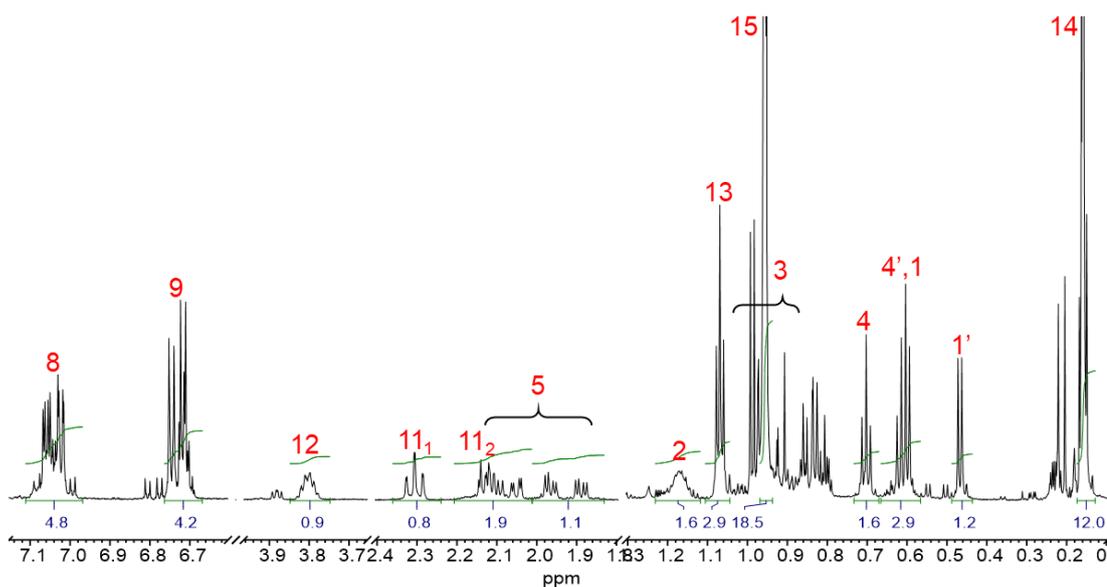
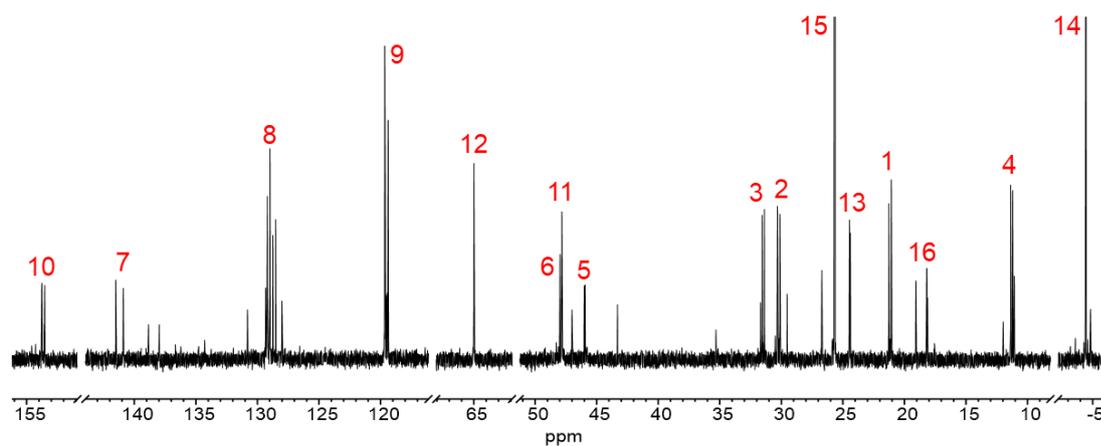**Figure A.2** ^{1}H NMR (CDCl$_3$, 700 MHz) spectra of BP-OH.

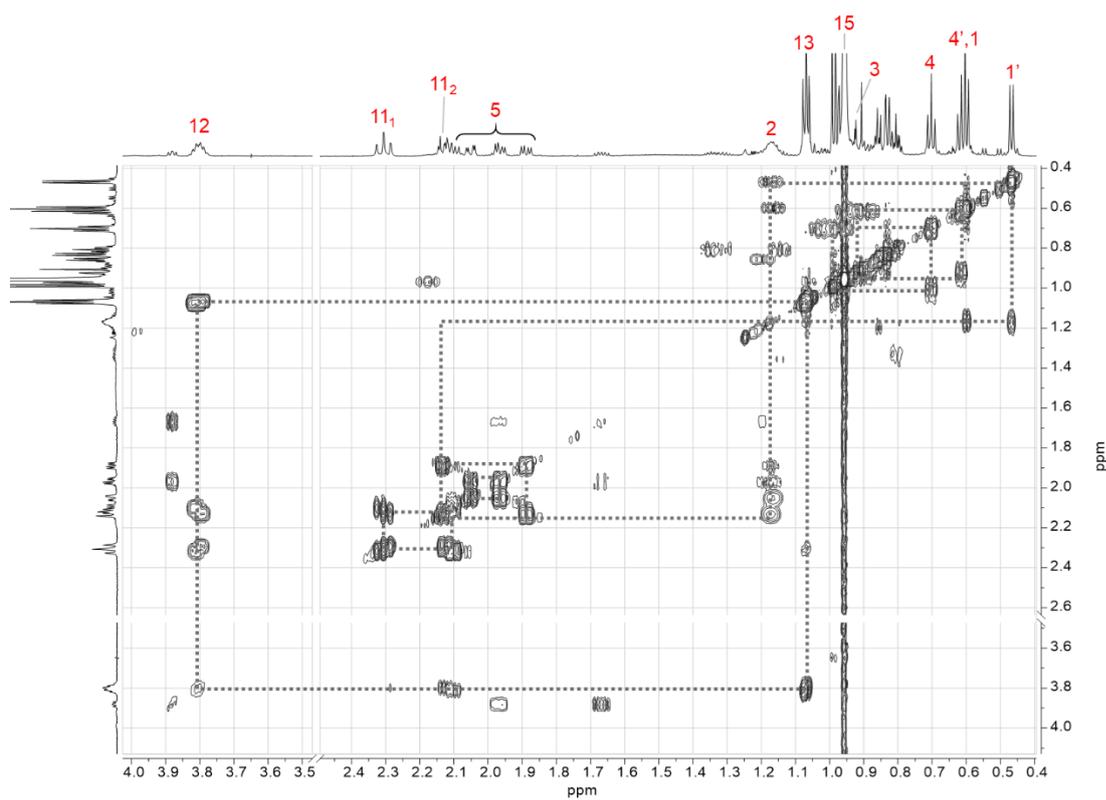**Figure A.3** ^{13}C NMR (CDCl$_3$, 175 MHz) spectrum of BP-OH.

Figure A.4 Section of ^{1}H-^{1}H COSY NMR spectrum of BP-OH.

Figure A.5 a) and b) sections of HSQC-NMR spectrum of BP-OH.
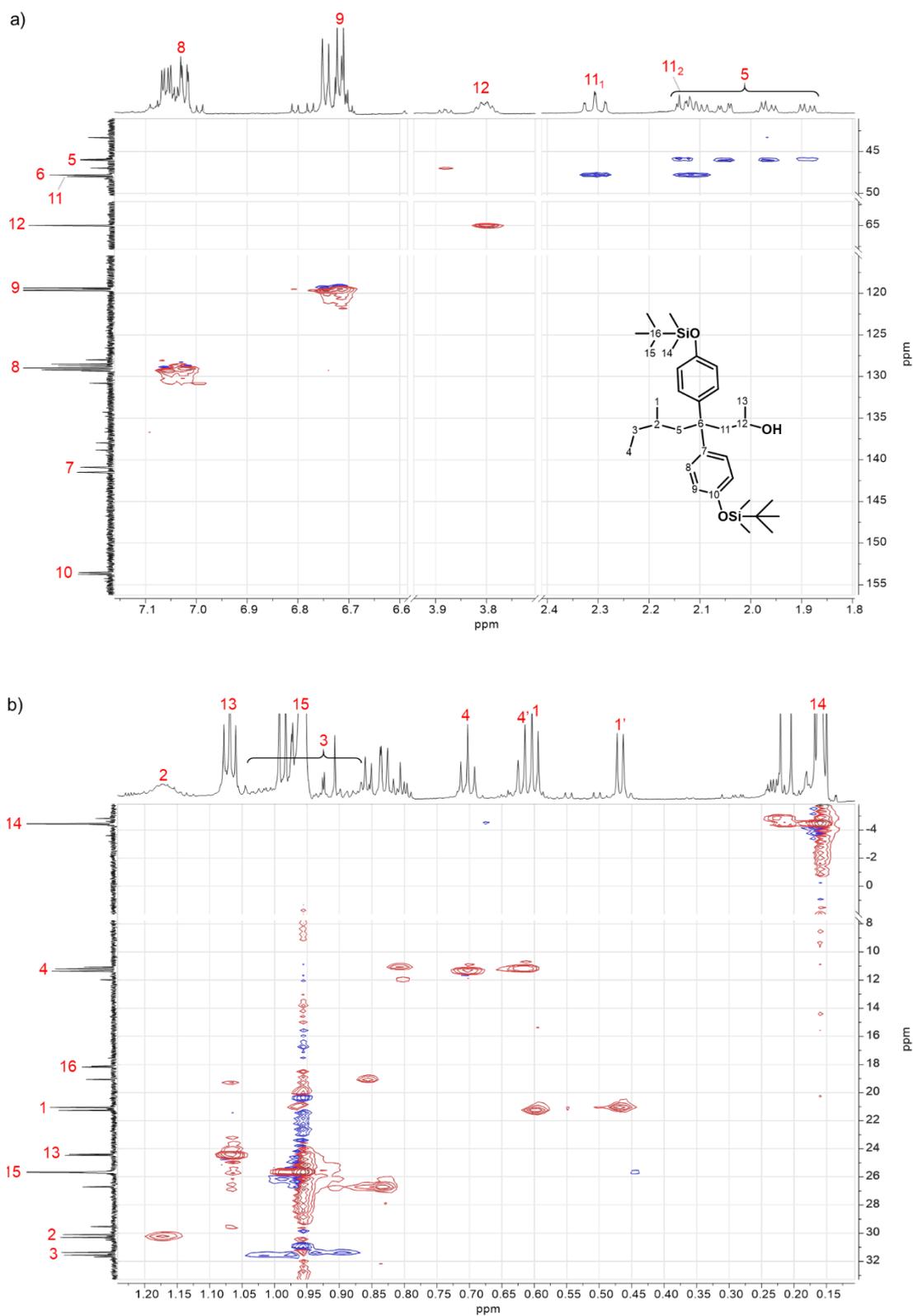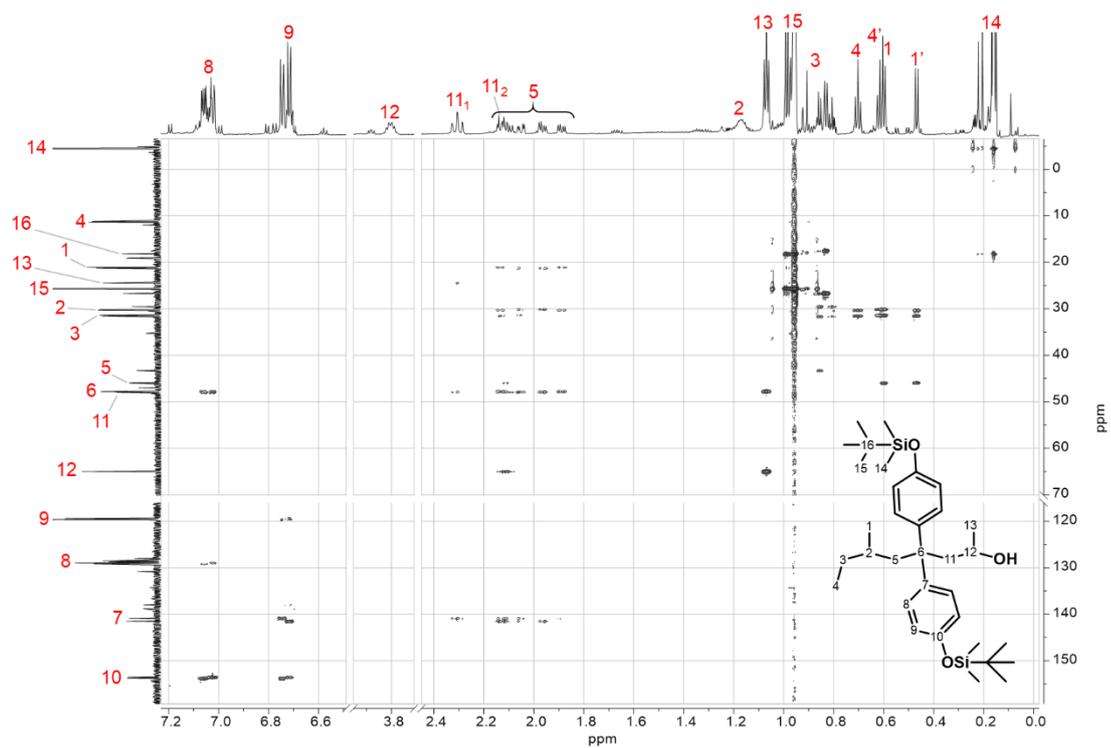
Figure A.6 HMBC-NMR spectrum of BP-OH.

2. NMR CHARACTERISATION OF BP-Br
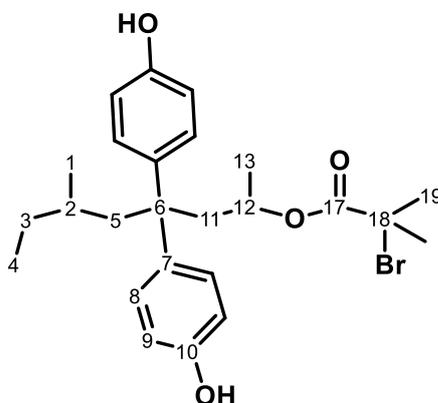
Figure A.7 Molecular structure of BP-Br.
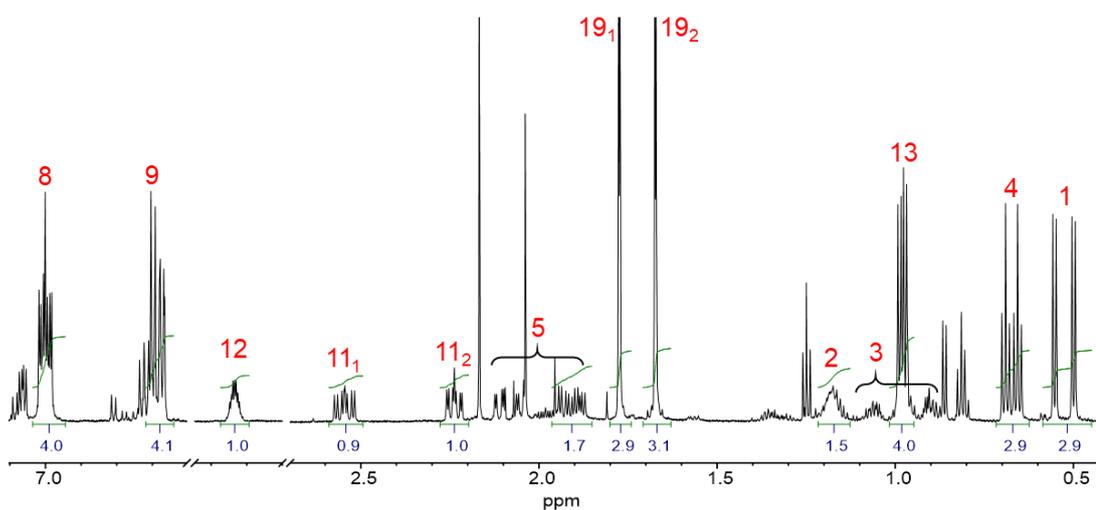
Figure A.8 ^{1}H NMR (CDCl$_3$, 700 MHz) spectra of BP-Br.
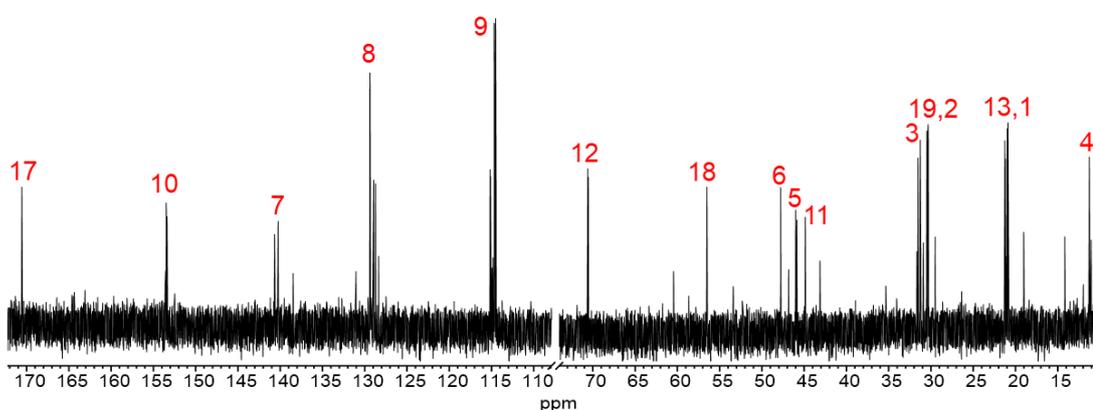
Figure A.9 ^{13}C NMR (CDCl$_3$, 175 MHz) spectrum of BP-Br.
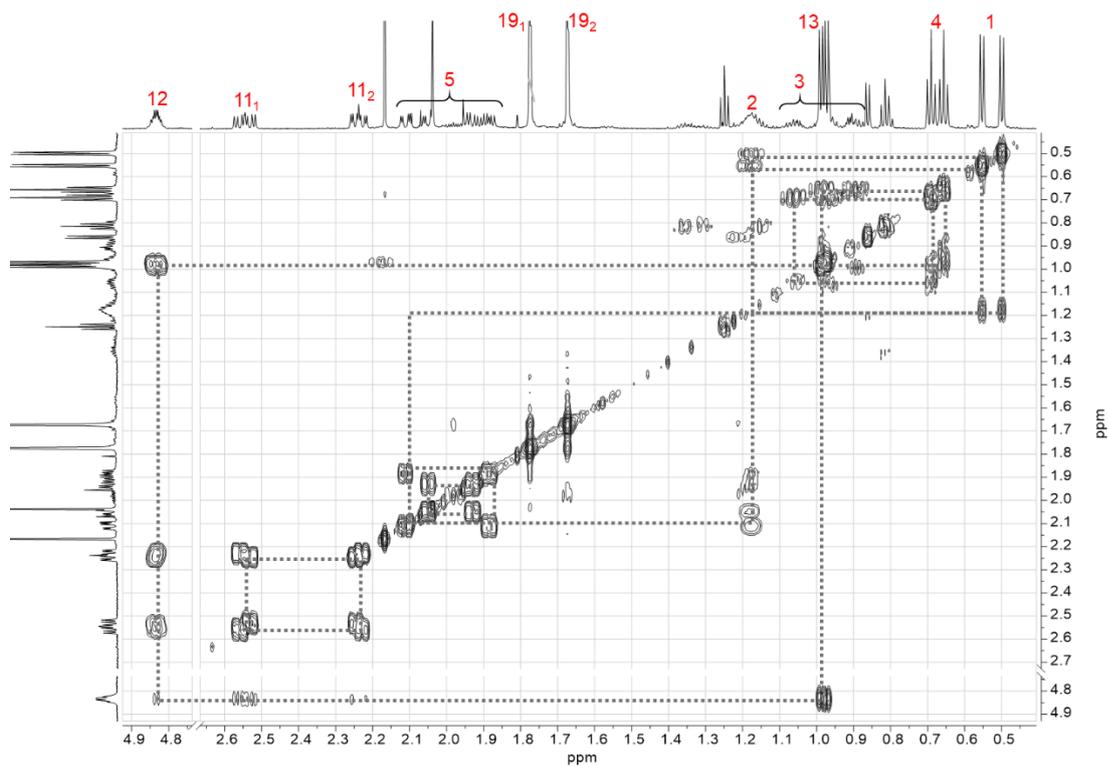
Figure A.10 Section of ^{1}H-^{1}H COSY NMR spectrum of BP-Br.
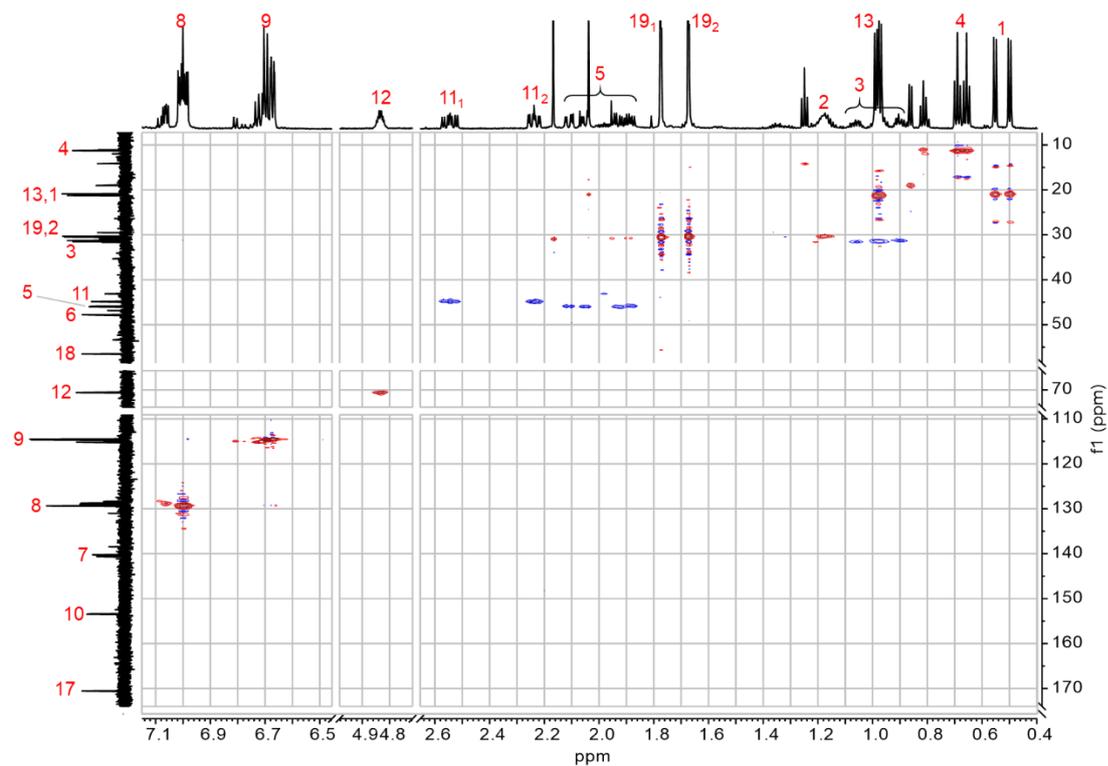
Figure A.11 HSQC-NMR spectrum of BP-Br.
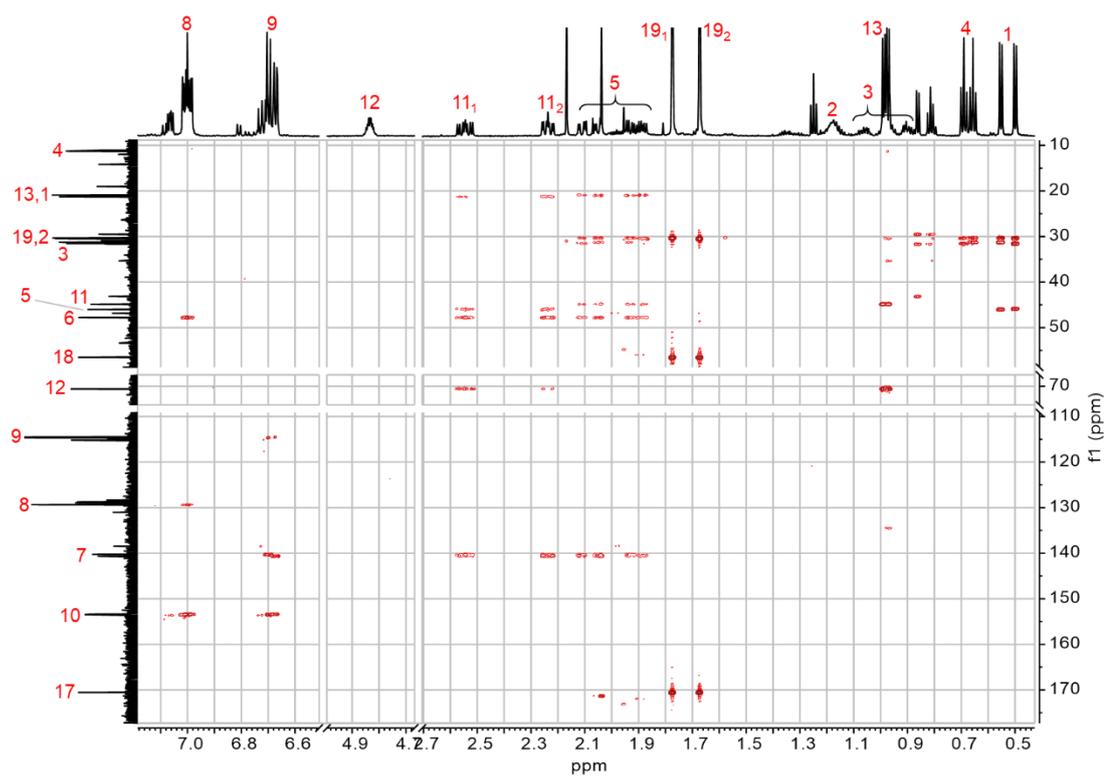
Figure A.12 HMBC-NMR spectrum of BP-OH.
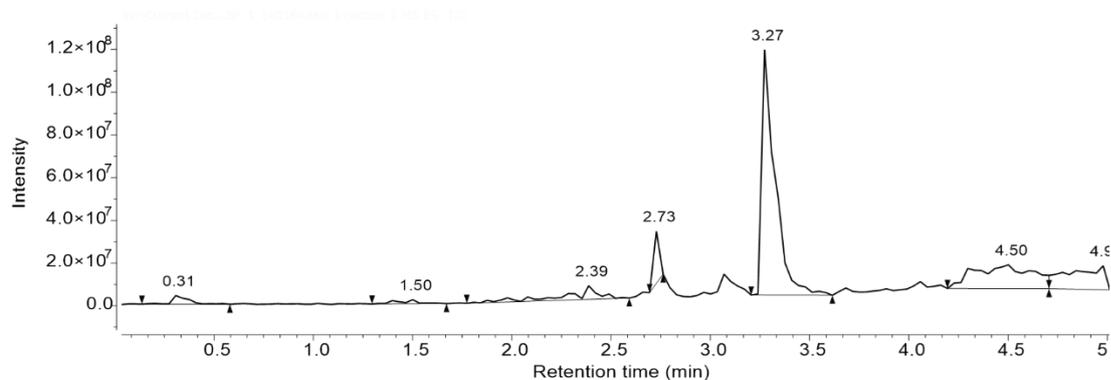
3. MS SPEC CHARACTERISATION OF BP-Br

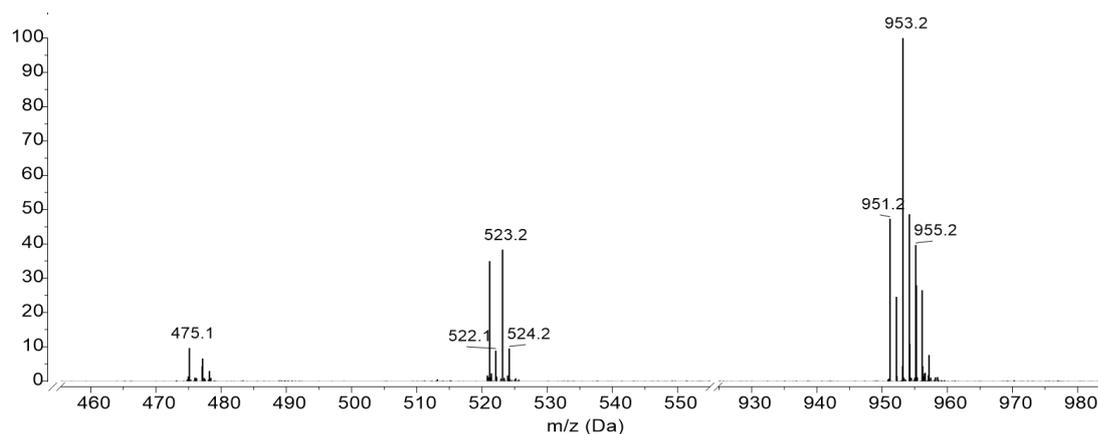**Figure A.13** TIC of LRMS (ESI-TOF) of BP-Br.
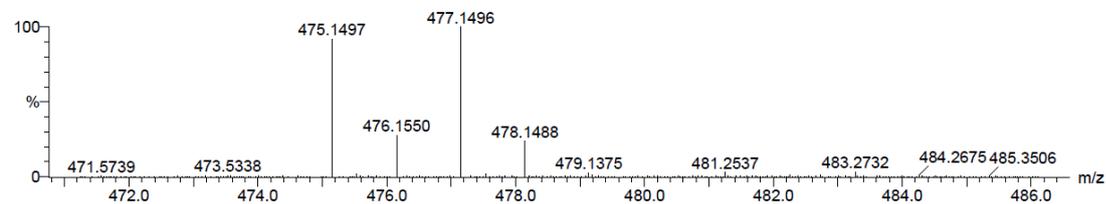

Figure A.14 LRMS (ESI-TOF) of peak at 3.27 min of BP-Br.

Figure A.15 HRMS (ESI-TOF) of peak m/z 475.1 of BP-Br.